



UNIVERSITY OF  
CAMBRIDGE



## Root Problems in Human Variation

Jason Jacob Gellis

Darwin College

May 25th, 2020

This thesis is submitted for the degree of Doctor of Philosophy

Word count: 42,734

This thesis is the result of my own work and includes nothing which is the outcome of work done in collaboration except as declared in the preface and specified in the text.

It is not substantially the same as any work that has already been submitted before for any degree or other qualification except as declared in the preface and specified in the text.

It does not exceed the prescribed word limit for the Faculty of Human, Social, and Political Sciences Degree Committee.

## Preface

The work here was designed and carried out under supervision of Professor Robert A. Foley

Chapter 6 included additional assistance and collaboration from Doctor Christopher N. Foley (not related), who helped code and test the Flexible Discriminant Analysis machine learning classifier.

Chapters 3-6 are structured as papers in preparation for submission to, or already submitted to Academic Journals. Therefore, there is a degree of overlap in their materials. While this format is intentional, all chapters are linked by a common theme.

Chapter 4 has been submitted to the Journal of Anatomy

Chapter 5 has been submitted to the Journal of Anatomy

Chapter 6 has been published PLOS ONE

Chapter 7 has been submitted to Science

For Shannon, always

## Acknowledgements

This dissertation is the product of a process much bigger than any one person. I am forever in gratitude to -

My family, Shannon Shafer, Penelope Gellis, and Maxwell Gellis; Richard and Teresa Gellis, Isaac Gellis, Ron and Diane Shafer, and Steve Shafer. Whose love and support have lifted me up and carried me through.

My supervisor, Professor Robert Foley, whose wisdom, patience, humour, and friendship have guided me through some of the greatest moments of my life, this dissertation included.

To Professor Marta Mirazón-Lahr, who has been a source of support and friendship, who graciously and generously included me in her research in Kenya as part of the In-Africa Project, who gave me access to the materials at the Duckworth Laboratory used in this dissertation, and who along with Professor Foley, has cared for my family and me.

To my family at the Leverhulme Centre for Human Evolutionary Studies, the Department of Archaeology, Darwin College, and the University of Cambridge -

Robert Foley, Marta Mirazón-Lahr, Federica Crivellaro, Laura van Holstein, Benjamin Utting, Keaghan Yaxley, Sarah Paris, Pippa Milligan, Lucia Nadal-Urias, Robert Attenborough, Jason Hodgson, Enrico Crema, Sarah Kaewart, Jonathan Goodman, Keziah Conroy, Alex Wilshaw, Frances Rivera, Fabio Lahr, Christopher Foley, Mahala Le May, Ana Belén Marín-Arroyo, Amaury Triaud, Hannah Grey, Thomas O'Mahoney, Lob Forey, Silvia Hogg, Trish Biers, The Duckworth Laboratory, The Turkana Basin Institute, Johnny at The Brew Project for fuelling late nights and early mornings, and all my B3 students over the years.

I thank the Duckworth Laboratory, University of Cambridge, for permission to study materials within its collections.

Thank you to family, the Department of Archaeology, Darwin College, The Cambridge Philosophical Society, The European Society for the Study of Human Evolution, and the State of California for funding opportunities.

# Table of Contents

<b>Preface</b> .....	<b>ii</b>
<b>Acknowledgements</b> .....	<b>iv</b>
<b>Table of Contents</b> .....	<b>v</b>
<b>List of Tables</b> .....	<b>ix</b>
<b>List of Figures</b> .....	<b>xi</b>
<b>Abstract</b> .....	<b>1</b>
<b>Chapter 1: Introduction</b> .....	<b>2</b>
<b>1.1 Dental Anthropology - Tooth crowns</b> .....	<b>2</b>
<b>1.2 Dental Anthropology - Tooth roots</b> .....	<b>7</b>
<b>1.3 Aims of this dissertation</b> .....	<b>12</b>
1.3.1 Patterns and predictions of tooth root and canal number and morphology.....	13
1.3.2 Tooth root morphospace and the phenotypic set .....	13
1.3.3 Identification and classification of geographic and population substructure.....	14
<b>Chapter 2: Biology of tooth crowns and roots</b> .....	<b>15</b>
<b>2.1 Tooth crowns</b> .....	<b>15</b>
<b>2.2 Tooth Roots</b> .....	<b>17</b>
2.2.1 The eruptive and penetrative phases .....	17
2.2.2 Teeth with more than one root .....	18
<b>2.3 Developmental basis of root variation</b> .....	<b>19</b>
<b>2.4 Morphogenetic gradients</b> .....	<b>19</b>
<b>2.5 Genetic/sex chromosomal influences</b> .....	<b>20</b>
<b>2.6 Environmental influences on tooth root development</b> .....	<b>22</b>
<b>Chapter 3: Materials and Methods</b> .....	<b>24</b>
<b>3.1 Human samples</b> .....	<b>24</b>
3.1.1 American Museum of Natural History .....	24
3.1.2 Duckworth Laboratory .....	25
3.1.3 Smithsonian National Museum of Natural History .....	25
<b>3.2 Dental formula and anatomical terms</b> .....	<b>28</b>
3.2.1 Dental formula .....	28
3.2.2 Anatomical terms.....	28
<b>3.3 Computed tomography</b> .....	<b>29</b>
3.3.1 Use of cone beam computed tomography for visualizing internal and external features of tooth roots.....	29
3.3.2 Imaging of osteological collections used in this dissertation.....	31
3.3.3 Analysis of CT images.....	31
<b>3.4 Root and canal traits</b> .....	<b>33</b>
3.4.1 Root number .....	33
3.4.2 Canal number.....	34
3.4.3 Root and canal orientation .....	35
3.4.4 Root morphology .....	37
3.4.5 Canal shape and orientation .....	41
<b>3.5 Inter-trait association and independent observations</b> .....	<b>45</b>

3.6 Data set and data imputation.....	46
<b>Chapter 4: Patterns of variation in canal and root number in human post-canine teeth ...</b>	<b>47</b>
4.1 Abstract .....	47
4.2 Introduction .....	47
4.2.1 Root and canal formation .....	48
4.3 Materials and Methods .....	49
4.4 Results .....	50
4.4.1 Root and canal number.....	50
4.4.2 Inter-trait correlation.....	52
4.4.3 PGLM of relationship between canal and root number in individual teeth .....	53
4.4.4 PGLM of canal and root number in geographical groups .....	57
4.5 Discussion .....	61
4.5.1 Differences in root and canal number .....	62
4.5.2 Variance across teeth and between the maxilla and mandible .....	62
4.5.3 Differences in geographical groups .....	65
4.6 Conclusions .....	67
<b>Chapter 5: Canal number and orientation are predictors of external root morphology.....</b>	<b>68</b>
5.1 Abstract .....	68
5.2 Introduction .....	68
5.3 Materials and Methods .....	71
5.4 Results .....	72
5.4.1 Maxillary Premolars .....	72
5.4.2 Maxillary molars .....	73
5.4.3 Mandibular Premolars .....	75
5.4.4 Mandibular Molars .....	75
5.4.5 Chi-Square test of independence between internal and external root morphology.....	79
5.4.6 Predictions of External Root Morphology.....	84
5.5 Discussion .....	88
5.5.1 Predictive power of canal number, morphology, and orientation on external root morphology.....	89
5.5.2 Constrained phenotypes and the most frequent phenotype .....	90
5.5.3 Biomechanical explanations .....	92
5.6 Conclusions .....	92
<b>Chapter 6: A novel system for determining tooth root phenotypes.....</b>	<b>93</b>
6.1 Abstract .....	93
6.2 Introduction .....	93
6.3 Materials and Methods .....	96
6.4 Results .....	98
6.4.1 Global root phenotype system .....	98
6.5 Recording tooth root phenotypes.....	98
6.5.1 Root number or absence .....	99
6.5.2 Canal number or absence .....	99
6.5.3 Anatomical locations of canals and roots .....	100
6.5.4 External Root Morphology.....	101
6.5.5 Canal configuration .....	102

6.6 The phenotypic set within the morphospace of root diversity .....	104
6.7 Case Study 1 - Geographical variation in phenotype diversity.....	107
6.8 Case Study 2 - Hominid Classification .....	113
6.9 Discussion .....	116
6.10 Conclusions .....	119
<b>Chapter 7: Tooth root deep phenotyping can identify population substructure in modern humans .....</b>	<b>120</b>
7.1 Abstract .....	120
7.2 Introduction .....	121
7.3 Materials and Methods .....	123
7.4 Results .....	125
7.4.1 Maxilla and mandible, all teeth, Geographical level 1: Major Human Subdivisions .....	126
7.4.2 Maxilla and mandible, all teeth, Geographical level 2: Continental Groups.....	129
7.5 Discussion .....	132
7.5.1 Diversity of root phenotypes and classical human biogeographical categories .....	133
7.5.2 Comparison of genome ancestry patterns and root phenotype distributions. ....	134
7.5.3 The problem of scale and classificatory criteria in human populations .....	137
7.5.4 Archaic and older AMH admixture.....	138
7.5.5 The potential of AI and Machine learning approaches .....	140
7.6 Conclusions .....	140
<b>Chapter 8: Conclusions.....</b>	<b>142</b>
8.1 Summary of conclusions.....	142
8.2 Tooth roots as a model phenotype .....	143
8.3 Evolutionary and methodological issues.....	145
8.3.1 The use of key teeth vs. the total phenotypic set.....	145
8.3.2 Tooth root morphospace .....	145
8.3.3 The phenotypic set .....	146
8.4 Evolutionary implications and applications .....	148
8.5 Machine learning methods in human evolutionary studies.....	150
8.6 Strengths, limitations, and future directions .....	151
<b>Chapter 9: Appendices .....</b>	<b>153</b>
9.1 Glossary .....	153
9.1.1 Tooth and Mandibular Anatomy.....	153
9.1.2 Directional Terms.....	156
9.1.3 Tooth identity .....	156
9.2 List of individuals used in this dissertation .....	157
9.3 Chapter 4 supplementary statistics .....	181
9.3.1 Tukey Pair-wise comparisons by tooth .....	181
9.3.2 Tukey pair-wise comparisons by geographical region .....	182
9.4 Chapter 6: Most prevalent phenotypes by geographical grouping .....	182
9.5 Chapter 7: Canonical variables with outliers.....	185

**Chapter 10: References ..... 186**

## List of Tables

Table 1.1: Previous investigations of Double-Rooted Mandibular Canines .....	8
Table 2.1: Genes expressed in varying structures during tooth root development.....	21
Table 3.1: Sample populations used in this dissertation .....	26
Table 3.2: Tooth counts of the right side of the maxillary and mandibular dental arcades...	32
Table 3.3: Number of roots in teeth of the right side of the maxilla and mandible by tooth	33
Table 3.4: Number of canals per tooth in the right side of the maxilla and mandible by tooth .....	34
Table 3.5: Anatomical orientation of canals in the right side of the maxilla and mandible by tooth.....	35
Table 3.6: Description of external tooth root morphologies at the midpoint.....	38
Table 3.7: Counts of external root morphologies in the right side of the maxilla and mandible by tooth .....	39
Table 3.8: Type and number of teeth with pegged roots in the right side of the maxilla and mandible.....	40
Table 3.9: Type and counts of roots showing fusion morphologies in the right side of the maxilla and mandible .....	41
Table 3.10: Counts of canal shapes and configurations in the right side of the maxilla and mandible by tooth .....	43
Table 4.1: Counts of teeth used in this study .....	49
Table 4.2: Number of roots from teeth in the right side of the maxilla and mandible by tooth .....	51
Table 4.3: Number of canals per tooth in the maxilla and mandible by tooth.....	51
Table 4.4: Regression parameters for GEE extended PGLM regression of the association between canal-to-root number by tooth, ranked by odds ratios from greatest to least.....	54
Table 4.5: Regression parameters for PGLM testing the association between canal and root number by tooth in geographic groups, ranked by odds ratio from greatest to least. ....	58
Table 5.1: Results of Chi-Square test of independence and Cramer's V for P <sup>3s</sup> .....	79
Table 5.2: Results of Chi-Square test of independence and Cramer's V for M <sup>1s</sup> .....	80
Table 5.3: Chi-Square test of independence and Cramer's V for P <sub>3</sub> .....	81
Table 5.4: Chi-Square test of independence results and Cramer's V for M <sub>1s</sub> .....	82
Table 5.5: Chi-Square test of independence and Cramer's V for M <sub>2</sub> trait – C-shaped root and canal .....	83
Table 6.1: Previous typological studies of tooth roots and canals .....	94
Table 6.2: Tooth counts of the right side of the maxillary and mandibular dental arcades...	96
Table 6.3: Hominid material used for case study 2 .....	97
Table 6.4: Summary table of five phenotypic elements .....	104
Table 6.5: Permutation of one element results in variation of phenotype codes.....	105
Table 6.6: Phenotype codes for total sample with highest frequency by tooth .....	106
Table 7.1: Tooth counts of the right side of the maxillary and mandibular dental arcades..	123
Table 7.2: List of samples used in this study by major geographical and continental groups .....	123
Table 7.3: Step-wise phenotype comparisons of cumulative variance explained between groups - G1: Major Human Subdivisions .....	127
Table 7.4: Confusion table for FDA of Geographical Level 1: Major Human Subdivisions ...	127

Table 7.5: True positive, true negative, false positive, and false negative rates of FDA for Geographical Level 1: Major Human Subdivisions .....	128
Table 7.6: Cumulative variance explained between groups - Geographical Region 2: Continental Group .....	130
Table 7.7: Confusion table for Geographical Region 2: Continental Group .....	130
Table 7.8: True positive and true negative rates for FDA of Geographical Region 2: Continental Group .....	131
Table 9.1: Collection information for individuals used in this dissertation .....	157
Table 9.2: Tukey Pair-wise comparisons of from GLM model of canal to root number by tooth .....	181
Table 9.3: Tukey pair-wise comparisons of canal to root number by geographical region..	182
Table 9.4: A-E provide the most prevalent phenotype codes for each geographical group	182

## List of Figures

Figure 1.1: Cluster analysis of Hanihara’s (2008) worldwide data set on non-metric tooth crown variation.....	5
Figure 1.2: Dendrograms of population ancestry and admixture based on dental phenotype and genomic data.....	7
Figure 2.1: Different stages of tooth crown development.....	16
Figure 2.2: Eruptive and Penetrative phases of tooth root development.....	17
Figure 2.3: Apical view of formation of (A) single and (B) multiple roots.....	18
Figure 3.1: Map of archaeological sites for individuals used in this dissertation.....	24
Figure 3.2: Human population sample sizes by collection.....	25
Figure 3.3: Human population sample sizes by location and sex.....	26
Figure 3.4: Map of archaeological sites for individuals used in this dissertation adapted to show the five major human populations.....	27
Figure 3.5: Anatomical surfaces and directions.....	29
Figure 3.6: Representative CBCT images of different canal system configurations.....	30
Figure 3.7: Horos Dicom Viewer 2D orthogonal view used to assess root and canal morphologies.....	31
Figure 3.8: Locations of measurements taken in Horos Dicom Viewer.....	33
Figure 3.9 : Axial slices of roots at midpoint. Eight morphologies are identified.....	37
Figure 3.10: Vertucci’s widely used canal classification system.....	42
Figure 3.11: Root canals morphology.....	43
Figure 4.1 : The sites on the apical foramen where the inter-radicular processes (IRP’s) form determines the location and orientation of each tooth root.....	48
Figure 4.2: Pearson correlation of root number to canal number.....	53
Figure 4.3: PGLM prediction curves with error bars for canal to root number for individual teeth.....	55
Figure 4.4: Proportion of canal to root number for individual teeth.....	56
Figure 4.5: Estimated marginal means derived from Tukey pair-wise comparisons of canal to root number by tooth.....	57
Figure 4.6: PGLM prediction curve for root to canal number by population.....	58
Figure 4.7: Marginal effects of canal to root count in individual teeth by geographical group.....	59
Figure 4.8: Estimated marginal means derived from Tukey pair-wise comparisons of PGLM of canal to root number by geographic group.....	60
Figure 4.9: Proportions of roots to canals in individual teeth by geographic group.....	61
Figure 5.1: Canal number and morphology does not always follow external number and form.....	69
Figure 5.2: Rare and infrequent root morphologies.....	70
Figure 5.3: Axial CT slices showing external root morphologies at the middle third and apical third.....	71
Figure 5.4: Counts of canal shapes and orientations in roots of maxillary premolars by canal number.....	73
Figure 5.5: Counts of canal shapes and orientations in roots of maxillary molars by canal number.....	74
Figure 5.6: Counts of canal shapes and orientations in single rooted mandibular premolars by canal number.....	75

Figure 5.7: Counts of canal shapes and orientations in roots of mandibular molars by canal number .....	76
Figure 5.8: Most frequent phenotype of external root morphology and internal canal count and configuration .....	77
Figure 5.9: Most frequent phenotypes of external root morphology and internal canal count and configuration for maxillary and mandibular premolars and molars.....	78
Figure 5.10: Standardized residuals of Chi-Square test for P <sup>3</sup> s .....	80
Figure 5.11: Standardized residuals of Chi-Square test for M <sup>1</sup> s .....	81
Figure 5.12: Standardized residuals of Chi-Square test for P <sub>3</sub> s .....	82
Figure 5.13: Standardized residuals of Chi-Square test for M <sub>1</sub> s .....	83
Figure 5.14: Standardized residuals of Chi-Square test for M <sub>1</sub> s .....	83
Figure 5.15: MLR of canal number to canal configuration and root morphology in P <sup>3</sup> s .....	84
Figure 5.16: MLR of canal number to canal configuration and root morphology in M <sup>1</sup> s. ....	85
Figure 5.17: MLR of canal number to canal configuration and root morphology in P <sub>3</sub> s. ....	86
Figure 5.18: MLR of canal number to canal configuration and root morphology in M <sub>1</sub> s. ....	87
Figure 5.19: MLR of canal number to canal configuration and root morphology for M <sub>2</sub> C-shaped roots and canals.....	88
Figure 6.1: Root and canal number do not always conform to one another .....	95
Figure 6.2: Flow chart for determining and recording phenotype element 1 - root number or absence.....	99
Figure 6.3: Flow chart for determining and recording phenotype element 2 - canal number. ....	100
Figure 6.4 Flow chart for determining and recording phenotype element 3 - anatomical location of canals.....	100
Figure 6.5: Flow chart for determining and recording phenotype element 4 - external root morphology .....	101
Figure 6.6: Flow chart for determining and recording phenotype element 5 - canal morphology and configuration.....	102
Figure 6.7: Flow chart for determining and recording phenotype element 5 - canal morphology and configuration (isthmus canals).....	103
Figure 6.8: Five phenotypic elements of a lower left 1 <sup>st</sup> mandibular molar.....	103
Figure 6.9: Counts of phenotypes in individual teeth. ....	105
Figure 6.10: Left - Combinations of individual root types form multiple root complexes. ..	106
Figure 6.11: Number of phenotypes permutations present in geographical subdivisions... ..	108
Figure 6.12: Dirichlet Distribution of relative proportions of maxillary phenotypes within global populations. ....	111
Figure 6.13: Dirichlet Distribution of relative proportions of mandibular phenotypes within global populations. ....	112
Figure 6.14: Phenotype codes found in the hominid sample.....	114
Figure 6.15: Standardized residuals of Chi-Square test for hominid genera and phenotype codes .....	116
Figure 7.1: Geographical Level 1: Major Human Subdivisions .....	126
Figure 7.2: Canonical variable plots for all maxillary and mandibular teeth from Geographical level 1: Major Human Subdivisions .....	129
Figure 7.3: Geographical Region 2: Continental Groups .....	129
Figure 7.4: Canonical variable plot for all maxillary and mandibular teeth from Geographical level 2: Continental groups.....	132

Figure 7.5: Phylogenetic tree of human populations based on ancient and contemporary genomics .....	139
Figure 8.1: Morphospace, phenotypic sets and observed phenotypes.....	147
Figure 9.1: Canonical variables 1-4 for G1: Major Human Subdivisions. No outliers removed. ....	185

## Abstract

This dissertation is an investigation of post-canine tooth root morphology in a global sample of modern humans. Tooth roots are variable in number, shape and orientation, and internal canal form and number do not necessarily covary with external morphology. However, this variation is poorly understood in anthropological and biological contexts. This is, in part, due to the inaccessibility of tooth roots for metric and morphological assessment. Early studies relied on x-rays, which are problematic when visualizing root structures, which are often curved or layered one on top of another. Computed tomography (CT) allows for clear visualization of tooth roots, and has revealed a previously unknown, complex combination of external and internal morphologies.

Using CT scans from a global sample of humans ( $n = 945$ ) a novel phenotype system is developed comprised of five elements: Root presence/absence (E1), canal root presence/absence (E2), canal location (E3), external root morphology (E4), and canal morphology and configuration (E5). Together, these five elements capture the external and internal morphology of the tooth root complex and are used to carry out four objectives: (1) to test and describe patterns of variation and divergence between root and canal number in individual teeth and between populations; (2) to develop a predictive model of tooth root morphology based on canal count and configuration; (3) to identify and define the total tooth root phenotypic set of the human sample; (4) to investigate if and how the total phenotypic set can delineate and define geographic and population structure in our sample. Novel statistical approaches are developed and used to ascertain complex patterning.

Results indicate that there are clear differences between patterns of root to canal number both within and between teeth of the maxilla and mandible, and that these patterns are different between populations; that root canal number and orientation are powerful predictors of external root morphology; that the combined phenotype elements capture variation within and between populations; and that the combined phenotype elements can accurately identify and delineate population substructures. These findings are discussed in terms of evolutionary and developmental biology and biomechanics, and population structure and diversity.

## Chapter 1: Introduction

### 1.1 Dental Anthropology - Tooth crowns

In many ways, teeth are unlike any other elements of the skeleton. The three dental tissues, enamel, dentine and cementum, are composites of calcium phosphate and organic materials, and comprise the hardest parts of the human body. Bone develops within the body as a mineralized connective tissue comprised of living cells, blood vessels, and nerves. In contrast, the components of teeth are mineralized epithelial tissues (Miller, 2013). Enamel, the only 'bony' material visible on the surface of the body contains no cells, blood vessels, or nerve supply (Ash, 2013). Dentine, which develops from contact with epithelium during morphogenesis, also contains no living cells, instead passing cells from the internal pulp through microscopic tubules (Li et al., 2017). Only cementum, the outer casing to the root, resembles bone (Kovacs, 1971). However, while it contains living cells and collagen, it contains no blood supply, and serves only as an attachment for the ligaments binding teeth to their sockets (Versiani et al., 2019). But perhaps, the greatest difference between teeth and the rest of the skeleton is that dental tissues experience no tissue turnover during the lifetime of an organism. While bone is continually replaced, maintained, and remodelled by cellular and physical activity, once formed, teeth retain only the structures determined by their development. Thus, teeth are easier to understand in relation to the genetic and evolutionary pathways which have guided and shaped their morphology.

Because of their complex biology, teeth have been the subject of many studies in anthropology, medicine, vertebrate palaeontology and zoology. Long recognized by 19th century naturalists as rich sources of evolutionary information and morphological diversity, it was not until the 20th century that anything resembling the modern field of 'dental anthropology' arose. Aleš Hrdlička (1920) produced what is considered the first major work - a detailed assessment of the presence, absence, and degree of expression of shovel-shaped incisors in Asian and American Indian populations in contrast to European and African populations. Hrdlička's contemporary, palaeontologist and odontologist W.K. Gregory (1921), classified dental traits as low (i.e. primitive) or high (i.e. civilized). Though his interpretations reflect the views of human origins and race of the late 19th/early 20th centuries, Gregory's analyses of cusp number, retention or loss of the Y5 *Dryopithecus*

pattern, and presence or absence of accessory cusps, emphasized the recognition and importance of primitive and derived traits that inform modern cladistic methods. Campbell's (1925) monograph on the dentition and palate of Australian Aboriginals integrated Hrdlička and Gregory's observations of population specific morphologies, and includes information on crown *and* root counts. Campbell's work is considered a cornerstone in dental anthropology for its characterization of non-European dental variation, and directly inspired morphological studies of the Bantu (Shaw, 1931) and Native Americans (Nelson, 1938; Goldstein, 1948). Characteristic of this early phase of dental anthropology is the focus on identifying and discussing dental traits such as molar number and groove pattern (Drennan, 1929; Hjellman, 1929) and the racial distribution of three-rooted mandibular molars (Tratman, 1938). However, it was recognized by contemporary practitioners, and the fields of palaeontology and human evolution at large, that in regard to how tooth morphology was distributed within and between human populations, "... the greater part of the world still remains in a state of dental darkness" (Keith, as quoted in Shaw, 1931).

Intensive interest in comparative dental morphology can be traced to Albert A. Dahlberg at the University of Chicago and P.O. Pederson from the University of Copenhagen. Dahlberg produced extensive works on the morphologies of Southwest Native Americans at the tribal level, which resulted in a number of major early publications, as well as dental casts and genealogical records (A A. Dahlberg, 1945; A.A. Dahlberg, 1945; Dahlberg, 1950). His extensive comparative data led to the production of a series of reference plaques which standardized rank scales of morphological variables of the teeth (Dahlberg, 1956). Running in parallel to Dahlberg, Pedersen (1949) produced his monograph *The East Greenland Eskimo Dentition*; which included extensive comparative data for Arctic and European populations. This period is capped off by Brothwell's (1963) publication of *Dental Anthropology*; which compiled studies of tooth morphogenesis, human and fossil hominin root crown morphology and variation, tooth wear, and importantly, a number of important papers on trait variation and affinities between Native Americans and Asians, and their distinctiveness from European populations.

The last third of the 20th century is most responsible for shaping dental anthropology into the field it is today. By this time, Garn (1971, 1977) recognized the role that genetics played in tooth crown morphology, and how this could be applied to studies of modern human populations. Using shovel teeth variation as an example, Molnar (1975)

discussed how the variability and frequencies of crown morphologies could delineate the major groups of mankind (included in this study are Sino-American, European, and Inuit populations). Molnar identified several broad issues for using dental morphologies in population studies. The first was that more often than not, the occurrence of a particular trait could be found within all the major groups of humanity; and that it was the frequency of a trait's occurrence that was useful for population studies. The second was that multiple traits were required for assessment of population affinities. Thus, human population dental variation is a question of number and degree, and it is crucial to consider as many variables as possible. Looking back, Molnar's observations seem obvious, as modern studies of genetics and morphology have shown that a single trait cannot divide the world's populations, but at the time they were ground-breaking.

Dental studies of population history and relationships come into focus during the late 1980's and 1990's when many of the discrete, non-metric traits (e.g. Carabelli's cusp, shovel-shaped incisors) long used to characterize and study dental morphology were formally described and standardized into 27 traits comprising the Arizona State University Dental Anthropology System (ASUDAS (Turner II et al., 1991)). This system has been applied to a number of data sets to test hypotheses of population histories and affinities, and human origins. Two milestone studies of human dental variation by Chris Stringer and Joel Irish gave strong supporting evidence to the 'out-of-Africa' model. Stringer et al. (1997) included the Krapina Neanderthals as an out-group in their cladistic analysis of modern human dental variation. Their results showed that Krapina Neanderthals had greater dental similarity to Sub-Saharan Africans and Australasians compared to European populations. Irish (1998) built and analysed a substantial database of Sub-Saharan African dental variation of living and fossil groups. His results showed that the mean measure of divergence between dental traits were significantly smaller between Sub-Saharan African and fossil groups than any other modern groups; leading him to conclude that traits distinctive of Sub-Saharan African populations represented ancestral characters found in fossil hominins and extant primates.

Irish and Guatelli-Steinberg (2003) expanded Irish's database to include 21 dental traits from 14 groups of modern humans and fossil members of East and South African robust and gracile australopithecines, and of the genus *Homo*. In regard to the Sub-Saharan sample, the authors concluded that the intraregional heterogeneity, relative distance

affinity to modern samples, and phenetic resemblance to Plio-Pleistocene ancestors, provided additional evidence consistent with an African origin of modern humans. The authors also noted a decrease of ancestral traits in populations with further temporal and spatial distance from Africa. There are two big take-aways from this. The first is that in aggregate, Sub-Saharan dentitions contain a suite of traits that surpass in number and/or variation, dental traits found in other human populations, which is consistent with a single African origin hypothesis (Turner, 1971; Irish, 1998; Reyes-Centeno et al., 2015). The second is, Sino-American populations are relatively reduced in their number and variation, suggesting that these populations, compared to all other populations are the most dentally “derived,” due to their loss of ancestral traits (Turner, 1971; Irish, 1998; Townsend et al., 2009; Reyes-Centeno et al., 2017). Situated between the two are three broad groups: Sahul-Pacific, Sunda-Pacific and Western Eurasian populations (Figure 1.1).

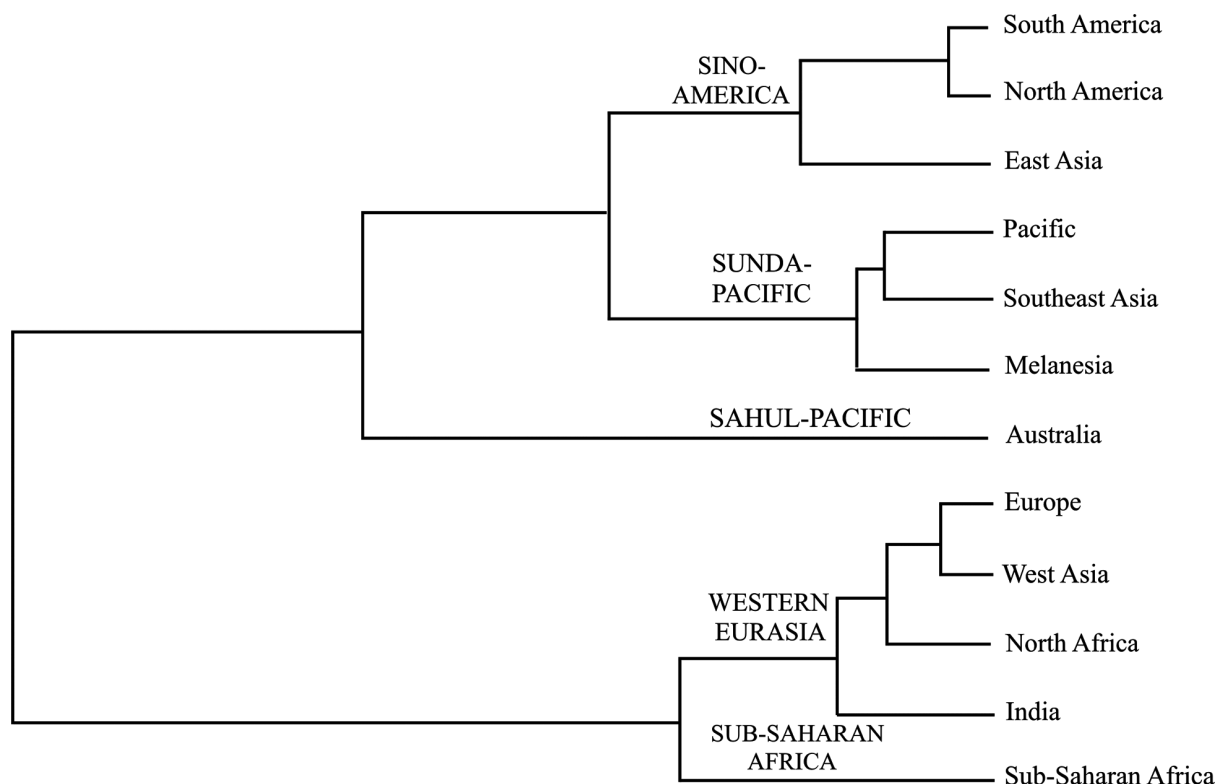


Figure 1.1: Cluster analysis of Hanihara’s (2008) worldwide data set on non-metric tooth crown variation (mean measure of divergence values and unweighted pair- group method using arithmetic averages tree). Figure from Scott et al., 2018.

The past few decades have also seen the integration of genomics and dental anthropology. The utility of a trait for historical and/or evolutionary analyses depends on how significantly its underlying genetics contribute to variation. Researchers have focused on three areas: tooth size, number, and morphology. Simple measures of tooth length, breadth, and height, and their resulting indices (e.g. crown areas) have been used to assess populations of modern humans (Hanihara and Ishida, 2005) and primates (Scott and Lockwood, 2004), both living and dead, as well as fossil hominins (Wood and Abbott, 1983; Wood and Uytterschaut, 1987; Martínón-Torres et al., 2008). However, these type of measures appear to be only useful for broad morphological characterizations, as crown size has been found to poorly discriminate closely related hominin species, and may be more a product of environmental influence than genetics (Dempsey and Townsend, 2001; Townsend et al., 2009; Evans et al., 2016). Hypo- and hyperdontia appear in varying frequencies in all populations. However, a growing body of evidence suggests that supernumerary teeth are linked to either tooth size (Brook, 2009), associated with conditions related to alveolar disruption such as cleft lip and palate (Haque and Alam, 2015; Nicholls, 2016), or inflammatory processes, pressures, and/or injuries affecting the development of the dental lamina (Mallineni, 2014). Tooth crown traits are widely assumed to be heritable, selectively neutral, evolutionarily conservative, and, importantly for populations studies, generated by the evolutionary process underlying founder effects, population bottleneck, and populations drift (see Scott et al., 2018 for an indepth discussion). Debate continues concerning which dental traits, and in what combination, preserve the most information (Rathmann and Reyes-Centeno, 2020). However, dental morphologies have proven to be among the strongest candidates for assessing population affinities and histories in the absence of genomic data (Hubbard et al., 2015; Rathmann et al., 2017; Scott et al., 2018).

While morphology does not always reach consensus with genetics, there exists a high degree of congruence (Figure 1.2) between population distances and histories based on dental phenotypes and genetic markers of population identity (Sofaer et al., 1972; Brewer-Carias et al., 1976; Hubbard et al., 2015; Rathmann et al., 2017; Reyes-Centeno et al., 2017; Rathmann and Reyes-Centeno, 2020).

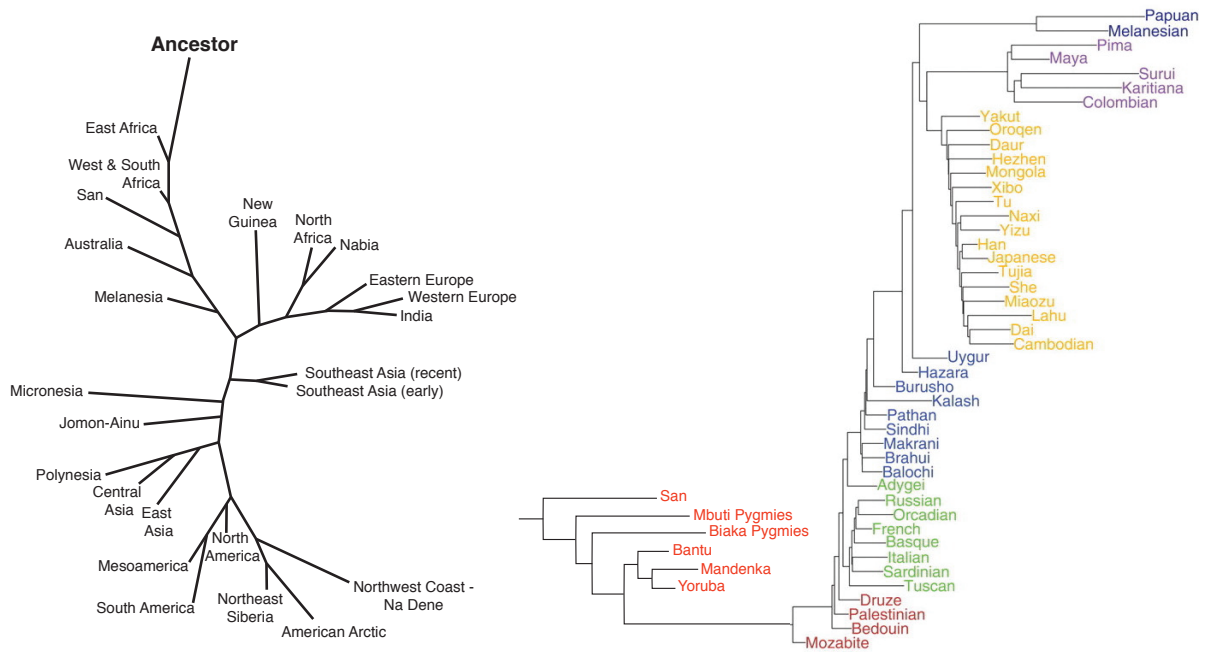


Figure 1.2: Dendrograms of population ancestry and admixture based on dental phenotype and genomic data. **Left:** *Homo sapiens'* evolution distance from the common ancestor based on mean measure of distance scores. Unrooted tree using 11 dental phenotype traits, where presumed ancestral condition was 0 or 1 compared to frequencies for 24 recent regional groups; groups closest to ancestor have least derived set of dental traits (Scott et al., 2018). **Right:** Individual ancestry and population dendrogram derived from 650,000 single-nucleotide polymorphisms in samples from the Human Genome Diversity Panel (Li et al., 2008) representing 51 populations from sub-Saharan Africa, North Africa, Europe, the Middle East, South/Central Asia, East Asia, Oceania, and the Americas. Branches are coloured according to continents/regions (Li et al., 2008).

## 1.2 Dental Anthropology - Tooth roots

Connecting tooth crowns to the jaws are the tooth roots. Tooth roots have received little attention in anthropology. Published information is overwhelmingly biased towards clinical studies and case reports. Like many of the early tooth crown studies discussed in 1.1, studies of roots were primarily descriptive of root number, and the occasional metrical analysis (Taylor, 1899; Black, 1902; Campbell, 1925; Drennan, 1929; Shaw, 1931; Tratman, 1938; Nelson, 1938; Abrahams, 1947; Pedersen, 1949; Selmer-Olsen, 1949; Moorrees, 1957; Brabant, 1964; Moss et al., 1967; Barnes, 1969; Miyabara, 1994). In fact, when observable (e.g., removable from the jaws, loose individual teeth), there appears to be little about the gross morphology of tooth roots, besides root count, that distinguishes them at all. Evidence of this can be found in century's worth of dental anthropological papers (cited in this chapter), including the ASUDAS, whose only traits for tooth roots includes root number and the presence or absence of the Tomes' root (Turner II et al., 1991).

In modern humans, maxillary premolars are reported as having the most variation of all teeth. This variation is in regard to root number, with a higher percentage of P<sup>3</sup>s having two roots (or at least bifurcated apices), while P<sup>4</sup> is typified by one root. Three rooted maxillary premolars (P<sup>3</sup> and P<sup>4</sup>) have been documented in modern humans (Shaw, 1931; Nelson, 1938; Abrahams, 1947; Carns and Skidmore, 1973; Vertucci and Gegauff, 1979; Caliřkan et al., 1995) but are extremely rare. Scott and Turner (Scott et al., 2018) report a world frequency of 4.9-66.7% for two-rooted premolars. Their results show that Sub-Saharan Africans have the highest frequency at 65%, 40% in West Eurasian populations, 20-30% in East Asian populations, and 5-15% in Northeast Siberians and all Native Americans.

Maxillary molars are generally three rooted; though molars with two, four (Christie, Peikoff, & Fogel, 1991; Ahmed & Abbott, 2012) and five (Fahid and Taintor, 1988) roots have been reported. Variation in root number has been recorded for three rooted M<sup>2</sup>s; with Australian Aboriginals having the highest reported percentage at 95.8% (Campbell, 1925). Sub-Saharan Africans also have a high frequency of three-rooted M<sup>2</sup>s at 85%, Western Eurasians and East Asians ranging from 50-70% and American Arctic populations ranging from 35-40% (Scott et al., 2018). Three European samples by Fabian, Hjelmmann, and Visser (in Brabant, 1964) report an average of 56.6%, in accordance with Scott and Turner (Scott et al., 2018). Inuit populations are lower with East Greenland populations at 23.7% (Pedersen, 1949) and 30.7-31.3% in two prehistoric Alaskan populations (Scott, 1991).

Double rooted mandibular canines are rare outside of European populations in which they attain a frequency of 4.9 -10% (Table 1.1). Alexandersen (1963) compiled data from several European countries as well as two Danish Neolithic samples, and two medieval samples. His study is the most comprehensive population study to date, and his findings suggest that the double rooted canine trait is a European marker.

Table 1.1: Previous investigations of Double-Rooted Mandibular Canines

Population	n	Number of Canines		Reference*
		1 root	2 roots	
Hungarians	1707	1604	103 (6.0%)	Hillebrand (1909)
Alemanni	507	476	31 (6.1%)	Schwerz (1928)
Germans	315	295	20 (6.4%)	Fabian (1928)
Finnish	98	93	5 (4.9%)	Hjelmmann (1929)
Dutch	2488	2365	123 (4.9%)	Visser (1948)
French	282	254	28 (10 %)	Huche (1954)
Bantu	62	61	1 (1.6%)	Shaw (1931)

<b>Pecos Tribe</b>	94	94	0	Nelson (1938)
<b>East Greenland Inuit</b>	72	71	1 (1.3%)	Pedersen (1949)
<b>Danish Neolithic †</b>				
- <b>2000 B.C.E.</b>	4	4	0	
- <b>1500 B.C.E.</b>	103	96	7 (5.6%)	Alexandersen (1963)
<b>Middle Ages 1500 A.C.E.</b>				
- <b>Æbelholt</b>	312	289	23 (8.0%)	
- <b>Naestved</b>	310	291	19 (5.1 %)	Alexandersen (1963)

\*All data in this table is reproduced from Alexandersen (1963).

† Dates and designation given by Alexandersen (1963).

In contrast to the maxilla, the most frequent form of mandibular P<sub>3s</sub> and P<sub>4s</sub> is single rooted; though P<sub>3s</sub> are occasionally two-rooted or, more rarely, three rooted (Barker et al., 1974; Kakkar and Singh, 2012; Fathi et al., 2014). Three rooted P<sub>3s</sub> appear to be an ancestral form, and appear in late Pleistocene humans from East Asia (Liao et al., 2019). Multiple roots are very rare in P<sub>4s</sub>. Some of the variation in mandibular premolars is related to the presence of the Tomes' root (see Chapter 3 for descriptives). Tomes' root appears in 10% of P<sub>3s</sub> and P<sub>4s</sub> of the Pecos Native American Tribe (Nelson, 1938), 36.9% of P<sub>3s</sub> and 8.4% for P<sub>4s</sub> in the Bantu (Shaw, 1931), and >25% for Sub-Saharan African groups (Scott et al., 2018). In contrast, P<sub>3</sub> Tomes' roots account for 0-10% of Western Eurasian populations and 10-15% of North and East Asian population (Scott and Turner, 1997).

Unlike their maxillary counterparts, mandibular molars are less variable in root number. Scott et al. (2018) report the presence of supernumerary root - radix entomolaris (see Chapter 3 for descriptives), in 20-30% of North and East Asian Inuits, compared to other human populations where its frequency is less than 15%. The trait is almost non-existent in Sub-Saharan African populations though it does appear with some frequency (8-15%) in Southeast Asian Populations. Tratman (1938) claimed the trait showed a distinct dichotomy between European and Asian populations, as did Pedersen (1949). The trait also appears in 15.6% of North American Athabascans and Algonquin Native American tribes (De Pablo et al., 2010).

Single rooted M<sub>2s</sub> are common in Chinese populations with a frequency as high as 40% (Zheng et al., 2011). These roots usually have a C-shaped canal (Chapter 3 for a discussion of this feature) which has a strong ethnic component as there is a high prevalence in East Asian populations (Fan et al., 2004a; Zheng et al., 2011; Fernandes et al.,

2014). The trait has a low frequency of 0-10% in Sub-Saharan Africans (Scott and Turner, 1997), 1.7% in Australian Aboriginals (Campbell, 1925), and 4.4% in the Bantu (Shaw, 1931). Pedersen (1949) reports the trait in 22% of Greenland Eskimos, Nelson (1938) reports a frequency of 30.4% of Pecos Native Americans, and Scott (1991) reports the trait in 28.2-32.7% of Kachemak and Koniag populations.

Root number appears to reveal very little about population structures and affinities in the way that crown morphologies do. The broad picture is that Sub-Saharan African populations and Australian Aboriginals have a predilection towards multi-rooted forms, with some reduction in Sino-American populations. However, outside of these two groups the picture is less clear. For example, while Native American populations trend towards a reduction in premolar root number, they also trend towards an increase in molar root number. Morphologies that appear in European and Chinese populations are relatively non-existent in others. It is possible that there is simply not enough morphological variation in roots (ASUDAS includes only two- root number and Tomes' root) for them to be important for modern human populations studies.

Compared to modern humans, studies of non-human primate and fossil hominin tooth roots have proved more rewarding. Externally, the roots of non-human primate and fossil species appear to be highly variable in number and morphology. For example, root morphologies described as 'plate-like' and 'dumb-bell' shaped, have been described in great apes, cercopithecoids, and Plio-Pleistocene hominins (Kullmer et al., 2011; Kupczik et al., 2019). Tomes' root appears in the Chinese Middle Pleistocene and European Early Pleistocene members of *Homo* (PRADO-SIMÓN et al., 2012; Xing et al., 2018). Ward et al. (1982) described the cross sections of australopith anterior teeth as 'ovoid'. Robinson's (1956) description of robust and gracile australopithecine roots make note of the 'plate-like' form; while Keith's (1913) writings on the Krapina Neanderthals described and classified the taurodont forms common to the species. Australopiths regularly had multi-rooted premolars (Robinson, 1954, 1956; Wood et al., 1988a; Brook et al., 2014; Moore et al., 2016; Kupczik et al., 2018).

For fossil hominins, the trend is towards reduction in root number, especially in the premolars. The ancestral hominin phenotype has been proposed as three-rooted maxillary premolars, and two-rooted mandibular premolars (Abbott, 1984; Hamon et al., 2012). The trend for reduction in premolar root number appears 3.4 -2.4 Ma, and coincides with

dietary shifts towards meat and/or softer cooked foods (Luca et al., 2010). By 1.8 Ma, *Homo erectus* has fewer tooth roots, especially M<sup>3</sup>'s, than earlier members of our genus, and *H. erectus* premolars are frequently bifurcated (Abbot, 1984) or single rooted (Anton, 2003). This trend in root number reduction continues through more recent members of genus *Homo* including some specimens allocated to *H. heidelbergensis* and *H. neanderthalensis* (FitzGerald, 1998; Benazzi et al., 2011; Zanolli and Mazurier, 2013).

Until relatively recently, studies of tooth roots suffered due to the inaccessibility of roots within the jawbones. Early studies required radiographs, which only offer two-dimensional analysis. This is awkward when dealing with structures that are curved or layered one on top of another. Other methods are more destructive and required the sectioning of bones and fossils. Now, Computerized Tomography (CT) and micro-CT ( $\mu$ CT) scans allow researchers to bypass destructive techniques and the limited imaging of radiographs, enabling a new series of inquiries into the internal and histological structures of skeletal material.

CT technology has revealed in great detail that the complexity of the root canal system does not correspond with external morphology. Canal number and morphology do not always conform to number and morphology of roots, and teeth can have multiple canals and canal configurations within a single root. While the numerical relationship between canals and roots is poorly understood, these findings have expanded studies of fossil hominin taxonomy (Wood et al., 1988; Moore et al., 2013, 2016) and classification (Emonet et al., 2012; Prado-Simón et al., 2012; Moore et al., 2013). Investigators have determined that variation between maxillary and mandibular premolar root and canal number and morphology is found in non-human primates (Moore et al., 2013), and is taxonomically distinctive in South African Plio-Pleistocene hominins (Moore et al., 2016).

Though the relationship between root and canal number and morphology appears to hold untapped dental phenotypic information, it remains little explored outside of premolars. This is surprising as there is a wealth of information, especially concerning canal morphology, in the clinical literature. Multiple typologies exist for canal number and morphology (discussed in Chapters 3 and 6), and countless studies and case reports have been published on canal and root number in virtually every population. The first problem is the lack of synthesis between the two features. Moore et al. (2013) developed a typology that incorporated internal and external count and morphology. However, it is limited to

premolars, whose variation does not encompass the entirety of variation found across all teeth. Here arises the second problem: the entirety of internal and external canal and root morphology, and the relationship between the two is unknown. Without reconciling these elements, the utility of tooth roots for population and evolutionary studies will remain at the level of comparing independent traits, rather than examining the overall integration and interaction of the root complex as a whole.

The variation of human tooth root phenotypes in an evolutionary framework is the central focus of this dissertation. I hope to use the availability of 3D scanned data to build a picture of this variation as a phenotypic set, made of the different components that comprise roots (e.g., canal and root number, morphology, etc.). To do so requires the development and application of new methodologies and approaches that will be presented and discussed here, as well as explorations of the patterns of variation in developmental, functional, evolutionary and geographical contexts. The major themes are outlined below.

### 1.3 Aims of this dissertation

In this dissertation CT imaging will be used to investigate internal and external morphological variation of tooth roots in a global sample of modern humans. As discussed above, and within each chapter, there is considerable variation in canal and root number and morphology; and the nature of this variation, its origins, and how it is partitioned within and between groups is poorly understood. The aim of this dissertation is: (1) to investigate and define the human tooth root morphospace; (2) to develop a comprehensive classification system that captures in external and internal morphology of individual tooth roots - the phenotypic set; (3) to build a developmental and predictive model of tooth root morphology based on canal count and configuration; and (4) to investigate if and how the total phenotypic set delineate and classify geographic and population structure in our sample. While the samples are modern humans, the methodology is developed and presented in a way that can be applied to all members of the hominid lineages. Because the terminology applied to teeth often varies between the anthropological, palaeontological, and clinical literature, a glossary has been provided in appendices section 9.1. Chapter 2 discusses the biology underlying tooth root growth and development. Chapter 3 discusses

the osteological material used in this dissertation, how data was collected from this material, and how these data were analysed.

### 1.3.1 Patterns and predictions of tooth root and canal number and morphology

Chapter 4 investigates the relationship between canal and root number. Canal and root formation are comprised of a series of reciprocal cellular interactions in the dental papilla of the developing tooth (Jernvall and Thesleff, 2000); and the complexity underlying tooth root phenotypic diversity begins with these two traits. Roots vary in canal and root number, and canal number does not always covary with root number. However, why this should be is unknown. This chapter tests hypotheses of canal to root ratio in and between teeth, maxilla and mandible, and major human population groups. Results are discussed in the context of spatial and biomechanical models, with implications for hominin dental evolution and phylogeny.

Because the external elements of tooth roots (dentin and cementum) encompass the nerves, blood supply, and pulpal material of the canal during root morphogenesis, it is possible that external morphology is somehow determined by internal morphology. Chapter 5 presents the first test of how canal number and orientation predict external root morphology. Furthermore, we identify the most frequent internal and external morphologies in individual roots of the tooth root complex across all teeth, and their contribution to phenotypic variation.

### 1.3.2 Tooth root morphospace and the phenotypic set

Chapter 6 introduces a novel system for determining tooth root phenotypes and explores the variation of tooth root morphospace and the phenotypic set. The concept of a phenotype set has its origins in behavioural ecology where it is used to describe an organism's range of possible behaviours and life-history strategies (Bennett, 1983). However, it has been extended to define the finite range of phenotypes possible in other branches of biology (Wang et al., 2009; Martin, 2014). We identify and describe five elements (E) that best capture variation in root and canal anatomy. They are: root presence/absence (E1), canal root presence/absence (E2), canal location (E3), external root morphology (E4), and canal morphology and configuration (E5).

On their own, each element is appropriate for binary classification of a trait's presence or absence, and frequency within and between populations. However, for reasons which will be tested and discussed throughout this dissertation, each element of the tooth root phenotype is in some way dependent on another element. Thus, the true phenotypic set is defined by considering root traits in aggregate.

### 1.3.3 Identification and classification of geographic and population substructure

The diversity of root phenotypes provides an opportunity to explore whether distinct clusters of elements correspond to distinct clusters of modern humans at multiple geographic scales. Having defined the phenotypic set and testing its underlying developmental processes, Chapter 7 introduces novel applications of machine learning methods to classify and delineate geographic groups and populations based on root phenotypes. Traditional "distance statistics" use traits to summarize between-group differences. Our question is about classification, not just similarity and difference. Because the high dimensionality of the phenotypic set means that the number of phenotypes used for classification can quickly exceed the number of individuals being classified, we employ novel statistical methods for testing dental phenotypes. Machine learning methods applied in this chapter down-weight, and in some cases, remove non-influential phenotypes (e.g., phenotypes with a high degree of intrapopulation heterogeneity), in order to identify phenotypes that effectively identify and partition population substructure.

## Chapter 2: Biology of tooth crowns and roots

### 2.1 Tooth crowns

Tooth development begins with neural crest cells (Li et al., 2017). These multipotent cells are unique to vertebrates and give rise to multiple tissues including craniofacial cartilage and bone. Neural crest cells (ectomesenchyme) interact with two types of cells: oral epithelial and mesenchymal cells. Oral epithelial cells form the enamel organ, an aggregate of cells responsible for the formation of enamel, initiation of dentin formation, and establishment of the shape of tooth crowns (Miller, 2013). Mesenchymal cells condense below the enamel organ where they form the dental papilla, which generates dentin and tooth pulp. As neural crest cells arise from neural tissue they migrate to the mandible and maxilla where they integrate the oral epithelial and mesenchymal cells, aiding the development of teeth (ibid).

Tooth formation is initiated by dental placodes – localized thickenings within the oral epithelium (Figure 2.1) and along a band of epithelial tissue (Jernvall and Thesleff, 2000). These dental placodes lead to outgrowths in epithelial band which correspond to positions of the future deciduous teeth (Miller, 2013). While crown formation is a continuous process, it can be delineated into a series of three distinguishable stages: the bud, cap, and bell stages (Nelson and Ash, 2010). It is the shape of the epithelial enamel organ that defines each stage. The bud stage is a round, localized growth of epithelial cells surrounded by ectomesenchyme cells. As the rounded epithelial bud increases in size its surface becomes concave. Then appear the primary and secondary enamel knots that initiate the cap stage (Figure 2.1). During the cap stage the epithelial cells comprising the enamel organ remain attached to the dental lamina, while the underlying mesenchyme forms the dental papilla. The tissue surrounding these two structures develop into what is known as the dental follicle, which protects and stabilizes the tooth during formation and eruption. Together, the enamel organ, dental papilla, and dental follicle constitute the tooth germ.

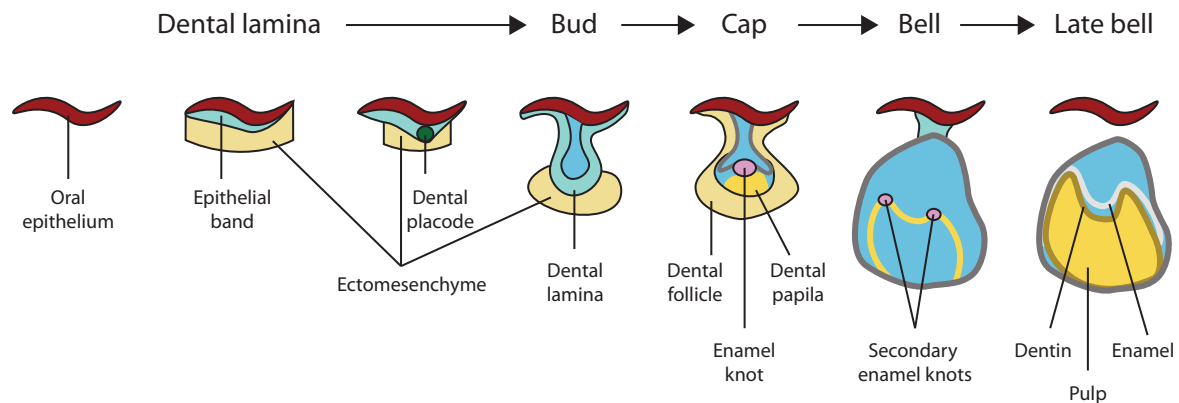


Figure 2.1: Different stages of tooth crown development.

Further growth of the papilla and enamel organ result in the bell stage (Butler, 1956; Kovacs, 1971). During the bell stage the cells of the enamel organ differentiate into four layers, (1) cuboidal cells on the surface of the enamel organ form the outer enamel epithelium (OEE) which serves to bring nutrients to the (2) inner enamel epithelium (IEE), columnar cells of the enamel organ closest to the papilla which become ameloblasts that form tooth enamel. Sandwiched between the OEE and IEE are (3) stellate reticulum cells adjacent to the OEE; and (4) the stratum intermedium cells adjacent to the IEE, both of which assist ameloblasts in enamel formation. Together, the stellate reticulum and stratum intermedium form a structure called the cervical loop. There is evidence that the cervical loop acts as a stem cell “reservoir” which allows the continuous growth of teeth in ungulates and rodents (Li et al., 2017), or the creation of Hertwig’s Epithelial sheath (HERS) which is responsible for the growth of tooth roots (discussed below in 2.2.1).

Towards the end of the bell stage, cells on the border of the dental papilla form odontoblasts, which elongate and form a matrix of collagen fibres called pre-dentin. This pre-dentin matrix calcifies into dentin, a process known as dentinogenesis. Once several layers of dentin have formed, the ameloblasts of the IEE undergo amelogenesis, a process in which ameloblasts deposit an enamel matrix (Orban and Bhaskar, 1980). Thus, dentinogenesis and amelogenesis govern the formation of dentin and enamel respectively. The bell stage marks the differentiation of the enamel organ from the surrounding dental lamina, resulting in the degeneration of the anterior dental lamina underlying the primary teeth (Nelson and Ash, 2010). However, dental lamina posterior to the primary teeth remains active as the jaw elongates and the permanent dentition develops.

## 2.2 Tooth Roots

Tooth root development can be split into two phases: the eruptive and penetrative (Figure 2.2). The eruptive phase commences when roots begin to develop and ends when the tooth crown is in occlusion. The penetrative phase begins after the tooth crown is in occlusion and ends when the apices of the tooth root complete formation. Both phases can be seen on the root surface. During the eruptive phase, the root surface is smooth while the surface formed during the penetrative phase is rough (Kovacs, 1971). Further, the proportion of smooth to rough surface appears vary among species, with the smooth surface decreasing from carnivore to herbivore (Kovacs, 1971). Amongst modern humans, the proportion is generally two-thirds smooth to one-third rough (Kovacs, 1971).

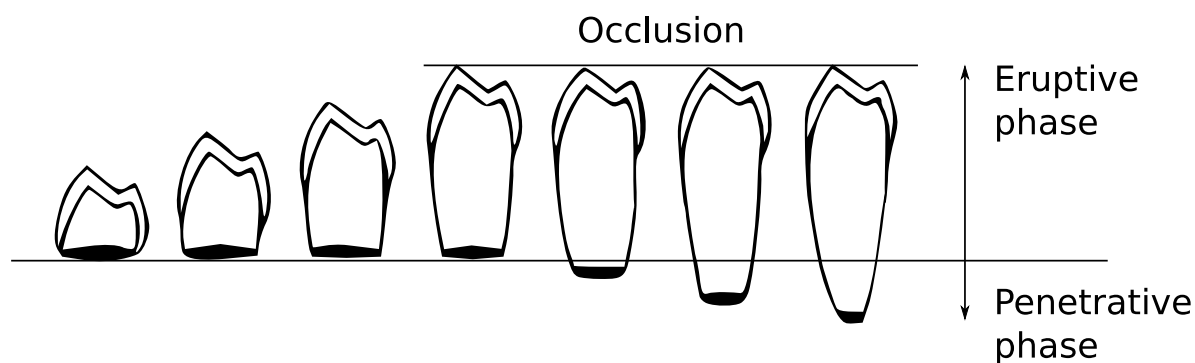


Figure 2.2: Eruptive and Penetrative phases of tooth root development. Figure modified from Kovacs (1971).

### 2.2.1 The eruptive and penetrative phases

Upon completion of the tooth crown the cervical loop forms a double layer of cells known as Hertwig's epithelial root sheath (HERS). It is the HERS that determines length, curvature, thickness, and number of roots. HERS extends around the dental papilla covering all but the basal portion where it forms an epithelial diaphragm over the apical foramen of the developing root. As the dental papilla expands the HERS encases it and to form the architecture of the root. Inside the root sheath, ameloblasts induce odontoblasts in the dental papilla to form dentin, which forms the bulk of the root. Simultaneously, mesenchymal cells in the dental papilla differentiate into cementoblasts and secrete cementoid to the external surface of the root sheath. The secreted cementoid gradually matures into a smooth, calcified cementum. During this process the epithelial diaphragm remains in a stationary position relative to the inferior and superior border of the mandible

and maxilla respectively. Thus, the root sheath is not actually growing *into* the jaw but *away* from it. Once the tooth is in occlusion the epithelial diaphragm no longer remains stationary. Instead, it begins to extend towards the base of the alveolar socket and the apices of the root begin to close.

### 2.2.2 Teeth with more than one root



Figure 2.3: Apical view of formation of (A) single and (B) multiple roots. Arrows indicate location of interradicular process formation and extension. Illustration from Ten Cate's Oral Histology, 8<sup>th</sup> Edition (Miller, 2013).

As in single rooted teeth, multi-rooted teeth have eruptive and penetrative phases, and extension of HERS, dentin and cementum formation all follow the same basic developmental and physiological processes. During the eruptive phase, as the epithelial diaphragm begins narrowing, 'tongue like' extensions caused by differential growth rates in the HERS begin to divide the primary apical foramen (Figure 2.3). As these extensions of the epithelial diaphragm contact opposing epithelial extensions, they fuse and divide the epithelial diaphragm into two or three new openings. These sub-divisions of the primary apical foramen are called inter-radicular processes. The epithelial diaphragm surrounding the opening to each root continues to form at an equal rate of growth. Deviations in the process lead to variations in root morphology (e.g., Taurodontism, supernumerary roots, and pyramidal-shaped roots). The rate at which HERS narrows also determines the length of the root – if HERS narrows rapidly, the root will be shorter; if HERS narrows slowly then the root will be longer.

## 2.3 Developmental basis of root variation

The biological basis for tooth root variation stems from developmental changes during root growth (Shields, 2005; Wright, 2007). This variation is established early in the roots' development and is, in part, influenced by the size of the tooth germ. A small increase in tooth germ size will lead to an expansion in cell count and reproduction in the HERS (Shields, 2005). Tooth germ size also effects molecular signalling governing the development of interradicular processes which can lead to differing degrees of fusion and bifurcation (ibid). However, explanations for external tooth root morphology recorded in the literature (see Chapter 3 for a further discussion) are non-existent. Chapter 5 tests the hypothesis that it is canal form and count that predicts external morphology.

Variation in tooth root number is the direct consequence of several growth processes operating during root development. These include: (1) sites on the apical foramen where inter-radicular processes originate; (2) the number and relative degree of development of each root; (3) the timing and appearance of intra-radicular processes; and (4) the timing of the fusion of each intra-radicular process (Kovacs, 1967; Nanci, 2012). The sites on the apical foramen where the inter-radicular processes form determine the location of each tooth root. So, in a tooth with mesial and distal roots, two inter-radicular processes arise from the buccal and lingual borders of the apical foramen, forming mesial and distal secondary apical foramina upon fusion (Nanci, 2012).

## 2.4 Morphogenetic gradients

Teeth have been observed to exist on a gradient in which adjacent teeth are more similar to one another than non-adjacent teeth (Butler, 1937, 1939, 1963). For example, lateral incisors are more similar to central incisors than they are to canines, while molars are more similar to one another than they are to premolars. Butler (ibid) conceptualized these gradients as morphogenetic fields in which different tooth types are determined by where they develop in the jaws. For Dental Anthropology, Dahlberg (1945b) adapted and extended Butler's (1937, 1939) morphogenetic fields of mammalian teeth from three (incisor, canine, and molar) to four fields corresponding to four morphological classes of human teeth: incisors, canines, premolars and molars. Dahlberg (1945b) assigned each field a 'key' tooth — the most mesial member of each field, with exception of the mandibular central incisor

— which he deemed the most developmentally and evolutionary stable tooth in terms of size, numerical variation (e.g., root or cusp number), and/or morphological variation.

Several theories have been proposed to explain patterns of morphological gradients in tooth rows: including morphogenetic field theory (Butler, 1937, 1939, 1956), the clone model (Osborn, 1978), the odontogenetic homeobox code model (McCollum and Sharpe, 2001), cooperative genetic interaction (Mitsiadis and Smith, 2006), and the inhibitory cascade model (Kavanagh et al., 2007). Though consensus has not been reached, Mitsiadis and Smith's (2006) cooperative genetic interaction model provides a synthesis of the molecular processes underlying patterned morphogenetic fields so far. Briefly, the differential expression of homeobox genes — clusters of regulatory genes that are spatially and temporally expressed during regulatory development (Gehring, 1993) — within the ectomesenchyme (Section 2.1 & Figure 2.1) leads to variation in the number, shape and size of teeth via modulation of signalling molecules. While the majority of this work has focused on development and patterning of tooth crowns, there is expected carry over to tooth roots due to shared developmental process. However, for reasons discussed below (Section 2.5), the genomic pathways of tooth root development are poorly understood.

For Dental Anthropology, Dahlberg (1945b) adapted and extended Butler's (1937, 1939) morphogenetic fields of mammalian teeth from three (incisor, canine, and molar) to four fields corresponding to four morphological classes of human teeth: incisors, canines, premolars and molars. Dahlberg (ibid) assigned each field a 'key' tooth — the most mesial member of each field, with exception of the mandibular central incisor — which he deemed the most developmentally and evolutionary stable tooth in terms of size, numerical variation (e.g., root or cusp number), and/or morphological variation.

## 2.5 Genetic/sex chromosomal influences

While the developmental order and concomitant molecular processes of tooth development are well understood (Kovacs, 1971; Wright, 2007; Miller, 2013; Li et al., 2017), the specific molecular process that initiates and controls the rate of growth in HERS, and consequent root and canal number, and form are unknown (Huang and Chai, 2013). Various genes have been proposed as targets for study (Table 2.1). However, due to the 'entwined' nature of multiple genes to one another and to growth and development, and the reciprocal

nature of cell interactions in tooth root development, there exists little in the way of linking individual genes to tooth root shape and form.

Table 2.1: Genes expressed in varying structures during tooth root development\*

Gene	Dental epithelium	Dental papilla	Dental follicle	Cementoblast
<i>Tgf-beta1</i>	+			
<i>Bmp2</i>	+	+	+	
<i>Bmp3</i>		+		+
<i>Bmp4</i>	+	+		
<i>Bmp7</i>	+	+		+
<i>Egf</i>			+	
<i>Egfr</i>	+			
<i>Fgf1</i>	+			
<i>Fgf2</i>	+			
<i>Fgfr1</i>	+			
<i>Fgfr2</i>	+			
<i>Notch1</i>	+			
<i>Notch2</i>	+			
<i>Notch3</i>	+			
<i>Shh</i>	+			
<i>Ctgf</i>	+		+	
<i>Timp1</i>		+		
<i>Timp2</i>	+			
<i>Timp3</i>	+			
<i>IGF</i>	+			
<i>HGF</i>	+			
<i>Msx1</i>		+	+	
<i>Msx2</i>	+	+	+	+
<i>Runx2</i>		+		
<i>Nfic</i>		+		
<i>Smad4</i>	+	+	+	+

**BMP** = bone morphogenetic protein; **FGF** = fibroblast growth factor; **HGF** = hepatocyte growth factor; **IGF** = insulin-like growth factor; **Nfic** = nuclear factor I $\alpha$ ; **Shh** = Sonic hedgehog. + = gene expression. \*Table modified from Huang and Chai (2013).

It has been suggested that chromosomal aneuploidy can affect the mitotic cell growth cycle of teeth. Rao et al. (1997) report that deletions of a homeobox gene within the pseudoautosomal regions of X and Y-chromosomes result in short or underdeveloped teeth and roots for those with Turner syndrome (45, X females). Individuals with Klinefelter's syndrome, a condition in which males have an extra chromosome, exhibit retardation of skeletal maturation including tooth development (Tanner et al. 1959). Taurodontism has also been linked with Klinefelter's syndrome (Wright, 2007; Giambersio et al., 2019), where

males (47, XXY) show larger tooth crowns than typical males (46, XY). However, differences in root size and morphology due to chromosomal abnormalities may have different aetiologies than those governing typical development. Unfortunately, the literature is silent on this.

## 2.6 Environmental influences on tooth root development

While the selective pressures on, and the adaptive nature of tooth crowns has been well explored (Hylander, 1975; Kay, 1975; Macho and Spears, 1999; Dempsey and Townsend, 2001), studies of tooth root function and evolution are largely absent from the literature. In an adaptive context, the common assumption has long been that tooth root surface area linearly increases from  $P^3s/P_{3s}$  to  $M^3s/M_{3s}$ , concomitant with increases in bite force magnitudes (Du Brul, 1977; Ward and Molnar, 1980; Bouvier, 1986; Spears and Macho, 1998; Macho and Spears, 1999). However, recent work has shown that for several species of primates, including humans, tooth root surface area is relatively similar in premolars, increases in first molars, and decreases posteriorly (Spencer, 2003; Ledogar et al., 2016; Kupczik et al., 2018). Thus, for humans, bite-force magnitude is highest at  $M^1s/M_{1s}$ , and lowest at  $M^3s/M_{3s}$ . The emerging consensus is that tooth root surface area is responsive to selection based on differences in masticatory loading; but that differences in diet and chewing mechanics produce different patterns of increasing and decreasing tooth root surface along the tooth row. Unfortunately, the adaptive and/or selective role of tooth root morphology (e.g., round, plate-like, etc.) is unknown.

The impact of masticatory forces on tooth root orientation and splay have elucidated some aspects of the effect of diet on morphology of the total root complex. When chewing, the highest bite forces are generated when force vectors are aligned parallel with the long axis of the tooth and root(s) (Baragar and Osborn, 1987). This explains the switch from anteriorly to posteriorly oriented roots in modern humans, as force vectors stemming from orofacial geometry and orientation of the masticatory muscles mirror this orientation (Dempster et al., 1963; Holly Smith, 1986). The impact of masticatory forces on tooth root splay also explain the difference between three rooted maxillary molars which are subjected to increased medio-lateral loads (Macho and Spears, 1999), and two rooted mandibular molars which must resist chewing forces to their inter-cuspal regions (Spears and Macho,

1998). A recent study of Great Apes and South African hominins attributes changes in root splay to dietary preferences (Kupczik et al., 2018), but to date there are no studies linking environmental influence to external root morphology.

## Chapter 3: Materials and Methods

### 3.1 Human samples

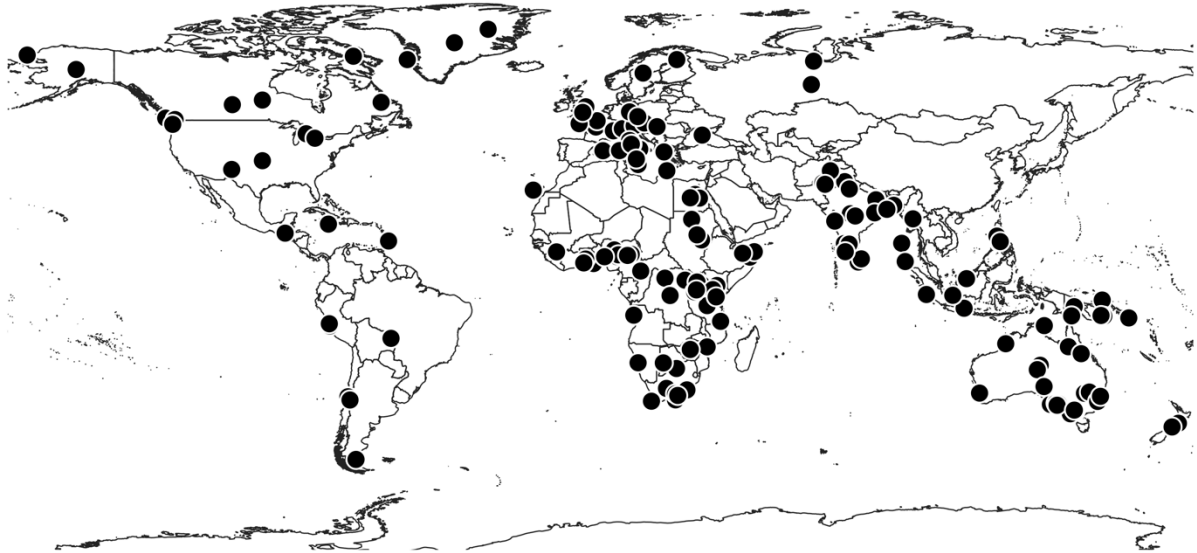


Figure 3.1: Map of archaeological sites for individuals used in this dissertation.

The 945 individuals used in this dissertation were recovered from archaeological sites across the globe (Figure 3.1). These individuals are stored in osteological collections at the Smithsonian National Museum of Natural History, Washington D.C., USA (SI), American Museum of Natural History, New York, USA (AMNH), and the Duckworth Laboratory (DW) at the University of Cambridge Leverhulme Centre for Human Evolutionary Studies, Cambridge, England (summarized in Figure 3.2). Only adult individuals, based on the eruption, occlusion, and closed root apices of  $M^3/M_3$ 's (or  $M^2/M_2$ 's in the case of congenitally absent  $M^3/M_3$ 's), were used in this dissertation.

#### 3.1.1 American Museum of Natural History

The 186 individuals from the AMNH collection are comprised of humans from Point Hope, Alaska, North America (Figure 3.2, right). These individuals are attributed to the Ipiutak (500 BCE – 500 CE) and Tigara (1300-1700 CE) cultures (Rainey, 1941, 1947, 1971; Larsen and Rainey, 1948). Information on sex (Figure 3.3) and antiquity come from the AMNH archives and publications associated with the collection (ibid).

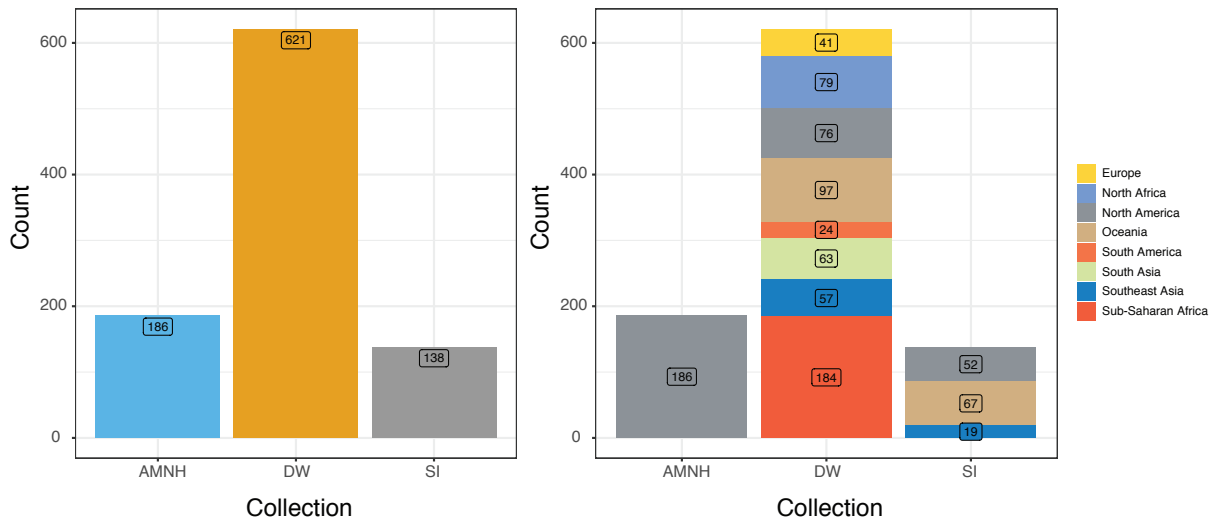


Figure 3.2: Human population sample sizes by collection. **Left:** Bar plot of counts for entire sample ( $n = 945$ ). **Right:** Counts of samples divided up by collection, and geographic locations given by collection records. A complete list of the individuals used in this study, their collection information, antiquity, sex, and locality based on available records is listed in Appendix 9.2.

### 3.1.2 Duckworth Laboratory

The majority of individuals ( $n = 621$ ) used in this dissertation come from the DW Laboratory collections. The DW is comprised of several private collections as well as research collections from the University of Cambridge Departments of Zoology, Anatomy, and Museum of Archaeology and Anatomy (Mirazón-Lahr, 2011). The oldest individuals studied in this dissertation come from the archaeological sites of Badari, Egypt (4000-3200 BCE), Jebel Moya, Sudan (100 BCE-500 CE) and Ngada, Egypt (4400-4000 BCE), in North-East Africa. The majority of the remaining individuals are  $\sim 200$  years old. In many cases information on exact locality, age, and age of death, is unavailable. Information on sex (Figure 3.3) comes from DW archives. A complete list of the DW individuals used in this study, their collection information, antiquity, sex, and locality based on available records is listed in Appendix 9.2.

### 3.1.3 Smithsonian National Museum of Natural History

The 138 individuals from the SI collection are from Oceania, Southeast Asia, and Greenland. Individuals from Oceania belong ( $n = 67$ ) to four different populations: Australia (Aboriginal), New Zealand (Maori), the Philippines, and Papua New Guinea. Individuals from Southeast Asia ( $n = 19$ ) are from Indonesia. Inuit individuals comes from the North-West coast of Greenland ( $n = 52$ ). While all SI individuals were recovered from archaeological

sites, information on exact locality, age, and age of death, is unavailable. However, information on sex was provided by collections management at the SI (Figure 3.3).

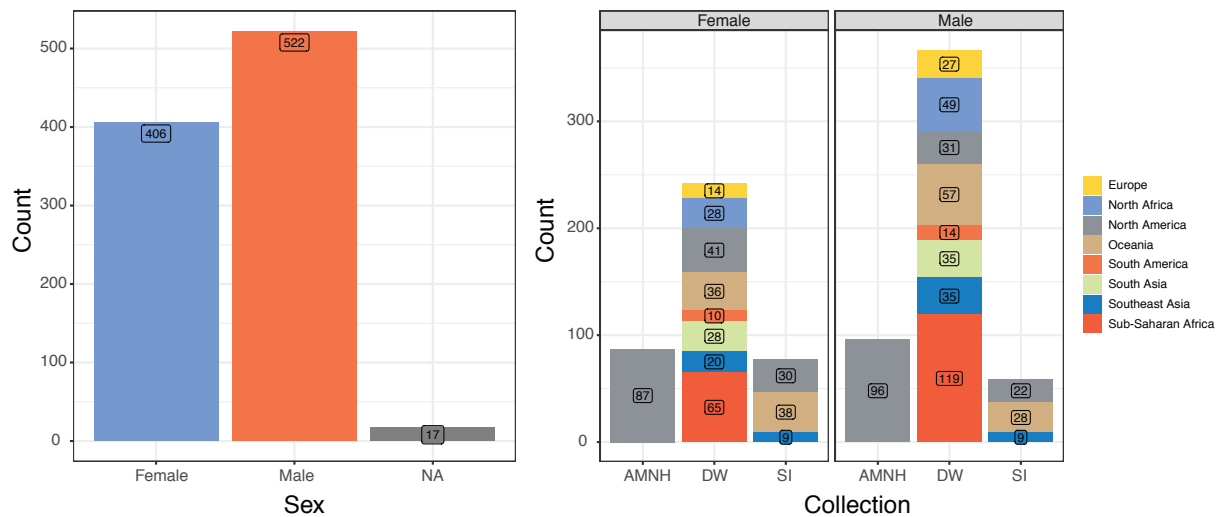


Figure 3.3: Human population sample sizes by location and sex. **Left:** Bar plot of sex for entire sample (n = 945). **Right:** Sex divided up by collection and geographic locations given by collection records. Individuals of undetermined sex ('NA') are not included in the plot on the right to improve readability. They are: AMNH (NA = 3), DW (NA = 12), and SI (NA = 2). A complete list of the individuals used in this study, their collection information, antiquity, sex, and locality based on available records is listed in Appendix 9.2.

The populations studied in this dissertation have been, at their broadest level, grouped into five major human populations: Sub-Saharan Africa, West-Eurasia, Sahul-Pacific, Sunda-Pacific, and Sino-Americas (Table 3.1 & Figure 3.4).

Table 3.1: Sample populations used in this dissertation

Populations*	Male	Female	Unknown	Total
Sahul-Pacific	84	74	9	167
Sunda-Pacific	42	28	3	73
Sub-Saharan Africa	119	65	-	184
West Eurasia	111	70	2	183
Sino-Americas	163	168	7	338
Total	519	405	21	945

These groupings are derived from two major works. The first is Cavalli-Sforza's *The History and Geography of Human Genes* (1994), a synthesis of global genetics with nearly half a century's worth of geographical, ecological, linguistic, archaeological, and paleoanthropological research. Among the author's many conclusions are that all available evidence points to 1) an African origin for *H. sapiens*; and 2) the fact that a series of dispersal and admixture events can classify and map where major human populations (as

listed above) and their subsequent subdivisions originated and dispersed through the ancient world. The volume (1994:317) also recognises that dental data “on northern Asia, southeast Asia, and the Americas are generally in excellent agreement with those from single genes.” The dental data they refer to are crown and root trait frequencies collected and analysed by Christy Turner (Busse and Carpenter, 1976; Nichol et al., 1984; Turner, 1987; Turner II, 1989). These data, along with later core collected works on dental crown traits and biogeography utilising the ASUDAS (Scott, 1988; Turner II et al., 1991; Stringer et al., 1997; Irish, 1998; Hanihara, 2013; Scott et al., 2018), form the second basis for major human geographical subdivisions presented here. These researchers (ibid) have shown that teeth are effective for identifying the same prehistoric population identities and movements discussed by Cavalli-Sforza (1994), as well as capturing the phenotypic diversity within populations, and the differences that arise between them after extended periods of isolation. The most current collections of dental anthropological research (Rathmann et al., 2017; Scott et al., 2018; Rathmann and Reyes-Centeno, 2020) are increasingly in accordance with the most recent genomic studies (Pickrell and Reich, 2014; Fu et al., 2016; Skoglund et al., 2016; Rathmann et al., 2017; Posth et al., 2018; Reich, 2018), further reinforcing the utility of teeth as phenotypic records of human biogeography and evolutionary history.

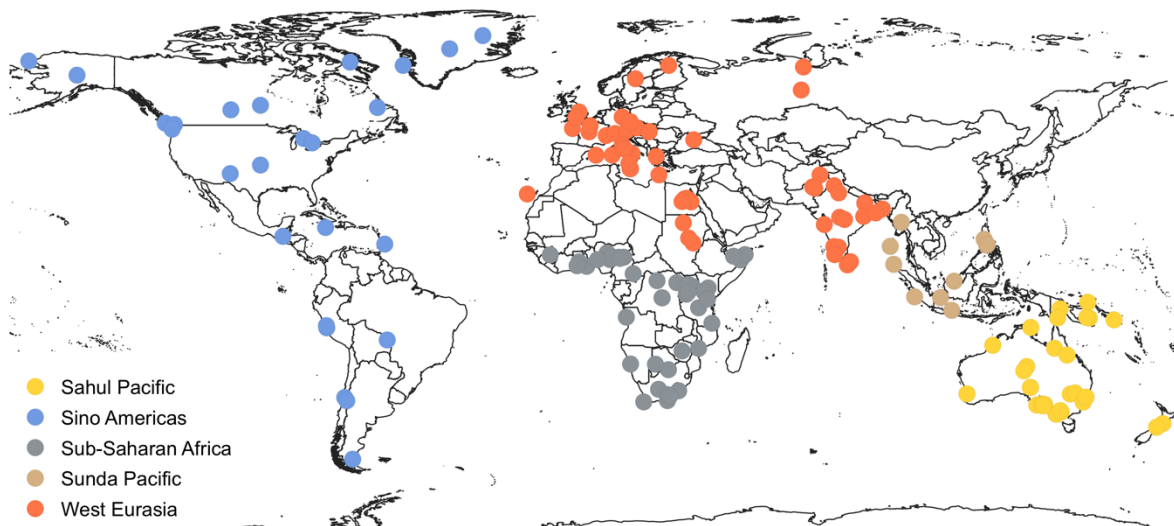


Figure 3.4: Map of archaeological sites for individuals used in this dissertation adapted to show the five major human subdivisions.

## 3.2 Dental formula and anatomical terms

### 3.2.1 Dental formula

There exist several formulae for differentiating the dentition. I have opted for one common to the anthropological and clinical literature. Categorically, incisors are indicated by an I, canines a C, premolars with P, and molars with M. Tooth numbers are labelled with super- and subscripts to differentiate the teeth of the maxilla and mandible respectively. For example,  $M^1$  indicates the 1st maxillary molar while  $M_1$  indicates the 1st mandibular molar. Numerically, incisors are numbered either 1 or 2 for central and lateral incisors respectively. Canines are marked 1 as there exists only one canine in each quadrant of the jaws. Through the course of evolution, apes and old world monkeys have lost the first and second premolars of their evolutionary ancestors (Novacek, 1986; White et al., 2012), thus the remaining 2 premolars are numbered 3 and 4.

### 3.2.2 Anatomical terms

Unlike the anatomical surfaces and directions used for tooth crowns, there exists no formula for tooth roots. In this dissertation, classical anatomical terms applied to tooth crown surfaces – mesial, buccal, distal, lingual, or combinations of (e.g., mesio-buccal) – are used to label the location of roots and canals and their features (Figure 3.5, A & B). Labelling order begins with mesial (M), followed by buccal (B), distal (D), and then lingual (L). Additionally, the term axial (A) is used to describe a single root, or a centrally located canal within a single-rooted tooth. Intermediate locations combine adjacent anatomical locations (e.g., mesio-buccal becomes MB). Fused roots are appended with an 'F'. For example, fused mesial and lingual roots are labelled MLF. Because anatomical location rather than anatomical surface is being employed, buccal (B) replaces labial for anterior teeth when describing roots.

This labelling system extends to features of the roots, such as canal number or external morphology (Figure 3.5 C). For example, a root with two canals in the mesial root and one in the distal root, would be labelled M2D1. The terms and abbreviations for external and internal root morphologies are further discussed below, and the application of

the labelling system is expanded upon in Chapter 6, which describes a novel tooth root phenotyping system. In this chapter it is used for descriptive purposes.

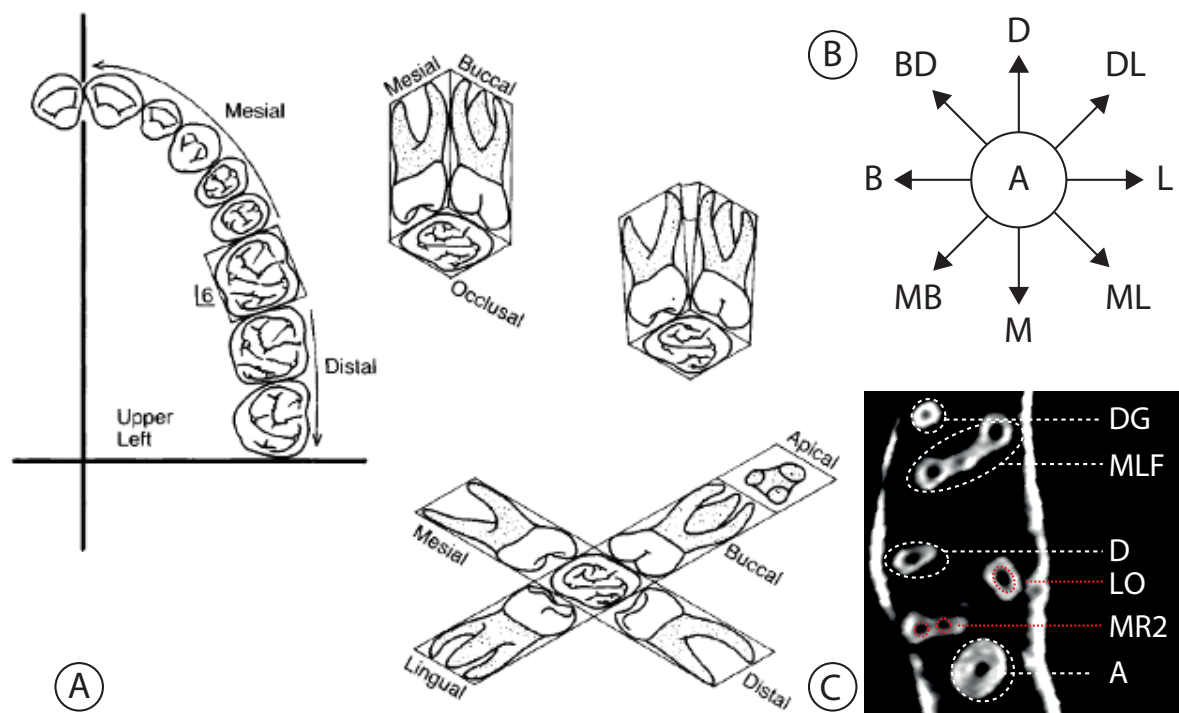


Figure 3.5: **A:** Anatomical surfaces and directions. From Hillson (1996, p10). **B:** Directional labels of classical anatomical terms and their intermediate locations (M = Mesial, B = Buccal, D = Distal, L = Lingual, MB = Mesio-buccal, BD = Bucco-distal, DL = Disto-lingual, ML = Mesio-lingual). **C:** Labelling of root and root features using anatomical surfaces and directions. A = axial, MR2 = a mesial root with two round canals, LO = a lingual root with a single oval canal, MLF = a mesio-lingual fused root, DG = distal globular shaped root.

### 3.3 Computed tomography

#### 3.3.1 Use of cone beam computed tomography for visualizing internal and external features of tooth roots

In clinical settings (e.g., dental, hospital, etc.), cone beam computed tomography (CBCT) is widely utilized to visualize internal and external structures of the crown and root(s) (see Martins and Versiani (2018) for an in-depth discussion of this topic). An important parameter supporting reliability of visualization for the study of root and canal anatomy is voxel size. In 3D medical imaging a single voxel is a cubic representation of a single value of space within a cubic volume. For example, a hypothetical 300x300x300 cubic volume would have 27,000,000 voxels. Thus, the lower the voxel size relative to the volume of 3D CBCT, the greater the resolution. Compared to micro-CT ( $\mu$ CT) which operates on the micron scale (a thousandth of a millimetre) for increased resolution, CBCT uses larger voxel sizes at the

millimetre scale which results in a relatively decreased resolution. However, CBCT has been proven to be reliable for detecting root canal number and morphology in specific teeth or individual roots (Blattner et al., 2010; Michetti et al., 2010; Domark et al., 2013; Pécora et al., 2013). Maret et al. (2014) compared in vitro CBCT images of different voxel sizes (76, 200, and 300  $\mu\text{m}$ ) with  $\mu\text{CT}$  (41  $\mu\text{m}$ ) and observed discrepancies of hard tissue morphology (i.e. cervical margins, cusp tips, incisal edges) were only significant at 300 $\mu\text{m}$  ( $P = .01$ , Wilcoxon test). These studies (additionally, see Martins and Versiani (2018) for an extensive overview of CBCT and  $\mu\text{CT}$  on root canal anatomy by tooth) have shown that CBCT can clearly and accurately detect structures such as root number, canal number, and configuration of the main root canal systems (Figure 3.6).

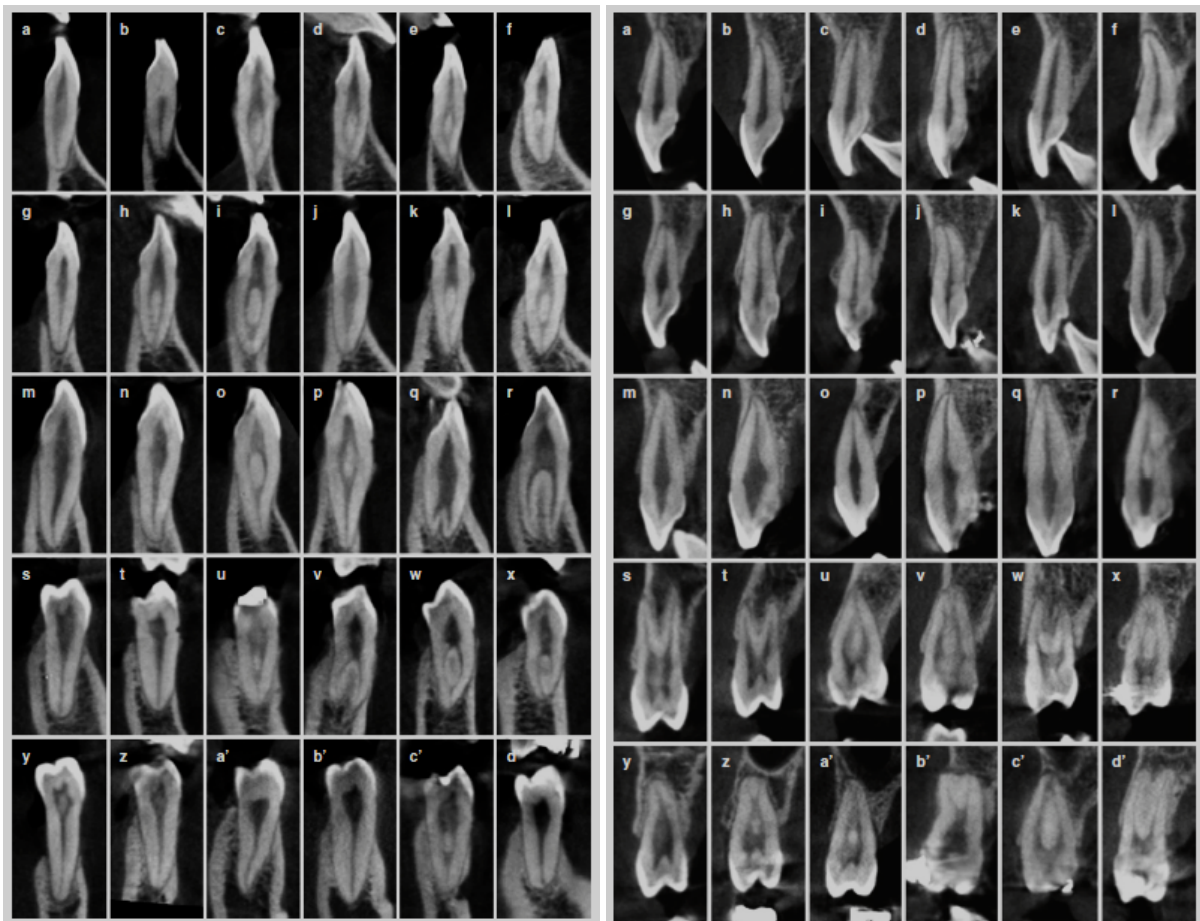


Figure 3.6: Representative CBCT images of different canal system configurations on maxillary (left) and mandibular (right) teeth. (a–f) Central incisors, (g–l) lateral incisors, (m–r) canines, (s–x) first premolars, and (y–d') second premolars.

### 3.3.2 Imaging of osteological collections used in this dissertation

Using cone-beam computed tomography (CBCT, here shortened to CT), we analysed teeth from the right sides of the maxillary and mandibular dental arcades of individuals ( $n=945$ ) from osteological collections housed at the Smithsonian National Museum of Natural History (SI), American Museum of Natural History (AMNH), and the Duckworth Laboratory (DW) at the University of Cambridge (Table 3.1, Appendix 9.2). Full skulls from the SI and AMNH were scanned by Dr. Lynn Copes (2012) using a Siemens Somatom spiral scanner (70  $\mu\text{A}$ , 110 kV, slice thickness 1.0 mm, reconstruction 0.5 mm, voxel size  $\text{mm}^3$ :  $1.0 \times 1.0 \times 0.3676$ ). Full skulls of specimens from the DW were scanned by Professor Marta Mirazón-Lahr and Dr. Frances Rivera (Rivera and Mirazón Lahr, 2017) using a Siemens Somatom Definition Flash scanner at Addenbrooke's Hospital, Cambridge England (80  $\mu\text{A}$ , 120kV, slice thickness 0.6mm, voxel size  $\text{mm}^3$ :  $0.3906 \times 0.3906 \times 0.3$ ). For all collections, crania and mandibles were oriented on the rotation stage, with the coronal plane orthogonal to the x-ray source and detector. Permission to use the scans has been granted by Dr. Copes, Professor Mirazón-Lahr, and Dr. Rivera.

### 3.3.3 Analysis of CT images

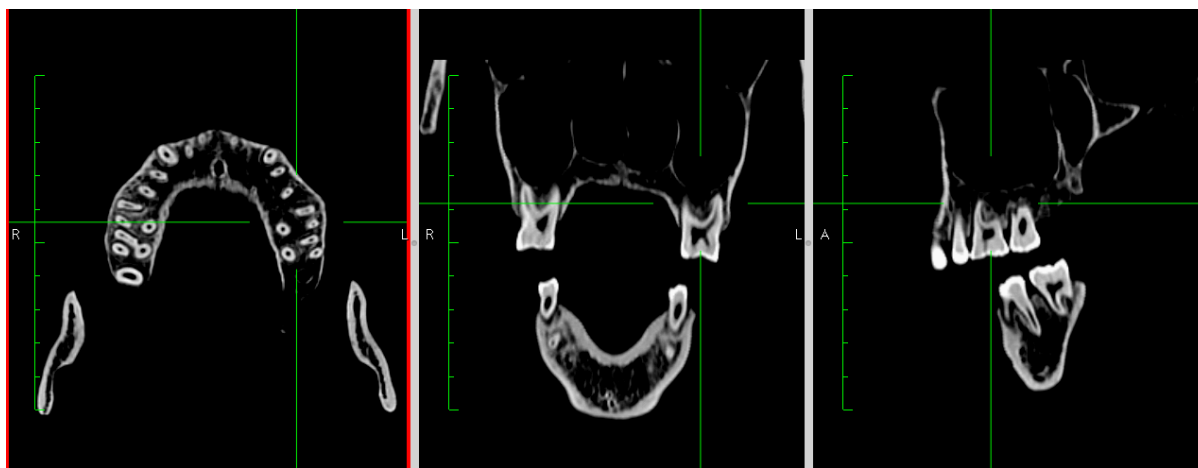


Figure 3.7: Horos Dicom Viewer 2D orthogonal view used to assess root and canal morphologies. Left: Coronal view at mid-point of roots. Centre: Anterior view at midpoint of roots. Right: Lateral view at midpoint of roots.

Transverse CT cross sections of roots and canals from 5,970 teeth (Table 3.2) were assessed in the coronal, axial, and sagittal planes across the CT stack, using measurement tools in the Horos Project Dicom Viewer (Figure 3.7) version 3.5.5 (<https://www.horosproject.org>, 2016). While information for all teeth from both sides of

the maxillary and mandibular arcades was recorded, only the right sides were analysed in subsequent chapters to avoid issues with asymmetry and artificially inflated sample size. Only permanent teeth with completely developed roots were used for this dissertation.

Table 3.2: Tooth counts of the right side of the maxillary and mandibular dental arcades.

Tooth	n	Tooth	n	Total
<b>Maxilla</b>		<b>Mandible</b>		
I <sup>1</sup>	204	I <sub>1</sub>	204	408
I <sup>2</sup>	248	I <sub>2</sub>	247	495
I <sup>2</sup> CON	1	I <sup>2</sup> CON	1	-
C <sup>1</sup>	406	C <sub>1</sub>	295	701
P <sup>3</sup>	515	P <sub>3</sub>	343	858
P <sup>4</sup>	467	P <sub>4</sub>	313	780
M <sup>1</sup>	697	M <sub>1</sub>	410	1,107
M <sup>2</sup>	596	M <sub>2</sub>	385	981
M <sup>3</sup>	362	M <sub>3</sub>	278	640
M <sup>3</sup> CON	28	M <sup>3</sup> CON	25	-
Total	<b>3,495</b>	-	<b>2,475</b>	<b>5,970</b>

**Superscript** = maxilla, **subscript** = mandible. **I** = incisor, **C** = canine, **P** = premolar, **M** = molar. **CON** = congenitally absent teeth.

Root and canal number are determined by applying the Turner Index (1991), which compares the point of bifurcation relative to total root or canal length, as measured in Horos Dicom Viewer from the cemento-enamel junction (CEJ) to the root apex/canal apical foramen (Figure 3.8). When this ratio is greater than one-third (33%) of the total root or canal length, the root or canal is classified as multi-rooted. When the ratio is less than one-third (33%) the root or canal is considered single rooted, or with a bifid apical third. Individual root/canal number for analysis is recorded as a simple numerical count (e.g., 1,2,3, etc.). Using measurement tools in Horos Dicom Viewer, the midpoint of the root was measured halfway between the CEJ and the apices of the root/s (Figure 3.8). It is by these methods that data were acquired for the analyses described and carried out through this dissertation.

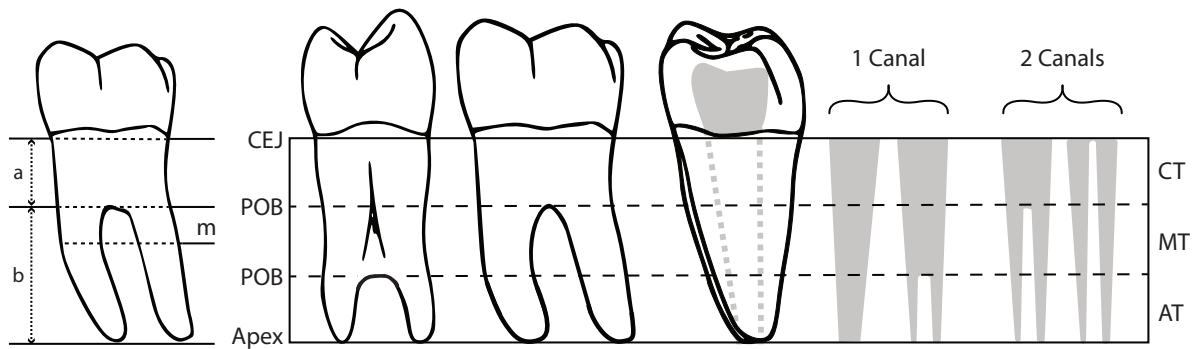


Figure 3.8: **Left:** Locations of measurements taken in Horos Dicom Viewer of (a) CEJ to point of bifurcation, (b) point of bifurcation to root apices, (m) mid-point between CEJ and root apices. **Right:** Determination of root and canal number. Distal view of single-rooted premolar with bifurcation of the apical third of the root. Lingual view of double-rooted mandibular molar. Distal root of double-rooted mandibular molar with examples of canal counts in solid grey. Dotted grey lines indicate canal/s position in root. CEJ = Cemento-enamel junction, POB = Point of bifurcation, Solid grey = canals. CT = cervical third, MT = middle third, AT = apical third.

### 3.4 Root and canal traits

#### 3.4.1 Root number

Root number has been shown to be variable in modern humans and extinct hominins (Carlsen and Alexandersen, 1991; Shields, 2005; Orhan and Sari, 2006; Emonet and Kullmer, 2014; Scott and Irish, 2017; Irish et al., 2018). In aggregate, the number of roots in teeth from the collected sample are between one and four (Table 3.3). Anterior teeth almost always having a single root, the exception being two double-rooted mandibular canines, premolars between one and three roots, and molars between one and four roots. Entomolaris (En) - three-rooted mandibular molars in which the third root extends from the disto-lingual side of the tooth, appear in 18.05 % M<sub>1s</sub>, 1.23% of M<sub>2s</sub>, and 5.94% of M<sub>3s</sub>. Paramolaris (Pa) - three-rooted mandibular molars in which the third root extends from the disto-buccal side of the tooth, appear in 3.63% of M<sub>3s</sub>.

Table 3.3: Number of roots in teeth of the right side of the maxilla and mandible by tooth

Tooth	Root number	n	Total Roots	% of teeth*	Tooth	Root number	n	Total Roots	% of teeth*
<b>Maxilla</b>					<b>Mandible</b>				
I <sup>1</sup>	1	204	204	100.00	I <sub>1</sub>	1	204	204	100.00
I <sup>2</sup>	1	248	248	100.00	I <sub>2</sub>	1	247	247	100.00
C <sup>1</sup>	1	406	406	100.00	C <sub>1</sub>	1	293	297	99.32
						2	2		0.68
P <sup>3</sup>	1	295	739	57.28	P <sub>3</sub>	1	341	345	99.42
	2	216		41.94		2	2		0.58
	3	4		0.78					

<b>P<sup>4</sup></b>	1	405	530	86.72	<b>P<sub>4</sub></b>	1	313	313	100.0
	2	61		13.06					
	3	1		0.22					
<b>M<sup>1</sup></b>	1	2	2,060	0.29	<b>M<sub>1</sub></b>	2	336	894	81.95
	2	28		4.02		3En	74		18.05
	3	666		95.55					
	4	1		0.14					
<b>M<sup>2</sup></b>	1	56	1,561	9.39	<b>M<sub>2</sub></b>	1	49	727	12.73
	2	117		19.63		2	330		85.71
	3	421		70.64		3	1		0.26
	4	2		0.34		3En	5		1.30
<b>M<sup>3</sup></b>	1	89	831	24.59	<b>M<sub>3</sub></b>	1	20	563	7.19
	2	82		22.65		2	231		83.09
	3	186		51.38		3En	16		5.76
	4	5		1.38		3Pa	11		3.96

\* From Table 3.2. Congenitally absent teeth not included in statistics for this table.

En = Entomolaris, Pa = Paramolaris.

### 3.4.2 Canal number

Canal number is highly variable, especially in post canine teeth; and several studies have shown that canal number is not always concomitant with root number (Peiris et al., 2015; Ahmed and Hashem, 2016; Versiani et al., 2019). However, canal number and its relationship to root number is neglected in the literature. Teeth from this sample contain between one and six canals (Table 3.4), and it is not uncommon for a single root to contain two or more canals, especially in the molars. With the exception of I<sup>1</sup>, all single rooted anterior teeth have a double canaled variant. Molars have the most canals per tooth, with M<sup>1</sup>s showing the most variation in canal number. With the exception of I<sup>1</sup>, canal number frequently exceeds root number (Table 3.4).

Table 3.4: Number of canals per tooth in the right side of the maxilla and mandible by tooth

Tooth	Canal number	n	Total Canals	% of teeth*	Tooth	Canal number	n	Total Canals	% of teeth*
	<b>Maxilla</b>					<b>Mandible</b>			
<b>I<sup>1</sup></b>	1	204	204	100.00	<b>I<sub>1</sub></b>	1	180	228	88.24
						2	24		11.76
<b>I<sup>2</sup></b>	1	247	249	99.60	<b>I<sub>2</sub></b>	1	208	286	84.21
	2	1		0.40		2	39		15.79
<b>C<sup>1</sup></b>	1	405	407	99.75	<b>C<sub>1</sub></b>	1	273	317	92.54
	2	1		0.25		2	22		7.46
<b>P<sup>3</sup></b>	1	82	959	15.92	<b>P<sub>3</sub></b>	1	254	435	74.05
	2	422		81.94		2	86		25.07

<b>P<sup>4</sup></b>	3	11		2.14	<b>P<sub>4</sub></b>	3	3		0.87
	1	233	708	49.89		1	300	326	95.85
	2	228		48.82		2	13		4.15
	3	5		1.07					
<b>M<sup>1</sup></b>	4	1		0.22	<b>M<sub>1</sub></b>	2	27	1,431	6.59
	2	4	2,431	0.57		3	167		40.73
	3	355		50.93		4	205		50.00
	4	333		47.78		5	10		2.44
<b>M<sup>2</sup></b>	5	4		0.57	<b>M<sub>2</sub></b>	6	1		0.24
	6	1		0.14		1	2	1,107	0.52
	1	8	1,910	1.34		2	93		24.16
	2	21		3.52		3	241		62.60
<b>M<sup>3</sup></b>	3	408		68.46	<b>M<sub>3</sub></b>	4	49		12.73
	4	159		26.68		1	10	748	3.60
	1	32	1,065	8.84		2	86		30.94
	2	24		6.63		3	162		58.27
	3	239		66.02					
	4	67		18.51					
						4	20		7.19

\* From Table 3.2. Congenitally absent teeth not included in statistics for this table.

### 3.4.3 Root and canal orientation

The orientation of roots in the tooth root complex is relatively unexplored in the literature. However, the orientation of these structures have been shown to relate to dietary and phylogenetic differences (Wood et al., 1988; Moore et al., 2015; Kupczik et al., 2018). The majority of teeth follow a similar pattern of having axially (A) oriented, buccal (B) and lingually (L) oriented, or mesially (M), distally (D), and lingually (L) oriented canals and roots (Table 3.5). Other orientations, for example MB1DB1ML1DL1R, are relatively rare, and only appear in molars. In cases where there are multiple canals appear in a single root these are almost always found in the mesial or buccal orientations (e.g., M2D1L1, B2L1).

Table 3.5: Anatomical orientation of canals in the right side of the maxilla and mandible by tooth

Tooth	Orientation	n	% of teeth*	Tooth	Orientation	n	% of teeth*
	<b>Maxilla</b>				<b>Mandible</b>		
<b>I<sup>1</sup></b>	A	204	100.00	<b>I<sub>1</sub></b>	A	180	88.24
					B1L1	24	11.76
<b>I<sup>2</sup></b>	A	247	99.60	<b>I<sub>2</sub></b>	A	208	84.21
	B1L1	1	0.40		B1L1	39	15.79
<b>C<sup>1</sup></b>	A	405	99.75	<b>C<sub>1</sub></b>	A	273	92.54
	B1L1	1	0.25		B1L1	22	7.46

<b>P<sup>3</sup></b>	A	82	15.92	<b>P<sub>3</sub></b>	A	254	74.05
	B1L1	421	81.75		B1L1	86	25.07
	B1L2	1	0.19		M1D1L1	3	0.87
	B2L1	6	1.17				
	M1D1	1	0.19				
	M1D1L1	4	0.78				
<b>P<sup>4</sup></b>	A	233	49.89	<b>P<sub>4</sub></b>	A	300	95.85
	B1L1	228	48.82		B1L1	13	4.15
	B2L1	3	0.65				
	B2L2	1	0.21				
	M1D1L1	2	0.43				
<b>M<sup>1</sup></b>	B1L1	3	0.43	<b>M<sub>1</sub></b>	M1D1	27	6.59
	M1D1	1	0.14		M1D1L1	12	2.93
	M1D1L1	354	50.80		M2D1	156	38.05
	M1D1L2	2	0.29		M2D1L1	59	14.39
	M1D2	1	0.14		M2D2	144	35.12
	M1D2L1	1	0.14		M2D2L1	3	0.73
	M1L1	1	0.14		M2D3	5	1.22
	M2D1	1	0.14		M3D1	1	0.24
	M2D1L1	327	47.07		M3D2	2	0.49
	M2D1L2	2	0.29		M3D3	1	0.24
	M2D2L1	1	0.14				
	M2D2L2	1	0.14				
	M3D1L1	1	0.14				
	MB1DB1ML1DL1	1	0.14				
	<b>M<sup>2</sup></b>	A	8		1.34	<b>M<sub>2</sub></b>	A
B1L1		20	3.36	B1D1L1	1		
M1B1D1L1		1	0.17	B2L1	2		
M1D1		1	0.17	B2L2	1		
M1D1L1		408	68.46	M1B1D1	7		
M1D2L1		2	0.33	M1D1	93		
M2D1L1		153	25.67	M1D1L1	1		
MB1DB1ML1DL11		2	0.33	M1D2	1		
ML3D1		1	0.17	M2D1	229		
			M2D1L1	4			
			M2D2	42			
			M3D1	2			
<b>M<sup>3</sup></b>	A	32	8.84	<b>M<sub>3</sub></b>	A	10	
	B1L1	17	4.70		B2L1	1	
	B2D1L1	1	0.28		M1B1D1	8	
	M1B1D1L1	2	0.55		M1B2D1	1	
	M1D1	7	1.93		M1D1	84	
	M1D1L1	235	64.92		M1D1L1	9	
	M1D1L2	1	0.28		M2B1D1	2	
	M1D2	3	0.83		M2D1	147	
	M1D2L1	1	0.28		M2D1L1	9	
	M2D1	1	0.28		M2D2	6	
	M2D1L1	45	12.43		M3D1	1	
	M2D2	11	3.04				
	MB1DB1ML1DL1R	5	1.38				
	ML3D1	1	0.28				

\* From Table 3.2. Congenitally absent teeth not included in statistics for this table. **A** = axial, **M** = mesial, **B** = Buccal, **D** = Distal, **L** = Lingual.

### 3.4.4 Root morphology

External root morphology has been described inconsistently in the literature, and the full range of variants, is unknown. External root morphology was assessed at the measured mid-point of the root, bounded by the CEJ and root apices (Figure 3.9). The midpoint was chosen as a point of inspection because (a) the root has extended far enough from the CEJ, and in the case of multi-rooted teeth, from the neighbouring roots to be structurally and developmentally distinct (Miller, 2013); and, (b) it does not reflect the morphological alterations common to the penetrative phase in which the apical third of the root becomes roughened and/or suffers ankylosis and concrescence due to penetration of jaw bones (Kovacs, 1971).

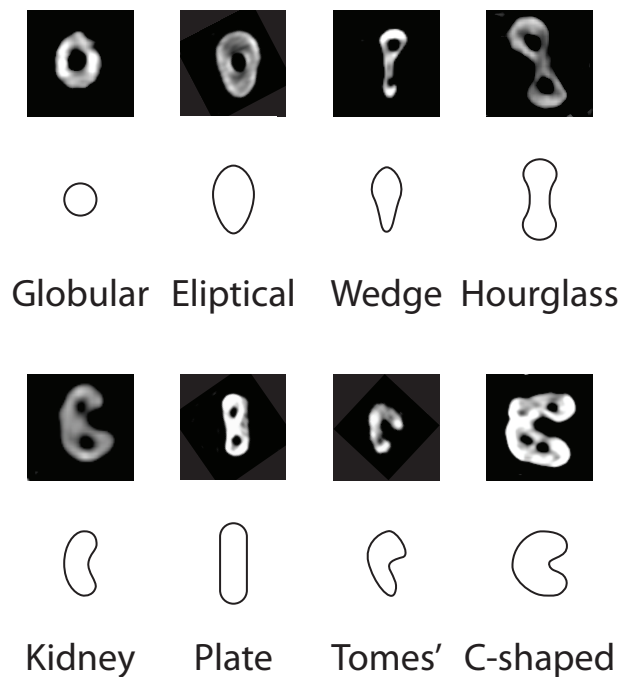


Figure 3.9 : Axial slices of roots at midpoint. Eight morphologies are identified

Some of these rarer morphologies, such as Tomes' and C-shaped roots (Tomes, 1923; Fernandes et al., 2014), are well defined in the literature. Others, such as 'plate-like' and 'dumb-bell' or 'hourglass' are poorly defined, and sometimes used interchangeably (Robinson, 1956; Kullmer et al., 2011; Kupczik et al., 2019). However, these forms are noticeably different (Figure 3.5). Additionally, two new morphologies are identified and described: wedge and kidney shaped. In this dissertation, existing and new morphologies

are clearly described and named (Table 3.6). The descriptions are based on previous studies and the author's analysis of 10,169 roots used in this study.

Table 3.6: Description of external tooth root morphologies at the midpoint

Morphology	Description	Reference
Globular (G)	Round or circular in shape. While this form varies greatly in size, it is relatively invariant in shape in that all edges are relatively equidistant from the centre.	(Nelson and Ash, 2010)
Elliptical (E)	While size, and distance of the edges from the centre vary, elliptical shaped roots are distinct from others in that they look like a squashed circle. Sometimes these forms are perfectly symmetrical and other times they resemble an egg. However, a consistent feature are their continuously smooth edges which are concentric to the canals.	(Kovacs, 1971; Nelson and Ash, 2010; Moore et al., 2013)
Wedge (W)	Wedge shaped roots are easily distinguished by their 'tapered' appearance. Sometimes these forms take the shape of a triangle with three edges and corners, while other times they appear more teardrop shaped with a slight constriction in the middle. One end is always noticeably wider than the other.	<b>This dissertation.</b>
Hourglass (H)	Hourglass shaped roots have often been confused with plate-shaped roots, or occasionally, elliptical roots. However, this form is distinct and easily identified by its bulbous ends and constricted centre. This constriction can be so pronounced that the root appears almost as a lemniscate in cross-section.	<b>This dissertation,</b> but see Robinson, (1956), Kullmer et al., (2011), and Kupczik et al., (2019), for complementary/contradictory definitions.
Kidney (K)	Kidney shaped roots are defined by their opposite convex and concave sides. Sometimes these curvatures are pronounced, and other times they are more subtle. However, these two features are always apparent, and distinct from other forms.	<b>This dissertation.</b>
Plate (P)	Plate shape roots are similar to hourglass and elliptical roots in their dimensions but are easily distinguished by their flat edges. In some variants the corners are rounded, while in others they are square.	<b>This dissertation,</b> but see Robinson, (1956), Kullmer et al., (2011), and Kupczik et al., (2019), for complementary/contradictory definitions.
Tomes' (T)	Tomes' roots have been documented for nearly a century and appear in a number of classification systems including the ASUDAS. They are single rooted teeth that appear to be 'splitting' into two roots. In cross section they sometimes look like c-shaped molar roots. However, one of their distinguishing features is that they are only found in mandibular premolars.	(Tomes, 1923; Turner, 1991)
C-shaped (Cs)	C-shape molar roots are primarily found in the second molars of the mandible, though they rarely appear in the first and third mandibular molars as well. There is a substantial clinical literature covering their distinct morphology and prevalence. Unlike Tomes' roots they do not appear to be splitting into two roots. Rather, they are a single, continuous root structure. Like kidney shaped roots they have opposite convex and concave sides. However, their curvature is more	(Fan et al., 2004a; Fernandes et al., 2014; Gu et al., 2016)

pronounced, in nearly a 180° arc with ends that are parallel to one another.

External root morphologies appear in different frequencies in each tooth, and some morphologies do not appear in some teeth at all (Table 3.7). The number of morphologies increase posteriorly along the tooth row, and M<sub>1</sub>s have the most morphologies. Part of this is due to the number of bifid (Bi) variants (e.g., EBi, PBi, etc.), as well as the presence of pegged and fused roots (Tables 3.8 and 3.9, respectively).

Table 3.7: Counts of external root morphologies in the right side of the maxilla and mandible by tooth

Tooth	External morphology	n	% of roots*	Tooth	External morphology	n	% of roots*
<b>Maxilla</b>				<b>Mandible</b>			
<b>I<sup>1</sup></b>	E	69	33.82	<b>I<sub>1</sub></b>	E	13	6.37
	G	117	57.35		G	1	0.49
	P	8	3.92		K	3	1.47
	W	10	4.91		P	177	86.76
<b>I<sup>2</sup></b>	E	120	48.39	<b>I<sub>2</sub></b>	W	10	4.90
	G	25	10.08		E	7	2.83
	P	97	39.11		H	1	0.40
	W	6	2.42		K	10	4.05
<b>C<sup>1</sup></b>	E	149	36.70	<b>C<sub>1</sub></b>	P	219	88.66
	EBi <sup>†</sup>	1	0.25		W	10	4.05
	G	4	0.99		E	54	18.18
	P	135	33.25		G	6	2.02
	W	117	28.83		H	6	2.02
<b>P<sup>3</sup></b>	E	10	1.35	<b>P<sub>3</sub></b>	K	2	0.67
	G	402	54.40		P	141	47.47
	H	80	10.83		W	87	29.29
	HBi	40	5.41		WBi	1	0.34
	K	38	5.14		E	62	17.97
	KBi	5	0.68		G	14	4.06
	P	143	19.35		H	1	0.29
	PBi	12	1.62		K	3	0.87
W	9	1.22	P	145	42.03		
<b>P<sup>4</sup></b>	E	24	4.53	<b>P<sub>4</sub></b>	T	75	21.74
	G	106	20.00		TBi	8	2.32
	H	70	13.21		W	37	10.72
	HBi	21	3.96		E	122	38.98
	K	31	5.85		G	21	6.71
	KBi	3	0.57		HBi	1	0.32
	P	266	50.19		K	1	0.32
	PBi	4	0.75		P	155	49.52
W	4	0.75	T	9	2.88		
<b>M<sup>1</sup></b>	E	500	24.27	<b>M<sub>1</sub></b>	TBi	1	0.32
					W	3	0.96
				E	20	2.24	

	G	266	12.91		G	76	8.50
	H	11	0.53		H	188	21.03
	K	49	2.38		HBi	61	6.82
	P	668	32.43		K	73	8.17
	PBi	4	0.19		KBi	4	0.45
	W	536	26.02		P	437	48.88
	WBi	2	0.09		PBi	17	1.90
					W	18	2.01
<b>M<sup>2</sup></b>	E	451	28.89	<b>M<sub>2</sub></b>	CS	33	4.54
	G	371	23.76		CSBi	1	0.14
	H	9	0.58		E	33	4.54
	HBi	2	0.13		G	15	2.06
	K	80	5.12		H	143	19.67
	KBi	1	0.06		HBi	17	2.34
	P	262	16.78		K	206	28.34
	W	241	15.43		KBi	4	0.55
					P	256	35.21
					PBi	5	0.69
					W	1	0.14
<b>M<sup>3</sup></b>	E	105	12.64	<b>M<sub>3</sub></b>	CS	6	1.07
	G	338	40.67		E	75	13.32
	H	12	1.44		G	72	12.79
	HBi	5	0.60		H	49	8.70
	K	41	4.93		HBi	4	0.71
	P	115	13.84		K	182	32.33
	PBi	5	0.60		KBi	3	0.53
	W	103	12.39		P	155	27.53
					PBi	2	0.36
					W	4	0.71

\* from Table 3.3, **Bi** = bifid. Congenitally absent teeth not included in statistics for this table.

Pegged (Mi) roots while globular in cross section, are their considered their own distinct morphology as they are a form of microdontia (Daito et al., 1992). They are relatively rare in our sample and only appear in M<sup>3</sup> and M<sub>3</sub> (Table 8).

Table 3.8: Type and number of teeth with pegged roots in the right side of the maxilla and mandible

Tooth	External morphology	n	% of roots*	Tooth	External morphology	n	% of roots*
	<b>Maxilla</b>				<b>Mandible</b>		
<b>M<sup>3</sup></b>	Mi	5	0.60	<b>M<sub>3</sub></b>	Mi	6	1.07

\* from Table 3.3

Fused roots are almost always found in the molars and are more common in the maxillary molars (Table 3.9). In almost all cases fusion includes the mesial (M) root, and it is not uncommon for fused roots to have some degree of bifurcation (Bi).

Table 3.9: Type and counts of roots showing fusion morphologies in the right side of the maxilla and mandible

Tooth	External morphology	n	% of roots*	Tooth	External morphology	n	% of roots*
	<b>Maxilla</b>				<b>Mandible</b>		
<b>P<sup>4</sup></b>	MLFBi	1	0.19	<b>M<sub>2</sub></b>	MDF	13	1.79
<b>M<sup>1</sup></b>	MDF	4	0.19	<b>M<sub>3</sub></b>	MDF	5	0.89
	MLF	1	0.05				
<b>M<sup>2</sup></b>	MLFBi	3	0.15				
	DLF	8	0.39				
	DLFBi	8	0.39				
	BLF	3	0.19				
	DLF	8	0.51				
	DLFBi	2	0.13				
	MDF	12	0.77				
	MDFDLF	4	0.26				
	MDFMLF	2	0.13				
	MDFMLFBi	1	0.06				
	MLF	60	3.84				
	MLFBi	21	1.35				
	MLFBiDLF	1	0.06				
	MLFBiMDF	1	0.06				
	<b>M<sup>3</sup></b>	MLFDLF	23	1.47			
MLFDLFBi		3	0.19				
MLFMDF		4	0.26				
DLF		15	1.81				
MDF		14	1.68				
MDFDLF		1	0.12				
MLF		25	3.01				
MLFBi		8	0.96				
MLFBiDLF	2	0.24					
MLFDLF	36	4.33					
MLFMDF	1	0.12					

\* from Table 3.3. M = Mesial, B = Buccal, D = Distal, L = Lingual, F = Fused, Bi = bifid apex. Ex: MLF = mesio-lingual fused roots, MLFBi = mesio-lingual fused roots with bifurcation. Congenitally absent teeth not included in statistics for this table.

### 3.4.5 Canal shape and orientation

Canal shape and orientation is probably the best described aspect of tooth root morphology due to its importance in clinical dentistry. Canals are the first tooth root structure to form (Orban and Bhaskar, 1980; McCollum and Sharpe, 2001), and exhibit a wide degree of variation within and between different tooth types (Vertucci et al., 1974; Vertucci and Gegauff, 1979; Vertucci, 2005; Versiani et al., 2019). Multiple typologies have been developed to classify canal shapes and configurations (see chapter 6 for a full

discussion). The most widely used typology was devised by Vertucci (1974; 2005), which defines 8 canal configurations (Figure 3.10). This typology does not account for accessory or lateral canals, and instead focuses on the primary canal structures extending from the pulp chamber to the apical foramen/foramina.

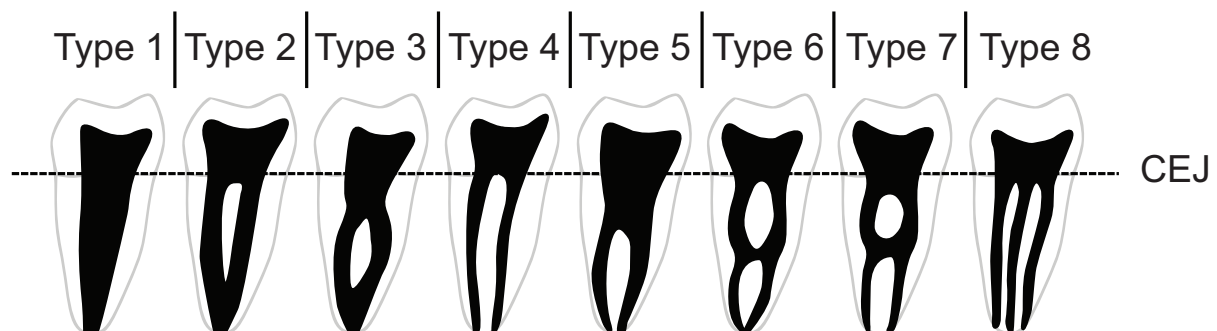


Figure 3.10: Vertucci's widely used canal classification system. Root and canal number do not always conform to one another. Black area represents pulp chambers and various canal configurations. Figure is modified from Vertucci et al. (1974).

In terms of morphology, canals can easily be grouped into three shapes: round, labelled R-shaped; oval, labelled O-shaped; and isthmus (Figure 3.11) labelled i-shaped. The first two are common to all teeth, while the third is predominantly found in the mandibular molars and Tomes' roots. Canal isthmuses are two canals connected by a 'ribbon' of variable completion; their variations have been well documented in the clinical literature (Hsu and Kim, 1997; Versiani et al., 2019), and are delineated by five, clearly classified variations (Figure 3.7). Here, these five variations are labelled i1-i5. Canal orientation has been extensively studied by clinical practitioners (see Versiani et al., 2018 for an in-depth review).

Canal configuration and count are intertwined (discussed above, and in Chapter 4) and thus we have extended our canal count to also reflect a simplified version of Vertucci's (1974) typology based on a system of thirds (Figures 3.8 & 3.11). Here, single, oval or round canals are labelled O or R. With exception to canal isthmuses, multi-canaled roots were found to always have round canals (see Chapter 5 for a discussion). Thus, the prefix R is used to delineate single and multi-canal configurations based on divisions into thirds.

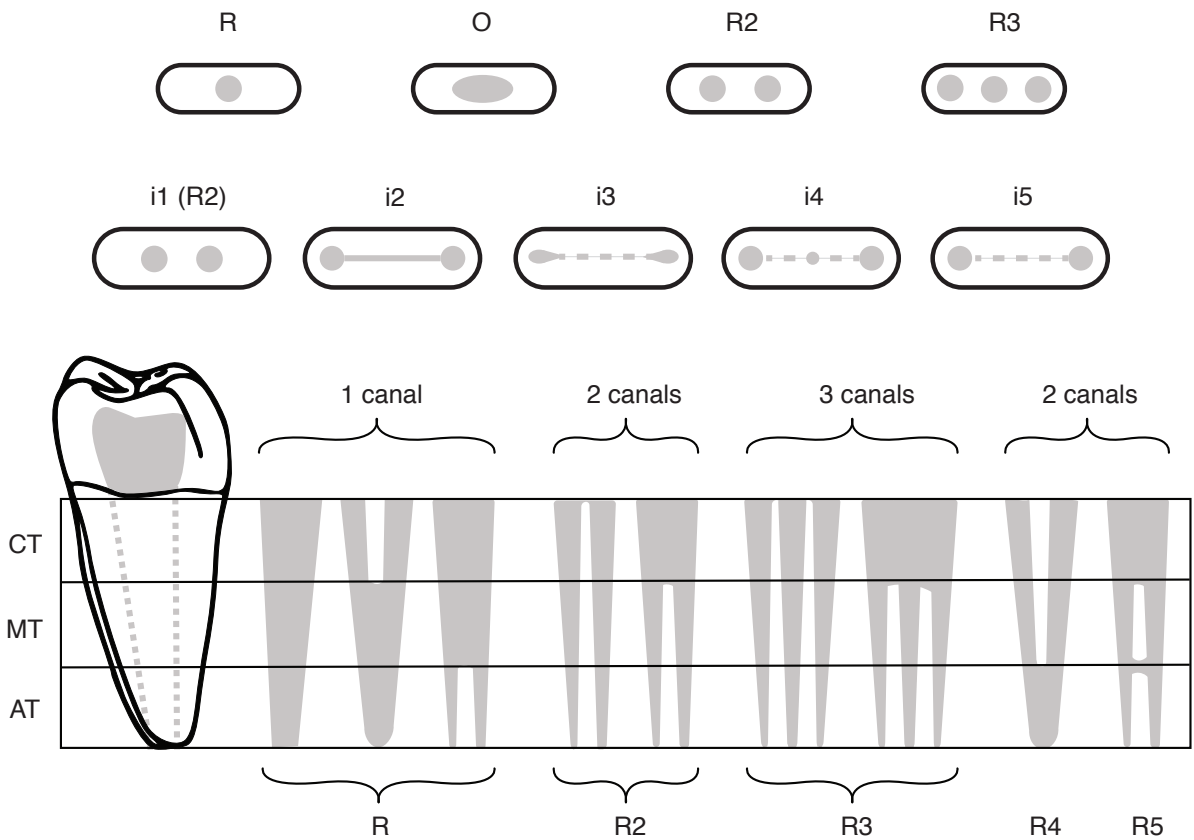


Figure 3.11: Root canals are almost always round or oval (top). Isthmus canals are characterized by a 'ribbon' of tissue between two round canals (middle). Canals frequently join and separate. Using a system of thirds after Turner (1991), canal count can easily be determined bottom).

Single round (R) and ovoid (O) canals are the most common canal morphologies and configurations in nearly all teeth of both jaws (Table 3.10). Interestingly, R canals are most prevalent in maxillary teeth while O canals are most prevalent in mandibular teeth. Isthmus canals (i2-i5) appear with less frequency than single (R and O) and double-canaled (R2-R5) variants and are mostly found in the mandibular molars. The double canaled R5 orientation appears the least. No R3 variants appear in this sample.

Table 3.10: Counts of canal shapes and configurations in the right side of the maxilla and mandible by tooth

Tooth	Canal morphology	n~	% of canalst	Tooth	Canal morphology	n~	# of canalst
<b>Maxilla</b>				<b>Mandible</b>			
I <sup>1</sup>	O	22	10.78	I <sub>1</sub>	O	110	48.25
	R	182	89.22		R	70	30.70
I <sup>2</sup>	O	84	33.73		R2	5	4.39
	R	163	65.46		R4	18	15.79
					i2	1	0.88
				O	140	56.68	
				R	68	27.54	

	R4	1	0.80		R2	6	2.43
					R4	31	12.55
					i2	1	0.40
					i5	1	0.40
<b>C<sup>1</sup></b>	O	227	55.77	<b>C<sub>1</sub></b>	O	204	64.35
	R	178	43.74		R	73	23.03
	R5	1	0.49		R2	1	0.63
					R4	15	9.46
					R5	1	0.63
					i2	3	1.89
<b>P<sup>3</sup></b>	O	67	6.99	<b>P<sub>3</sub></b>	O	177	40.69
	R	458	47.76		R	84	19.31
	R2	120	25.03		R2	21	9.66
	R4	75	15.64		R4	1	0.46
	R5	7	1.46		i2	2	0.92
	i2	6	1.25		i3	1	0.46
	i5	9	1.88		i4	2	1.38
					i5	59	27.13
<b>P<sup>4</sup></b>	O	193	27.26	<b>P<sub>4</sub></b>	O	179	54.91
	R	163	23.02		R	121	37.12
	R2	70	19.77		R2	5	3.07
	R4	90	25.42		R4	1	0.61
	R5	3	0.85		i5	7	4.29
	i2	11	3.11				
	i5	2	0.56				
<b>M<sup>1</sup></b>	O	357	14.69	<b>M<sub>1</sub></b>	O	225	15.83
	R	1,379	56.75		R	142	9.99
	R2	149	12.26		R2	261	36.73
	R4	134	11.03		R4	86	12.10
	R5	14	1.15		R5	5	0.70
	i2	33	2.72		i2	105	14.78
	i3	3	0.25		i3	30	4.22
	i4	1	0.08		i4	10	1.41
	i5	13	1.07		i5	30	4.22
<b>M<sup>2</sup></b>	O	284	14.87	<b>M<sub>2</sub></b>	O	295	26.66
	R	1,245	65.18		R	90	8.13
	R2	53	5.55		R2	139	25.11
	R4	69	7.23		R4	99	17.89
	R5	4	0.42		R5	2	0.36
	i2	45	4.71		i2	68	12.29
	i3	7	0.73		i3	22	3.97
	i4	1	0.16		i4	12	3.25
	i5	11	1.15		i5	13	2.35
<b>M<sup>3</sup></b>	O	120	11.27	<b>M<sub>3</sub></b>	O	202	27.01
	R	740	69.48		R	185	24.73
	R2	44	8.26		R2	58	15.51
	R4	25	4.69		R4	72	19.25
	i2	21	3.94		i2	31	8.29
	i3	3	0.56		i3	5	1.34
	i4	1	0.28		i4	1	0.40
	i5	8	1.50		i5	13	3.48

~ n column list times each variant appears. However, R2, R4, R5, and i2-i5 are two-canaled variants and are counted twice, and R3 is a three-canaled variant which is counted three times, to calculate % of canals. † = Table 3.4. Congenitally absent teeth not included in statistics for this table.

### 3.5 Inter-trait association and independent observations

The inter-relationships of dental traits have been well studied in clinical and anthropological contexts. Tooth dimensions are strongly correlated with one another (Garn et al., 1965, 1968; Harris and Lease, 2005), as are eruption sequences (Smith, 1991; Ash, 2013; Fleagle, 2013), timing of mineralization (Reid et al., 1998; Nelson and Ash, 2010; Miller, 2013), and agenesis (Garn et al., 1963; Nieminen, 2009). However, non-metric crown and root traits are poorly correlated and usually expressed independently of one another (Corruccini, 1976; Markowski, 1995; Scott et al., 2018). In population studies (discussed in Chapter 1, sections 1.1 and 1.2) the working assumption is that non-metric crown and root traits are expressed independent of one another, and show little or no interaction with metric crown and root dimensions, or tooth anagenesis (Scott and Irish, 2017).

An exception to the above, nonmetric traits expressed on members of the same morphogenetic field (see Chapter 2, section 2.4) sometimes do show significant correlations (Scott, 1977; Scott and Irish, 2017). While a 'key tooth' (i.e., the most mesial) might be the most developmentally and evolutionary stable tooth in a morphogenetic field, it does not always exhibit the full frequency or degree of expression of traits within that field (Butler, 1963). For example, five-cusped M<sub>1</sub>s appear in 85 -100% of all human populations, while M<sub>2</sub>s have a relatively higher frequency of four-cusped molars (Scott and Turner, 1997; Hemphill, 2002). Other traits, such as the protostylid appear with greatest frequency in M<sub>1</sub>s, but with a higher degree of expression in M<sub>2</sub>s and M<sub>3</sub>s (Scott and Turner, 1997). Teeth with reduced size or that are congenitally absent are nearly exclusive to M<sub>3</sub>s and do not appear in M<sub>1</sub>s or M<sub>2</sub>s at all (Daito et al., 1992; Kirkham et al., 2005). In tooth roots, the Ento- and Paramolaris variants are almost always found in M<sub>1</sub>s (Carlsen and Alexandersen, 1990; Calberson et al., 2007) while C-shaped variants are almost always found in M<sub>2</sub>s (Fernandes et al., 2014). Thus, when working with multiple teeth in the same morphogenetic fields there is an increased risk in violating statistical assumptions of independence. This is problematic for dental anthropologists who want to capture and analyse the total variation within all teeth, but instead must limit their analyses to a single tooth. When an unusual trait appears with higher frequency in non-key tooth (i.e., not the most mesial) within a morphogenetic field, the working solution has been for researchers to use this single tooth as the 'key tooth' for representing that particular trait in a sample (Turner II et al., 1991).

However, the researcher must consider how this might affect their choice of statistical model.

Dental inter-relationships are usually assessed with a wide variety of correlational methods (see Scott and Irish, 2017 for a full discussion). For example, interclass correlation coefficients, and principal components or factor analysis are often applied to metric traits, while contingency and/or tetrachoric coefficients are appropriate for non-metric traits depending on how they are treated (e.g., presence/absence, breakpoints, etc). In this dissertation, correlational methods and tests of independence are applied to metric and non-metric traits root traits. Additionally, regression and classification models are applied to predict canal-to-root number, canal morphology to external root morphology, and population identity. Each of these studies requires different statistical approaches and tests, each with their own underlying assumptions. These are addressed in a chapter by chapter basis within the materials and methods sections for each study.

### 3.6 Data set and data imputation

Data were analysed with the R Project for Statistical Computing, version 3.6.3 (<https://www.R-project.org>, 2017). Because the osteological materials used in this study were recovered from excavation sites, many of the individuals comprising our sample are missing one or more teeth. As the mechanism causing these missing data are unrelated to the values of any variables used in analysis (missing completely at random), our observed values are essentially a random sample of the full data set and not biased (Sterne et al., 2009). Thus, multiple imputation is appropriate for our data set (Garson, 2015; Zhang et al., 2017). Using the missMDA package, we performed multiple imputation on missing data in preparation for analysis (Josse and Husson, 2016). The missMDA package imputes data so that imputed values have no weight on the results (i.e., all methods are performed on observed values only). Thus, missMDA serves to replace missing entries with plausible values, resulting in a dataset that can be analysed by any statistical method, free from errors generated by missing and/or NA values.

## Chapter 4: Patterns of variation in canal and root number in human post-canine teeth

### 4.1 Abstract

Descriptive morphology of tooth roots traditionally focuses on number of canals and roots. However, how or if canal and root number are related is poorly understood. While it is often assumed that canal number is concomitant with root number and morphology, in practice canal number and morphology do not always covary with external root features. To investigate the relationship between canal and root number, post-canine teeth were examined and quantified from computerized tomography scans from a global sample of 945 modern humans. We tested the hypotheses that canal to root ratios differ between teeth, and that canal to root ratios differ across populations. Results indicate that not only is root number dependent on canal number, but that this relationship becomes more variable as canal number increases, varies both between individual teeth and by population, and changes as populations increase in distance from Sub-Saharan Africa. These results show that the ratio of canal number to root number is an important indicator of variation in dental phenotypes.

### 4.2 Introduction

Tooth root anatomy varies in canal and root number, and canal number does not always covary with root number. Various aspects of this have been studied in modern humans (Kovacs, 1971; Ackerman et al., 1973; Vertucci and Gegauff, 1979; Hsu and Kim, 1997; Zorba et al., 2014; Ahmed et al., 2017), extant hominoids (Kupczik et al., 2005; Emonet et al., 2012; Moore et al., 2013), and fossil hominins (Wood et al., 1988; Plavcan and Daegling, 2006; Kupczik et al., 2009; Kupczik and Hublin, 2010; Le Cabec et al., 2013; Moore et al., 2016). However, the numerical relationship between canals and roots is poorly understood. This study investigates the relationship and variability between canal and root number in a global sample of modern humans (n=945). Specifically, we asked (1) what is the relationship between root number and canal number; (2) does this relationship vary by tooth; and (3) does the relationship between canal and root number vary by populations?

### 4.2.1 Root and canal formation

Tooth canal and root formation are comprised of a series of reciprocal cellular interactions in the dental papilla of the developing tooth (Jernvall and Thesleff, 2000). Central to the process is Hertwig's epithelial root sheath (HERS), which is derived from the cervical loop of the enamel organ and is thought to be responsible for root number, shape and length (Miller, 2013; Luder, 2015). Following crown formation, mesenchyme cells form the blood vessels, nerves, and connective tissue of the pulp cavity and root canals (Wright, 2007). Simultaneously, the HERS extends apically, interacting with the mesenchyme cells of the developing canal structures, and differentiating into odontoblasts responsible for dentin and cementum production (Li et al., 2017).

During root morphogenesis, the HERS produces inter-radicular processes (IRP's), finger-like protrusions adjacent the cervical foramen of the tooth crown. The extension and fusion of opposing IRPs across the cervical foramen create multiple secondary foramina which, in turn, form multiple tooth roots (Kovacs, 1971; Orban and Bhaskar, 1980); and it may be that number and orientation of IRP's are responsible for the variation in canal and root forms (Figure 4.1). While molecular regulation and tooth morphogenesis have been extensively studied in tooth crowns, the mechanisms responsible for variation in canal and root structures are poorly understood. Because of its extensive role in root formation, HERS has been an area of focus; and several studies have shown that disturbances in formation of the HERS results in abnormalities in root number and shape (see Luder, 2015 for a review).

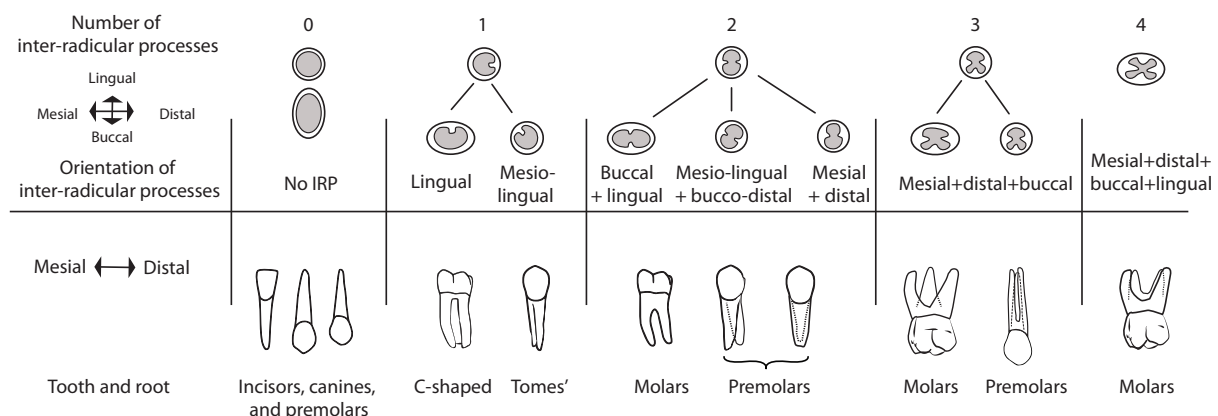


Figure 4.1 : The sites on the apical foramen where the inter-radicular processes (IRP's) form determines the location and orientation of each tooth root. For example, in a tooth with mesial and distal roots, two inter-radicular processes arise from the buccal and lingual borders of the apical foramen, forming mesial and distal secondary apical foramina upon fusion. Grey = apical foramina.

Though internal and external internal morphogenesis of root structures are concurrent processes, the completed structures do not always covary. There is great variation and complexity in root canals. It is easy to conceptualize canals as round holes which taper towards the roots' apex. However, many teeth have multiple canals within a single root. These canals can join and separate in unpredictable places and the more ovoid the cross-section of the root, the greater the propensity for canal complexity (Vertucci and Gegauff, 1979; De Pablo et al., 2010; Ahmed et al., 2017). Possible causes of divergence in canal and root number have been attributed to uneven deposition of dentin on the walls of the canal (Manning, 1990), trauma to the HERS by radiation or chemical interference (Fischischweiger and Clausnitzer, 1988), and/or failure of the HERS to fuse on different sides of the root (Nelson and Ash, 2010; Miller, 2013).

### 4.3 Materials and Methods

In this chapter, we analysed root and canal number from post-canine teeth (Table 4.1) from the right sides of the maxillary and mandibular dental arcades of individuals (n= 945) housed in the osteological collections at the Smithsonian National Museum of Natural History (SI), American Museum of Natural History (AMNH), and the Duckworth Laboratory (DW) at the University of Cambridge Leverhulme Centre for Human Evolutionary Studies (See Chapter 3, Table 3.1).

Table 4.1: Counts of teeth used in this study\*

Tooth	n	Tooth	n	Total
<u>Maxilla</u>		<u>Mandible</u>		
<b>P<sup>4</sup></b>	467	<b>P<sub>4</sub></b>	313	780
<b>M<sup>1</sup></b>	697	<b>M<sub>1</sub></b>	410	1,107
<b>M<sup>2</sup></b>	596	<b>M<sub>2</sub></b>	385	981
<b>M<sup>3</sup></b>	362	<b>M<sub>3</sub></b>	278	
<b>Total</b>	2,637	-	1,729	4,366

\* Teeth are from the right sides of the maxillary and mandibular dental arcades. Table is not based on imputed values.

Data were analysed with the R Project for Statistical Computing, version 3.6.3 (<https://www.R-project.org>, 2017). Because the Poisson distribution is typically used for count data, a Poisson general linear model (PGLM) was used to test for the predictive

relationship between root and canal number by tooth and population groups at the  $p = 0.05$  significance level (Zeileis et al., 2008).

A key assumption underlying PGLM is the independence of observations (Hoffmann, 2004). Thus, the inclusion of multiple teeth from the same individuals may violate assumptions of independence for PGLM. To account for this, we fit our PGLM with Generalized Estimating Equations (GEE). GEE estimates population-averaged parameters and their standard errors based on a number of assumptions: (1) The response variables are correlated or clustered; (2) There is a linear relationship between the covariates and a transformation of the response; and (3) within-subject covariance has a correlation structure (Zeger and Liang, 1986; Diggle et al., 2002). Based on Pearson correlation analysis of canal and root number (see section 4.4.2), we used Auto Regressive Order 1 (AR1) correlation structure for our GEE covariance matrix. While GEE estimates of model parameters are valid regardless of the specified correlation structure, the AR1 correlation structure is appropriate because it (a) has no distributional assumptions (Zuur et al., 2009); (b) can accurately model covariance for cross-sectional individual and clustered studies (Müller et al., 2009; Muoka et al., 2021); (c) accurately models within-subject correlation decreasing across time and/or space (Agresti, 2002); and (d) assumes observations within and individual are non-independent (Zeger and Liang, 1986). Thus, AR1 is appropriate at the individual and population levels, and for the temporospatial distances within and between individuals and groups within our sample. GEE was carried out using 'geepack: Generalized Estimating Equation Package' version 1.3.2 (Halekoh et al., 2006). Stepwise model selection was tested and quantified using Akaike Information Criteria (stepAIC). Tukey's multiple comparison test was used for pair-wise analysis of population groups. (Full statistical output is presented in Appendix Section 9.3).

## 4.4 Results

### 4.4.1 Root and canal number

Tables 4.2 and 4.3 report counts for number of roots and canals from teeth belonging to the right side of the maxilla and mandible. The number of roots in teeth from the sample are between one and four (Table 4.2). In this sample, teeth with four roots are limited to maxillary molars and appear with a relatively low frequency compared to 2 and 3

rooted teeth. Premolars, especially P<sub>3</sub> and P<sub>4</sub>, are predominantly single-rooted, while the majority mandibular molars in this sample are double-rooted. Entomolaris (En), or three-rooted molars, appear in 18.05 % M<sub>1</sub>s, 1.23% of M<sub>2</sub>s, and 5.94% of M<sub>3</sub>s, and paramolaris (Pa) appears in 3.63% of M<sub>3</sub>s.

Table 4.2: Number of roots from teeth in the right side of the maxilla and mandible by tooth

Tooth	Root number	n	Total Roots	% of teeth*	Tooth	Root number	n	Total Roots	% of teeth*
<b>Maxilla</b>					<b>Mandible</b>				
<b>P<sup>3</sup></b>	1	295	739	57.28	<b>P<sub>3</sub></b>	1	341	345	99.42
	2	216		41.94		2	2		0.58
	3	4		0.78	<b>P<sub>4</sub></b>	1	313	313	100.0
<b>P<sup>4</sup></b>	1	405	530	86.72		2			
	2	61		13.06					
	3	1		0.22					
<b>M<sup>1</sup></b>	1	2	2,060	0.29	<b>M<sub>1</sub></b>	2	336	894	81.95
	2	28		4.02		3En	74		18.05
	3	666		95.55					
	4	1		0.14					
<b>M<sup>2</sup></b>	1	56	1,561	9.39	<b>M<sub>2</sub></b>	1	49	727	12.73
	2	117		19.63		2	330		85.71
	3	421		70.64		3	1		0.26
	4	2		0.34		3En	5		1.30
<b>M<sup>3</sup></b>	1	89	831	24.59	<b>M<sub>3</sub></b>	1	20	563	7.19
	2	82		22.65		2	231		83.09
	3	186		51.38		3En	16		5.76
	4	5		1.38		3Pa	11		3.96

\* From Table 4.1. En = Entomolaris, Pa = Paramolaris. Table is not based on imputed values.

Teeth in this study contain between one and six canals (Table 4.3), and canal count often exceeds root count. Molars have the most canals per tooth, with M<sub>1</sub>s showing the most variation.

Table 4.3: Number of canals per tooth in the maxilla and mandible by tooth

Tooth	Canal number	n	Total Canals	% of teeth*	Tooth	Canal number	n	Total Canals	% of teeth*
<b>Maxilla</b>					<b>Mandible</b>				
<b>P<sup>3</sup></b>	1	82	959	15.92	<b>P<sub>3</sub></b>	1	254	435	74.05
	2	422		81.94		2	86		25.07
	3	11		2.14		3	3		0.87
<b>P<sup>4</sup></b>	1	233	708	49.89	<b>P<sub>4</sub></b>	1	300	326	95.85
	2	228		48.82		2	13		4.15
	3	5		1.07					
	4	1		0.22					
<b>M<sup>1</sup></b>	2	4	2,431	0.57	<b>M<sub>1</sub></b>	2	27	1,431	6.59
	3	355		50.93		3	167		40.73
	4	333		47.78		4	205		50.00

	5	4		0.57		5	10		2.44
	6	1		0.14		6	1		0.24
<b>M<sup>2</sup></b>	1	8	1,910	1.34	<b>M<sub>2</sub></b>	1	2	1,107	0.52
	2	21		3.52		2	93		24.16
	3	408		68.46		3	241		62.60
	4	159		26.68		4	49		12.73
<b>M<sup>3</sup></b>	1	32	1,065	8.84	<b>M<sub>3</sub></b>	1	10	748	3.60
	2	24		6.63		2	86		30.94
	3	239		66.02		3	162		58.27
	4	67		18.51		4	20		7.19

\* From Table 4.1. Table is not based on imputed values.

#### 4.4.2 Inter-trait correlation

Pearson product-moment correlation coefficients (Figure 4.2) were computed to assess linear correlation between root number (RN) and canal number (CN) for teeth used in this study (Table 4.1). The majority of variables have negligible to weak positive or negative correlation coefficient strength values of  $0.01 - \pm 0.30$  (Akoglu, 2018). Within individual tooth types moderate to strong correlation coefficient values of  $0.31 - \pm 0.69$  (ibid) are found in P<sup>4</sup> RN:P<sup>4</sup> CN (0.46), M<sup>3</sup> RN:M<sup>3</sup> CN (0.47), M<sub>2</sub> RN:M<sub>2</sub> CN (0.35), and M<sub>3</sub> RN:M<sub>3</sub> CN (0.50). With the exception of P<sup>3</sup> RN:P<sup>4</sup> CN (0.46), P<sup>3</sup> RN:P<sup>4</sup> CN (0.65), P<sub>3</sub> CN:P<sub>4</sub> CN (0.43), M<sup>3</sup> RN:M<sup>2</sup> CN (0.31), and M<sub>2</sub> CN:M<sub>3</sub> CN (0.31), there are no significant correlations of RN to CN across different teeth.

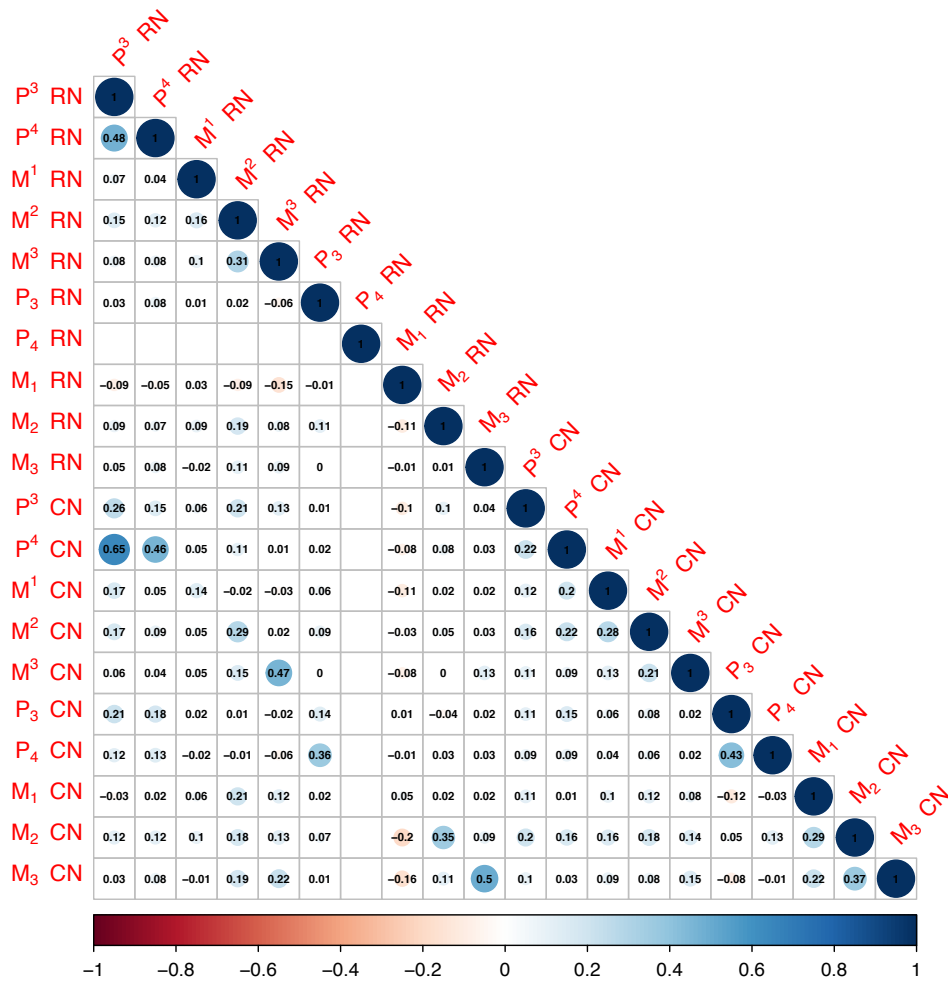


Figure 4.2: Pearson correlation of root number (RN) to canal number (CN). Significance level = 0.05. Significant positive correlation coefficients in blue. Significant negative correlation coefficients in red. Blank cells in P<sub>4</sub> RN:P<sub>4</sub> RN due to all P<sub>4</sub>s having the same level (i.e., one root. See Table 4.2).

#### 4.4.3 PGLM of relationship between canal and root number in individual teeth

While independent variables are uncorrelated, uncorrelated variables are not always independent. To address this, we fit PGLM with GEE to account for low levels of correlation between some traits (Figure 4.2), and to account for using multiple teeth from the same individuals, which may violate assumptions of variable independence. PGLM fitted with GEE was used to directly test the linear relationship of root to canal number by tooth - in other words, to see how the relationship between canal and root number varies across different tooth types. StepAIC determined that inclusion of canal counts, and individual teeth as independent variables provided the most parsimonious predictive model (- none, df = 0, AIC = 22537; - canal count, df = 1, AIC 22741; - Tooth, df = 10, AIC 22994). To avoid emphasizing results against one tooth we fitted the model without an intercept. GLM of individual teeth

reveal that for P<sup>3</sup>, M<sup>1</sup>-M<sup>3</sup>, and M<sub>1</sub>-M<sub>3</sub>, as canal count increases, so does root count (Table 4.4). Interestingly, this is not the case for P<sub>3</sub> and P<sub>4</sub>. In the maxilla, the greatest increase in root to canal number is found in M<sup>1</sup> (99.99%), and similar relationships are found in M<sup>2</sup> and M<sup>3</sup>. Maxillary premolars remain relatively stable, with a minimal increase (0.03%) in P<sup>3</sup>, and no increase in root number in P<sup>4</sup>. Mandibular molar (M<sub>1</sub>-M<sub>3</sub>) roots are comparatively similar to one another in their odds ratios, especially M<sub>1</sub> and M<sub>2</sub>; while surprisingly, mandibular premolars (P<sub>3</sub>-P<sub>4</sub>) show that as canal number increases root number does not.

Table 4.4: Regression parameters for GEE extended PGLM regression of the association between canal-to-root number by tooth, ranked by odds ratios from greatest to least\*

	Estimate	Odds ratio	Std. error	Wald	P-value
<i>Canal number</i>	0.117	1.124	0.007	251.300	< .0001
<b>Maxilla</b>					
M <sup>1</sup>	0.693	1.999	0.025	750.400	< .0001
M <sup>3</sup>	0.650	1.916	0.025	683.700	< .0001
M <sup>2</sup>	0.648	1.911	0.025	651.900	< .0001
P <sup>3</sup>	0.000	1.000	0.018	0.000	0.990
P <sup>4</sup>	-0.091	0.913	0.011	69.100	< .0001
<b>Mandible</b>					
M <sub>3</sub>	0.356	1.428	0.022	264.800	< .0001
M <sub>2</sub>	0.127	1.382	0.025	207.100	< .0001
M <sub>1</sub>	0.287	1.330	0.028	106.700	< .0001
P <sub>4</sub>	-0.119	0.887	0.008	248.000	< .0001
P <sub>3</sub>	-0.127	0.881	0.008	236.100	< .0001

\*Model fitted without intercept.

Prediction curves differ for each tooth, and the maxilla and mandible as a whole (Figure 4.3). Similar tooth groups have similar prediction curves — P<sub>3</sub>, P<sub>4</sub>, and P<sup>4</sup>; M<sub>3</sub>, M<sub>2</sub>, and M<sub>1</sub>; and M<sup>1</sup>, M<sup>2</sup>, M<sup>3</sup>; and these differ between the maxilla and mandible. As prediction curves diverge from the 1:1 canal-to-root ratio, root number decreases, though this does not necessitate a concomitant reduction in canal number.

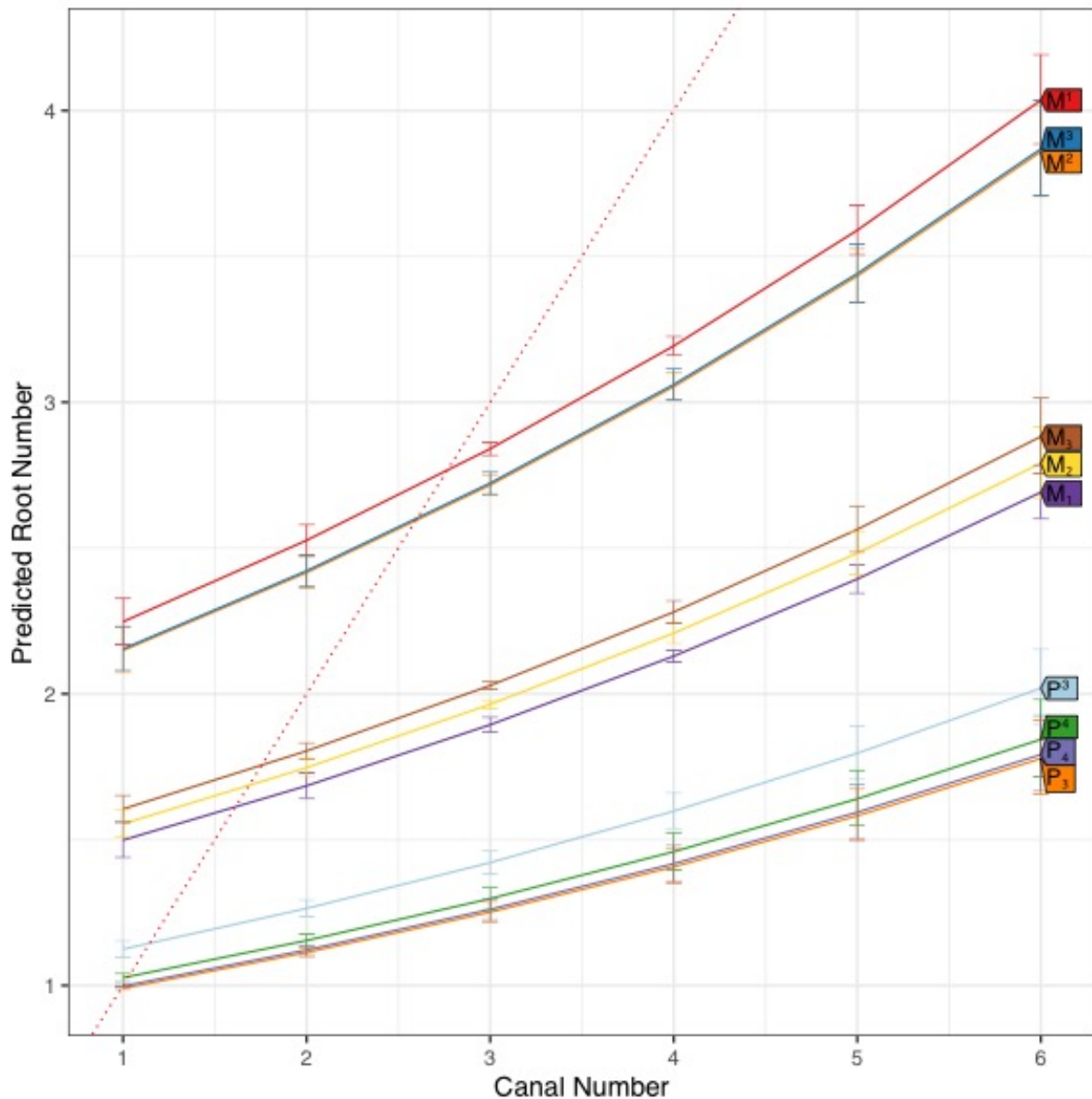


Figure 4.3: PGLM prediction curves with error bars for canal to root number for individual teeth. Dotted red line represents 1:1 canal to root relationship (i.e., what would be observed if there was a simple 1:1 relationship between roots and canals). Over prediction in the number of roots for single canaled  $M^1$ - $M^3$ 's is owing to very small sample of individuals with one root to one canal (see Tables 4.2 and 4.3 for counts).

Figure 4.4 plots proportions of canal to root number of individual teeth within the sample. Different patterns are clearly evident across all teeth and between the maxilla and mandible and help to explain groupings of individual tooth prediction curves in Figure 4.2. There is a slight over-prediction in the number of roots for single canaled  $M^1$ - $M^3$ 's owing to 1) very small sample of individuals with one root to one canal for these teeth (see Table 4.4 for counts); and 2) because we have used a fixed non-parametric model to capture the non-linearity between canal and root number. Variation in canal to root number decreases in the premolars while increasing in the molars, though this variation does not covary between

opposing individual maxillary and mandibular teeth. The greatest variation is found in the maxillary molars ( $M^1$ - $M^3$ ) while the least is found in  $P_4$ .

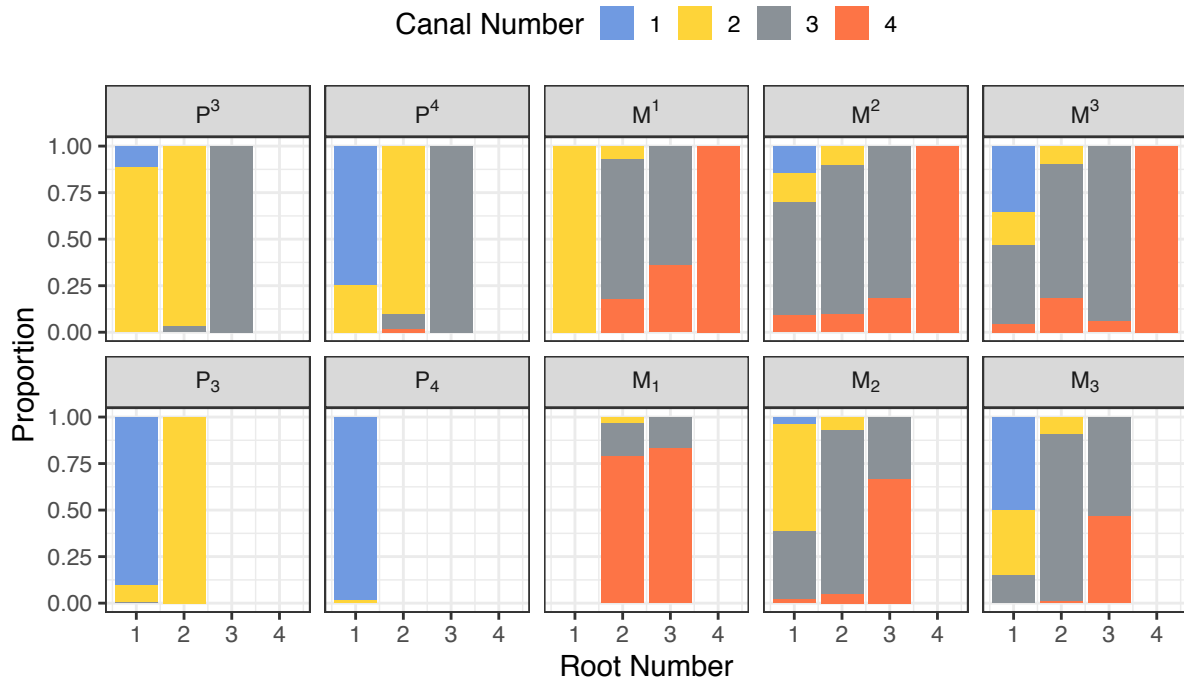


Figure 4.4: Proportion of canal to root number for individual teeth. 5 canaled teeth = 14, 6 canaled teeth = 2, are included in calculations of proportions but are not visualized on this plot due to small sample size.

Tukey pair-wise comparisons (Figure 4.5) for PGLM of root to canal number by tooth show that prediction curves and canal-to-root proportions plotted in Figures 4.2 and 4.3 reflect significant differences between teeth. Full statistical output is presented in appendix section 9.3.1, Table 9.2.

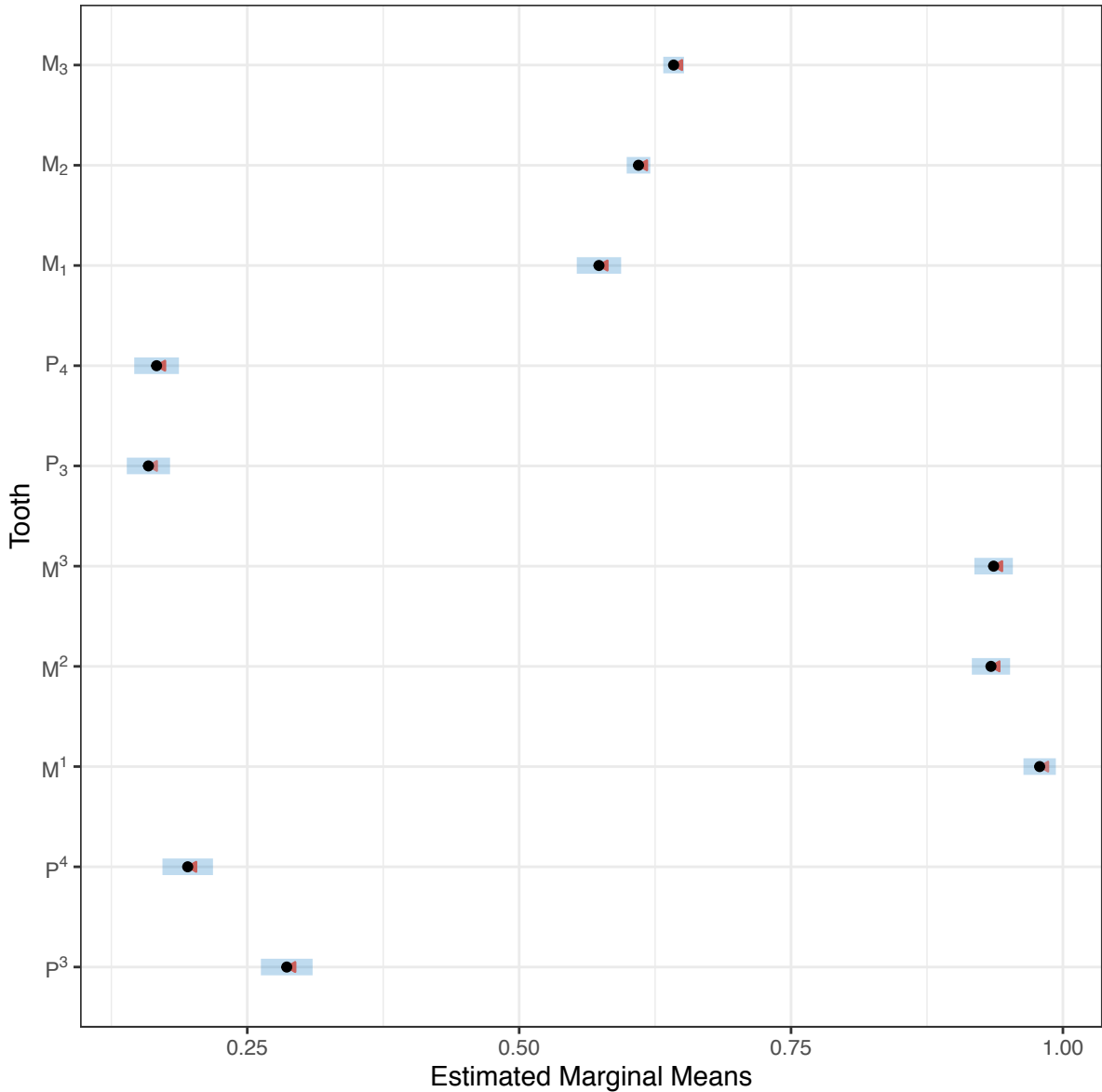


Figure 4.5: Estimated marginal means derived from Tukey pair-wise comparisons of canal to root number by tooth. Black dot = mean value; Blue bar = confidence intervals. The degree to which red comparison arrows overlap reflects the significance ( $p = 0.05$ ) of the comparison of the two estimates. Full statistical output is presented in Appendix Section 9.3, Table 9.2.

#### 4.4.4 PGLM of canal and root number in geographical groups

We used GEE and PGLM to test the linear relationship of root to canal number by tooth across population groups (Table 4.5). StepAIC determined that inclusion of canal counts, individual teeth, and geographic groups as independent variables provided the most parsimonious predictive model ( - none,  $df = 0$ , **AIC = 22529**; - GEO,  $df = 5$ , AIC = 22539; - canal count,  $df = 1$ , AIC 22659; - Tooth,  $df = 10$ , AIC 22853). To avoid emphasizing results against one geographical region or tooth we fitted the model without an intercept.

Table 4.5: Regression parameters for PGLM testing the association between canal and root number by tooth in geographic groups, ranked by odds ratio from greatest to least\*.

Populations	Estimate	Odds ratio	Std. error	Wald	P-value
Canal number	0.329	1.389	0.002	29139.9	< .0001
Sub-Saharan Africa	-0.211	0.810	0.007	816.8	< .0001
Sino-Americas	-0.235	0.790	0.006	1749.3	< .0001
Sunda-Pacific	-0.250	0.779	0.010	658.8	< .0001
West Eurasia	-0.238	0.789	0.007	1065.3	< .0001
Sahul-Pacific	-0.258	0.773	0.007	1206.2	< .0001

\* Model fitted without intercept.

Individual teeth of geographical groups are relatively similar in their odds ratios and prediction curves; and follow a similar pattern of divergence from a 1:1 canal-to-root ratio (Figure 4.6). Prediction curves for Sub-Saharan African populations are closest to the 1:1 canal-to-root ratio, while Sino-American populations are the furthest.

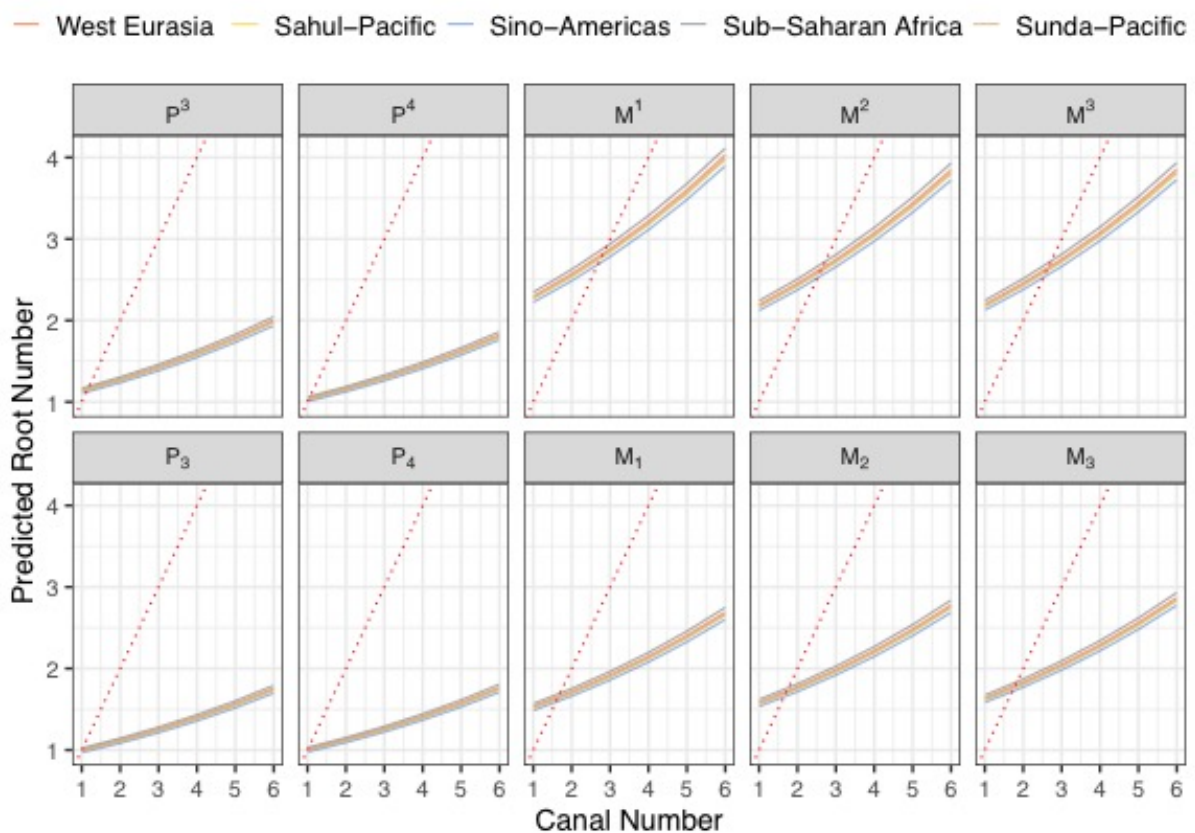


Figure 4.6: PGLM prediction curve for root to canal number by population. Dotted red line represents 1:1 root to canal relationship. Over prediction in the number of roots for single canaled M<sup>1</sup>-M<sup>3</sup>'s is owing to very small sample of individuals with one root to one canal (see Figure 4.2 for counts).

Marginal effects quantify how both groups vary differently in their canal to root ratios (Figure 4.7) when the explanatory variable (canals) changes by one unit. For all teeth, the Sino-American groups have the lowest percentage of change in root number as canal number increases, while Sub-Saharan Africans show a higher percentage of change in root number change as canal number increases.

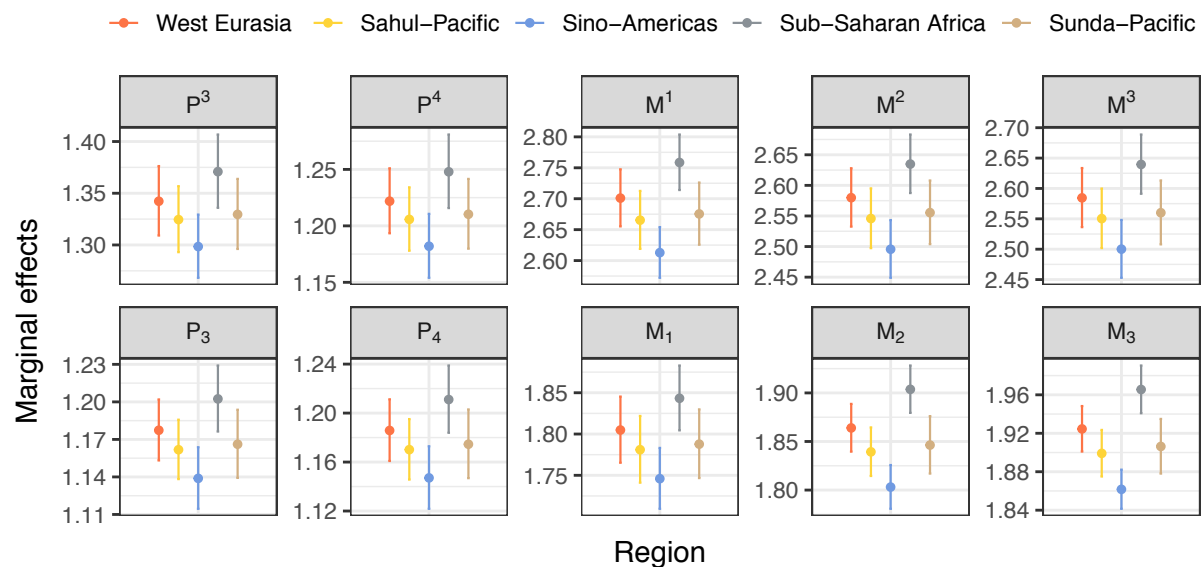


Figure 4.7: Marginal effects of canal to root count in individual teeth by geographical group.

Different patterns in proportions of roots to canals are complex but help clarify patterns in prediction curves and marginal effects in populations (Figure 4.7). Several clear patterns arise: (1) As canal and root number increases, there is a trend for first premolar, and then mandibular teeth to reduce in presence until only maxillary molars are left (4 canals: 4 roots). (2) Within populations, patterns vary, and are inconsistent. For example, while canal-to-root ratios of West Eurasian, Sahul- and Sunda-Pacific populations are represented relatively evenly, 3:3 canal-to-root P<sup>3</sup>s are only present in Sub-Saharan African populations, while 3:3 canal-to-root M<sup>1</sup>'s are only present in Sino-American populations. (3) There is a trend for root number reduction but not canal number reduction in Sino-American populations. Tukey pair-wise comparisons of GLM of canal to root number by population (Figure 4.8) show that patterns in prediction curves (Figure 4.6) and canal-to-root proportions (Figure 4.9) reflect significant populations.

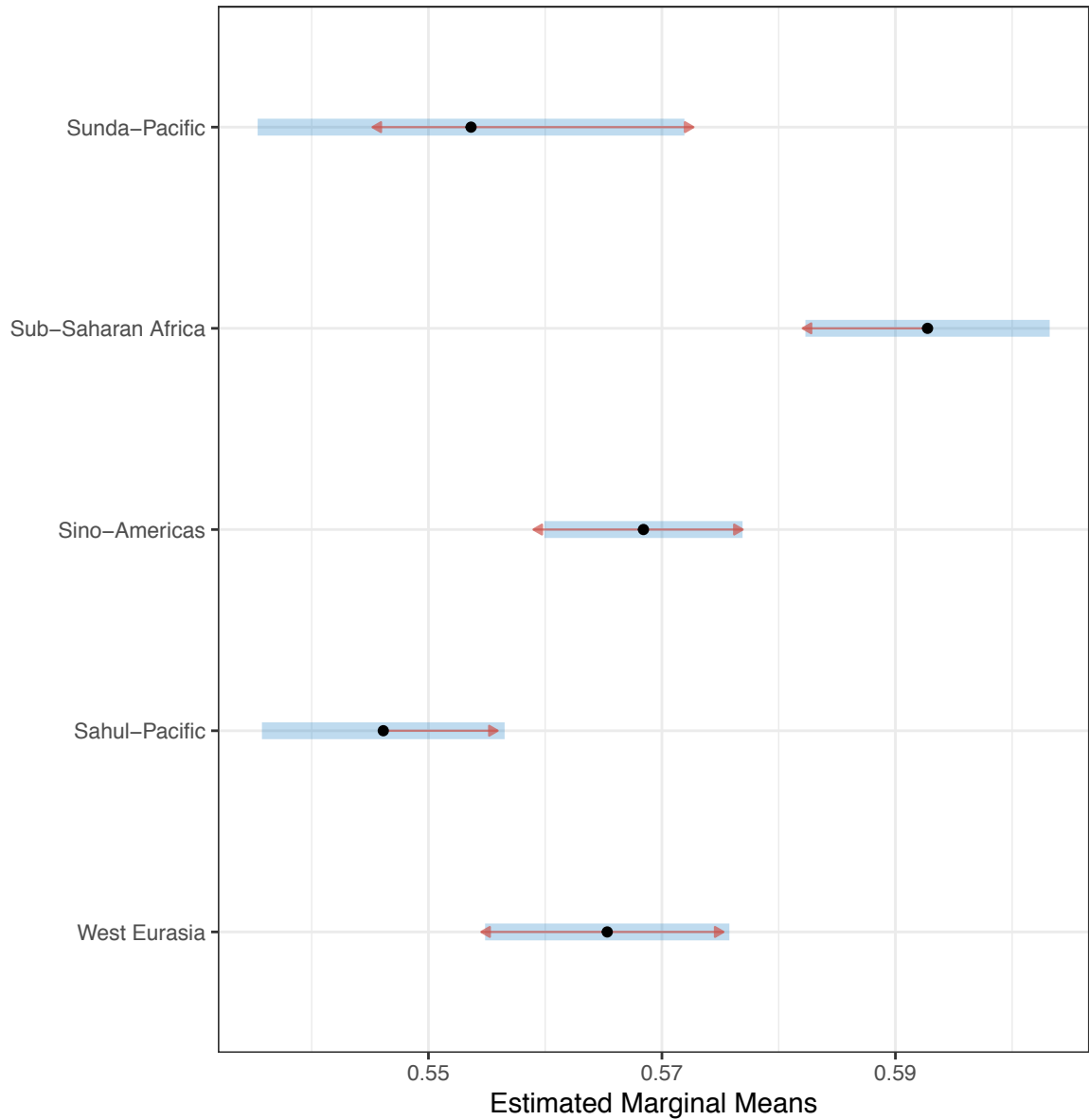


Figure 4.8: Estimated marginal means derived from Tukey pair-wise comparisons of PGLM of canal to root number by geographic group. Black dot= mean value; Blue bar = confidence intervals. The degree to which red comparison arrows overlap reflects the significance ( $p = 0.05$ ) of the comparison of the two estimates. Full statistical output is presented in Appendix section Table 9.3, Table 9.3.2.

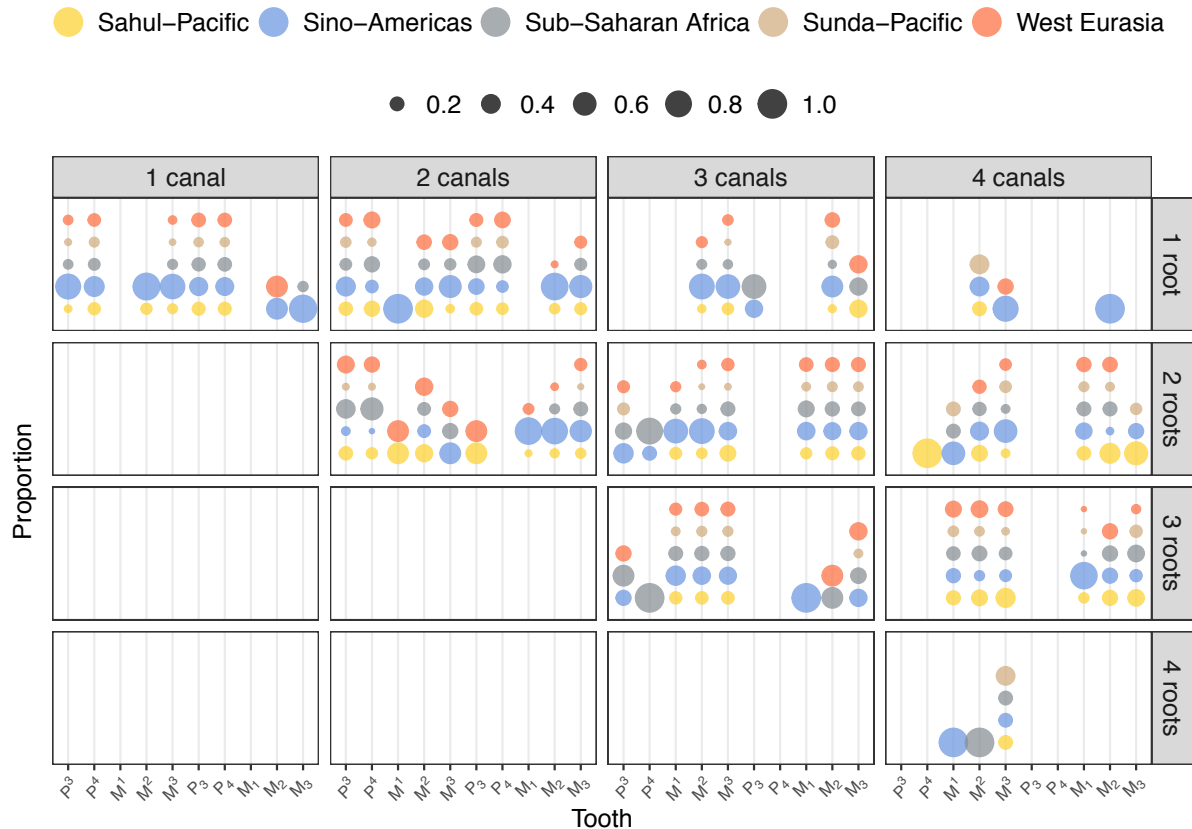


Figure 4.9: Proportions of roots to canals in individual teeth by geographic group. Proportions are calculated over individual teeth, with columns summing to one. Owing to low sample size we removed specimens with five and six canals.

## 4.5 Discussion

In the analyses presented above we have been able to show that there is little to no correlation between root and canal number in teeth. However, because uncorrelated random variables are not always independent, we extended our PGLM with GEE to develop a predictive model of the relationship between canal and root number, globally and by region, and we show that this relationship is not perfectly linear. We have found that canal number predicts root number, and that the greater the number of canals the more complex, and less predictable the number of roots. This relationship varies by maxillary and mandibular teeth and tooth row. Similar estimates (Table 4.4) and PGLM curves of tooth types (Figure 4.3) seem to lend support to the morphogenetic field model in which teeth within a field are more similar to one another than to teeth of another field (Butler, 1937, 1963; A.A. Dahlberg, 1945); especially for molar fields in both jaws. These results raise a number of issues: what does the complexity of canal to root number relationships mean developmentally? Why does this complexity vary across particular tooth types? How does

divergence in canal and root number vary between maxillary and mandibular teeth in total, by population, and individually?

#### 4.5.1 Differences in root and canal number

Currently, there is no consensus as to why canals and roots should differ in number, given that canal formation precedes root formation. Clusters of blood vessels entering the dental papilla early in tooth formation coincide with the positions where roots will eventually form (Miller, 2013). The HERS and expanding dental pulp form around these nerves and blood vessels before dentin formation. Thus, each root must contain at least one canal for the pulp, and the nerve and blood supply that precede the formation of the surrounding root structure. It is possible that number, size, and configuration of blood and nerve supplies is, in part, responsible for variation in canal number with the roots, and not variation in the number and orientation of the interradicular processes alone.

#### 4.5.2 Variance across teeth and between the maxilla and mandible

Why canal and root number should vary both within and between teeth of the maxilla and mandible is also unknown. Prediction curves and proportions of canal to root numbers show that the relationship between canals and roots within tooth types are similar to one another, i.e., maxillary molars are alike, while being significantly different from other tooth types, such as premolars and mandibular molars. Groupings of like teeth may lend support to morphogenetic field theory (Butler, 1937). These results suggest that the number of canals and roots within tooth types are relatively "fixed" with little intra-tooth type variation. We propose two possible explanations, the first functional, the second spatial.

Megadonty is a hallmark of early hominin evolution (Robinson, 1956; Wood and Abbott, 1983; Reed, 1997; Wood and Constantino, 2007); and heavy chewing requires large teeth. The majority of chewing actions occur on the broad occlusal surfaces of the post-canine teeth where, compared to anterior teeth, masticatory movements are complex combinations of antero-posterior, vertical and lateral movements (van Eijden, 1991; Ledogar et al., 2016). Chewing pressures on the maxillary teeth result from absorption of shearing and compressive forces generated by the active movement of the mandible (Ledogar et al., 2016). During mastication, maxillary molars are subjected to greater medio-

lateral directed loads than mandibular molars (Dempster et al., 1963; Spears and Macho, 1998). These medio-lateral forces are dissipated into the jaws via the tooth roots (Zwemer, 1985; Baragar and Osborn, 1987); and, in humans, are strongest at, and decrease posteriorly from M<sup>1</sup> (Gordon, 1984; Macho and Spears, 1999). Consequently, as root surface area decreases in M<sup>2</sup> and M<sup>3</sup>, so does root number ((Dempster et al., 1963); Table 4.2).

It is possible that where increased masticatory loadings are a selective pressure for larger teeth, an increased blood supply required for developing a larger tooth will result in an increase in canal number. This will, in turn, result in more roots. The increased mesio-distal and bucco-lingual dimensions of premolars tooth crowns belonging to megadontic "robust australopiths" (*Paranthropus boisei*, *P. robustus*, *P. aethiopicus*), support such a hypothesis. These "hyper-robust" hominins regularly had multi-rooted/canaled premolars (Robinson, 1954, 1956; Wood et al., 1988; Brook et al., 2014; Moore et al., 2016; Kupczik et al., 2018), and the ancestral hominin phenotype has been proposed as three-root maxillary premolars, and two-root mandibular premolars (Abbott, 1984; Hamon et al., 2012). In modern humans, molars withstand the heaviest masticatory loadings while premolars are subjected to the least (Demes and Creel, 1988; Ledogar et al., 2016). That masticatory stresses produce high strains in the alveolar margin of the anterior maxilla (Ledogar et al., 2016) may act to increase canal and root number in the maxillary premolars compared to mandibular premolars. Developmentally, Shields (2005) proposed that tooth germ size influenced the number and development of IRP's. However, multiple studies have noted that tooth crown size (used as proxy for tooth germ size) does not always covary with root number and size in humans and hominoids (Abbot, 1984; Shields, 2005; Moore et al., 2013, 2016).

Different masticatory forces resulting from dietary demands have been shown to increase tooth root surface area, and thus size, in primates (Kovacs, 1971; Spencer, 2003; Kupczik and Dean, 2008; Ledogar et al., 2016). A possible selective mechanism to increase tooth root surface area would be to increase the number of roots, which would in turn enlarge the cervical base area of the crown (Kupczik et al., 2005). A study of *Gorilla gorilla*, *Pan troglodytes*, as well as of 26 fossil gracile and robust hominins from South Africa concluded that dietary adaptations produced mesio-distal expansion at the base of tooth roots in M<sup>1</sup>s (Kupczik et al., 2018). The authors (ibid) concluded that it was increases in root splay that accommodated higher masticatory loadings, but that the mesio-distal expansion

of the root bases in robust hominins might be an adaptive response to different jaw kinematics for chewing different food types — horizontally directed repetitive chewing in *P. boisei* (Demes and Creel, 1988; Wood and Constantino, 2007), versus multi-directional loading of *P. robustus* (Macho, 2015). However, the extant and fossil species from this study are already characterized by multi-rooted molars and premolars (Sperber, 1973; Wood et al., 1988; Kupczik et al., 2005; Shields, 2005); so it is difficult to discern if mesio-distal expansion of the roots is an adaptive response to biomechanical pressures, a by-product of additional roots, or both. If root splay is in fact the primary adaptive response to increased masticatory loading, the selective pressures underlying what point single root surface area/size stops increasing and root differentiation begins have yet to be elucidated.

Alternatively, variation may arise from space required for growing teeth in the developing jaws. Consider that maxillary and mandibular 1st molars are the first adult teeth to erupt (at 6-7 years) followed by the anterior teeth (7-10 years), premolars (10-12 years), followed by 2nd (12-13 years) and 3rd molars (17-21 years). In this spatial scenario maxillary and mandibular 1st molars have the greatest number of roots and canals, while late forming and erupting premolars have the least as they are sandwiched between 1st molars and the already erupted anterior teeth. Constrained variation, especially in the premolars may be explained by limited space for growth and development, while maxillary and mandibular molars have spatial restrictions on their growth and development limited by dimensions of the palate and by the ascending ramus of the mandible.

Biomechanical and spatial explanations need not be mutually exclusive. It may be the case that canal, and root variation found in modern humans is a product of reduction in space as a consequence of reduced selection for intensive biomechanical chewing pressures in early human evolutionary history. Premolar root number has been documented as more variable than in all other tooth types (Sperber, 1973; Wood et al., 1988; Kupczik et al., 2005; Shields, 2005). Contrary to the molarization of the robust Paranthropines, the reduction of premolar root number is present in South-African gracile hominins. Robinson (1956) and Sperber (1974) report predominantly (84%) double-rooted maxillary premolars in a sample of *Australopithecus africanus*, though single (8%) and triple-rooted (8%) variants do occur. *A. africanus* mandibular premolars are reported as having single C-shaped (also referred to as Tomes' root) and double-rooted mandibular molars (Robinson 1952, 1956; Sperber, 1974, Moore et al., 2016). Thus, this trend for reduction in premolar root number appears

early in human evolutionary history (3.4 -2.4 Ma) and coincides with dietary shifts towards meat and/or softer cooked foods (Luca et al., 2010), and reduction of hominin tooth crowns, jaws and face (Wood and Collard, 1999; Plavcan and Daegling, 2006). At 1.8 Ma *Homo erectus* has fewer tooth roots, especially M<sup>3</sup>/M<sub>3s</sub>, than earlier members of our genus, and *H. erectus* premolars are frequently single rooted (Anton, 2003). This trend in root number reduction continues through more recent members of genus *Homo* including some specimens allocated to *H. heidelbergensis* and *H. neanderthalensis* (FitzGerald, 1998; Benazzi et al., 2011; Zanolli and Mazurier, 2013).

#### 4.5.3 Differences in geographical groups

Sino-American and Sub-Saharan African populations are significantly different from one another (Figure 4.8), and these differences can be explained by reduction in root number in the former. Compared to all other groups, Sino-Americans have the greatest proportion of single rooted teeth across all populations while Sub-Saharan African populations have the smallest (Figure 4.9). This trend is present regardless of canal number. The exception to this is the presence of three-rooted mandibular molars (ento- and paramolaris root forms) in Sino-Americans (Carlsen and Alexandersen, 1990). This form represents a relatively rare root polymorphism, and appears with frequencies around 30-50% in East Asian, Inuit, and Aleut populations; 5-15% in Southeast Asian and Pacific populations; compared to 1% in European and Sub-Saharan African populations (Scott et al., 2018).

As with individual teeth, there is no clear explanation for changes in canal to root number between populations. The reasons may be biomechanical in nature and relate to different diets between populations. However, this is unlikely as the Sino-American populations included in this study (primarily comprised of North American First peoples, see Appendix section 9.2, Table 9.1), did not pursue uniform subsistence strategies. However, the effect of different diets on tooth root and canal morphologies is poorly understood, with only a few studies centred on non-human primates, and gracile and robust Australopiths (see Kupczik et al., 2018 for an overview).

The study of dental traits have an extensive history and utility for characterizing and assessing the biological relationships within and populations (see Scott et al., 2018 for a

comprehensive review). Dental morphology has been shown to be under strong genetic control and minimally affected by environmental factors (Corruccini et al., 1986; Dempsey and Townsend, 2001). The evolutionary trend of teeth has also been described as towards reduction in size and simplification in morphology (Scott and Turner, 1988). While the authors of these studies were describing tooth crowns, tooth roots are presumably operating under the same genetic and environmental constraints, and evolutionary trends.

Marginal effects (Figure 4.7) and canal to root proportions (Figure 4.9) support evidence of simplification in terms of reduction. Sub-Saharan Africans and Sino-Americans are furthest in distance from one another in time and space, and the former group shows the greatest variation in root and canal number, while the latter shows a reduction. For example, Sino-Americans have a higher proportion of single rooted, double-canaled  $M_2$ 's and  $M_3$ 's than all other groups. Additionally, congenitally absent  $M_3$ 's are common (>25%) in Sino-American populations (Turner II et al., 1991; Daito et al., 1992; Rakhshan, 2015; Scott et al., 2018). Compared to Sub-Saharan African populations, Western Eurasia, Sahul- and Sunda-Pacific groups have reduced variability, though not as much as Sino-Americans. These three groups share similar linear relationships (Figure 4.6) and canal to root proportions (Figure 4.9), though marginal means of West Eurasian and Sunda-Pacific populations reveal their canal to root relationships are more similar to Sub-Saharan Africa, while Sahul-Pacific is closer to Sino-Americans.

Recent studies have highlighted the decrease of genetic and phenotypic diversity in human populations with increasing distance from Sub-Saharan Africa (Handley et al., 2007). This decrease in diversity has been interpreted as evidence of an African origin for anatomically modern humans. Reduced intra-population diversity has been ascribed to an "Out of Africa" migration, and sequence of founder events due to rapid expansions and colonization of the world (Prugnolle et al., 2005; Liu et al., 2006; Li et al., 2008). This reduction in diversity has been recorded in human dental (Hanihara and Ishida, 2005; Hanihara, 2008), craniofacial (Betti et al., 2009; Hanihara and Ishida, 2009), and morphometric traits (Manica et al., 2007), further supporting genetic hypotheses of this single, African origin and subsequent expansions. Our results also support such a pattern with some exceptions. For example, three rooted  $M_1$ 's, sometime referred to as *Radix entomolaris* (see Calberson, De Moor and Deroose, 2007 for a review), increase in Sino-American populations (Figure 4.9) while appearing in low frequency in other populations;

especially Sub-Saharan Africa (Scott et al., 2018). This trait has been most commonly attributed to genetic drift (Scott et al., 2018), though a recent study has suggested archaic introgression (Bailey et al., 2019); however, see Scott, Irish and Martínón-Torres (2020) for a rebuttal.

## 4.6 Conclusions

This paper presents a novel investigation into the relationship between canal and root number in human post-canine teeth. In all cases, canal number is either equal to or exceeds root number, supporting our hypothesis that canal number precedes and is, in part, responsible for root number in all post-canine teeth. These canal to root relationships are significantly different between tooth types (i.e., molars and premolars), within and between the maxilla and mandible. Results indicate that Sub-Saharan African and Sino-American populations are significantly different in their canal to root numbers, and this difference represents an overall reduction in root number with distance from Africa, but not necessarily canal number. Canal to root relationships differ across all populations studied, however the reasons for these differences are not ultimately clear. To test population affinities and differences, future studies should include morphological distance-based analysis to test divergence, as well as consider additional biological, historical, linguistic and cultural data. Results also show that tooth types within and between the jaws have different linear relationships and that these relationships are significantly different. These results support biomechanical and spatial hypotheses related to tooth crown size in hominin evolution, and future studies should include root *and* canal count in their analysis.

## Chapter 5: Canal number and orientation are predictors of external root morphology

### 5.1 Abstract

Within the tooth root, canals can vary in shape and orientation, and it is not uncommon for a single root to contain multiple canals. Externally, root morphology also varies, though the range of variation, and its relation to canals remains little explored. This investigation of modern human post-canine teeth uses computerized tomography scans of a global sample of 945 modern humans to investigate the most frequent phenotypes of root and canal morphologies, and how canal number, shape, and orientation relate to external root morphology. Results (1) include descriptions of root and canal morphologies, counts, and configurations; (2) indicate that certain canal counts, morphologies, and orientations are significantly associated with certain external root morphologies; and can predict those external morphologies; and (3) and that this pattern varies in individual teeth and roots in the maxilla and mandible.

### 5.2 Introduction

The formation of tooth roots originates from complex interactions between Hertwig's epithelial root sheath (HERS) and the innervation and blood supply of the developing tooth (Huang and Chai, 2013; Miller, 2013). Nerve and vascular structures supporting the growing tooth enter the dental papilla at positions where the hard tissues (dentin and cementum) of the roots will eventually form (Miller, 2013). These structures eventually comprise part of the root canal pulp which differentiates into the dentine and cementum of the developing root.

The relationship between canal number and root number has been tested in the post-canine teeth of 945 humans, with results showing that canal number is equal to or exceeds root number across all teeth (Chapter 4). Results indicate that canal number predicts root number, and that tooth types (i.e., premolars and molars) within and between the maxilla and mandible share similar prediction curves of canal to root number. However, it is unknown if the number and configuration of these canal structures influence the shape

of the external morphology of tooth roots. This primary aim of this study is as test of the relationship between canal number and configuration, and external root morphology.

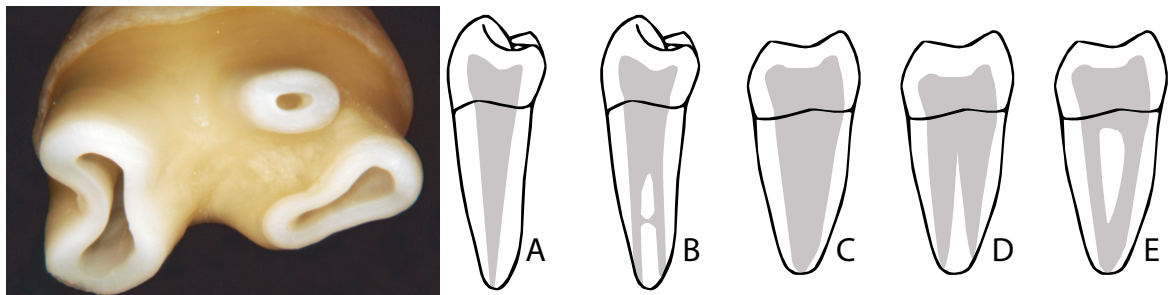


Figure 5.1: Left - Sectioned 1st maxillary molar showing canal morphology mimicking external morphology (Herbranson, 2015). Right - Canal number and morphology does not always follow external number and form. Grey area represents pulp chambers and various canal configurations. A and B are single-rooted mandibular premolars (distal view); C, D, and E are two-rooted mandibular molars (mesial view).

It is easy to conceptualize canals as round holes which taper towards the roots' apex, mirroring the external morphology of the root. In reality, the number and shape of canals does not always covary with number of roots, and many teeth have multiple canals within a single root (Figure 5.1 and see Chapter 4). Canals can be round, oval shaped, or one of several isthmus configurations; and multiple canals, when found in a single root, can join and separate in unpredictable places between the cemento-enamel junction (CEJ) and root apices (See Chapter 3, Figure 3.11). Several clinicians have developed typologies to classify root canal variation (Weine, 1969; Vertucci and Gegauff, 1979; Hsu and Kim, 1997; Fan et al., 2004a; Vertucci, 2005). The variation between systems is the result of technological restrictions (e.g., radiography, CT,  $\mu$ CT, etc.) and the appearance of accessory and lateral canals which extend from the pulp to the periodontal tissues surrounding the teeth; as some practitioners choose to include accessory canals in their typologies, while others focus on canal structures that extend from the pulp chamber and exit foramina in the apices of the root.

External root morphology has been less explored in the clinical literature, while the anthropological literature has generally emphasized root number and rare or infrequent morphologies (Figure 5.3). First described in *Homo neanderthalensis* molars (Keith, 1913), mandibular post-canine tooth roots and pulp canals are sometimes C-shaped (Figure 5.3A). This type of configuration consists of a root canal system in a 180-degree arc and is most common in 2nd mandibular molars (Fan et al., 2004a, 2004b; Fernandes et al., 2014). Also

common in Neanderthals, taurodont molars occur when the HERS fails to invaginate at the proper horizontal level (Figure 5.3C). As a result, the external shape of the root is enlarged, and the floor of the pulp chamber is displaced apically of the cemento-enamel junction. Mandibular premolars with a prominent mesial developmental groove of varying depth have been classified as Tomes' roots (Tomes, 1923 (Figure 5.3B)). This last feature is found in modern humans (Scott and Turner, 1997) and fossil members of *Homo* from the Chinese Middle Pleistocene and European Early Pleistocene (PRADO-SIMÓN et al., 2012; Xing et al., 2018).

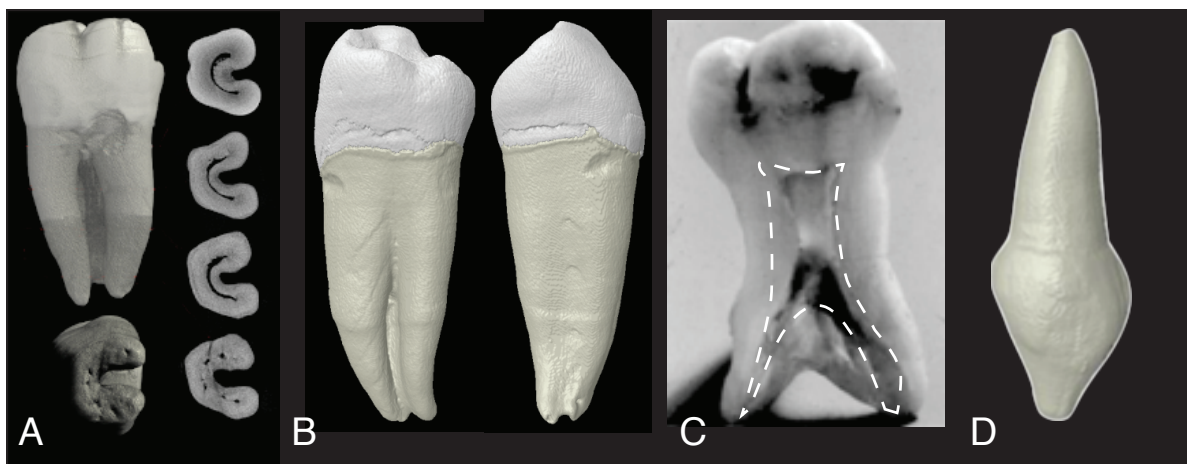


Figure 5.2: Rare and infrequent root morphologies: **A.** C-shaped tooth in (clockwise) lingual, cross-section with i2 canal configuration, and apical views. **B.** Tomes' root. Left = mesial view, right= distal view. **C.** Taurodont molar, apically displaced pulp chamber and canals outlined in white. **D.** Peg-shaped root. Images A,B, and D from the Root Canal Anatomy Project <http://rootcanalanatomy.blogspot.com/> (accessed 10 March 2019). Image C from <http://www.dentagama.com> (accessed 27th March 2019).

Externally, the roots of non-human primate and fossil species appear to be highly variable in number and morphology. For example, root morphologies described as 'plate-like' and 'dumb-bell' shaped, have been described in great apes, cercopithecoids, and Plio-Pleistocene hominins (Kullmer et al., 2011; Kupczik et al., 2019). However, in humans, emphasis has been on rare or infrequent morphologies, and identification of the total morphospace of external morphologies is under-explored. Further, what defines the most frequent phenotype (MFP) - root and canal number, external root morphology and in internal canal configuration - is unknown for humans. Chapter 3 describes multiple external root morphotypes derived from a global population of modern humans. Similar to the variation found in tooth cusp morphology (Turner and Nichol, 1991), these morphologies

exist as distinctive anatomical variants (Figure 5.4). Thus, it is possible that there is an untapped wealth of useful morphological features in tooth roots.

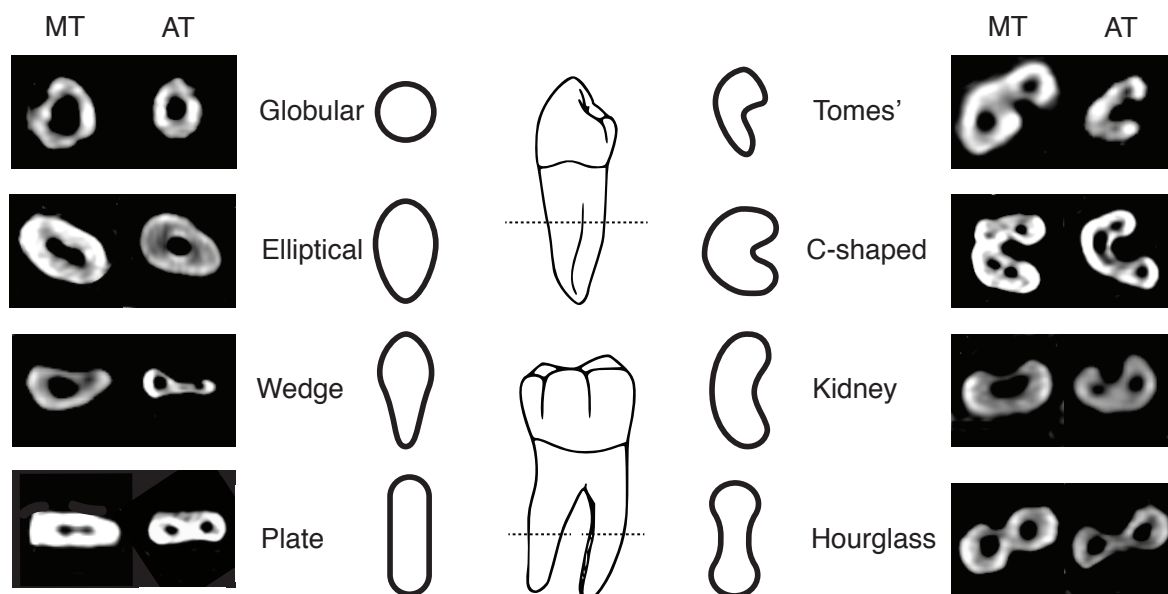


Figure 5.3: Left and right columns = axial CT slices showing external root morphologies at the middle third (MT) and apical third (AT). Centre illustrations = root morphologies at centre of root/s.

### 5.3 Materials and Methods

Only post-canine permanent teeth from the right side of the maxilla and mandible with completely developed roots were used for this study (See Chapter 4, Table 4.1). To assess counts of roots and canals (See Chapter 4, Tables 4.2 & 4.3), and morphology at the midpoint of the root (Figure 5.3) transverse CT cross sections of roots and canals were assessed in the Horos Project Dicom Viewer, version 3.5.5 (<https://www.horosproject.org>, 2016).

Data were analysed with the R Project for Statistical Computing, version 3.6.3. For basic descriptives, counts of traits for all teeth, combined by type, were included. However, primary analysis were carried out only for 'key teeth' (i.e.,  $P^3$ ,  $M_1$ ,  $P_3$ , and  $M_1$ ) as discussed in Chapter 3, Section 3.5 and Scott and Turner II (2015). Chi-Square test of independence was used to determine if there is a significant relationship between external root morphology and internal canal configuration at the  $p = 0.05$  significance level. A post-hoc analysis using Pearson residuals was used to determine which variables have the strongest association to one another and contribute to the Chi-Square statistic. Residual values past the threshold of  $\pm 3$  indicate a lack of fit. Cramer's V was used to measure the difference between observed

strengths of relationships between canal count and orientation to root morphology; with 0 = no relationship and 1 = perfect relationship. Because data do not meet the assumptions of a particular family of distribution (i.e., Gaussian), multinomial logistic regression (MLR) was used to test and model linear relationships between root morphology, and canal orientation and number. MLR uses a logarithmic function (logit) to reduce probability values between 0 and 1, with 0 indicating 0% predictive value, and 1 indicating 100% predictive value. Results report probability values between .50 and 1. Multinomial logistic regression was carried out using the "nnet" package (Venables and Ripley, 2002). Because C-shaped molars appear only in the M<sub>2S</sub>, a secondary analysis was carried out as M<sub>2</sub> should be considered the 'key tooth' for this trait (Turner II et al., 1991).

## 5.4 Results

CT scans of 4,366 post-canine teeth (See Chapter 4, Table 4.1) of 945 individuals from a global sample (See Chapter 3, Table 3.1) were used to test if canal number and orientation predicted external root morphology. Identification of the MFP of root morphology, canal count, and canal orientation are required for multinomial logistic regression. Counts of canal shapes and orientations in single and double-canaled roots were plotted to discern the MFP for descriptive purposes and to prepare for MLR (Figures 5.4-5.7). Results of Chi-Square test of independence and Kramer's V for the relationship between canal number and configurations, and external morphology are also reported.

### 5.4.1 Maxillary Premolars

The MFP of single-rooted, single-canaled maxillary premolars is plate-shaped (P) with an oval (O) shaped canal (n=861); and the majority of double-canaled variants are also plate-shaped, but with 2 round canals in an R4 (n=98) configuration (Figure 5.4). Plate-shaped single rooted premolars also have the most variation in canal orientations, with multiple forms appearing. The MFP of premolars with a single-canaled buccal root is globular (G) with a round (R) canal (n=525). Double-canaled buccal roots in premolars are rare and are minimally represented in this study (n=9). The majority of double-canaled buccal roots are hourglass (H) shaped with 2 round canals in an R2 configuration. Globular shaped roots with a single round canal account 99% of lingual roots of maxillary premolars.

A bifurcated, kidney (K) shaped root with an R2 canal configuration is the single representative of double-canaled lingual premolar roots in this sample.

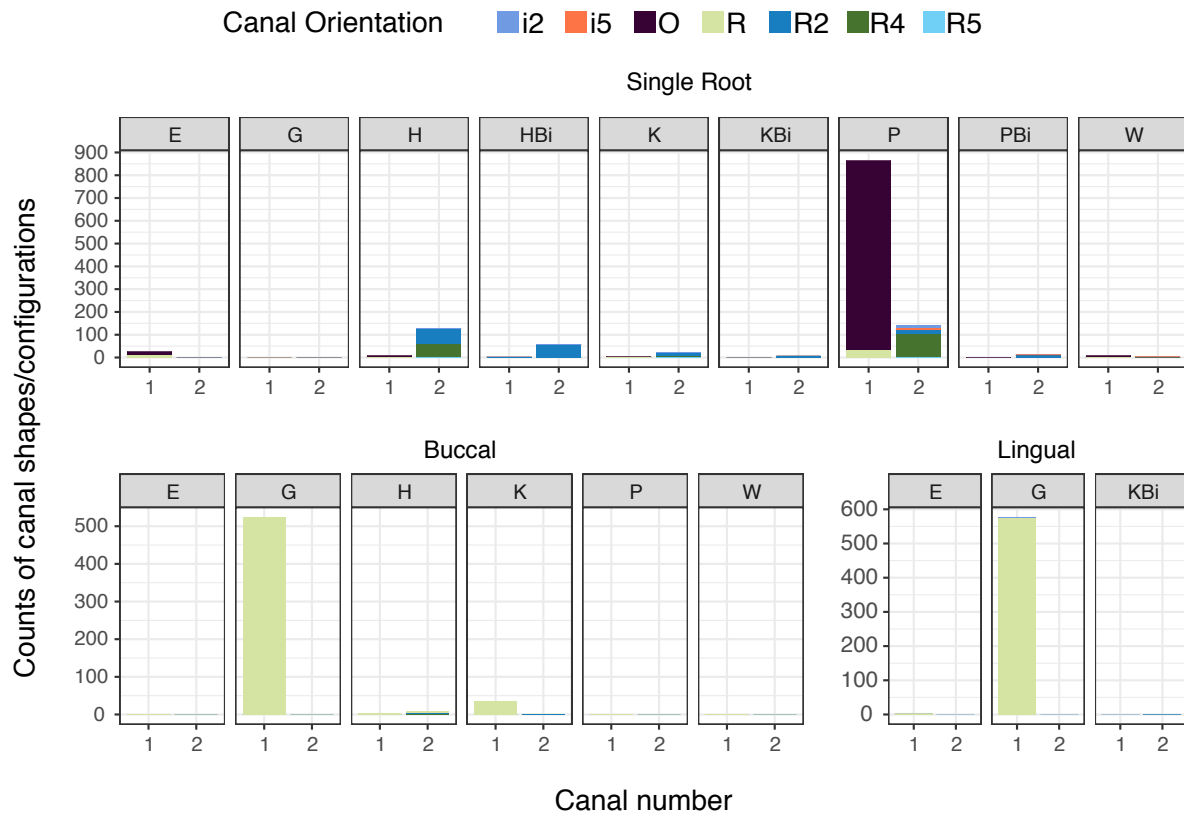


Figure 5.4: Counts of canal shapes and orientations in roots of maxillary premolars by canal number. Root forms: E = elliptical, G= globular, H = hourglass, K = kidney, P = plate, W=wedge. Bi = root form with apical bifurcation. Counts are calculated over combined root morphologies containing 1 or 2 canals.

#### 5.4.2 Maxillary molars

Maxillary molars can vary from 1-4 roots and 1-6 canals in total (Figure 5.5); and there is a wide range of variation in maxillary molar canal forms and root configurations. The MFP of single rooted, singled canaled maxillary molars is plate-shaped with an oval canal (n=215). No double-canaled single rooted maxillary molars are present in this study. The mesial root is the most diverse in external morphologies and internal configurations. For single-canaled variants, wedge (W) shaped mesial roots with a round canal are the MFP (n= 806). Wedge shaped with a R4 canal configuration are the MFP for two canaled variants (n=234). Due to the number of fused root configurations (MLF, MDF, DLF), maxillary molars tend to possess a diverse range of isthmus canal configurations. These are not limited to fused roots, and are present in plate, wedge, and hour-glass shaped roots too. The MFP of

maxillary buccal roots is globular with a single round canal (n=9), though kidney shaped roots with round and oval shaped canals are equally present. No double-canaled buccal root variants are present in the sample. Globular shaped roots with a single round canal account for 925 of distal maxillary molar roots, followed closely by elliptical shaped roots containing a single round canal accounting for 882. Distal roots are varied in their external morphology but constrained in their canal configurations; with most forms containing a single round canal. The single-canaled MFP is globular with a round canal. Globular shaped lingual roots are the MFP for single (n=1266) and rarer double-canaled (n=10) configurations.

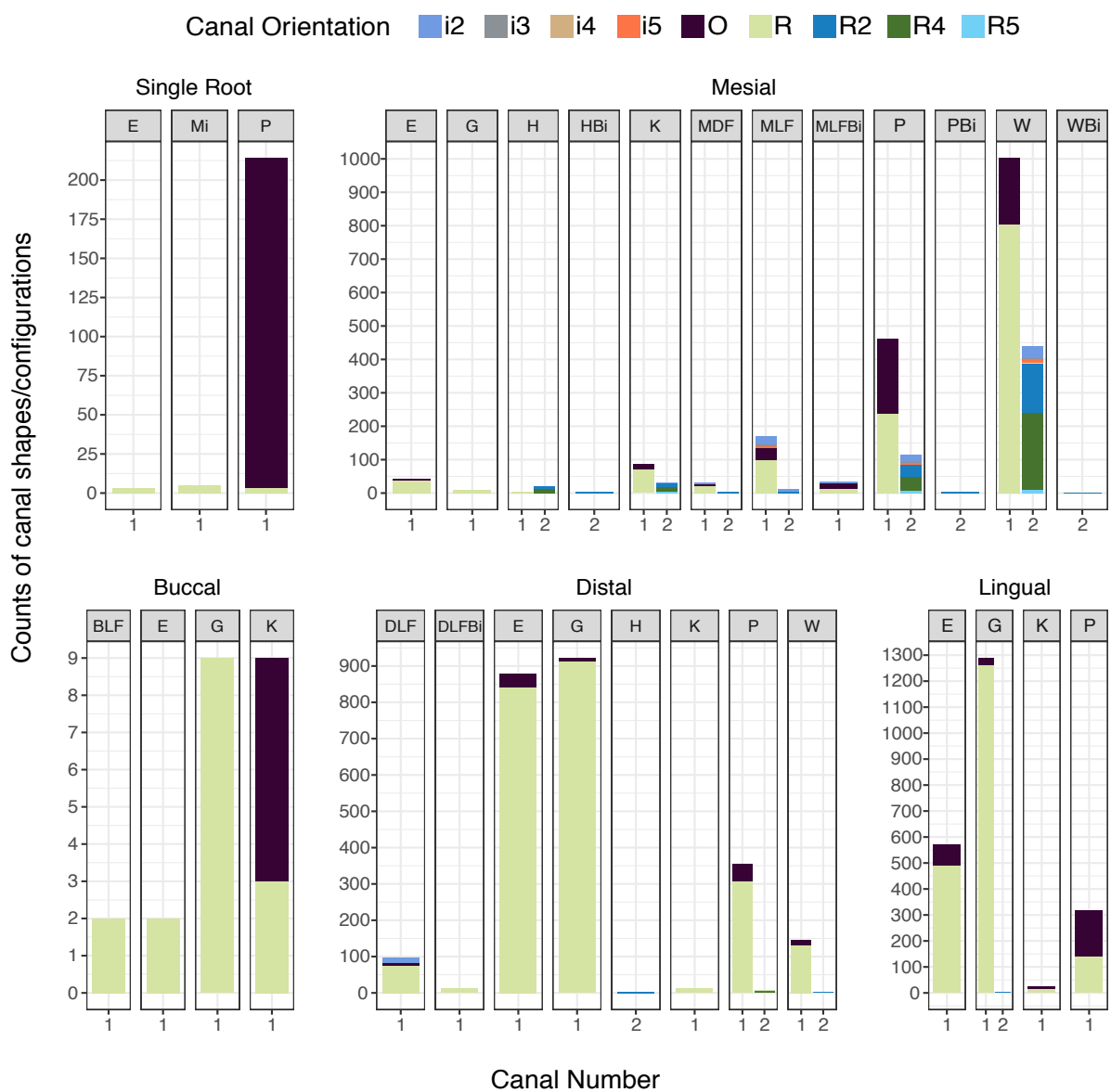


Figure 5.5: Counts of canal shapes and orientations in roots of maxillary molars by canal number. Root forms: E = elliptical, G= globular, H = hourglass, K = kidney, P = plate, W=wedge. BLF = Bucco-lingual fused, MDF = mesio-distal fused, MLF = mesio-lingual fused, DLF = Disto-lingual fused, Bi root form with apical bifurcation. Counts are calculated over combined root morphologies containing 1 or 2 canals.

### 5.4.3 Mandibular Premolars

Only single-rooted mandibular premolars appeared in the sample used for this study (Figure 5.6). The MFP of single rooted mandibular premolars is plate-shaped with an oval canal (n=1,328). Tomes' roots with varying configuration of isthmus canals, especially i5, are the MFP of double-canaled mandibular premolars (n=188).

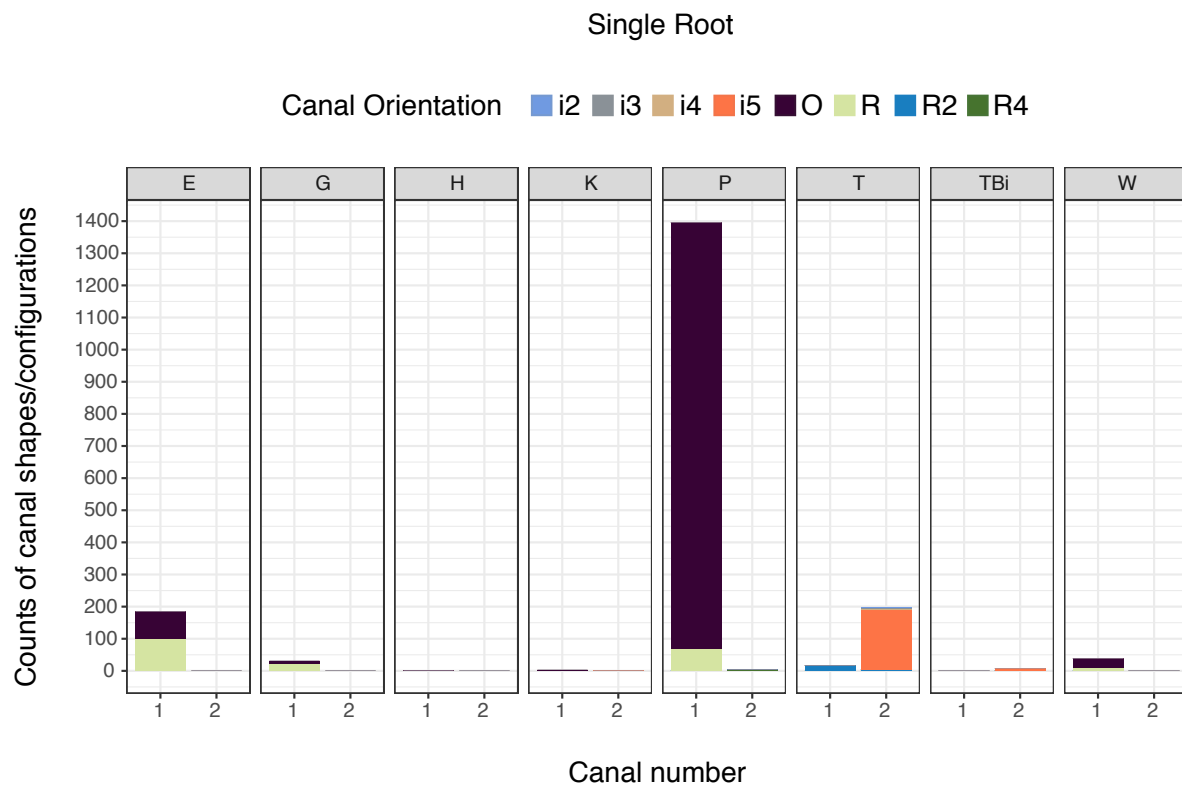


Figure 5.6: Counts of canal shapes and orientations in single rooted mandibular premolars by canal number. Root forms: E = elliptical, G= globular, H = hourglass, K = kidney, P = plate, W=wedge, Bi root form with apical bifurcation. Proportions are calculated over combined root morphologies containing 1 or 2 canals.

### 5.4.4 Mandibular Molars

Similar to their maxillary counterparts, mandibular molars have a wide diversity of external morphologies and internal canal configurations (Figure 5.7). Single rooted mandibular molars with a single canal are relatively rare; with the MFP being a pegged root with a round canal (n=6). Single rooted, double-canaled mandibular molars are predominantly C-shaped (n=41). Like Tomes' roots, C-shaped (Cs) teeth always have an isthmus canal variation (Figure 5.2); the dominant forms being i3 (n=10) and i4 (n=10). The MFP of single-canaled mesial roots is plate-shaped with an oval canal (n=479). Double-canaled mesial roots contain the most variations of mandibular root morphologies and canal

configurations, with the MFP being hourglass-shaped with and R2 canal configuration (n=719). Buccal roots are rare in mandibular molars, and in this sample (n=16). Here, globular shaped morphology with a single round canal is the MFP (n=10). The MFP of single-canaled distal mandibular molar roots is plate-shaped with an oval canal (n=1,010); though a large number are also kidney shaped (n=733). Double-canaled distal roots display great variation in root morphology and canal configuration. The MFP is plate-shaped with an i2 isthmus canal configuration (n=52). Globular roots with a single canal (n=81) and kidney shaped roots with 2 round canals (n=1) are the MFP for lingual roots.

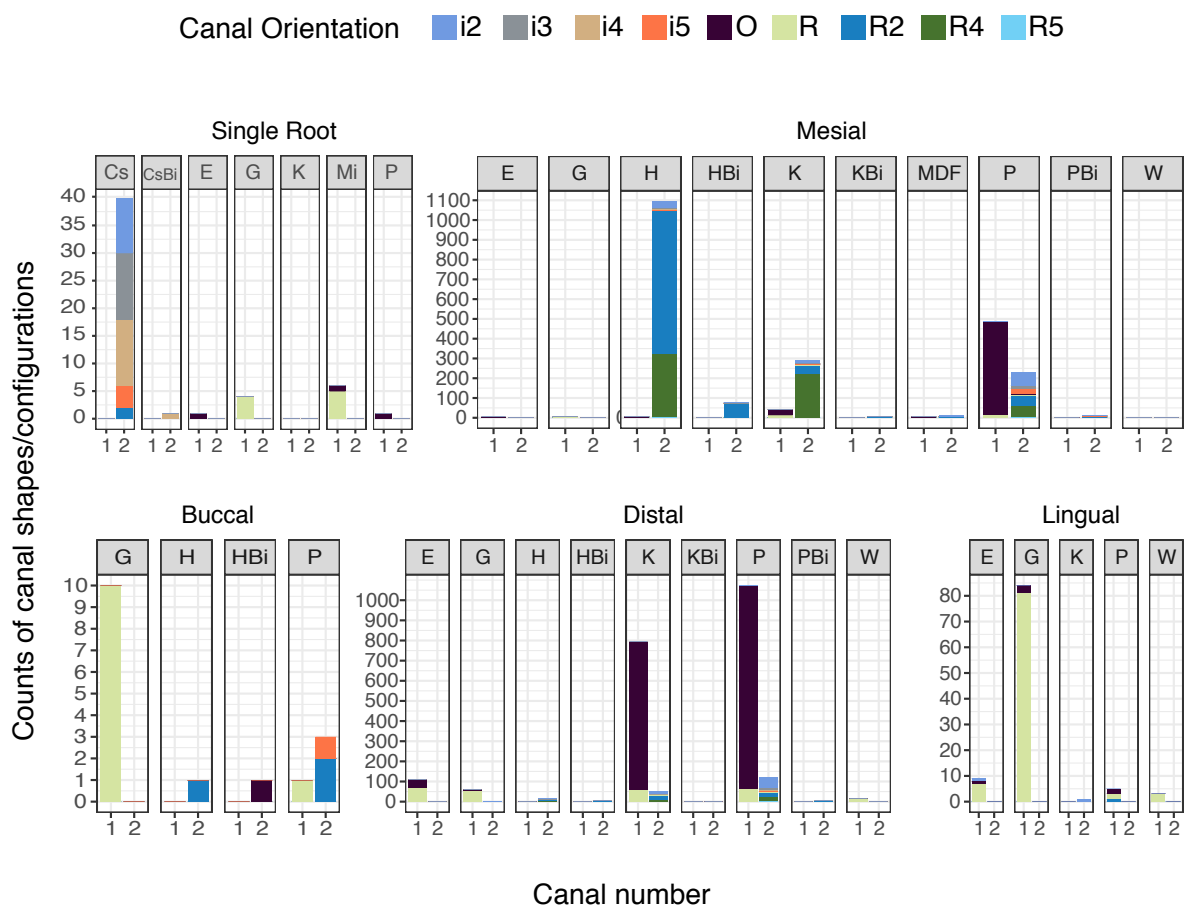


Figure 5.7: Counts of canal shapes and orientations in roots of mandibular molars by canal number. Root forms: E = elliptical, G= globular, H = hourglass, K = kidney, P = plate, W=wedge, Mi = pegged root, Cs = C-shaped, MDF = mesio-distal fused, Bi root form with apical bifurcation. Proportions are calculated over combined root morphologies containing 1 or 2 canals.

Figure 5.8 plots the MFP of external root morphology and internal canal morphology, count, and configuration in the roots of the maxilla, mandible, and jaws combined. For some roots there is no MFP found in the sample as either the roots show no MFP, or only the external form is invariant, and only varies in canal morphology and configuration.

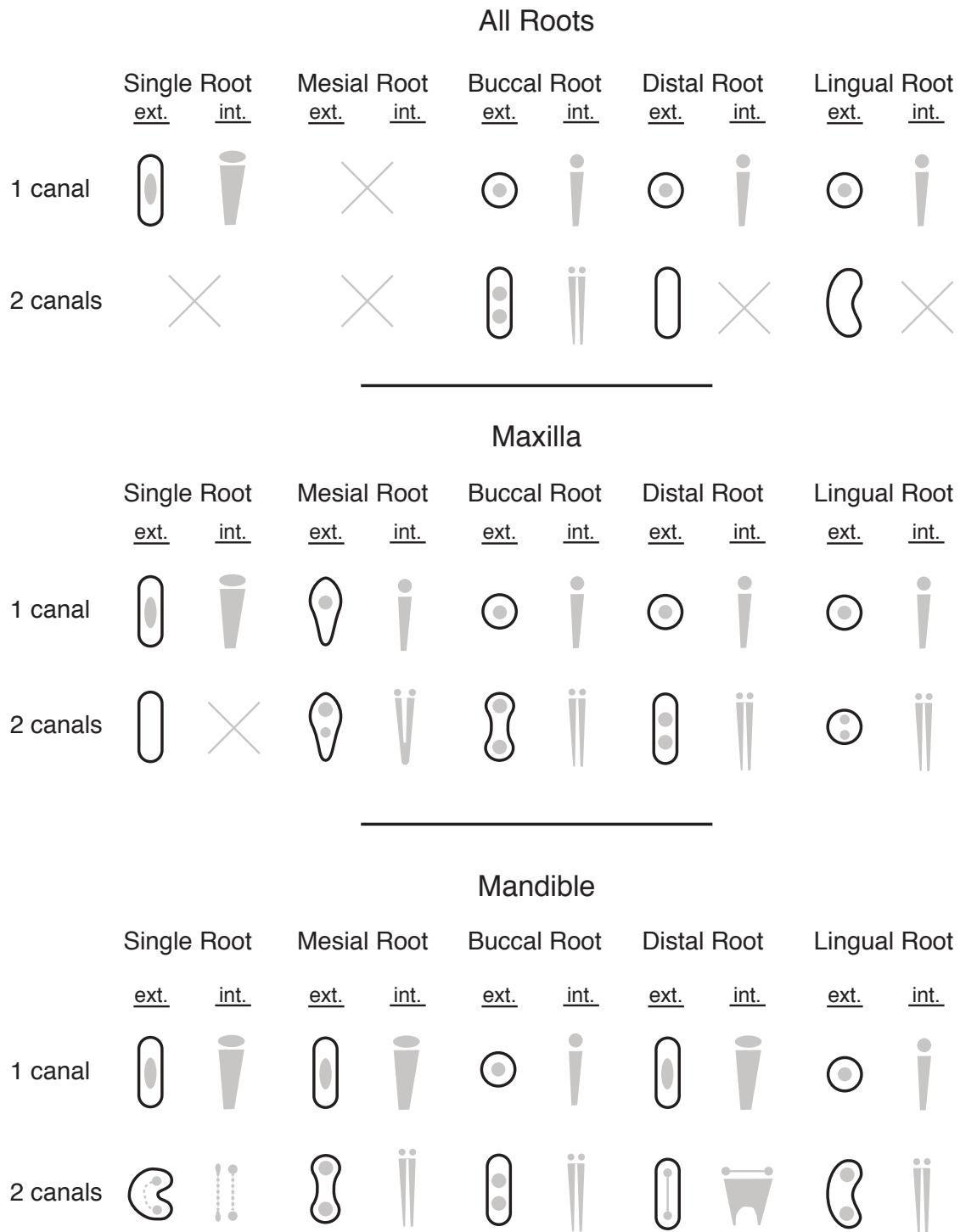


Figure 5.8: Most frequent phenotype of external root morphology and internal canal count and configuration. Solid grey = canal, ext. = external form, int. = internal configuration, X = no MFP, as all roots show different external *and* internal morphologies. Canal forms and descriptions are illustrated in Figure 5.2. **Top:** Pooled MFPs from all teeth of the maxilla and mandible by root. **Middle:** Pooled MFPs from all teeth of the maxilla. **Bottom:** Pooled MFPs from all teeth of the mandible.

Figure 5.9 shows the MFP for premolars and molars in the jaws. Based on these data, the MFP of maxillary and mandibular premolars are single rooted, with a plate-shape

external morphology and a single, oval canal. The MFP of maxillary molars is three roots with a wedge-shaped mesial root, and globular shaped distal and lingual roots, containing single, round canals. Mandibular molars are double rooted, with an hourglass mesial root containing two round canals, and a plate-shaped distal root with a single, oval canal. The MFPs are based on counts alone and do not reflect intra- or inter-population variability.

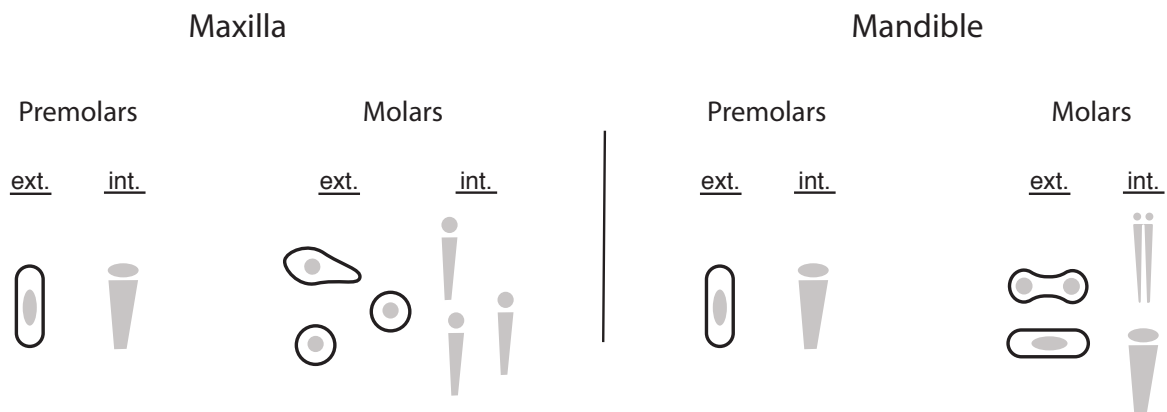


Figure 5.9: Most frequent phenotypes of external root morphology and internal canal count and configuration for maxillary and mandibular premolars and molars. Solid gray = canal, ext. = external form, int. = internal configuration. Figures are not in anatomical position but are aligned in a way that mimics their placement in the jaws.

Certain forms are in the clear majority. These are plate-shaped roots with single oval shaped canals, and globular shaped roots with single, round shaped canals (Figure 5.9). At least one of these external morphologies is found in all teeth in the maxilla and mandible with single and double canaled variants. While the plate-shaped, oval canaled form is the MFP for single-rooted teeth, it appears in multi-rooted teeth as well. Double canaled roots are more variable in their external morphologies and exhibit a number of canal configurations. This is less the case for the globular variant which rarely has more than one canal. The most common multi-canaled variant is the R2 configuration of two separate canals, followed by the R4 configuration of two distinct canals which are fused at their apices (Figure 5.2).

In multi-rooted forms, the pattern of external and internal morphologies is dissimilar between the molars of the maxilla and mandible (Figures 5.5, 5.7, & 5.8). Multi-rooted teeth show significantly more variation in external morphologies than single rooted teeth. For example, mesial and distal roots of multi-rooted maxillary molars have 12 and 8 external morphologies respectively, compared to only 3 external morphologies in single rooted

maxillary teeth. This variation is mirrored, especially in the case of maxillary molar mesial roots, by a high diversity of canal configuration. While single rooted maxillary teeth display 2 canal morphologies, mesial roots of multi-rooted teeth have 9, and distal roots display 7.

#### 5.4.5 Chi-Square test of independence between internal and external root morphology

A Chi-Square test was conducted to test independence of canal configurations and external root morphologies in P<sup>3</sup>s. Chi-Square statistics show that P<sup>3</sup> canal configurations and external morphology are significantly related in our sample, while Cramer's V shows a strong relationship between root and canal morphology for all roots (Table 5.1). There were not enough P<sup>3</sup>s with mesial or distal roots for inclusion with this study.

Table 5.1: Results of Chi-Square test of independence and Cramer's V for P<sup>3</sup>s

Root	$\chi^2$	df	<i>p</i> -value	Cramer's v
Single	497.20	42	0.005	0.43
Buccal	145.95	8	0.012	0.39
Lingual	491.00	2	0.003	1.0

Standardized residuals for individual roots of maxillary P<sup>3</sup>s reveal strong associations between certain internal configurations and morphologies (Figure 5.10). Noticeably, all bifurcated (Bi) root morphologies are strongly associated with double-canaled configurations (R2-R5, i1-i5), and weakly associated with single canal configurations. Non-bifurcated hourglass and kidney forms show similar associations with the exception of plate-shaped morphology, which is only associated with a single oval canal. Globular and elliptical shaped morphologies are strongly associated to single canal morphologies. The overall pattern, however, is of independence between canal configurations and external morphologies. For example, in lingual roots it is only the KBi morphology that is significantly related to canal configuration, while residuals for other morphologies fall with range of the Chi-Square distribution.

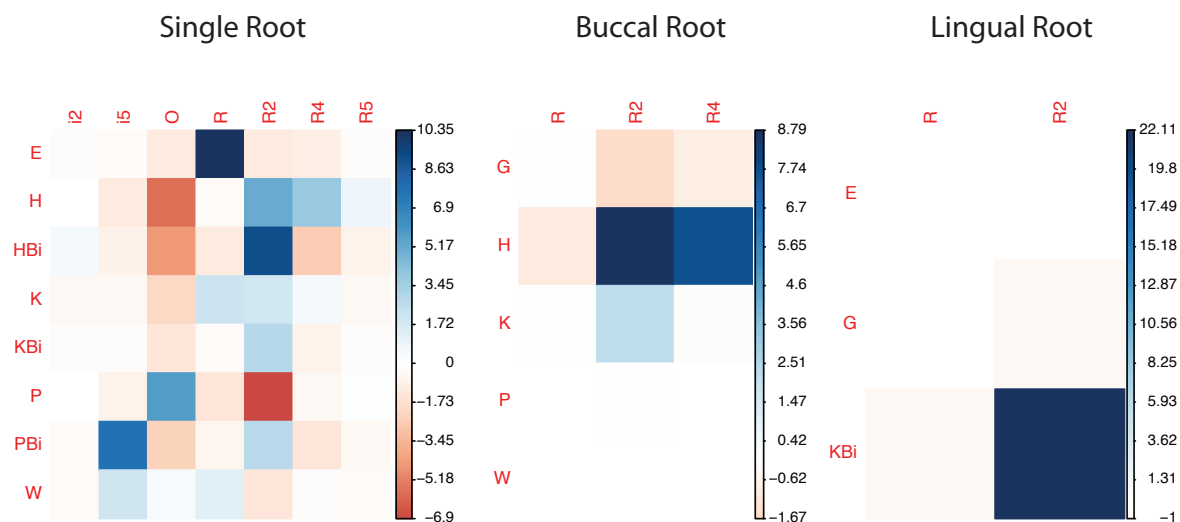


Figure 5.10: Standardized residuals of Chi-Square test for P<sup>3</sup>s. Cells with strong contribution to the  $\chi^2$  score are displayed in blue while cells with weak contribution are in red. x-axis= canal configurations, y axis = external root morphology.

Chi-Square statistics show that canal number and configurations, and external morphology are significantly related in M<sup>1</sup>s with the exception of mesial roots (Table 5.2). Standardized residuals for individual roots of M<sup>1</sup>s reveal similar patterns of strength of association between canal configurations and external morphologies (Figure 5.11). Fused roots (MLF, MDF, DLF) are strongly associated with isthmus canal configurations. Cramer's V shows a weak relationship between root and canal morphology for all maxillary molar roots here. As with P<sup>3</sup>s, the overall pattern is one of independence, with only a few pairings of external morphology and canal configuration falling outside the Chi-Square distribution (Figure 5.11). There were not enough M<sup>1</sup>s with single or buccal roots for this study.

Table 5.2: Results of Chi-Square test of independence and Cramer's V for M<sup>1</sup>s

Root	$\chi^2$	df	p-value	Cramer's v
Mesial	96.83	64	0.159	0.11
Distal	153.76	30	0.024	0.18
Lingual	328.8	16	0.004	0.30

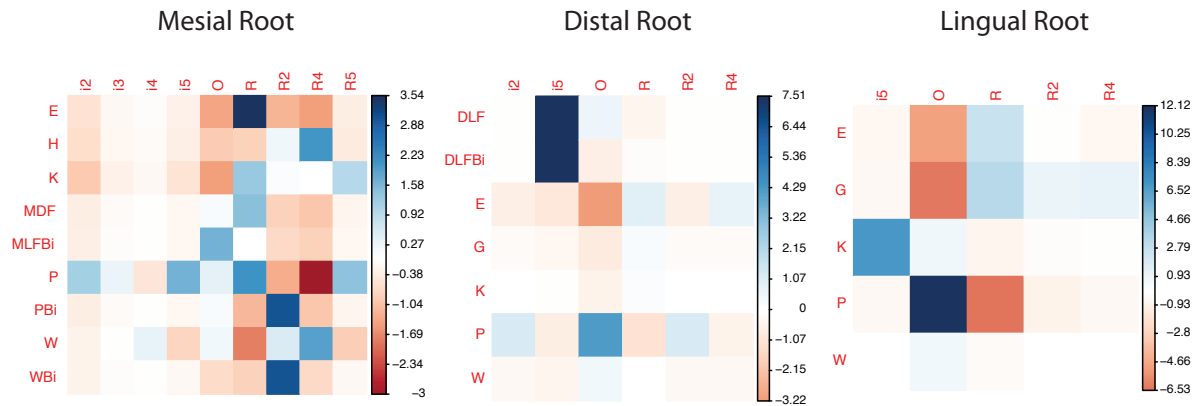


Figure 5.11: Standardized residuals of Chi-Square test for M<sup>1</sup>s. Cells with strong contribution to the  $\chi^2$  score are displayed in blue while cells with weak contribution are in red. x-axis= canal configurations, y axis = external root morphology.

The Chi-Square statistic show that canal number and configurations, and external morphology are significantly related in mandibular premolars, while Cramer's V indicates a strong relationship between internal and external morphologies (Table 5.3).

Table 5.3: Chi-Square test of independence and Cramer's V for P<sub>3</sub>

Root	$\chi^2$	df	p-value	Cramer's v
Single	1123.4	42	<.001	0.41

Standardized residuals for P<sub>3</sub>s are limited to single rooted variants (Figure 5.12). For single mandibular premolar roots, Tomes' (T) roots are exclusively associated with isthmus canal configurations, while globular (G) and elliptical (E) morphologies are only associated with single round canals. As with the roots of other teeth, plate-shaped roots have a strong association with oval shaped canals, while bifurcated teeth have a strong association with double-canaled configurations. Again, the overall pattern is of independence as very few of the canal configuration and root morphologies contribute to lack of fit.

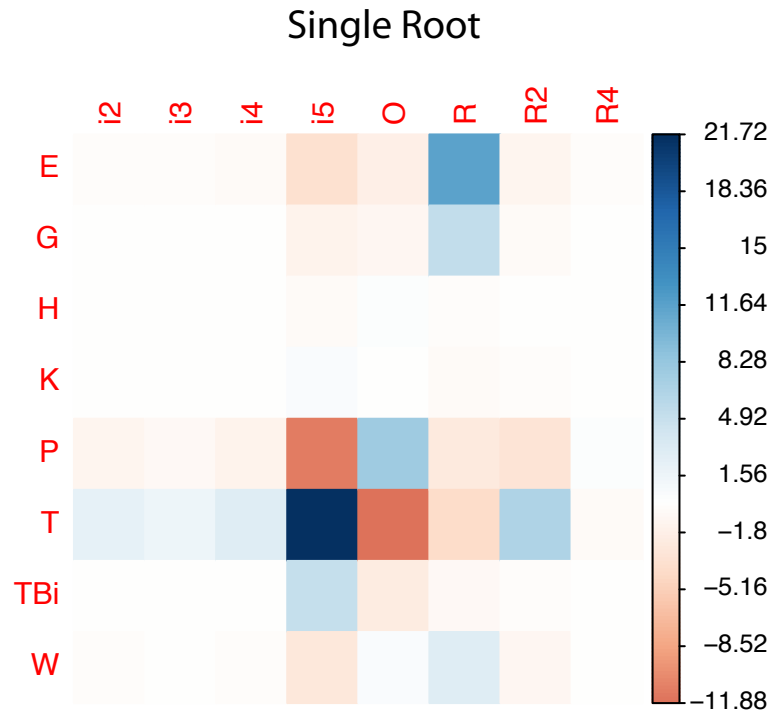


Figure 5.12: Standardized residuals of Chi-Square test for P<sub>3s</sub>. Cells with strong contribution to the  $\chi^2$  score are displayed in blue while cells with weak contribution are in red. x-axis= canal configurations, y axis = external root morphology.

Chi-Square statistics show that canal number and configurations, and external morphology are, with the exception of lingual roots, significantly related in mandibular molars (Table 5.4).

Table 5.4: Chi-Square test of independence results and Cramer's V for M<sub>1s</sub>

Root	$\chi^2$	df	p-value	Cramer's v
Mesial	723.91	40	<0.0001	0.38
Distal	630.78	64	<0.001	0.29
Lingual	9.34	4	0.053	0.25

Standardized residuals reveal that, like other teeth, bifurcated forms are most associated with double-canaled configurations (Figure 5.13). In most roots, plate (P) shaped roots are strongly associated with oval (O) shaped canals, the exception being the buccal root where the strongest relationships are between 2-canaled configurations. Globular (G) and elliptical (E) shaped roots are most associated with single round (R) and oval (O) canals, respectively. Very few of the canal configuration and root morphologies contribute to lack of fit.

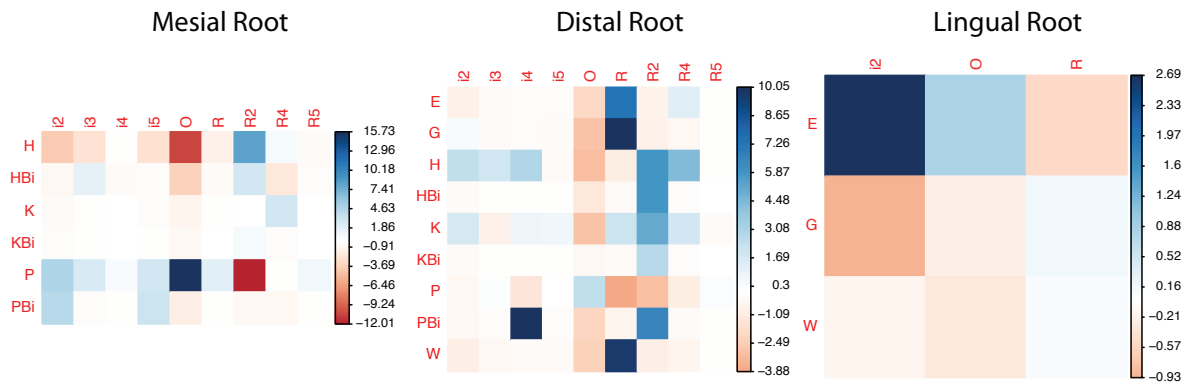


Figure 5.13: Standardized residuals of Chi-Square test for  $M_1$ s. Cells with strong contribution to the  $\chi^2$  score are displayed in blue while cells with weak contribution are in red. x-axis= canal configurations, y axis = external root morphology.

A separate analysis was carried out for  $M_2$  as it is the 'key tooth' for C-shaped roots and canals (A.A. Dahlberg, 1945; Turner II et al., 1991; Fernandes et al., 2014). Chi-Square statistics show that canal number and configurations, and external morphology are not significantly related in mandibular molars (Table 5.4).

Table 5.5: Chi-Square test of independence and Cramer's V for  $M_2$  trait – C-shaped root and canal

Root	$\chi^2$	df	p-value	Cramer's v
Single	0.545	2	0.761	0.0

Standardized residuals reveal that C-shape (Cs) molars are associated with, but independent from isthmus canals (Figure 5.14).

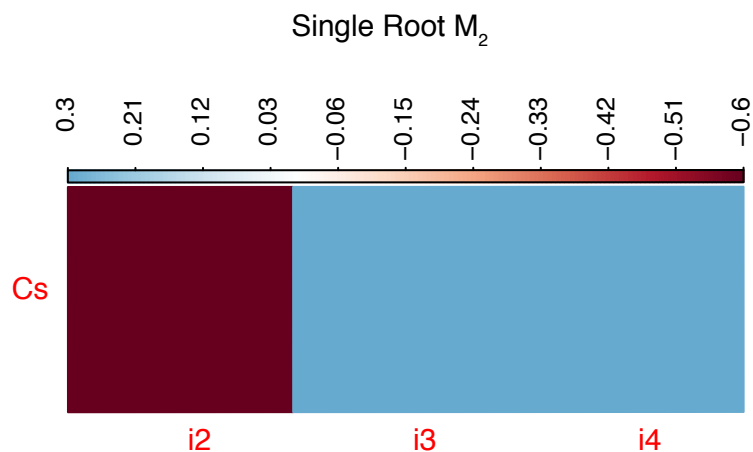


Figure 5.14: Standardized residuals of Chi-Square test for  $M_1$ s. Cells with strong contribution to the  $\chi^2$  score are displayed in blue while cells with weak contribution are in red. x-axis= canal configurations, y axis = external root morphology.

### 5.4.6 Predictions of External Root Morphology

Multinomial logistic regression (MLR) was used to test if canal number and configuration can predict external morphology in P<sup>3</sup> (Figure 5.15). Sample size of maxillary P<sup>3</sup>s with mesial and distal roots were too small, and/or with too few levels for inclusion with analysis. Regardless of canal number, single rooted maxillary premolars are plate shaped. A single oval canal predicts a plate-shaped root (96.4%), and the same morphology is predicted by a double-canaled i2 configuration (66.67%), double-canaled i5 configuration (50.00%), double-canaled R4 configuration (60.81%), and double-canaled R5 (99.98) configuration. A single round canal predicts a globular buccal root (93.97%), a double-canaled R2 configuration predicts an hourglass morphology (66.68%), while a double-canaled R4 configuration predicts an hourglass morphology (100.0%). A single round canal predicts globular lingual roots (99.39%), a double-canaled i2 configuration predicts globular lingual roots (99.39%), while and R4 canal configuration predicts a bifurcate kidney shaped morphology (100.0%)

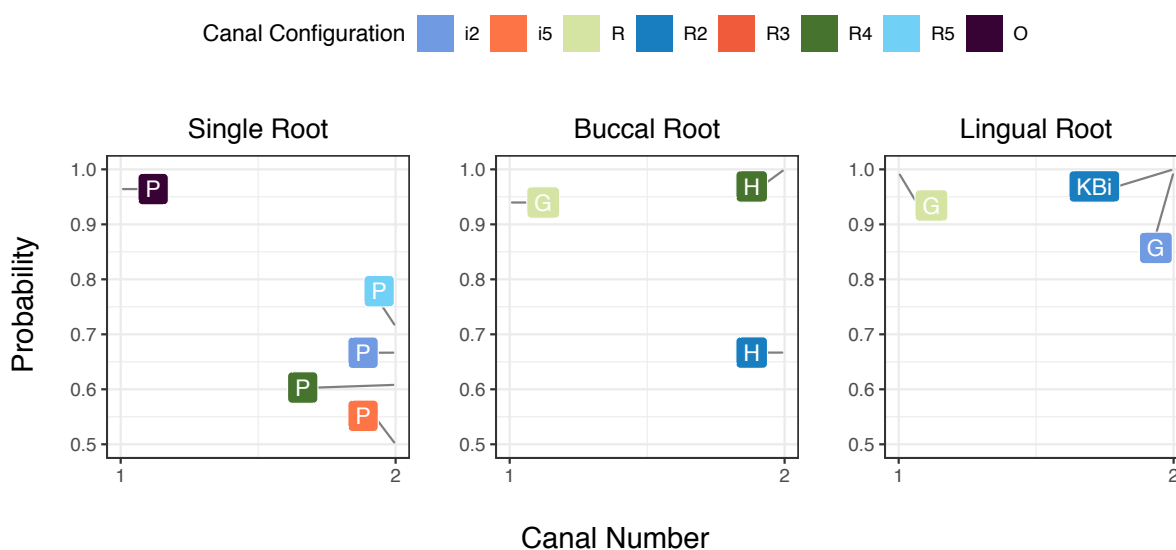


Figure 5.15: MLR of canal number to canal configuration and root morphology in P<sup>3</sup>s. Most frequent phenotype for single roots = plate-shaped (P); buccal roots = globular (G); lingual roots = globular (G).

Results of MLR for maxillary molars are presented in Figure 5.16. Sample size of single-rooted M<sup>1</sup>s was too small (n = 2) and with too few levels (n = 1) for inclusion in analysis. Sample size of M<sup>1</sup>s with buccal roots was also too small (n = 4) and with too few levels (n = 2) for inclusion in analysis. While the MFP of mesial roots is wedge shaped, there are no canal configurations that predict this shape with over 80.60% accuracy. The single-

canaled form is predicted by a round canal (61.02%) and an oval canal (70.73%). A number of isthmus canal variations appear, though it is the double-canaled R4 configuration that has the most predictive power (80.60%). Both i2 isthmus and R2 canal configurations have the most predictive power for double-canaled plate-shaped distal roots (100%). Single-canaled plate-shaped roots are predicted by oval canals (71.91%). Double-canaled kidney shaped lingual roots are predicted by i5 isthmus canal configurations (99.84%), while globular variants are predicted by R4 canal configurations.

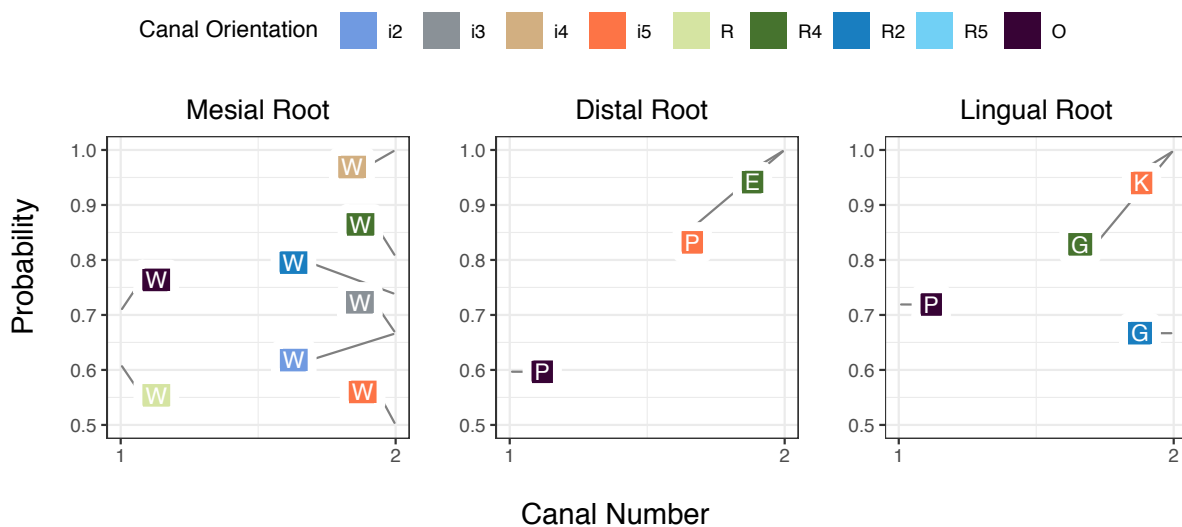


Figure 5.16: MLR of canal number to canal configuration and root morphology in M<sup>1</sup>s. Most frequent phenotype for single roots = plate-shaped (P); mesial roots = wedge (W); buccal roots = globular (K); distal roots = globular (G) lingual roots = globular (G).

All P<sub>3</sub>s used in this study were single rooted. The majority of double-canaled mandibular premolars are Tomes' roots (Figure 5.17), while single-canaled premolars are plate-shaped. All Tomes' shaped premolars have isthmus canal configuration while plate-shaped roots do not. A single oval canal predicts a plate-shaped single rooted mandibular premolar (89.7%), while R2 and R4 double-canaled variants predicts plate-shaped 50.00% and 99.99% respectively. Double-canaled mandibular premolars are either plate-shaped or a Tomes' root. Isthmus canal i2-i5 configurations predict the Tomes' root morphology; with i3 having the greatest predictive power (99.99%).

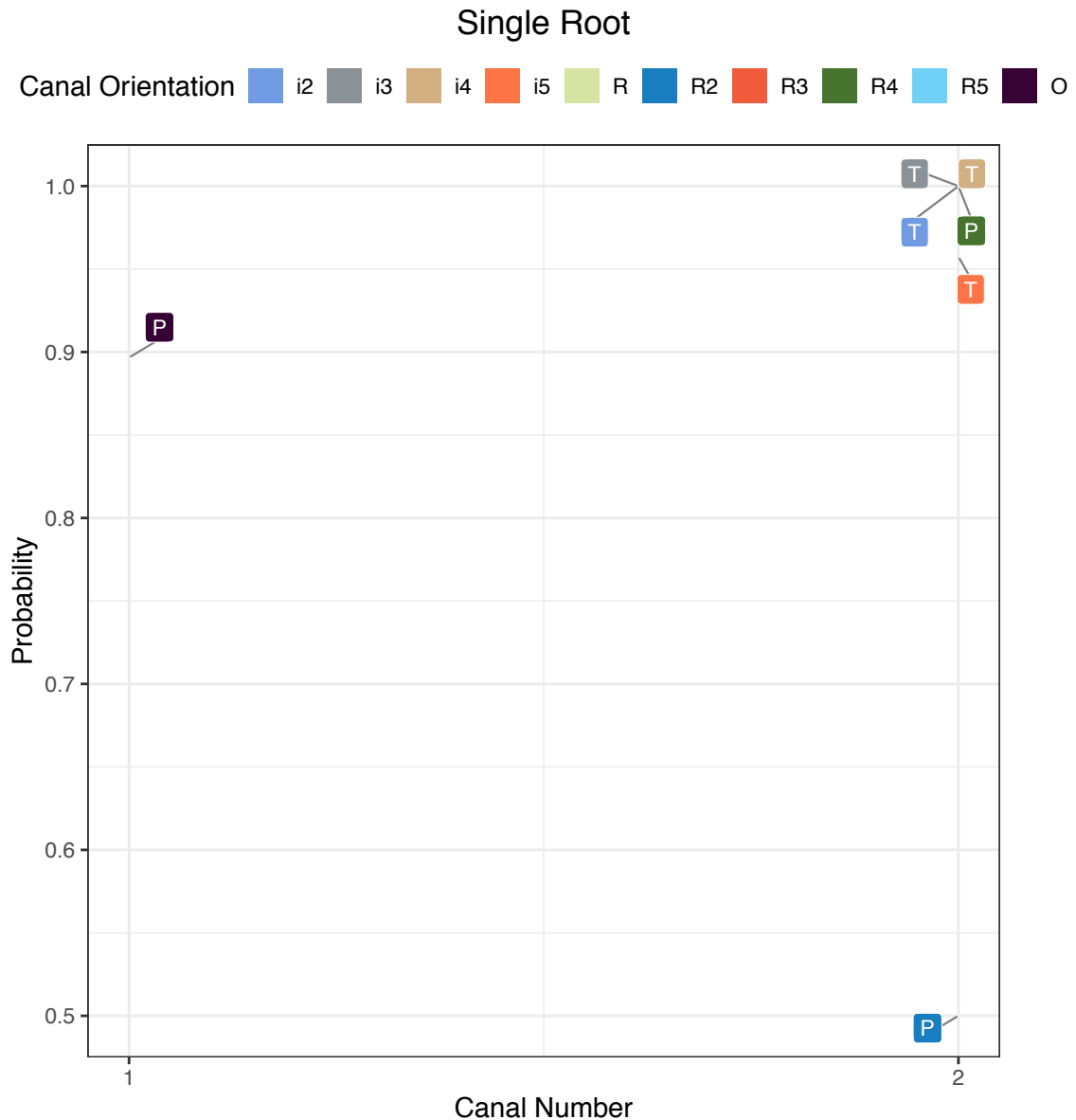


Figure 5.17: MLR of canal number to canal configuration and root morphology in P<sub>3</sub>s.

Results of MLR for M<sub>1</sub>s are presented in Figure 5.18. A single oval shaped canal has the greatest predictive power for single-canaled mesial mandibular molar roots (91.6%). Amongst a number of canal configurations, a two canaled R2 configuration is the best predictor for hourglass-shaped double-canaled mesial roots (79.6%). Distal roots are predominantly plate-shaped with varying canal shapes and configurations. An oval shaped canal predicts the single-canaled plate morphology at 56.2%, while double-canaled R5 morphology predicts plate-shaped morphology at 99.0%, followed by a number of isthmus canal variants. A single round canals predict globular shaped lingual roots (87.10%), and

kidney shaped is predicted by an i2 isthmus canal morphology in Double-canaled variants (99.9%). There were not enough single rooted  $M_{1s}$  or  $M_{1s}$  with buccal roots for this study.

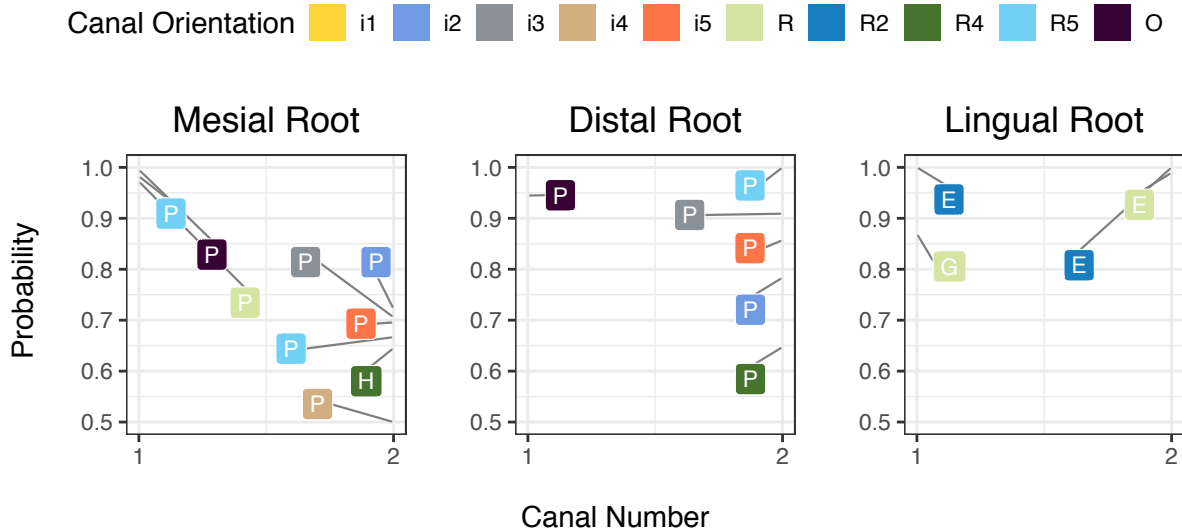


Figure 5.18: MLR of canal number to canal configuration and root morphology in  $M_{1s}$ .

Results of MLR for  $M_{2s}$  with C-shaped roots and canals are presented in Figure 5.19. C-shaped molars are characterised by isthmus canals (Fan et al., 2004a; Fernandes et al., 2014), and here they predict C-shaped roots 100.0% of the time. A single round canal predicts a single-rooted G-shaped morphology 99.99% of the time.

## Single Root $M_2$ - C-shaped trait

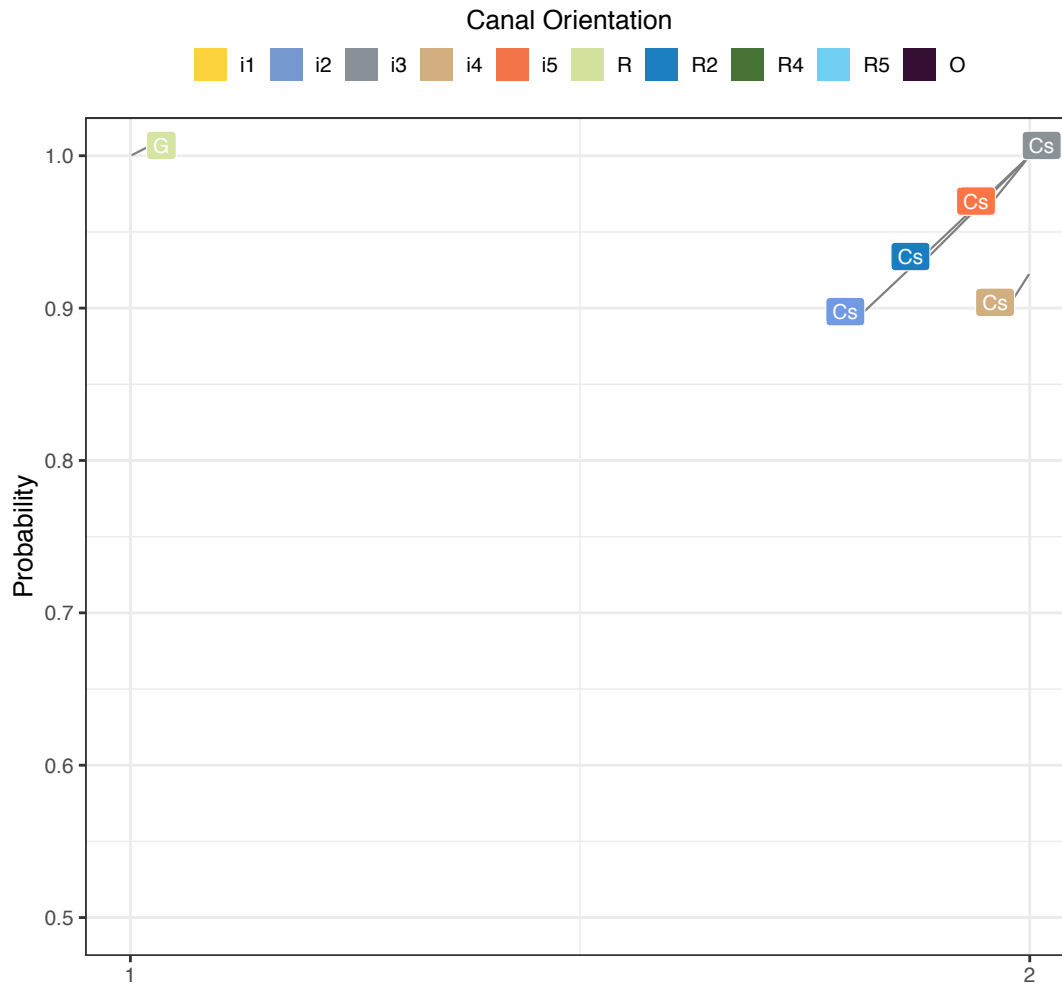


Figure 5.19: MLR of canal number to canal configuration and root morphology for  $M_2$  C-shaped roots and canals.

### 5.5 Discussion

This paper set out to (1) discover and describe the most frequent root and canal morphologies, and canal count and configurations in the post canine teeth of a global sample of modern humans; and (2) test the associative and predictive power of canal count and orientation on external root morphology. It has shown that there are MFPs for teeth within and between the maxilla and mandible; and that there is a significant associative and predictive power between internal and external tooth root morphologies.

### 5.5.1 Predictive power of canal number, morphology, and orientation on external root morphology

Chi-Square tests of independence indicate that canal morphology and orientation have varying degrees of independence and significant association with external root morphology (Tables 5.1-5.5). The overall pattern is one of independence, which is in accordance with previous studies of non-metric traits (see Section 3.5). Several clear patterns emerge. The first is that certain external morphologies mirror internal morphologies. This is especially noticeable between globular roots and round canals, and plate-shaped root and oval canals; as well as C-shaped and Tomes' roots with isthmus canals, and bifurcated forms with 2 canals (e.g., R2 configuration). Another interesting pattern is that in roots with an increased height to width ratio (i.e., plate, hourglass, elliptical, wedge, kidney), that wider roots are more strongly associated with double-canaled forms. This can be interpreted in several ways. The first is that two canals require a wider root. In this scenario, all 'wide' roots (i.e., plate, hourglass, kidney) have two canals, and the relationship is a spatial one. While this is true for this sample, the interpretation is problematic, as it is not apparent that root shape or canal count is a function of the physical dimensions of the root. Alternatively, while blood vessels do appear in locations that roots will eventually form (Miller, 2013), they may not be the prime determinants of root number and variation. During root morphogenesis, the developing root sheath produces inter-radicular processes (IRP's), finger-like protrusions adjacent to the cervical foramen of the tooth crown. The extension and fusion of opposing IRPs across the cervical foramen create multiple secondary foramina which, in turn, form multiple tooth roots (Kovacs, 1971; Orban and Bhaskar, 1980). It may be that number and orientation of IRP's is responsible for tooth root dimensions and/or shape alone. Future studies may be able to elucidate this by comparing location and measure of IRPs to root dimensions.

Based on the predictive power of canal number, morphology, and orientation, as well as Chi-Square tests of independence, the former explanation seems the better of the two. Multiple canaled forms do predict wider and/or bifurcated roots, and these predictions coincide with MFPs described in Figures 5.8 and 5.9. One root breaks this pattern - mesial wedge-shaped roots of maxillary molars. This root is predicted by nearly every double-

canaled variant and morphology, none of which mirror its external form. This suggests, again, that the relationship between canals and external morphology is a more a spatial one. However, this may be due to certain roots having more 'evolvability' than others (discussed below).

### 5.5.2 Constrained phenotypes and the most frequent phenotype

While tooth roots possess a great deal of external and internal morphological variation, the diversity of individual roots in this sample is overwhelmingly constrained to several forms stemming from the interactions between their internal and external features (Figures 5.8 and 5.9). Phenotypic variation is the raw material upon which selection and drift acts. However, phenotypic variation in organismal development is biased towards certain phenotypes (Smith et al., 1985; Arthur, 2004; Wilkins, 2007). While canal and root formation are comprised of a series of reciprocal cellular interactions (Jernvall and Thesleff, 2000), clusters of blood vessels entering the developing tooth coincide with the positions where roots will eventually form (Miller, 2013). These observations of root development suggest that the structures that help determine root number and position are present early in tooth morphogenesis and play some part in the 'developmental bias' of roots. There is a clear relationship between canal and root number, in which canal number is either equal to or exceeds root number. This supports the hypothesis that canal number precedes and is, in part, responsible for root number in teeth (Chapter 4). The results of this study support these earlier findings as canal number, morphology, and orientations are predictive of external root morphology, and the tooth root phenotypes of the phenotypic set.

Taken in the above context, these results raise several important questions. The first is why are tooth root phenotypes so constrained? The most obvious answer is that, like tooth crowns, roots are under strong genetic control; and disturbances due to genetic alterations may lead to morphological defects or inhibit or cease development. Plate-shaped, oval-canaled, and globular shaped, round canaled roots are the MFP in the study sample. These forms are not only present in Plio-Pleistocene hominins and non-human primates (Hillson, 1996; Chapter 5), but in early mammals of the Jurassic period as well (Luo and Wible, 2005; Luo et al., 2015); suggesting a deep evolutionary history for these forms.

Thus, it would appear that not only are root forms developmentally and phenotypically constrained, but that these constraints are shared in early mammalian lineages as well.

These constraints may be due to the evolutionary adaptability or, 'evolvability' of tooth roots. The capacity to generate novel, heritable phenotypic variation defines a trait's evolvability (Kirschner and Gerhart, 1998). At the cellular level, regulatory proteins act to promote or inhibit the number of random mutational steps needed to generate novel regulatory mechanisms (Kirschner and Gerhart, 1998). These regulatory processes are relevant to evolutionary processes as they can reduce constraints on change and the accumulation of non-lethal variants. The greater the number and specificity of a protein's functional requirements, the more resistant they are to change. Additionally, a protein's structural stability enhances its capacity to evolve by allowing it to accept a wider range of beneficial mutations while retaining its ability to fold to its original structure (Bloom et al., 2006). Together, the number, specificity, and stability of proteins helps explain evolution's extensive morphological and physiological diversity in light of taxon-wide conservation of core genetic, cellular, and developmental processes.

The concepts of developmental bias, evolvability, and phenotypic constraint, help inform the second question - if tooth roots are so phenotypically constrained, why do certain roots exhibit higher levels of diversity? Based on the above results, and the results discussed in Chapter 4, the presence of additional canals and canal configurations are responsible for different external root forms. This suggests that multiple canals, which conserve core genetic, cellular, and developmental processes of tooth morphogenesis, may have more 'evolvability' than single canaled forms. However, an equally plausible explanation is that canals act as a scaffolding around which the external components of roots differentiate and grow, and ultimately take their final shape from. The two need not be mutually exclusive, as the processes underlying the entirety of root morphogenesis are reciprocal (Jernvall and Thesleff, 2000).

In light of these two questions, what is interesting is that certain roots seem to be more variable than others. The most variable is the mesial root of maxillary molars which exhibits 12 external morphologies and 9 canal configurations. Why this root should exhibit so much variation while others do not is unknown. Additionally, its external morphology does not mirror internal morphology as there is no wedge-shaped canal, and the morphology is retained regardless of canal number or orientation. It has been observed that

mandibular premolars are the most variable teeth for humans, fossil hominins, and non-human primates (Wood and Abbott, 1983; Wood et al., 1988; Shields, 2005; Moore et al., 2013, 2015, 2016; Emonet and Kullmer, 2014). However, this study and the results of chapter 4 suggest that it is maxillary molars that are the most variable, not only in root number, but in exterior root morphology, canal number and morphology, and canal orientation. Unfortunately, tests of protein activation and inhibition on tooth root morphology are beyond the scope of this study.

### 5.5.3 Biomechanical explanations

Roots function to anchor the teeth to the jaws, and to absorb and transmit the directional forces of mastication. It may simply be that root variation in general, and MFPs in particular, are well adapted for this purpose. In a study of maxillary 1st molar root forms in non-human primates and South-African robust and gracile Australopiths, root shape, size, and orientation were found to correlate with diet, bite force, and chewing pattern (Kupczik et al., 2018). Tooth crown size is already known to correlate to diet in hominins (Moggi-Cecchi and Boccone, 2007) and non-human primates (Spencer, 2003; Kupczik et al., 2009), however the relationship between dietary strategy and masticatory forces to tooth roots is poorly understood. Biomechanical explanations do not negate developmental bias, evolvability, and/or phenotypic constraint. It may be that the MFPs of roots are under strong stabilizing selection in modern humans.

## 5.6 Conclusions

This paper presents the first investigation into the relationship between canal number, morphology, and orientation to external root morphology. The most frequent phenotypes are described for post canine teeth of the maxilla, mandible, and jaws combined. Result indicate that certain canal morphologies and orientations are strongly associated with and can predict external root morphology. It is unclear why internal and external variation is distributed the way it is, or why the internal and external structures of some roots are more variable than others. Future studies will need to further clarify the underlying developmental mechanisms of tooth root morphogenesis and consider biomechanical and dietary factors as well.

## Chapter 6: A novel system for determining tooth root phenotypes

### 6.1 Abstract

Human root and canal number and morphology are highly variable, and internal root canal form and count does not necessarily co-vary directly with external morphology. While several typologies and classifications have been developed to address individual components of teeth, there is a need for a comprehensive system, that captures internal and external root features across all teeth. Using CT scans, the external and internal root morphologies of a global sample of humans are analysed (n=945). From this analysis a method of classification that captures external and internal root morphology in a way that is intuitive, reproducible, and defines the human phenotypic set is developed. Results provide a robust definition of modern human tooth root phenotypic diversity. Our method is modular in nature, allowing for incorporation of past and future classification systems. Additionally, it provides a basis for analysing hominin root morphology in evolutionary, ecological, genetic, and developmental contexts.

### 6.2 Introduction

Dental anatomy is an area of special interest in human evolutionary studies. Teeth can provide information on diet, health, age and life history. Importantly, tooth development and morphology appear to be under relatively strong genetic control (see Bei, 2009 for a review), and potentially reflect phylogenetic patterns and signals of selection. While much research has focused on tooth crowns, there is a paucity of anthropological data on tooth roots. This was largely due to the inaccessibility of tooth roots for metric and morphological assessment. Early studies required x-rays, which are problematic when visualizing root structures, which are often curved or layered one on top of another. Other methods are destructive, requiring the sectioning of bones and fossils. The development of Computerized Tomography (CT) and micro-CT ( $\mu$ CT) allows researchers to bypass destructive techniques and the limited imaging of 2D radiographs (x-rays), transforming the potential for studying variation in tooth roots. The use of CT technology has bolstered the number of ento- and endodontic reports on tooth roots (Table 6.1). Several of these studies

have identified novel morphotypes of individual teeth, while others have re-evaluated existing morphologies within and between populations. However, there is a need for a comprehensive categorization system, that can be used for undocumented morphotypes, and is applicable for describing and classifying not just the total human tooth root phenotype, but the phenotypes of all hominoids.

Table 6.1: Previous typological studies of tooth roots and canals

Authors	Technique	Roots	Canals	Modern humans	Teeth
Tomes, 1923	Direct observation	Yes	-	Yes	Premolars
Keith, 1913	Direct observation	Yes	Yes	-	Molars
Ackerman et al., 1973	Radiography	Yes	Yes	Yes	Molars
Vertucci and Gegauff, 1974	Direct observation using dye	-	Yes	Yes	Maxillary premolars
Abbot, 1984	Direct observation, radiography	Yes	Yes	Yes	All teeth, focus on premolars
Turner et al., 1991	Direct observation	Yes	-	Yes	All
Carlsen and Alexandersen, 1991	Direct observation	Yes	-	Yes	Mandibular molars
Hsu and Kim, 1997	Sectioning of tooth, direct observation using dye	-	Yes	Yes	Maxillary and mandibular pre- and first molars.
Fan et al., 2004	Radiography	Yes	Yes	Yes	2nd mandibular molar
Moore et al., 2013	CT	Yes	Yes	-	Premolars
Ahmed et al., 2017	micro-CT	-	Yes	Yes	All

Externally, roots exhibit considerable variability in number, morphology, and size. For example, premolars have been reported as having between one and three roots (Vertucci and Gegauff, 1979; Kirilova et al., 2014), while maxillary and mandibular molars have between one and five roots (Cleghorn et al., 2006; Taylor, 2006; Roy, 2013; Fernandes et al., 2014). Studies of root morphologies have pointed out repeated forms such as 'plate-like' and 'dumb-bell', in the mandibular molars of humans, great apes, cercopithecoids, and Plio-Pleistocene hominins (Robinson, 1956; Kullmer et al., 2011; Kupczik et al., 2019); while

cross sections of australopith anterior teeth have been described as 'ovoid' (Ward et al., 1982). Interestingly, CT technology has also revealed that the complexity of the root canal system does not correspond with external morphology (Wood et al., 1988; Moore et al., 2013; Versiani et al., 2019). Canal number and morphology do not always conform to number and morphology of roots, and teeth can have multiple canals and canal configurations within a single root (Figure 6.1).

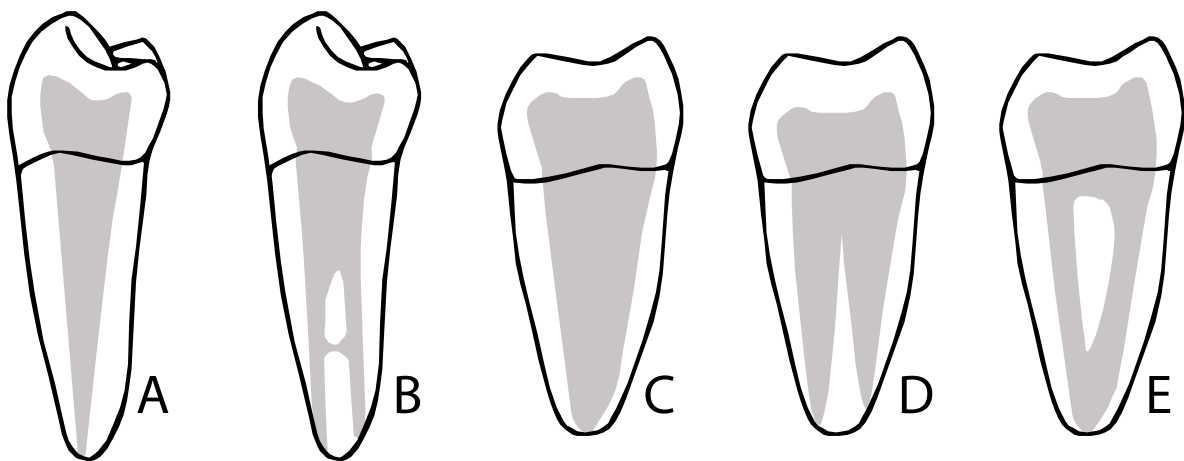


Figure 6.1: Root and canal number do not always conform to one another. Grey area represents pulp chambers and various canal configurations that have been described in the literature (Vertucci and Gegauff, 1979). **A** and **B** are single-rooted mandibular premolars (distal view); **C**, **D**, and **E** are two-rooted mandibular molars (mesial view). **A** and **C** are single canal configurations, **B** (Vertucci Type 7) and **E** (Vertucci Type 2), and **D** is a double canaled configuration.

In the presence of similar, rare, or infrequent external root morphologies (e.g. Tomes' roots, three rooted molars, etc.), canal morphology has proved useful for hominin classification (Emonet et al., 2012; Prado-Simón et al., 2012; Moore et al., 2013) and taxonomy, as researchers have shown that canal configurations can differentiate robust and gracile australopiths (Wood et al., 1988; Moore et al., 2013, 2016). Previous studies have provided systems for canal classification (Vertucci and Gegauff, 1979; Weine, 1984; Hsu and Kim, 1997; Fan et al., 2004a; Zheng et al., 2011); however, it is unclear how this variation relates to external morphology, or is partitioned between and across populations.

The aim of this study is to develop and provide a comprehensive tooth root classification system. We do this by analysing CT scans of maxillary and mandibular teeth from a global sample of modern human individuals (n=945). We treat roots both individually and, in the case of multi-rooted teeth, as a root complex. Classification is based on root number, canal number, external root shape, and internal canal shape and configuration. We

developed an element-based system for classifying all human root phenotypes. The purpose of the classification we present is to provide a method for the analysis of tooth root diversity in hominin evolution. The idea is to define the morphospace of phenotypic diversity, both potential and realized. This will thus comprise the "phenotypic set". The concept of the phenotypic set was originally developed in behavioural ecology to describe the range of possible strategies (Bennett, 1983) but has been extended to define the finite range of phenotypes possible in other branches of biology (Wang et al., 2009; Martin, 2014), of which a smaller number are likely to occur.

### 6.3 Materials and Methods

Using CT scans, we analysed both sides of the maxillary and mandibular dental arcades of individuals (n= 945) from osteological collections housed at the Smithsonian National Museum of Natural History (SI), American Museum of Natural History (AMNH), and the Duckworth Laboratory (DW) at the University of Cambridge (See Chapter 3, Table 3.1). Only permanent teeth with completely developed roots from the right side of the maxilla and mandible were used for this study (Table 6.2).

Table 6.2: Tooth counts of the right side of the maxillary and mandibular dental arcades.

Tooth	n	Tooth	n	Total
<b>Maxilla</b>		<b>Mandible</b>		
I <sup>1</sup>	204	I <sub>1</sub>	204	408
I <sup>2</sup>	248	I <sub>2</sub>	247	495
I <sup>2</sup> CON	1	I <sup>2</sup> CON	1	-
C <sup>1</sup>	406	C <sub>1</sub>	295	701
P <sup>3</sup>	515	P <sub>3</sub>	343	858
P <sup>4</sup>	467	P <sub>4</sub>	313	780
M <sup>1</sup>	697	M <sub>1</sub>	410	1,107
M <sup>2</sup>	596	M <sub>2</sub>	385	981
M <sup>3</sup>	362	M <sub>3</sub>	278	640
M <sup>3</sup> CON	28	M <sup>3</sup> CON	25	-
Total	<b>3,495</b>	-	<b>2,475</b>	<b>5,970</b>

**Superscript** = maxilla, **subscript** = mandible. **I** = incisor, **C** = canine, **P** = premolar, **M** = molar. **CON** = congenitally absent teeth.

All data were analysed with the R Project for Statistical Computing, version 3.6.3 (<https://www.R-project.org>, 2017). Counts and frequencies of most prevalent phenotypes by tooth were calculated (see Appendix section 9.4, Tables 9.4A-E). However, we are also

interested in estimating the probability of how phenotypes for each tooth are distributed within our observed phenotypes. To understand the probability, diversity, and distribution within our sample we used the Dirichlet Distribution to visualize phenotypes by their relative proportion in each tooth. Here, the counts of each distinct phenotype for each tooth are treated as a distinct category, or probability simplex, within a multinomial/categorical distribution. Unlike the Gaussian distribution which displays counts of individual phenotypes, the Dirichlet Distribution estimates the prevalence and probability of multiple phenotypes within each tooth. Thus, the Dirichlet is a distribution of probability distributions, which captures not only diversity of phenotypes, but evenness and richness of their distribution, and rarity as well.

Table 6.3: Hominid material used for case study 2\*

Genus & species	n	Element
<i>Homo sapiens</i>	2	Maxilla
<i>Pan troglodytes</i>	2	Maxilla
<i>Paranthropus boisei</i> (OH 5)	2	Maxilla
<i>Paranthropus robustus</i> (SK 48)	2	Maxilla
<i>Australopithecus africanus</i> (STS 71)	1	Maxilla

\* Section 6.8.

We conducted a small study classifying and comparing phenotype codes between hominid genera (Table 6.3). The *Homo sapiens* sample comes from the main sample (see Chapter 3, Table 3.1). The *Pan troglodytes* sample was provided by the Centre for Academic Research and Training in Anthropogeny (CARTA Subject IDs: 3990, 4074. Courtesy of the Centre for Academic Research and Training in Anthropogeny / Museum of Primatology at UC San Diego. <http://carta.anthropogeny.org>). *Pan troglodytes* were scanned on a Toshiba Aquilion MEC CT3 helical CT scanner (360µA, 135kV, slice thickness 0.5mm) at CARTA, San Diego, California. *Paranthropus boisei* was scanned on a Siemens Somatom Plus 40 (165µA, 120kV, slice thickness 1.0mm) at the Department of Radiology, University Clinic, Innsbruck Austria ("digital@archive of fossil hominoids - University of Vienna"). *Paranthropus robustus* was scanned on a Siemens Sensation 16 (250µA, 140kV, slice thickness 1.0mm) at Little Company of Mary Medical Centre Totiusstraat/ Street Groenkloof, South Africa ("digital@archive of fossil hominoids - University of Vienna"). *Australopithecus africanus* was scanned on a Siemens Somatom Plus 4 (129µA, 140kV, slice thickness 1.0mm) at

Selbypark Clinic, Johannesburg, South Africa ("digital@archive of fossil hominoids - University of Vienna").

For the hominid material a Chi-Square test of independence was used to determine if there is a significant relationship between hominid genera and phenotype codes at the  $p = 0.05$  significance level. Standardized residuals are used to determine which variables have the strongest association to one another and contribute to the Chi-Square statistic.

## 6.4 Results

The aim of this study was to produce a methodology and system for analysing the diversity of human tooth roots, and these are shown and described here as our results.

### 6.4.1 Global root phenotype system

We analysed CT scans of 5,970 teeth (Table 6.2) of 945 individuals from a global sample to identify morphologies which are useful for describing the tooth root complex of modern human teeth. In order to classify and analyse the human tooth root and canal system we devised a finite set of phenotype elements - each of which describes a property of the total root complex. Each element (E) within the set provides information on root (E1) and canal (E2) presence and absence; location of canals in roots (E3); external root form (E4); and (E5) internal canal forms and configurations (See Chapter 3 for a full description). Combined elements (for example root number and internal canal form combined together) can be treated as phenotypes or separated and analysed by their constituent parts. The system, described below, allows us to define a finite set of possible root phenotypes (the realized phenotypic set) and analyse diversity in a constrained morpho-space.

## 6.5 Recording tooth root phenotypes

This system works with categorical and numbering systems including, but not limited to, the Palmer Notation Numbering system, the FDI World Dental Federation System, simple abbreviations such as UP4 (upper 2<sup>nd</sup> premolar) or LM1 (lower first molar), or the super- and subscript formulas described in and used throughout this study.

### 6.5.1 Root number or absence

Roots are recorded by simple counts and represented with an R. For example, a two-rooted tooth would be coded as R2. Root number is determined using the Turner index (Turner II et al., 1991) as outlined in the methods chapter (Chapter 3). Congenitally absent teeth and roots are labelled CON, rather than 0 or NA. This is because congenital absence of a tooth is a heritable phenotypic trait, with different population frequencies (McKeown, 2002; Rakhshan, 2015). In the case of missing teeth, root number can often be recorded by counting the alveolar sockets. Figure 6.2 presents a workflow for recording E1 and its variants.

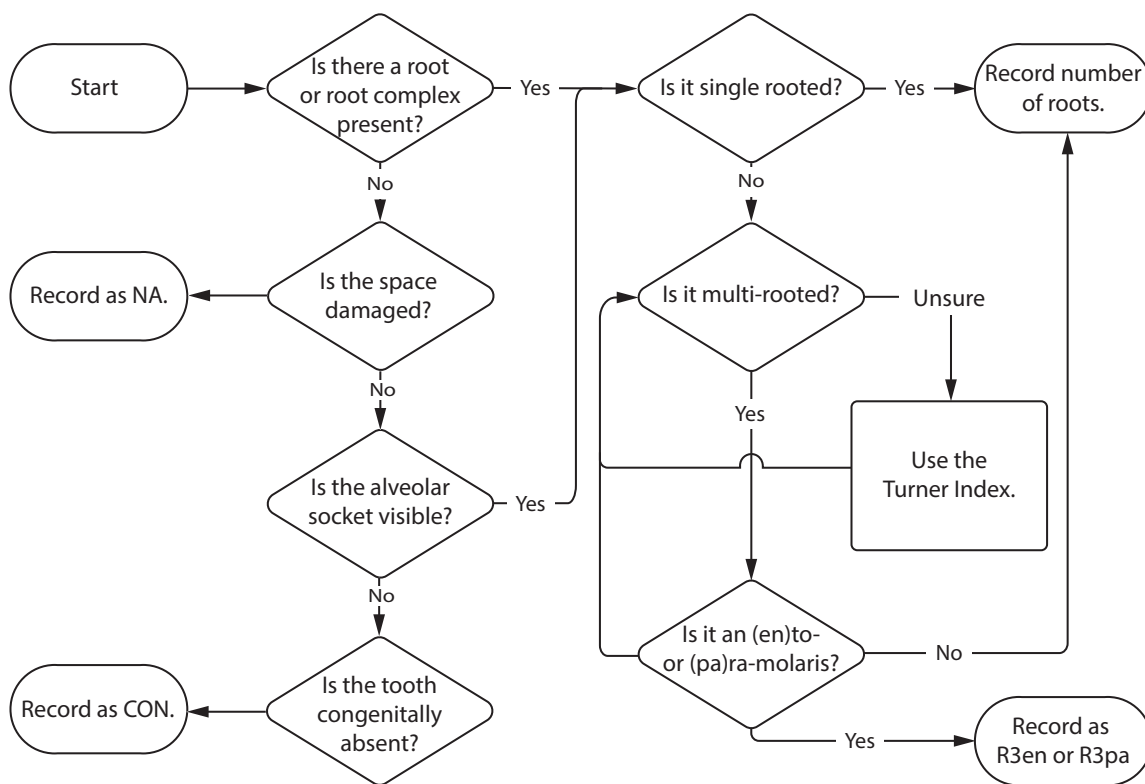


Figure 6.2: Flow chart for determining and recording phenotype element 1 - root number or absence.

### 6.5.2 Canal number or absence

Like root number, canal number is a simple count but represented with a C rather than an R. As discussed in the methods section (Chapter 3), the Turner index (1991), essentially a system of thirds, is applied to determine counts. Building on the above example, a two rooted, three canaled tooth would be coded as R2-C3. Figure 6.3 presents a workflow for recording E2 and its variants.

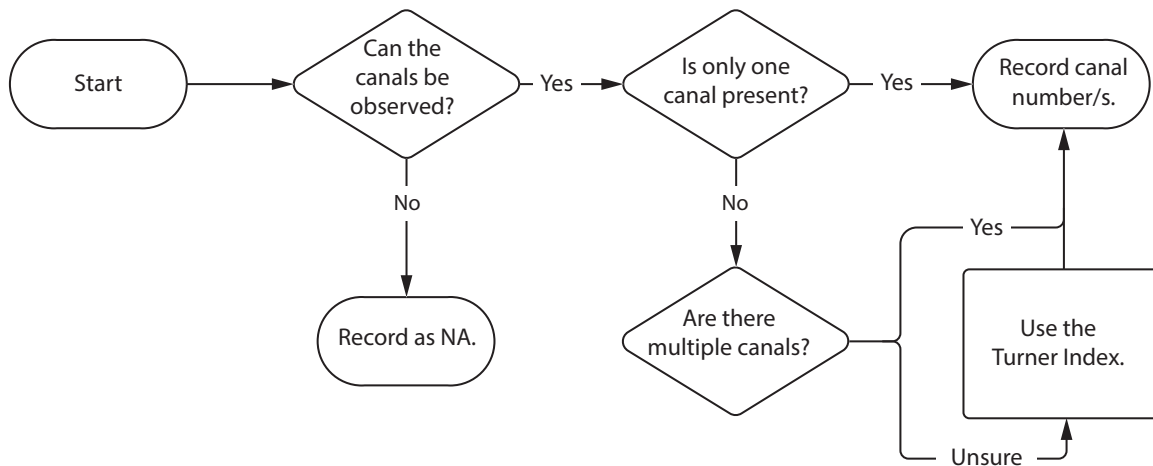


Figure 6.3: Flow chart for determining and recording phenotype element 2 - canal number.

### 6.5.3 Anatomical locations of canals and roots

The location canals and roots in the root complex are easily recorded following the anatomical directions common to any dental anatomy textbook and discussed in Chapter 3. Figure 6.4 presents a workflow for recording E3 and its variants. Labelling order begins with mesial (M), followed by buccal (B), distal (D), and lingual (L), inclusive of intermediate locations (e.g., mesio-distal). Continuing the above example, if two canals are found in the mesial root and one in the distal root, the root complex would be coded as R2-C3-M2D1.

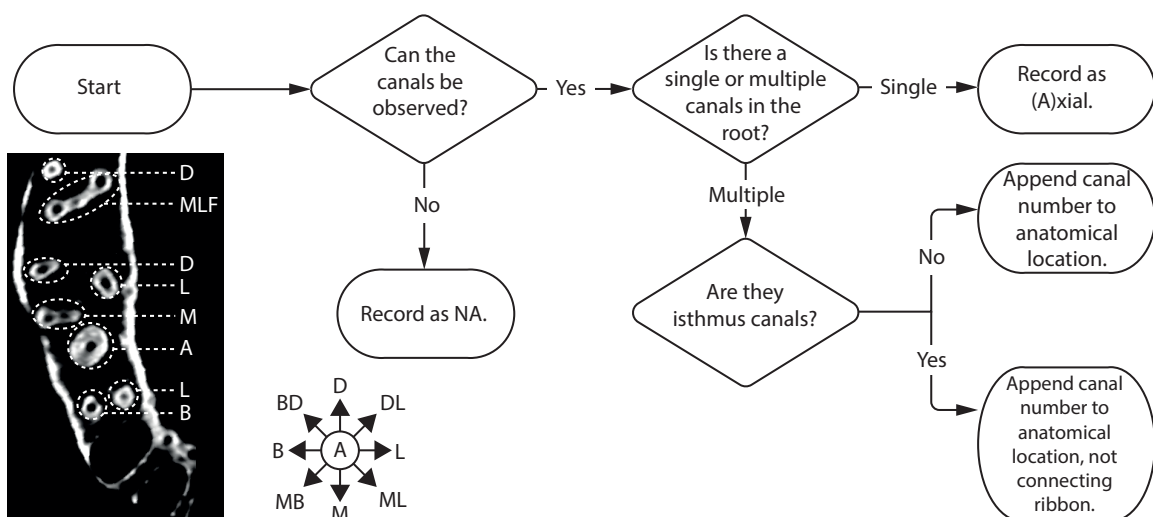


Figure 6.4 Flow chart for determining and recording phenotype element 3 - anatomical location of canals. Bottom left: Axial CT scan slice of right maxillary dental arcade. Anatomical directions: A = axial, M = mesial, MB = mesio-buccal, B = buccal, BD = bucco-distal, D = distal, DL = disto-lingual, L = lingual, ML = mesio-lingual, F = fused.

### 6.5.4 External Root Morphology

Figure 6.5 presents a workflow for recording E4 and its variants. Fused roots also fall under E4 and are simply recorded with F (for fused) appended to the anatomical locations of the fused roots.

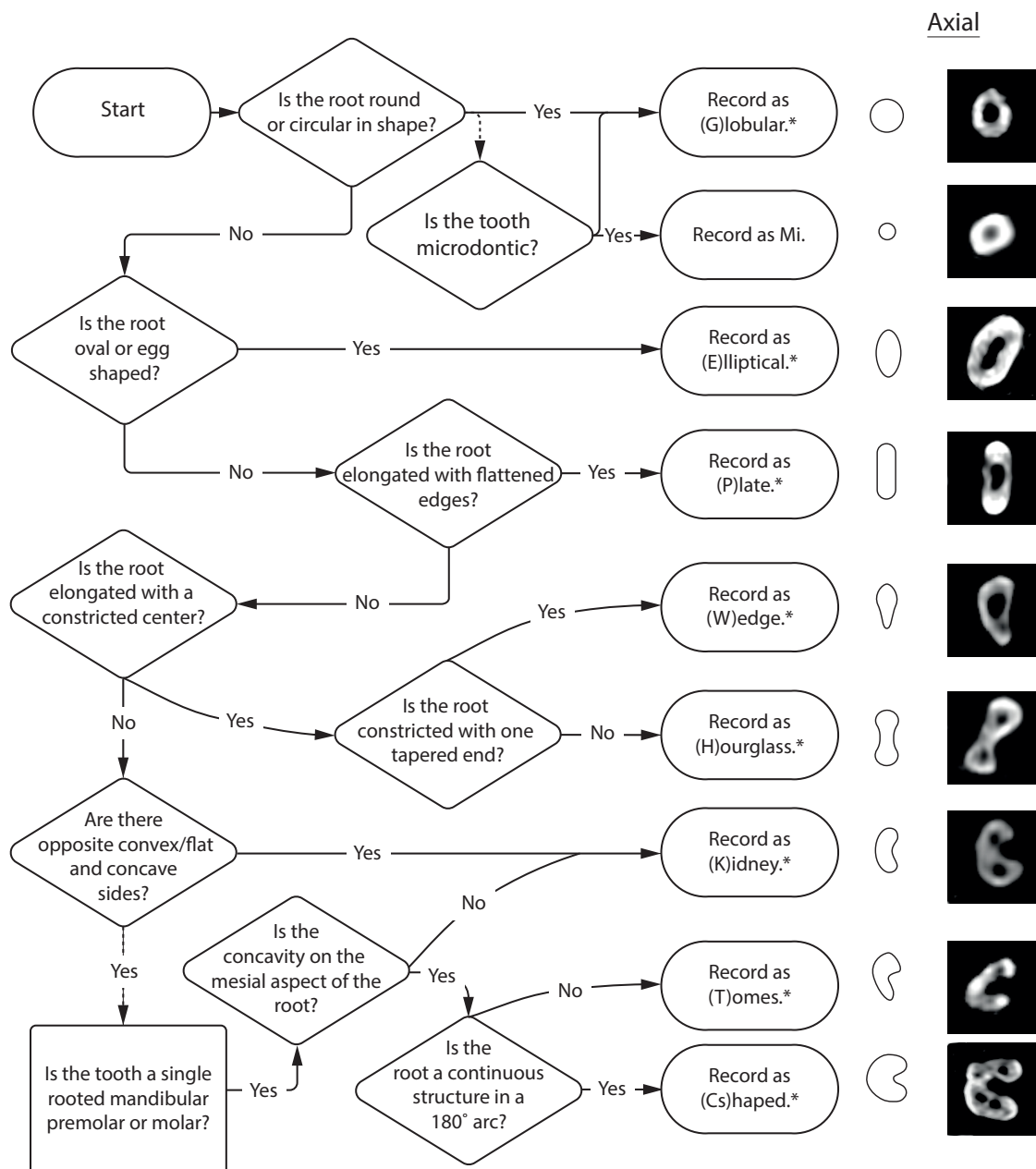


Figure 6.5: Flow chart for determining and recording phenotype element 4 - external root morphology. \*if root is bifurcated, append morphology with Bi. Ex: P = plate, PBi = plate-bifurcated. Right: axial CT slices showing external root morphologies.

For example, a mesial and buccal fused root, would be recorded as MBF. Though axial slices were used to determine these morphologies, morphologies can also be ascertained visually from extracted teeth, and occasionally the alveolar sockets of missing teeth (Scott et al.,

2018). A tooth with two roots, containing three canals – two in the mesial root and one in the distal root, with an hourglass and plate shaped mesial and distal roots, is coded as: R2-C3-M2D1-MHDP.

### 6.5.5 Canal configuration

Root canal configuration requires visualization of the canal system from the CEJ to the foramen/foramina. While  $\mu$ CT or CBCT provide the greatest resolution for visualising these structures, in certain cases 2D radiography is sufficient (see Versiani et al., 2018 for an indepth discussion and comparison of techniques). This simplified system will help the user to classify canal configurations as it is based on a system of thirds, rather than harder to visualize ‘types’. Figures 6.6 and 6.7 present a workflow for recording E5 and its variants.

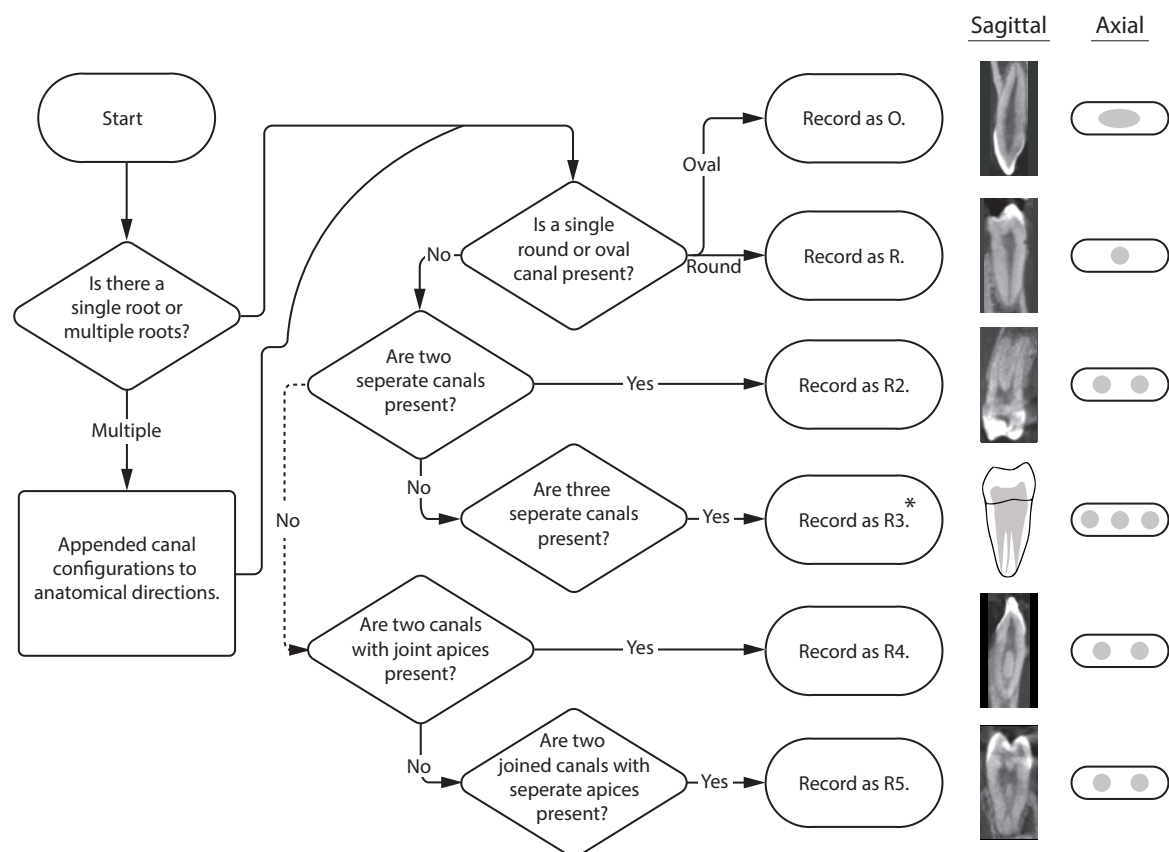


Figure 6.6: Flow chart for determining and recording phenotype element 5 - canal morphology and configuration. Right: sagittal CT slices showing canal morphologies. \*Because the R3 variant does not appear in this sample, the sagittal slice is represented by an illustration.

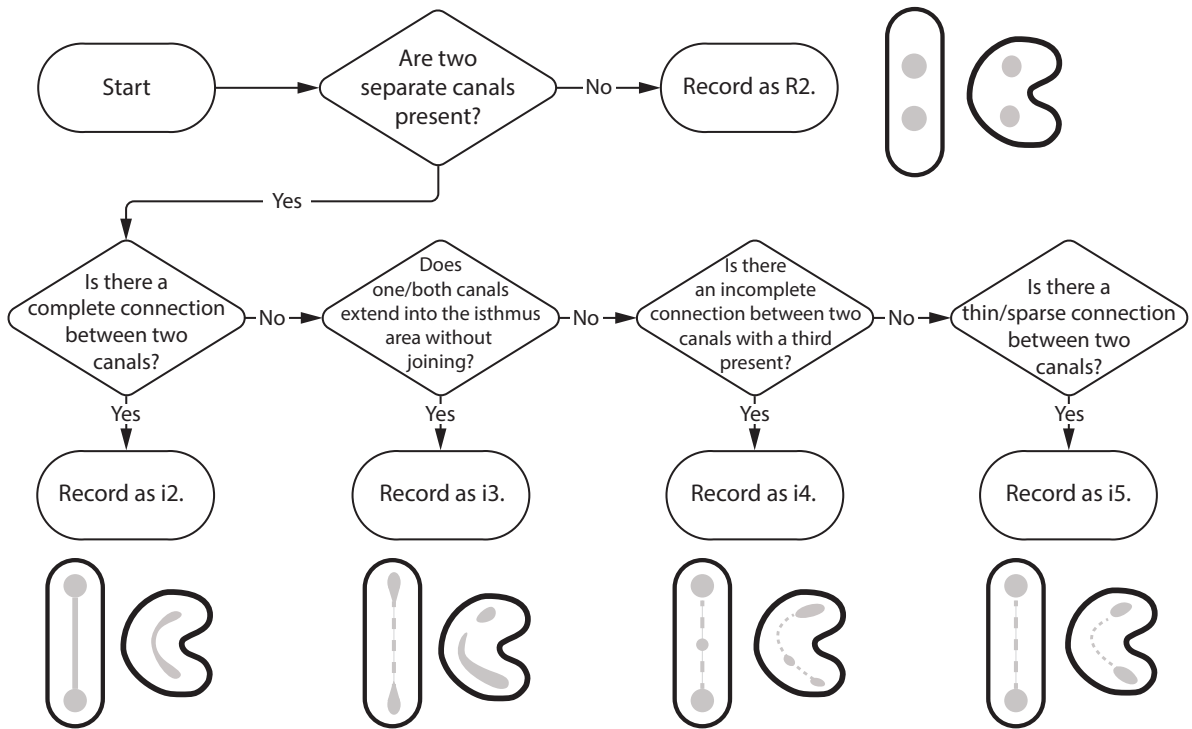


Figure 6.7: Flow chart for determining and recording phenotype element 5 - canal morphology and configuration (isthmus canals). Illustrations show external root morphologies including C-shaped root variants. Canal shape/configuration is in gray.

Finalizing the above example - two round canals in the mesial root and one ovoid canal in the distal root can easily be coded as MR2DO; completing the root complex phenotype code as: R2-C3-M2D1-MHDP-MR2DO (Figure 6.8). Thus, the five phenotype elements (summarised in Table 6.4) can be used to describe the root complex of the tooth.

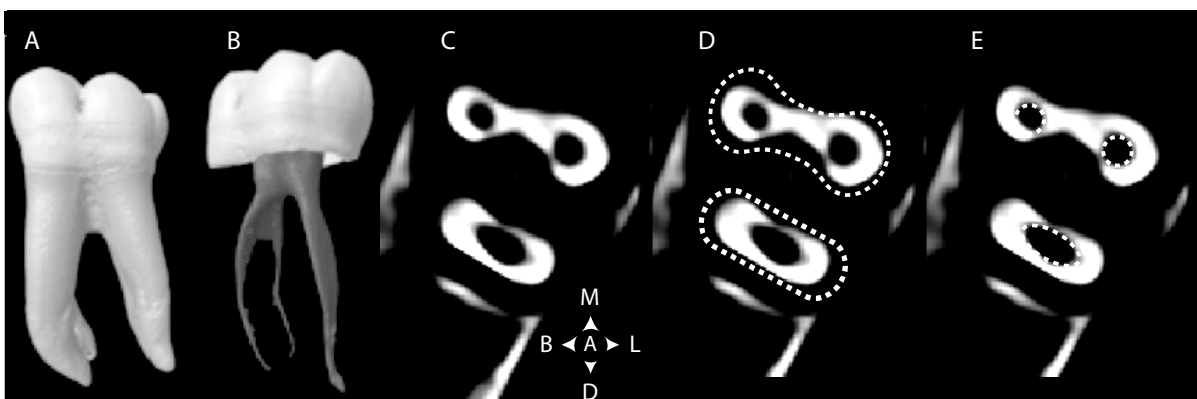


Figure 6.8: Five phenotypic elements of a lower left 1<sup>st</sup> mandibular molar (RM<sub>1</sub>-R2-C3-M2D1-MHDP-MR2DO). **A.** E1 - Root presence/absence; **B.** E2 - Canal presence/absence, **C.** E3 - Canal location, **D.** E4 - Canal morphology, **E.** E5 - Canal shape. Images A and B from the Root Canal Anatomy Project <https://rootcanalanatomy.blogspot.com/> (accessed 10 March 2019)

Table 6.4: Summary table of five phenotypic elements

Element	Description	Reference
E1	Element 1 records root number or absence. Roots are recorded as simple counts and represented with an R. For example, a two-rooted tooth would be coded as R2. Root number is determined using the Turner index (Turner II et al., 1991). Congenitally absent teeth and roots are labelled CON, rather than 0 or NA.	Figure 6.2
E2	Element 2 records canal number. Canals are recorded by simple counts and represented with a C. For example, a two-canaled tooth would be coded as C2. Canal number is determined using the Turner index (Turner II et al., 1991).	Figure 6.3
E3	Element 3 records root and canal location. Locations in the root complex are easily recorded following the anatomical directions common to any dental anatomy textbook. Labelling order begins with mesial (M), followed by buccal (B), distal (D), and lingual (L), inclusive of intermediate locations (e.g., mesio-distal).	Figure 6.4
E4	Element 4 records external root morphology as seen at the midpoint of the root between the CEJ and the root apex. If the root is bifurcated, the morphology is appended with Bi. Ex: P = plate, PBi = plate-bifurcated.	Figure 6.5
E5	Element 5 records canal configuration and morphology.	Figures 6.6 & 6.7

\* In the case of missing teeth, root number can often be recorded by counting the alveolar sockets.

## 6.6 The phenotypic set within the morphospace of root diversity

Across all teeth we identified five phenotype elements, and their constituent permutations, which can be used to capture external and internal morphology of the tooth root complex. In combination there exists 841 phenotype permutations derived from combinations of individual phenotype elements. These comprise our study's "phenotypic set" among the range of potential phenotypes. Anterior teeth have the least number of phenotypes, while molars have the greatest (Figure 6.9). The greatest number of phenotypes are found in the maxillary molars while the least are found in the anterior maxillary teeth.

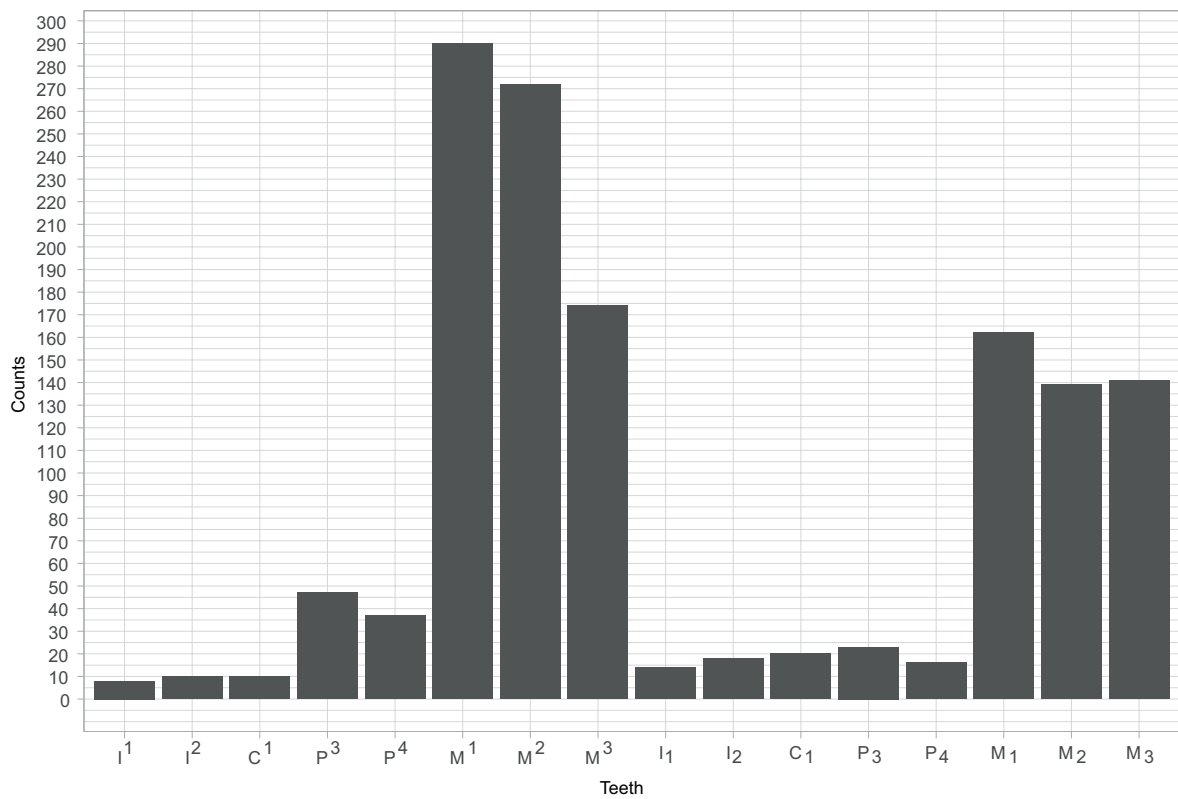


Figure 6.9: Counts of phenotypes in individual teeth.

The large number of phenotypes found in our sample can be explained by the permutations within each element. For example, Table 6.5 shows how permutations in one element can result in four nearly identical tooth roots with four different phenotype codes. Here, all these roots are identical in their phenotypic elements with the exception of their external morphology (E4).

Table 6.5: Permutation of one element results in variation of phenotype codes

E1	E2	E3	E4	E5	Code
R1	C1	A	<b>P</b>	O	R1-C1-A-P-O
R1	C1	A	<b>E</b>	O	R1-C1-A-E-O
R1	C1	A	<b>W</b>	O	R1-C1-A-W-O
R1	C1	A	<b>K</b>	O	R1-C1-A-K-O

E4 variants: P = Plate, E = elliptical, W = wedge, K = kidney.

Figure 6.10 visualizes how multiple combinations and orientations of these root types create the external morphological permutations and variations of the human tooth root phenotype.

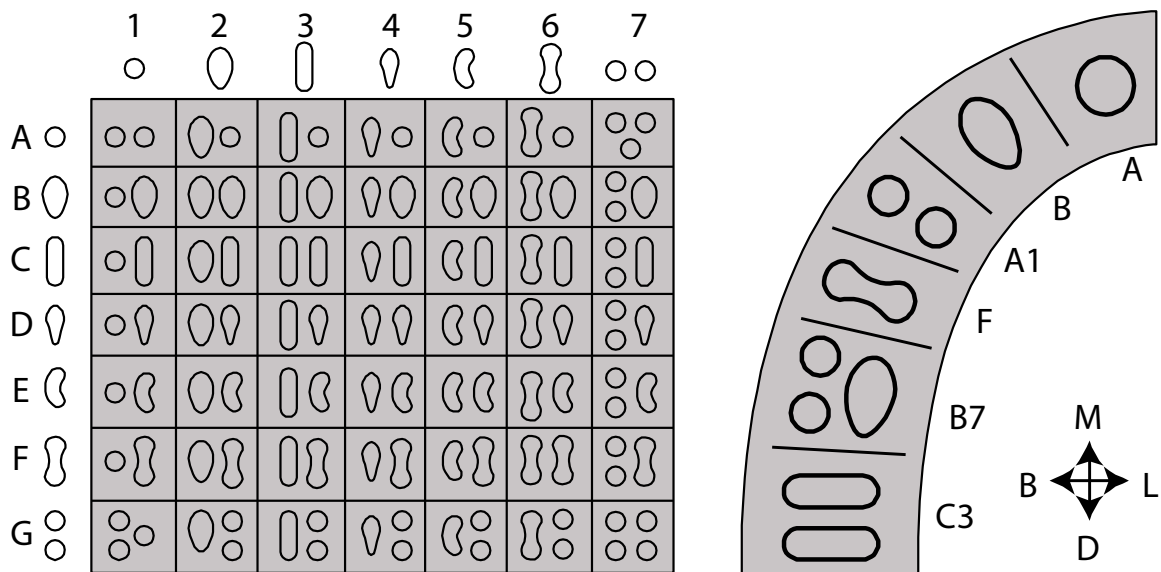


Figure 6.10: Left - Combinations of individual root types form multiple root complexes (e.g., C3 = one tooth with two plate shaped roots). Right - multiple root forms can appear in the tooth row.

Some phenotype permutations appear with greater frequency than others. Table 6.6 lists the most frequent phenotype permutations by tooth in our total global sample. Teeth with more roots result in a greater number of phenotype permutations per element, and thus, a reduced frequency of a 'dominant' phenotype. For example, though M<sup>1</sup>'s have the largest number of phenotypes (n=291) the dominant phenotype, R3-C3-M1D1L1-MWDGLG-MRDRLR, accounts for only 2.29% of the sample.

Table 6.6: Phenotype codes for total sample with highest frequency by tooth

Tooth	Phenotype Code	n	Frequency
<b>Maxilla</b>			
I <sup>1</sup> , n= 204	R1-C1-A-G-R	112	54.90
I <sup>2</sup> , n= 249	R1-C1-A-E-R	96	38.55
C <sup>1</sup> , n= 405	R1-C1-A-E-R	113	27.90
P <sup>3</sup> , n= 515	R2-C2-B1L1-BGLG-BRLR	177	34.37
P <sup>4</sup> , n= 468	R1-C1-A-P-O	170	36.32
M <sup>1</sup> , n= 697	R3-C3-M1D1L1-MWDELE-MRDRLR	16	2.29
M <sup>2</sup> , n= 597	R3-C3-M1D1L1-MWDGLG-MRDRLR	17	2.84
M <sup>3</sup> , n= 391	R3-C3-M1D1L1-MWDGLG-MRDRLR	33	8.42
M <sup>4</sup> n= 1	R1-C1-A-P-R	1	100.0
<b>Mandible</b>			
I <sub>1</sub> , n= 204	R1-C1-A-P-O	99	48.5
I <sub>2</sub> , n= 248	R1-C1-A-P-O	129	52.02
C <sub>1</sub> , n=295	R1-C1-A-P-O	113	38.31
P <sub>3</sub> , n= 343	R1-C1-A-P-O	110	32.07
P <sub>4</sub> , n=313	R1-C1-A-P-O	116	37.06
M <sub>1</sub> , n= 410	R2-C3-M2D1-MHDP-MR2DO	29	7.07
M <sub>2</sub> , n= 385	R2-C3-M2D1-MHDK-MR4DO	22	5.71
M <sub>3</sub> , n=303	R2-C3-M2D1-MKDK-MR4DO	13	4.29

Phenotypes with highest prevalence by tooth for each population are listed in Appendix 9.4 (Tables 9.4 A-E).

We have described above the morphological components that capture diversity in roots, and the 5-element system we have developed to summarize this. The method is designed to facilitate comparative qualitative and quantitative analyses of human, hominin and hominoid dental roots. There are many potential applications on both extant and extinct populations, and we illustrate two here, the first on human geographical variation, and the second on differentiation among hominids.

## 6.7 Case Study 1 - Geographical variation in phenotype diversity

Although genomes are now used extensively to map population affinities, morphological or phenotypic evidence still plays a role, and indeed are important for exploring genotype-phenotype relationships. While craniofacial elements have been widely used, tooth roots have not (Scott and Turner, 1997; Hanihara and Ishida, 2005, 2009; Buck and Viðarsdóttir, 2012). The system described above opens up the opportunity to use them comparatively and globally. We can briefly consider here one such use, a comparison of levels of phenotypic diversity by region.

We divided the global sample into five groups based on broad geographic regions – Sub-Saharan Africa, Sunda-Pacific, Sahul-Pacific, Sino-America, and West Eurasia. Temporally, these geographic groups are representative of the major population movements of the past 10,000 years, and are based on language, bioarchaeology, geography, cultural history, and dental crown variation (Irish, 1998; Irish and Guatelli-Steinberg, 2003; Hanihara and Ishida, 2005; Hanihara, 2013; Cavalli-Sforza et al., 2018; Scott et al., 2018). Tooth root phenotype diversity varies across regions (Figure 6.11).

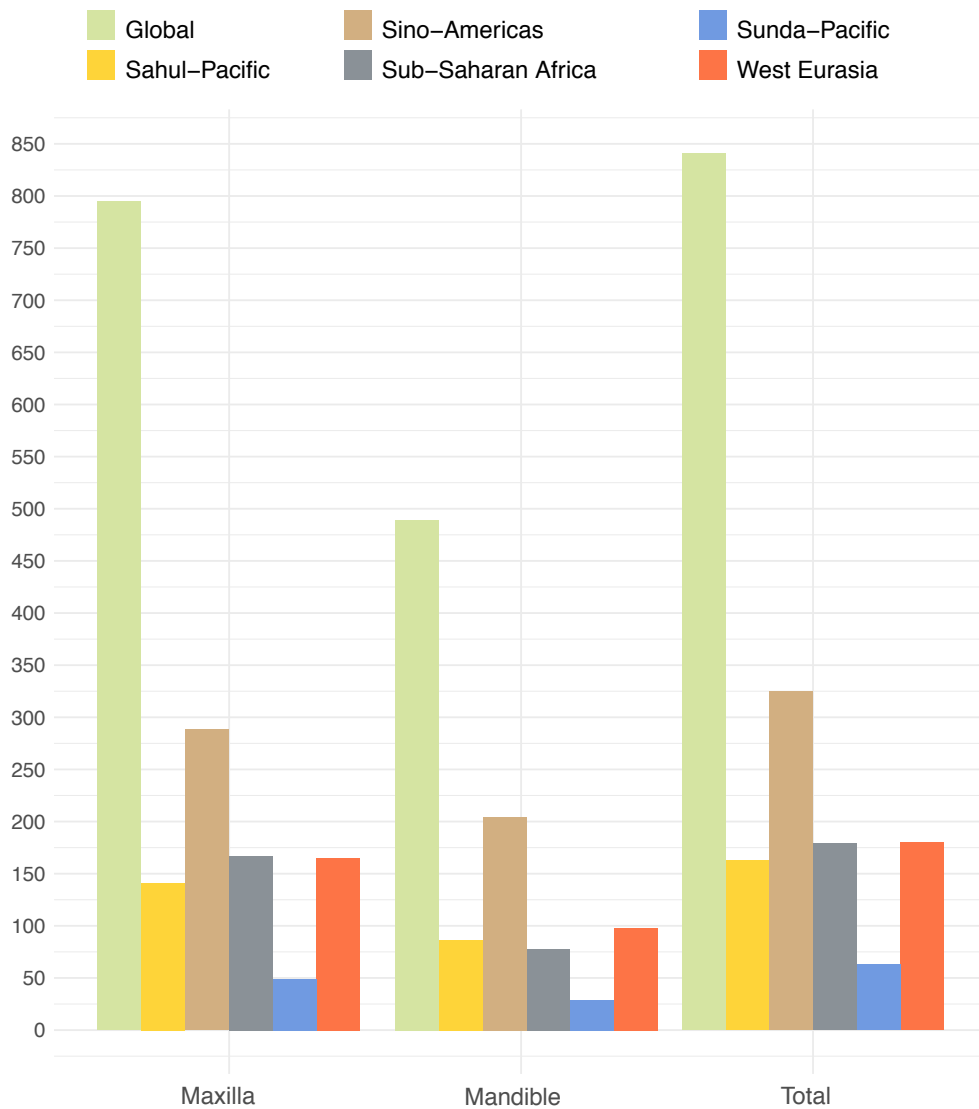


Figure 6.11: Number of phenotypes permutations present in geographical subdivisions.

The greatest number of phenotypes are found in Sino-American populations while the least are found in Sunda-Pacific. Again, as shown in Figure 6.11, the greatest number of phenotypes are found in the maxilla, and the least are found in the mandible. Tooth counts and phenotypes with highest prevalence by tooth for each population are listed in Appendix Table 9.4A-E. This is perhaps a surprising result, as studies of levels of cranial diversity decline with distance from sub-Saharan Africa (Manica et al., 2007; von Cramon-Taubadel and Lycett, 2008; Betti et al., 2009), suggesting that different phenotypes (and the resolution at which phenotypes are defined) may behave differently at a global scale. Experimentation with different and more resolved geographical sub-divisions are required to test this further.

Counts of the presence or absence of phenotypes across regions represents a relatively simple approach, but it is possible to use these data at a more sophisticated level. Dirichlet Distributions can be used to visualize the distribution of phenotype probability, variance, richness, and evenness (see Methods) for each tooth within global populations. Differences in distribution can be explained through the interactions of richness, evenness, and rarity on variation. Richness (i.e., number) and evenness are negatively correlated to one another, with variation being intermediate between the two (Wilsey et al., 2005; Pallmann et al., 2012). Thus, in distributions with higher peaks and narrower spread, variation is correlated with richness of phenotypes that are unevenly represented; while in distributions with low peaks and a wider spread, variation is correlated with low richness, but even representation of phenotypes. Regardless of these factors, the Dirichlet Distribution can help us visualize the probability of each phenotype for a tooth from population within the total sample. Figures 6.13 and 6.14 show Dirichlet distributions for the previously defined geographical regions. There is an overlap in distribution of phenotypes between populations due to shared permutations within one or more element, yet it is not always clear how variation is partitioned. For example, the low peak and wide dispersion for P<sup>3</sup>'s of Sunda-Pacific populations indicate a low number of phenotypes with near even representation. The most prevalent phenotype for this tooth and population is R2-C2-B1L1-BGLG-BRLR - 1 of 10 phenotypes found in Sunda-Pacific P<sup>3</sup>'s and appearing 6 times in a total sample of 19 teeth (Table 9.4D). While at a 31.57% frequency within the Sunda-Pacific population, the probability of finding this phenotype, for this tooth, in this population, from our observed phenotypes (n= 841) is only 9%.

Distribution of phenotypes within the Dirichlet can also elucidate hypotheses regarding phenotypic variability, gene flow, founder effect, and drift. For example, while there is overlap between phenotypes, the dominant phenotypes of each population, most notably Sub-Saharan Africa, are different from one another (Figures 6.12 & 6.13). Compared to other populations, Sub-Saharan Africa has a relatively wide and low curve, meaning the sample contains ample phenotypic variation but with even representation. Further, the dominant phenotype for Sub-Saharan Africa, R2-C3-M2D1-MHDP-MR2DO, has a probability of nearly 20%. The dominant phenotype for Sino-Americas, R2-C2-M1D1-MPDP-MODO, appears with a probability of 10%. The high peak but narrow curve of Sino-American m1's

indicate a high degree of variation but with very uneven representation of phenotypes surrounding the dominant type.

These results suggest that the high probability of the dominant Sub-Saharan African phenotype, and the relatively even representation of phenotypes surrounding it are the product of convergence via gene flow within a stable population. Not only is the dominant Sino-American phenotype different from the Sub-Saharan African geographical group, but it is highly represented at the expense of other intragroup phenotype permutations, suggesting drift via founder effect.

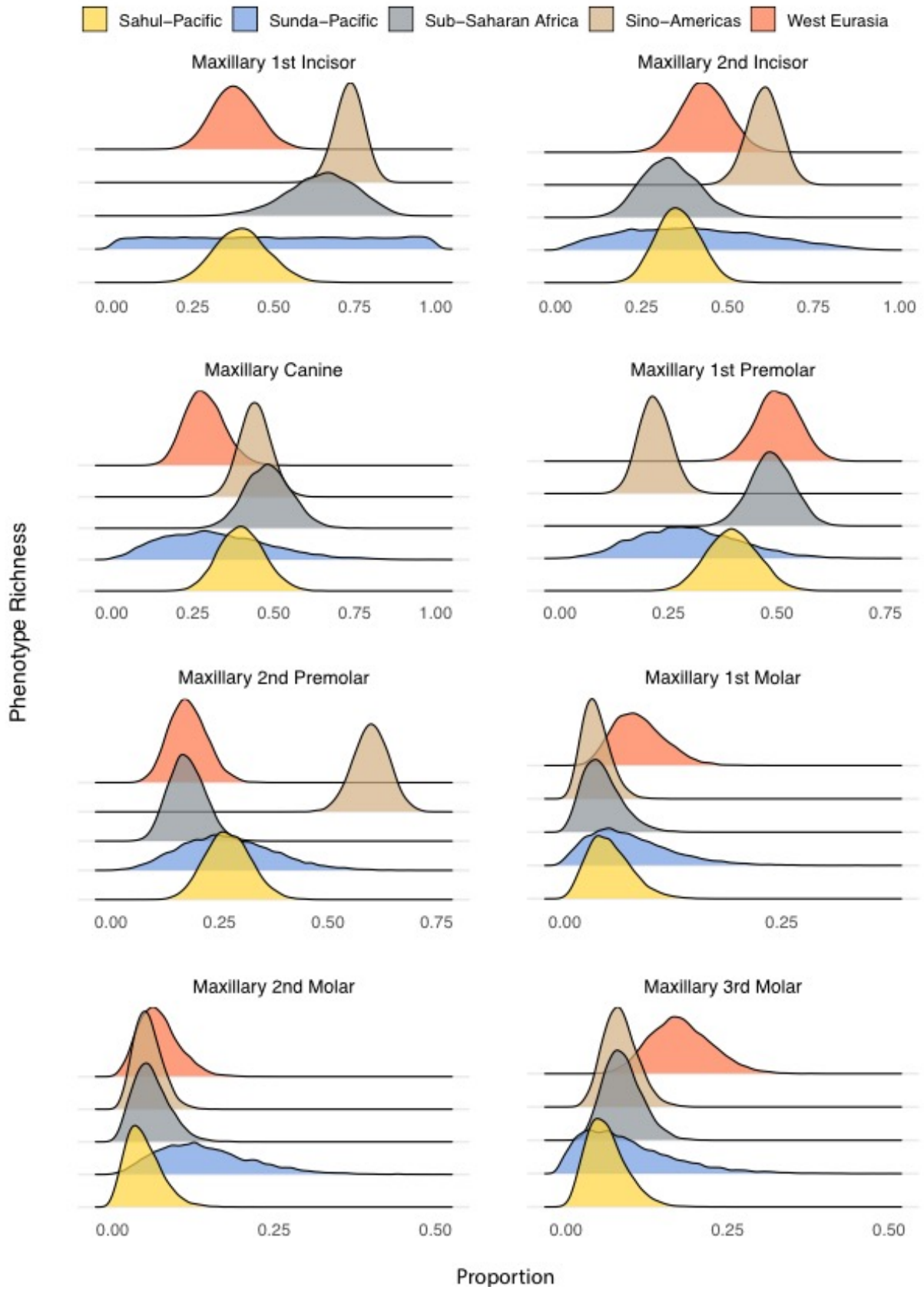


Figure 6.12: Dirichlet Distribution of relative proportions of maxillary phenotypes within global populations.

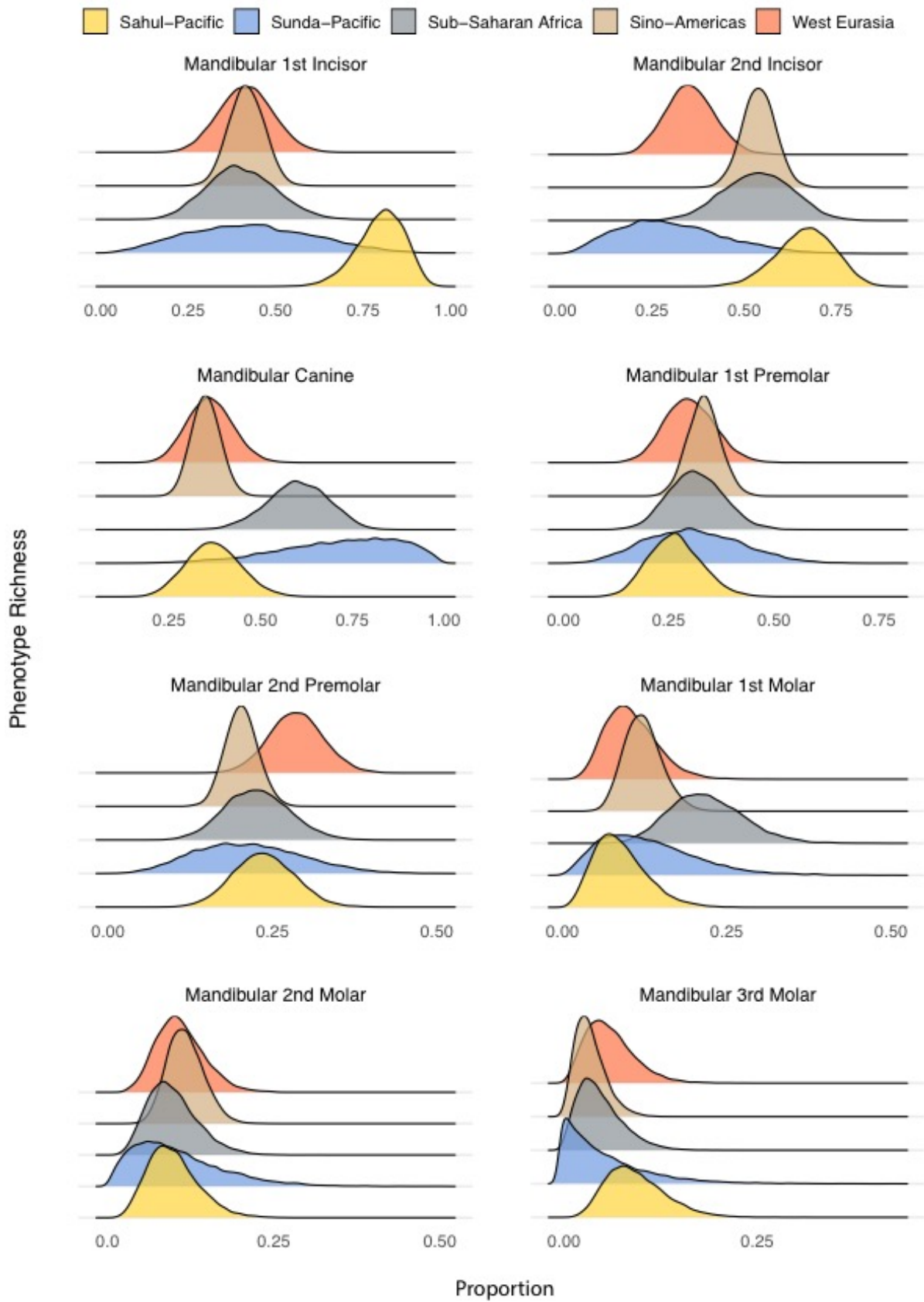


Figure 6.13: Dirichlet Distribution of relative proportions of mandibular phenotypes within global populations.

## 6.8 Case Study 2 - Hominid Classification

While the phenotype elements were derived from modern human tooth roots, there is no reason that the phenotype system cannot be applied to other hominids. Phenotypic differences have been routinely used to determine intraspecific and taxonomic patterns of relatedness; and dental features have played a major role in this (Corruccini and McHenry, 1980; Wood and Uytterschaut, 1987; Gómez-Robles et al., 2007; Moggi-Cecchi and Boccone, 2007; Quam et al., 2009; Xing et al., 2018), but with a few notable exceptions (Wood et al., 1988; Prado-Simón et al., 2012; Le Cabec et al., 2013; Moore et al., 2015, 2016), this has been based mostly on crowns rather than roots. To explore the potential of using the method developed here, 9 CT scans of fossil hominins and extant hominids were analysed to categorize their root phenotypes (Table 6.4). We can use these data to consider degrees of similarity across taxa. Figure 6.14 shows the phenotype codes in the maxillary teeth of four genera - *Homo*, *Pan*, *Australopithecus*, and *Paranthropus*.

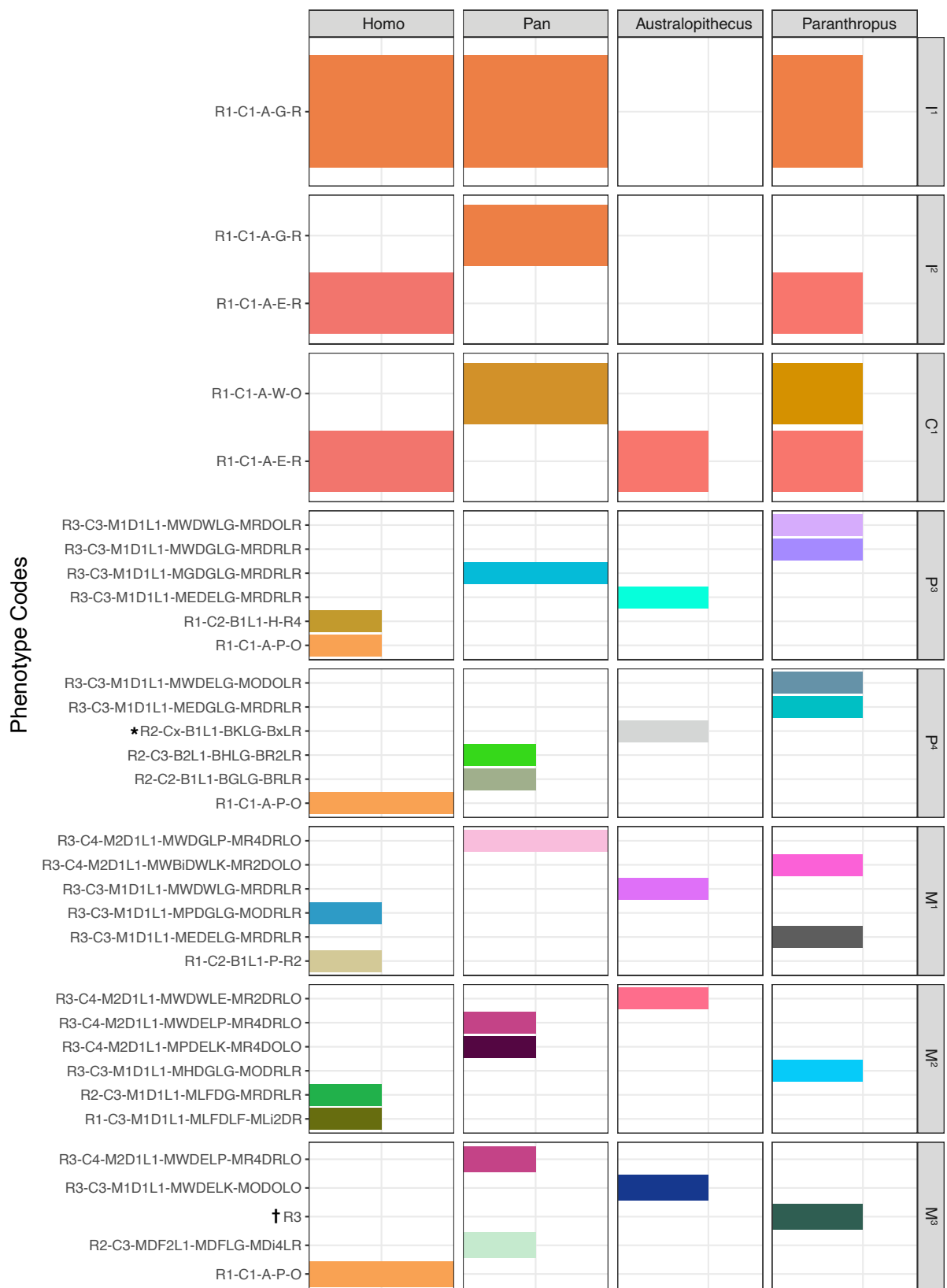


Figure 6.14: Phenotype codes found in the hominid sample (Table 3.3). Phenotype codes are color coded, and repeated phenotypes appear in different genera. Blank values indicate tooth was not present for classification.  
 \* Canal information not readable from CT scan. † Only information from element one is readable from CT scan.

There are clearly both overlaps and differences across the genera. No phenotypes are shared across *all* genera (however, this may be due to no anterior *Australopithecus* teeth being included); the number of unique phenotypes per genus is remarkably similar – eight for *Pan*, *Homo* and *Paranthropus*, and five for *Australopithecus*. Each genus shares phenotype element permutations with each other genus, with the highest shared number being between the anterior teeth of *Homo* and *Paranthropus*. *Pan*, *Homo* and *Paranthropus* have the highest number of phenotypes (11,11,12 respectively), while *Australopithecus* the fewest (6). However, this is likely due to the small sample size and no anterior teeth present for the *Australopithecus* scan.

Chi-Square statistics show that genera significantly differ in phenotypes ( $\chi^2 = 107.04$ ,  $df = 81$ ,  $p\text{-value} = 0.02$ ). Standardized residuals reveal how strongly associations between genera and certain phenotypes contribute to the Chi-Square statistic (Figure 6.15). Noticeably, the majority of three-rooted E1 permutations are strongly associated with *Australopithecus* and *Paranthropus* genera, while the majority of single and double-rooted E1 permutations are associated with *Pan* and *Homo* genera. The exception to this is phenotype code R2-Cx-B1L1-BKLG-BxLR associated with *A. africanus*, which is missing information for element 2, and giving a false signal. Particular morphologies, especially the wedge-shaped mesial root of three rooted forms are also strongly associated with fossil hominins and chimpanzees. If this represents an ancestral condition or is an adaptive form are unclear. While studies of fossil hominins have noted multi-rooted forms with comments on morphology (Wood et al., 1988), there is comparatively little discussion of how morphology is related to masticatory function and diet (Kupczik et al., 2018). These results show that our method may provide possible new avenues to exploring these issues.

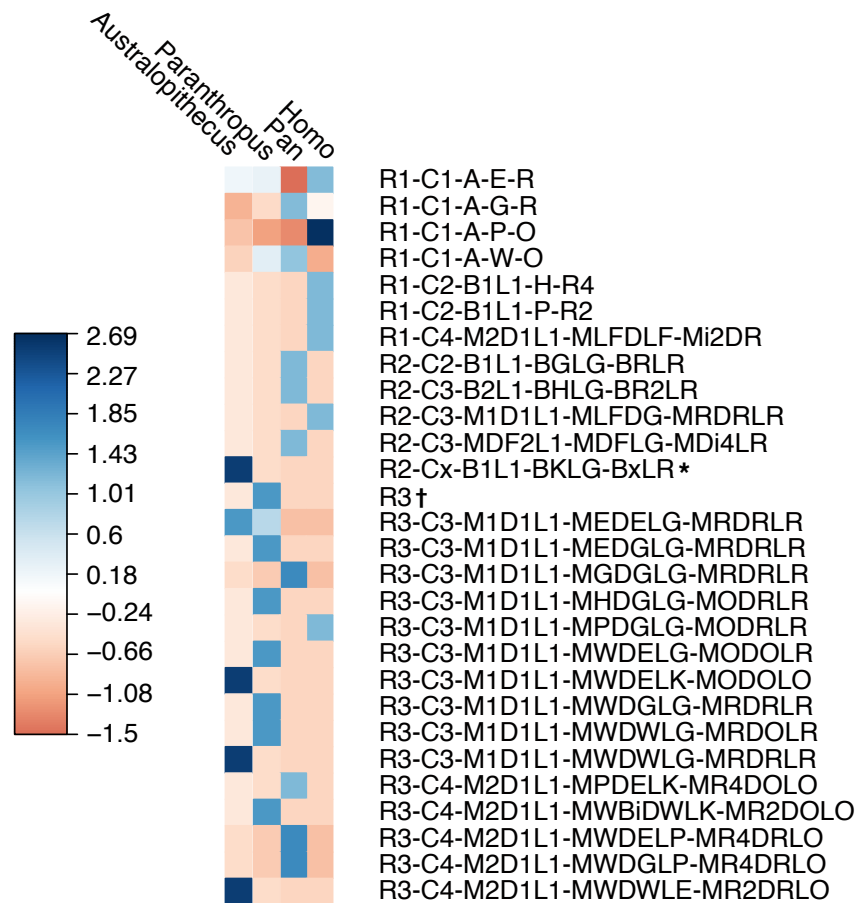


Figure 6.15: Standardized residuals of Chi-Square test for hominid genera and phenotype codes. Cells with strong contribution to the  $\chi^2$  score are displayed in blue while cells with weak contribution are in red. Residual values greater than 2 indicate that observed frequency is greater than expected frequency. Residual values less than 2 indicate that observed frequency is less than expected frequency. \* Canal information not readable from CT scan. † Only information from element one is readable from CT scan.

## 6.9 Discussion

This paper set out to present a method that would capture quantitatively and qualitatively the diversity of human tooth root phenotypes, using a modular approach. It has shown that it is possible to have a universal code for phenotyping roots, and that a global sample of modern humans demonstrates the high level of diversity within the elements comprising to the total tooth root phenotype. A more comprehensive set of tooth root data should reinforce and expand the broader toolset for studying human phenotypic diversity (e.g., tooth crowns, craniofacial morphometrics, genetics, etc.).

We would emphasize two elements of the approach. The first is the expansion of data available and the use of a universal and modular system. Scanning technologies have provided greater access to tissues, such as tooth roots, that were previously difficult to access for visual inspection, thus, permitting a much fuller and complete description of

these morphologies. The system we have developed is designed to be comprehensive and universal, so that any tooth can be placed within the set of attributes. The five elements - root presence/absence (E1), canal root presence/absence (E2), canal location (E3), external root morphology (E4), and canal morphology and configuration (E5) – but also allow for independent categorization, so that phenotypes can be put together combinatorically, or treated as individual components – for example, using just external root morphology. Although constructed for human variation, we have shown through preliminary case studies that the system can be extended across extant and fossil hominids, providing an additional tool for reconstructing evolutionary history, as well be used to map geographical patterns among contemporary human populations. Its broader applicability will be dependent upon an expansion in the number of scans available; while this is increasingly the case for fossil hominins, more regular scanning of more recent samples will be essential for studies of human diversity.

The advantages of this system, in addition to its universality, is that it allows for relatively simple qualitative and quantitative analysis. This is important, as there is increasing interest in mapping human diversity in different ways, using quantitative techniques (Stinchcombe and Hoekstra, 2008; Malaspinas et al., 2016; Matsumura et al., 2019); the abundance of dental remains provides an additional source of information. In addition, there is growing interest among geneticists to map phenotypic variation against genetic variation (Zichello et al., 2018), and to develop a better understanding of genotype-phenotype relationships. As teeth are generally to be considered strongly influenced by their genetic components (Corruccini et al., 1986; Dempsey and Townsend, 2001), they are an ideal system for testing these relationships. It is also the case, as we have seen in the brief case study of human geographical variation, that different phenotypes may behave differently across populations, and so tooth roots can become part of phenotype-phenotype comparisons. Such comparisons can be either phenetic, or phylogenetic, as the coding system is entirely suitable for cladistic analysis.

The second element relates to morphospace - an increasingly utilized concept in evolutionary biology (Mitteroecker and Huttegger, 2009; McGhee, 2015). The morphospace is the total available forms that a phenotype can take, limited by physical or biological properties. Evolution is, in a sense, following paths in morphospace (Savell et al., 2016). The phenotypic set is that part of the morphospace that is actually occupied. The method

proposed here has explored the available morphospace for human (and hominin) tooth roots and has provided a series of elements that describe it. There are a very large number of possible phenotypes under this system (in principle, the total number is combinatorial product of the five elements and their potential states, although in practice the number would be much smaller due to functional and physical constraints), but we have shown here that in a relatively large sample there are about 841 observable individual tooth phenotypes – in other words a small proportion of possible ones. Furthermore, the exploratory case study on geographical distribution of these phenotypes across the world, at a continental scale, shows that there are differences in how the various populations occupy the available morphospace. More detailed analysis is required to determine the basis for these differences. Further work is also required to determine how changing the geographic scale and basis for populational groupings will affect these observations – the one presented here is continental or even supra-continental but given the way in which adaptive process and genetic drift operate locally, it is likely that a much smaller scale approach is necessary. What is critical here is that the proposed method allows the realized and potential phenotypic sets of dental roots to be determined and analysed in potential evolutionary, developmental and functional contexts.

Finally, for the method to be worthwhile, it is necessary for it to be useful in relation to current hypotheses and research foci. Four uses are immediately apparent. First, current interest in the role of dispersals, not just the initial one from Africa (Forster and Matsumura, 2005; Lahr and Foley, 2005; Marean, 2015), but also the increasing genetic evidence for multiple later regional dispersals means that finding ways of linking the palaeoanthropological and archaeological record to the inferred genotypes requires diverse phenotypes, and methods such as this will be required (Kayser, 2010; Chen et al., 2012; Pagani et al., 2015; Reich, 2018). The second is in terms of earlier phases of human evolution; with the current evidence for interbreeding across hominin taxa (Wolf and Akey, 2018), it is necessary to have appropriate phenotypic systems – and roots are likely to be a good one – to tease out the phenotypic effects in such admixture (Rathmann et al., 2017; Reyes-Centeno et al., 2017). Third, there is considerable interest in modularity and integration in evolution, and the modular approach adopted here may provide a suitable model system for exploring these issues (Bastir and Rosas, 2005; Gómez-Robles and Polly, 2012). And finally, biomechanical and spatial studies of the hominid masticatory system can

draw functional and dietary information from root and canal number and morphology (Walker, 1981; Daegling and Grine, 1991; Benazzi et al., 2015; Ledogar et al., 2016).

## 6.10 Conclusions

This paper presents a novel method for defining and analysing the morphospace of the human tooth-root complex. The five elements of the system root presence/absence (E1), canal root presence/absence (E2), canal location (E3), external root morphology (E4), and canal morphology and configuration (E5), were designed to: 1) identify the elements that best describe variation in root and canal anatomy, 2) create a typology that is modular in nature and can be appended for undocumented morphotypes, and 3) is applicable to hominoids. Additionally, results demonstrate the utility and effectiveness of the classification system, and that diversity exists within and between global populations, and between genera of extant and fossil hominids. The system will provide a basis for future research in human evolution, human genotype-phenotype investigations, and the functional biology of the human masticatory system.

## Chapter 7: Tooth root deep phenotyping can identify population substructure in modern humans

### 7.1 Abstract

Mapping and accounting for human biological diversity has been a controversial and major research issue for over a century. A level of stability was established with early work in classical genetics, emphasizing intra-population variation. The impact of genomics has changed the situation, with greater emphasis on ancestry, admixture and dispersals. For both evolutionary and medical research, it is necessary to obtain a better grasp on the relationship between human genomic and phenotypic diversity. Machine learning methods offer the opportunity to develop new approaches to partitioning human global phenotypic diversity. In this paper we develop one such methodology and apply it to one phenotypic system – human tooth roots. Tooth roots are especially difficult to access, describe, and study, due to their concealment in the bony crypts of the jaws. Thus, classical anthropological analyses have been limited to root number and/or canal count. Advances in medical imaging techniques have allowed researchers to better visualize and describe additional morphologies, making available data from a much richer set of tooth-root phenotypes than previously known. This diversity provides unprecedented opportunities toward gaining better insight and resolution into population heterogeneity. This is difficult however, as the resulting root phenotype-space is vast and so efficiently incorporating these data into analyses presents major biological and computational challenges. To meet this challenge, we train a modern non-parametric machine learning classifier using a novel root phenotyping system and continental and sub-continental geographic data. We show that the trained classifier accurately matches root-samples to separate groups of modern humans. The results indicate (1) that tooth roots are well-suited for reconstructing population dynamics when used as a morphological proxy for DNA; and (2) that machine learning offer opportunities to establish patterns of variation in different phenotypic systems, and so explore how phenotypic domains may either covary or vary independently with each other and with genomic diversity.

## 7.2 Introduction

The nature of human biological diversity has been a central topic in evolution since the middle of the nineteenth century. While earlier notions of deep and fixed racial categories were replaced in the middle of the twentieth by more evolutionarily sound concepts of variable intra- and inter-specific variation based on populational thinking, the subject has become more complex with the rise of genomics. Multiple studies, using both contemporary and ancient DNA, and ranging from simple uniparental systems to whole genomes, have shown that it is possible to reconstruct both global and local patterns of ancestry (Skoglund et al., 2016; Nielsen et al., 2017; Posth et al., 2018; Reich, 2018). These have revealed a whole variety of outcomes, ranging from strong evidence for long term population continuity, abrupt boundaries between populations, rare or recurrent admixture and gene flow, and virtual complete replacements of populations. Despite this complexity, broad patterns of populational affinity and ancestry have been recognized.

The long-term, underlying pattern of this complexity is an African origin for the human species in a lineage that diverged from the ancestors of Neanderthals more than half a million years ago (Meyer et al., 2012), diversification within Africa prior to a series of dispersals into Eurasia in the last 100,000 years at least (Hershkovitz et al., 2018; Lipson et al., 2020), followed by subsequent further dispersals within and between continents, resulting in strong continental and sub-continental geographical structures (Henn et al., 2012). Overlain on top of this history of dispersals, or at least significant geographically directional gene flow, are repeated admixture events, both within the modern human species and with archaic hominin taxa (Li et al., 2008; Sankararaman et al., 2016; Nielsen et al., 2017).

This has shaped renewed interest in broader patterns of human diversity, particularly the question of the relationship between genetic diversity and phenotypic diversity (Rahim et al., 2008; Campbell and Tishkoff, 2010). This has been explored within human evolutionary history, where despite advances in aDNA methods, fossil bones provide the most comprehensive evidence. There have been numerous studies using different elements of the human phenotype to map human diversity in space and time and reconstruct history and adaptation from these (Irish, 1998; Irish and Guatelli-Steinberg, 2003; Hanihara and Ishida, 2005; Betti et al., 2009; Hanihara, 2013; Reyes-Centeno et al.,

2015; Rathmann et al., 2017; Matsumura et al., 2019; Rathmann and Reyes-Centeno, 2020). On the whole, they show an overlapping distribution of traits, but with clear groupings present. While this is in broad accord with the genomic evidence about the clinal nature of human phenotypic variation, it provides noisy information, and furthermore, different phenotypes can give different signals. For example, the most comprehensive analyses utilizing dental traits to track dispersals and migrations support evidence of a 'southern route' via a single dispersal out of the Horn of Africa, and through subsequent regions of southwestern Asia (Hanihara, 2013; Reyes-Centeno et al., 2017). These results are partially in conflict with the Reyes-Centeno et al.'s (2014, 2015) recent studies utilizing genomic and cranial phenotype data which supports multiple dispersals. The authors posit that conflicting results may be due to applying the same methodological framework to genomic and phenotypic data within their same study (ibid.).

Teeth have been a mainstay for anthropological studies of present and past populations. This is, in part, due to their resistance to chemical and physical destruction, they are generally well preserved in archaeological and paleontological contexts. Because they are under strong and relatively simple genetic control, the frequency of dental crown sizes and morphologies, much like blood group genes, fingerprint patterns, and other biological traits, can diverge and converge, in varying degrees, when human populations undergo temporal isolation or interbreeding (Hlusko et al., 2016; Stojanowski et al., 2018, 2019). Thus, the polymorphic features of teeth can be used to assess biogeographic history and population structure (Hanihara and Ishida, 2005; Irish, 2005; Irish and Konigsberg, 2007; Hanihara, 2008; Berg and Ta'ala, 2014; Ragsdale and Edgar, 2015; Rathmann et al., 2017), and, due to their prevalence in the fossil record, hominin dispersals, and evolutionary patterns and processes (Martín-Torres et al., 2007; Irish et al., 2013, 2018).

The model phenotypic set used to study geographical population structure are tooth roots, based on the full phenotypic coding system described in Chapter 6. Like tooth crowns, tooth roots are presumably under strong genetic control. Previous work has shown that root number is dependent on canal number, that canal number and orientation predict external root morphology, and that tooth root phenotypic diversity varies within and between populations (Chapters 3 and 4). The major biological and computational challenge is how to best utilize this phenotypic information to understand population heterogeneity at different geographical scales. Essentially, our problem is one of classification in which we

must reduce a large number and combination of predictors (phenotypes) into functions that can separate and identify groups. In this study we trained a machine learning classifier (Hastie et al., 1994) using phenotypic variation present in tooth roots, to identify population structure within a global sample of modern humans at two levels - Major Human Subdivisions and Continental Groups (Table 6.1); and so, test hypotheses of tooth root variation in relation to biogeographical and evolutionary contexts.

### 7.3 Materials and Methods

Using CT scans, we analysed post-canine teeth (Table 7.1) from the right sides of the maxillary and mandibular dental arcades of individuals (n= 945) from osteological collections housed at the Smithsonian National Museum of Natural History (SI), American Museum of Natural History (AMNH), and the Duckworth Laboratory (DW) at the University of Cambridge (Table 7.2). Because congenitally absent teeth are under genomic control they are include here for analysis (Rakhshan, 2015).

Table 7.1: Tooth counts of the right side of the maxillary and mandibular dental arcades.

Tooth	n	Tooth	n	Total
<b>P<sup>3</sup></b>	515	<b>P<sub>3</sub></b>	343	858
<b>P<sup>4</sup></b>	467	<b>P<sub>4</sub></b>	313	780
<b>M<sup>1</sup></b>	697	<b>M<sub>1</sub></b>	410	1,107
<b>M<sup>2</sup></b>	596	<b>M<sub>2</sub></b>	385	981
<b>M<sup>3</sup></b>	362	<b>M<sub>3</sub></b>	278	640
<b>M<sup>3</sup> CON</b>	28	<b>M<sub>3</sub> CON</b>	25	-
Total	<b>3,495</b>	-	<b>2,475</b>	<b>5,970</b>

Table 7.2: List of samples used in this study by major geographical and continental groups

G1: Major Human Subdivisions	<i>N</i>	G2: Continental Groups	<i>n</i>
Sahul-Pacific	164	Sahul-Pacific	164
Sino-Americas	338	Central America*	1
		North America	313
		South America	24
Sub-Saharan Africa	184	Sub-Saharan Africa	184
Sunda-Pacific	76	South-East Asia	76
West Eurasia	183	Europe	41
		North Africa	79
		South Asia	63

\*Central America has been removed from this the G2 level of analysis as there was only one individual belonging to this group, which violates our exclusion criteria.

Quantitative methods used to summarize between-group differences are commonly known as "distance statistics." Their most elementary measure is derived from the average of absolute differences of quantitative variable between individuals or groups. Pearson (1926) developed the poorly named, but of its time, "coefficient of racial likeness" (CRL) to test if differences/distance between groups was statistically significant. These types of statistics can be applied to morphological traits or as measures of genetic distance (Ramachandran et al., 2005; Hanihara, 2008; Henn et al., 2011), such as the fixation index ( $F_{ST}$ ). Modern studies rely on a combination of traditional frequentist statistics and multivariate techniques such as principal coordinates analysis (PCA) and factor analysis. Most distance statistics (e.g. Mantel test) used in dental anthropological studies (Scott, 1988; Hanihara, 2009; Scott et al., 2018) are measures of dissimilarity between trait frequencies; in which samples with identical frequencies would have a pairwise distance coefficient of 0.0, while deviations from zero would indicate dissimilarity/distance. Unfortunately, distance statistics were developed for metrical analyses and are of poor utility for qualitative/categorical traits.

In this study we investigate if tooth roots can delineate and classify populations. To do this we utilized flexible discriminant analysis (FDA) - a machine learning method in which a probabilistic classifier is trained on a sample of known observations (individuals comprising our human population) to determine a "boundary" between classes of known — individuals labelled by their geographic region and their total phenotype — and unknown observations. FDA accomplishes this by generating new linear axes from known predictor variables (labelled humans and their phenotypes), and then projecting data from those known categories on to a newly generated axes in a way that maximises separability between response categories (population groups). Unlike traditional linear discriminant analysis from which FDA is derived, FDA is particularly appropriate to our study for three reasons: (1) our data are a mixture of discrete and categorical data, and it would therefore be inappropriate to model them via a particular family of distribution (i.e. Gaussian); (2) FDA can produce results for nonparametric data through non-parametric regression (Hastie et al., 1994); (3) the need for variable selection and regularization due to the large number of phenotypic predictors (which we can assume not all of which might be helpful) and the relatively small sample size of our populations.

Because FDA uses non-linear combinations of predictors (splines), it is useful for modelling non-normality/non-linear relationships for more accurate classification, rather than prediction. Therefore, collinearity among the predictor variables rather than non-independence would greatly diminish the accuracy of this model. FDA adjust for collinearity by removing predictor variables with little or no predictive power for distinguishing groups (Hastie et al., 1994; Næs and Mevik, 2001). These non-influential predictors are either phenotypes with a high degree of intrapopulation homogeneity, or phenotypes which are so unique that they are erroneously classified to an incorrect population cluster. Thus, because FDA is not concerned with prediction (in this analysis) but with classification, non-independence of phenotypes does not affect the analysis. As a safeguard, to help attenuate issues associated with unique phenotypes we also introduced an exclusion criterion in which we exclude individuals with 2 or less shared phenotypes.

Flexible discriminant analysis (FDA) was carried out using the mda: Mixture and Flexible Discriminant Analysis package (Hastie and Tibshirani, 2017). Prior to FDA, data was randomly partitioned into training (80% of individuals) and test (20% of individuals) sets. For example, when all 945 individuals are used, 189 are randomly kept aside for testing. FDA then performs regularization and variable selection on the phenotypes belonging to the remaining 756 individuals to remove phenotypes which decrease classification accuracy (non-influential predictors). The remaining phenotypes of these individuals comprise the canonical variables - linear combinations of two or more phenotypes, which are mutually orthogonal variables comprising non-linear combinations of the phenotypes included in the classification model, to inform population classification. Summaries of classifications are presented in a confusion matrix - a table which describes the performance of the predictive classifier on the test data for which true values (population identity) is known. Correct and incorrect predictions are summarized as count values broken down by class. Confusion matrices also include values for accuracy, sensitivity, and specificity derived from true positive (TP), false negative (FN), true negative (TN), and false positive (FP) values.

## 7.4 Results

We used flexible discriminant analysis by optimal scoring (FDA) to predict multigroup classification of individuals from G1: Major Human Populations (Figure 7.1) from our

sample. Predictors (phenotypes) were reduced to a number of discriminate coordinate functions that separate groups. We also conducted a stepwise test of the phenotype elements (E1 - E5) to see which combination of elements (root number, canal number, orientation, external morphology, and canal orientation) gave the strongest classification and accuracy.

#### 7.4.1 Maxilla and mandible, all teeth, Geographical level 1: Major Human Subdivisions

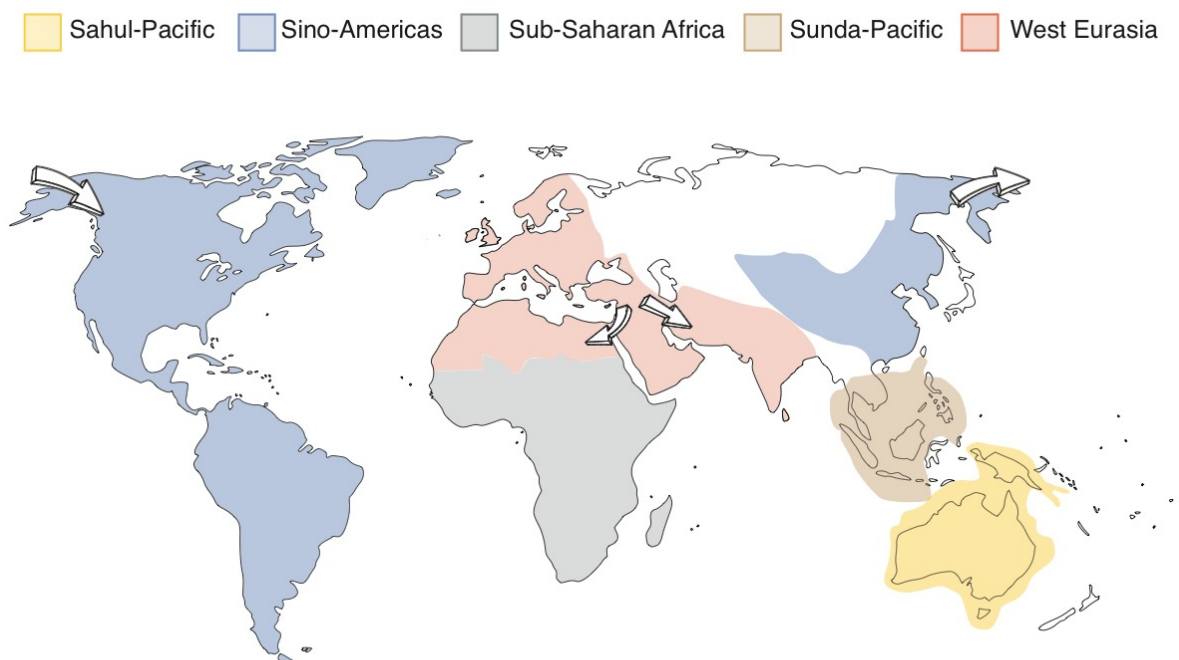


Figure 7.1: Geographical Level 1: Major Human Subdivisions

Scaling sum-of-squares for ascending combinations of phenotypic elements are reported in Table 7.2. These values represent the percent of between group variance explained by each dimension relative to the total amount explained. When all phenotypic elements (E1-E5) are used, FDA explains 96.96 percent of classification performance by canonical variable 3.

Table 7.3: Step-wise phenotype comparisons of cumulative variance explained between groups - G1: Major Human Subdivisions

# of individuals	CV1	CV2	CV3	CV4	DF	TME
<b>Root number (E1)</b>						
n = 756	69.29	96.09	99.69	100.0	13.87586	0.42593
<b>Root (E1) and canal number (E2)</b>						
n = 756	64.47	96.59	99.17	100.0	38.53111	0.28704
<b>Root number (E1), canal number (E2), and root orientation (E3)</b>						
n = 738	68.72	96.43	99.15	100.0	40.35739	0.26965
<b>Root number (E1), canal number (E2), root orientation (E3), and external root morphology (E4)</b>						
n = 595	64.26	92.79	97.02	100.00	175.8313	0.07731
<b>Root number (E1), canal number (E2), root orientation (E3), external root morphology (E4), and canal orientation (E5)</b>						
n = 423	62.95	88.53	96.95	100.00	177.5198	0.03073

CV = canonical variable. DF = degrees of freedom (per dimension), TME = Training misclassification error. Reference population for FDA = Sub-Saharan Africa. Reduction in number of individuals is due to FDA and exclusion criteria removing phenotypes with poor predictive power.

Table 7.3 presents a confusion table for the performance of FDA on our sample. Each row represents instances in a predicted class and each column represents instances in their actual class. When all elements (E1-E5) are used, FDA accurately predicts all instances for Sino-Americans. Other groups have minimal misclassification, with the most confusion occurring between Sahul- and Sunda-Pacific populations.

Table 7.4: Confusion table for FDA of Geographical Level 1: Major Human Subdivisions

	Sub-Saharan Africa	Sahul Pacific	Sino-Americans	Sunda-Pacific	West Eurasia
<b>Root number (E1)</b>					
Sub-Saharan Africa	<b>64</b>	7	7	2	12
Sahul-Pacific	19	<b>99</b>	21	23	77
Sino-Americans	22	15	<b>234</b>	9	20
Sunda-Pacific	0	2	1	<b>2</b>	2
West Eurasia	42	9	7	25	<b>35</b>
<b>Root (E1) and canal number (E1)</b>					
Sub-Saharan Africa	<b>126</b>	8	3	4	11
Sahul-Pacific	5	<b>99</b>	12	14	60
Sino-Americans	4	5	<b>236</b>	3	4
Sunda-Pacific	1	7	4	<b>19</b>	12
West Eurasia	11	13	15	21	<b>59</b>
<b>Root number (E1), canal number (E2), and root orientation (E3)</b>					
Sub-Saharan Africa	<b>124</b>	9	3	2	10
Sahul-Pacific	5	<b>95</b>	11	16	49
Sino-Americans	3	3	<b>235</b>	3	2
Sunda-Pacific	3	7	4	<b>18</b>	14
West Eurasia	9	14	11	21	<b>67</b>
<b>Root number (E1), canal number (E2), root orientation (E3), and external root morphology (E4)</b>					
Sub-Saharan Africa	<b>115</b>	1	0	0	2
Sahul-Pacific	0	<b>90</b>	1	7	13
Sino-Americans	0	0	<b>212</b>	1	1

Sunda-Pacific	0	1	0	<b>35</b>	4
West Eurasia	1	6	1	7	<b>97</b>
<b>Root number (E1), canal number (E2), root orientation (E3), external root morphology (E4), and canal orientation (E5)</b>					
Sub-Saharan Africa	<b>83</b>	0	0	0	1
Sahul-Pacific	0	<b>66</b>	0	6	2
Sino-Americas	0	0	<b>147</b>	0	0
Sunda-Pacific	0	0	0	<b>32</b>	0
West Eurasia	0	2	0	0	<b>82</b>

Rows = predicted classes, columns = actual classes, diagonal values in bold = correctly predicted classes. The confusion table visualizes sensitivity (true positive = **TP**), specificity (true negative = **TN**), type 1 errors (false positive = **FP**), and type 2 errors (false negative = **FN**) for FDA of groups. Outcomes between groups can be formulated in a 2X2 contingency table to calculate statistical measures of a binary classification test. For example, values from Table 6.3 for Sino-Americas and Sub-Saharan Africa would be entered into a contingency table with the following values: **TP** = 147, **TN** = 83, **FP** = 0, and **FN** = 0.

Table 7.4 presents true positive and true negative rates, and accuracy of FDA for G1. Most populations have 100% true positive and true negative rates, and accuracy. FDA is least accurate for predicting membership in Sahul-Pacific and Sunda-Pacific populations (94%).

Table 7.5: True positive, true negative, false positive, and false negative rates of FDA for Geographical Level 1: Major Human Subdivisions

	TPR	TNR	Accuracy
Sino-Americas : Sahul-Pacific	1.0	1.0	1.0
Sahul-Pacific : Sub-Saharan Africa	1.0	1.0	1.0
<b>Sahul-Pacific : Sunda-Pacific</b>	<b>1.0</b>	<b>0.84</b>	<b>0.94</b>
<b>Sahul-Pacific : West Eurasia</b>	<b>0.97</b>	<b>0.98</b>	<b>0.97</b>
Sino-Americas : Sub-Saharan Africa	1.0	1.0	1.0
Sino-Americas : Sunda-Pacific	1.0	1.0	1.0
Sino-Americas : West Eurasia	1.0	1.0	1.0
Sub-Saharan Africa : Sunda-Pacific	1.0	1.0	1.0
<b>Sub-Saharan Africa : West Eurasia</b>	<b>1.0</b>	<b>0.99</b>	<b>0.99</b>
Sunda-Pacific : West Eurasia	1.0	1.0	1.0

**TPR** = True positive rate (sensitivity): **TPR** = TP/(TP+FN).

**TNR** = True negative rate (specificity): **TNR** = TN/(TN+FP).

Accuracy = TP+TN/(TP+TN+FP+FN).

Figure 7.2 displays combinations of coordinate plots for canonical variables 1-3. which explain 96.95% of cumulative between-group variation and show clear separation between Sino-Americans and Sub-Saharan Africans to each other and to all other groups. Sino-Americans remain separate in the majority of combinations, followed by Sub-Saharan

Africa. Sahul- and Sunda-Pacific show overlap with one another and/or West Eurasian populations.

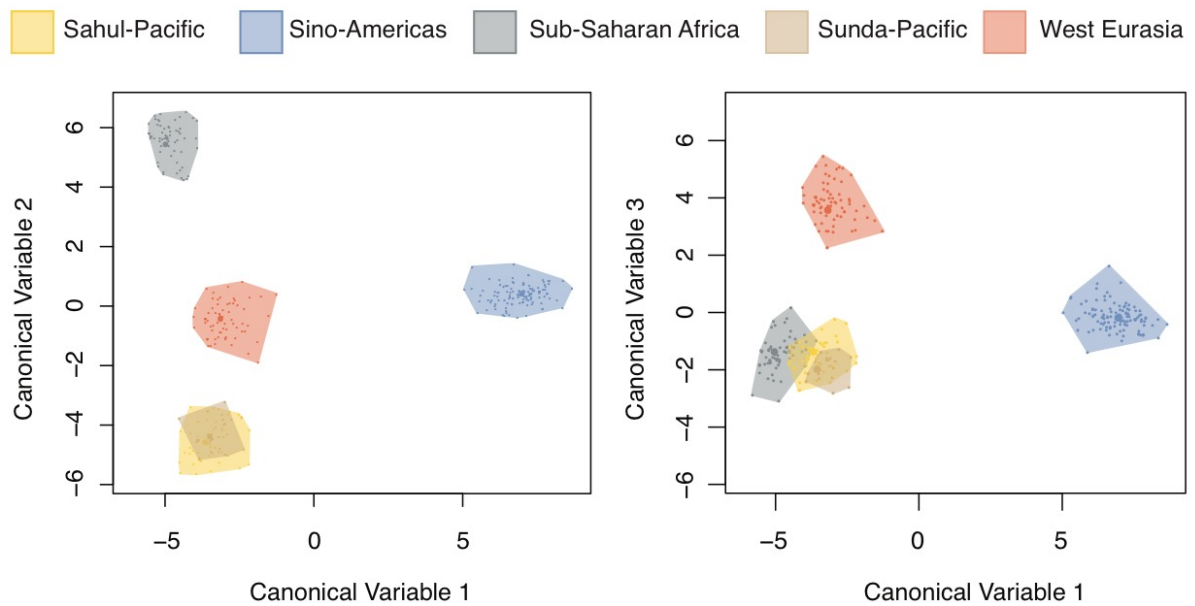


Figure 7.2: Canonical variable plots for all maxillary and mandibular teeth from Geographical level 1: Major Human Subdivisions. Canonical variables 1-3 explain 96.95% of cumulative variance between groups.

#### 7.4.2 Maxilla and mandible, all teeth, Geographical level 2: Continental Groups

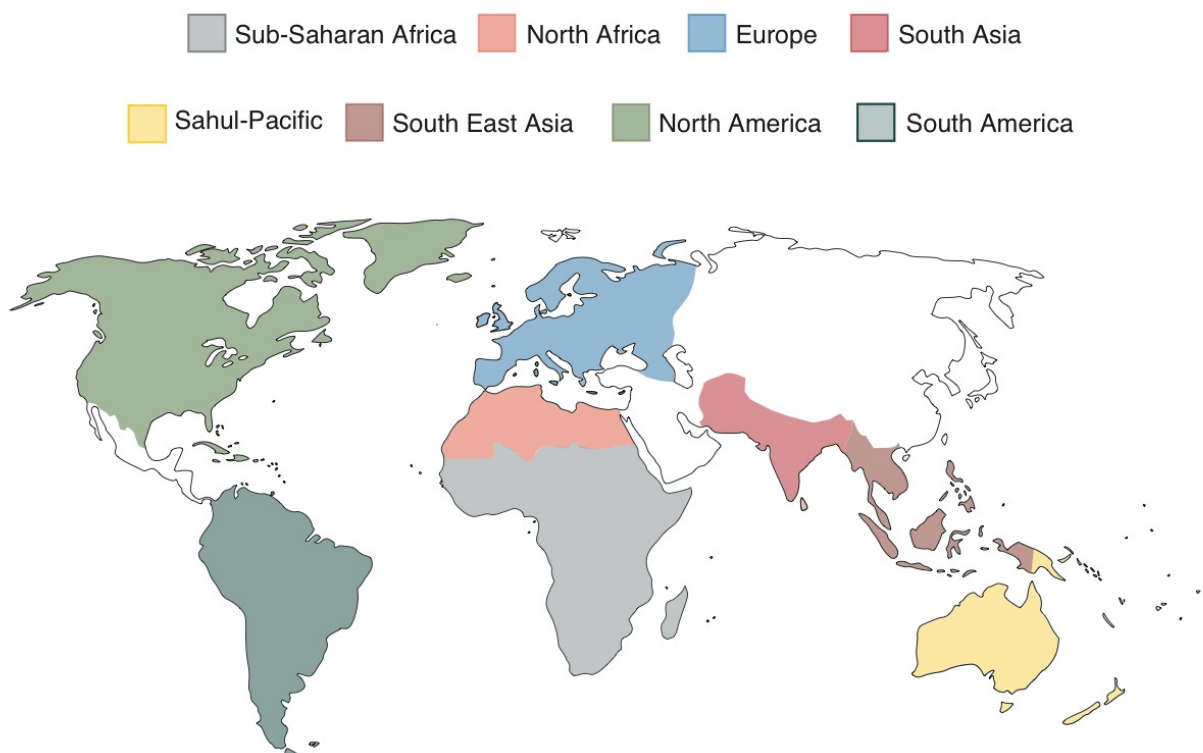


Figure 7.3: Geographical Region 2: Continental Groups. Central America has been removed from this level of analysis as there was only one individual belonging to this group, which violates our exclusion criteria.

Optimal scaling sum-of-squares for each dimension from Geographical Region 2: Continental Group (G2) are reported in Table 7.5. These values represent the percent of between group variance explained by each dimension relative to the total amount explained. 92.35 percent of classification performance is explained by the first 3 canonical variables, with minimal incremental increases between variables 3-7.

Table 7.6: Cumulative variance explained between groups - Geographical Region 2: Continental Group

Canonical Variable	V1	V2	V3	V4	V5	V6	V7
%	60.08	84.05	92.25	95.04	97.15	98.97	100.0

Degrees of freedom per dimension = 178.4111. Training misclassification error: 0.06147 (n = 423).

FDA accurately predicts all instances for Central America, South Asia, and South East Asia. Other groups have minimal misclassification, with the most confusion occurring between Sahul- and Sunda-Pacific populations (Table 7.6).

Table 7.7: Confusion table for Geographical Region 2: Continental Group

	Sub-Saharan Africa	Europe	North Africa	North America	Sahul-Pacific	South America	South Asia	South East Asia
Sub-Saharan Africa	<b>83</b>	0	0	0	0	0	0	0
Europe	0	<b>20</b>	4	0	1	0	6	0
North Africa	0	0	<b>31</b>	0	0	0	0	0
North America	0	0	0	<b>129</b>	0	1	0	0
Sahul-Pacific	0	1	0	0	<b>68</b>	0	1	6
South America	0	0	0	5	0	<b>11</b>	0	0
South Asia	0	0	0	0	0	0	<b>24</b>	0
South East Asia	0	0	1	0	0	0	0	<b>31</b>

Rows = predicted classes, columns = actual classes, diagonal values in bold = correctly predicted classes. Central America has been removed from this level of analysis as there was only one individual belonging to this group, which violates our exclusion criteria.

Table 7.7 presents and true negative rates, and accuracy of FDA for G2. Most populations have 100% true positive and true negative rates, and accuracy. FDA is least accurate for predicting membership between European and South Asian populations (88%). The majority of cases with reduced accuracy are associated with groups that are in close geographic proximity; for example, Europe and North Africa (93%), or Sahul-Pacific and South East Asia (94%).

Table 7.8: True positive and true negative rates for FDA of Geographical Region 2: Continental Group

	TPR	TNR	Accuracy
Sub-Saharan Africa : Europe	1.0	1.0	1.0
Sub-Saharan Africa : North Africa	1.0	1.0	1.0
Sub-Saharan Africa : North America	1.0	1.0	1.0
Sub-Saharan Africa : Sahul-Pacific	1.0	1.0	1.0
Sub-Saharan Africa : South America	1.0	1.0	1.0
Sub-Saharan Africa : South Asia	1.0	1.0	1.0
Sub-Saharan Africa : South East Asia	1.0	1.0	1.0
<b>Europe : North Africa</b>	<b>1.0</b>	<b>0.89</b>	<b>0.93</b>
Europe : North America	1.0	1.0	1.0
<b>Europe : Sahul-Pacific</b>	<b>0.95</b>	<b>0.99</b>	<b>0.98</b>
Europe : South America	1.0	1.0	1.0
<b>Europe : South Asia</b>	<b>100.0</b>	<b>0.80</b>	<b>0.88</b>
Europe : South East Asia	1.0	1.0	1.0
North Africa : North America	1.0	1.0	1.0
North Africa : Sahul-Pacific	1.0	1.0	1.0
North Africa : South America	1.0	1.0	1.0
North Africa : South Asia	1.0	1.0	1.0
North Africa : South East Asia	1.0	1.0	1.0
North America: Sahul-Pacific	1.0	1.0	1.0
<b>North America: South America</b>	<b>0.96</b>	<b>0.92</b>	<b>0.96</b>
North America: South Asia	1.0	1.0	1.0
North America: South East Asia	1.0	1.0	1.0
Sahul-Pacific: South America	1.0	1.0	1.0
<b>Sahul-Pacific : South Asia</b>	<b>1.0</b>	<b>0.96</b>	<b>0.99</b>
<b>Sahul-Pacific: South East Asia</b>	<b>1.0</b>	<b>0.84</b>	<b>0.94</b>
South America : South Asia	1.0	1.0	1.0
South America : South East Asia	1.0	1.0	1.0
South Asia : South East Asia	1.0	1.0	1.0

TPR = True positive rate (sensitivity):  $TPR = TP/(TP+FN)$ .

TNR = True negative rate (specificity):  $TNR = TN/(TN+FP)$ .

Accuracy =  $TP+TN/(TP+TN+FP+FN)$ .

Figure 7.4 displays combinations of coordinate plots for canonical variables 1-3, which explain 92.25% of cumulative between group diversity in G2. There is a clear separation of North and South American populations from all other groups. For several variables Central America is either separate from all groups or is grouped away from North and South America. This may be due to only one individual from Central America being included in this study. Clear groupings are present in all plots: South-East Asia groups with Sahul-Pacific; South Asia and Europe group with North Africa, while Sub-Saharan Africa primarily remains separated from other groups.

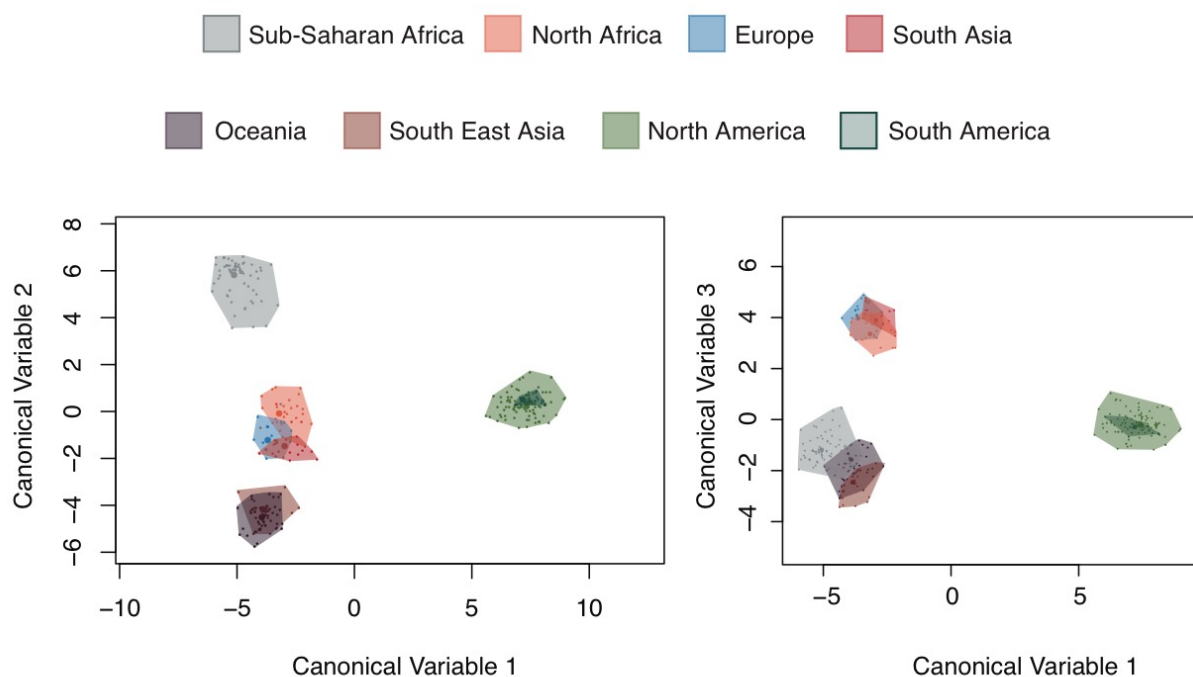


Figure 7.4: Canonical variable plot for all maxillary and mandibular teeth from Geographical level 2: Continental groups. Canonical variables 1-3 explain 92.25% of cumulative variance between groups.

## 7.5 Discussion

The results from these analyses are promising, indicating that the phenotypic patterns present across human populations can accurately classify those populations into groups that were based on other criteria such as geography or language. The results show that first, the combined five phenotypic elements give the strongest classificatory power; and second, that geographically based human populations can be identified and separated with a higher degree of discrimination than is seen in traditional methods. There are, however, a number of issues that require further discussion.

### 7.5.1 Diversity of root phenotypes and classical human biogeographical categories

It is well established, both through classic anthropological approaches and more recent genomic studies, that human populational variation is clinal (Handley et al., 2007; Hanihara, 2008), with no clear-cut boundaries between them. Nonetheless, geographical variation at the population level does exist, and reflects difference in ancestry as well as a history of admixture and gene flow. Research into the history of human diversity has depended upon identifying the broad pattern of human global phenotypic and genetic diversity. Given the lack of discrete boundaries, the challenge is to determine on what basis to categorize and classify the global populations, and the appropriate scale.

In the first set of analyses presented here, the higher-level categories consisted of the five units based on traditional geo-linguistic distributions – Sub-Saharan African, Sunda-Pacific, Sahul-Pacific, Sino-American and Western Eurasia. The division of humanity into five major groups (and further regional subdivisions) is based on geography, language, genetics, and, of course, dental variation. The first two, language and genetics, can be argued to be completely independent of one another. While true at the individual and group levels, there is a significant correspondence between genetics and language, and the process underlying both share common attributes (Carstairs-McCarthy and Ruhlen, 1997; Lieberman, 2006; Chen et al., 2012). As in genetics, language has geographic and temporal dependencies, with numerous characteristics that possess a 'phylogenetic' history. However, unlike genetics, the spread of language is horizontal, rather than vertical, proceeds at a faster pace, and can be adopted by assimilated but genetically different populations. Distance matrices for genomic and linguistic data indicate a separate grouping pattern for East Asians, Arctic populations, and Australian Natives from Caucasoid and Sub-Saharan African populations (Chen et al., 2012).

Using these categories allows comparability with classic analyses of dental phenotypic variation in the anthropological literature (Irish, 1998; Irish and Guatelli-Steinberg, 2003; Hanihara and Ishida, 2005; Hanihara, 2013; Scott et al., 2018). The results presented here suggest that tooth root phenotypes also pattern out in similar ways – for example, Sunda-Pacific and Sahul-Pacific are very similar, while the Sino-American group, probably subject to drift and founder effects, are the most distinct. The Sub-Saharan African

population is also distinct on Canonical Variable 2 (Figure 7.2). That the first three canonical variables account for 96% of the observed variation suggests that these results are fairly robust. Furthermore, the degree of discrimination between geographical groups is striking, much more so than in many other studies (the plots shown in Figure 7.2 have had the outliers removed for clarity of presentation given the very high number of positive and negative FDA scores, but the full dataset plots are provided in Appendix Section 9.5, Figure 9.1). Whether this is a result of the novel method employed here is discussed below.

### 7.5.2 Comparison of genome ancestry patterns and root phenotype distributions.

These population groupings are not monophyletic as currently understood on the basis of genomic research (in as much as the term monophyly can be applied to human populations but should be taken here to mean a higher degree of shared ancestry for each than would be the case for other populational groupings). It is not therefore clear whether the tooth root phenotypic patterning observed reflects ancestry or more recent admixture and gene flow. Recent studies of populations have primarily used genetic variation to detect population history (Li and Durbin, 2011; Ralph and Coop, 2013; Schiffels and Durbin, 2014). These results have built extensively on the original 'out of Africa' model of recent human evolution (Cann et al., 1987), where all living humans are descended from a relatively small ancestral African population, and non-Africans are the descendants of one or more dispersals across Eurasia (Winder et al., 2015). The earliest Eurasia split is between Asian and Pacific populations, and West Eurasians. After that, it is Sunda and Sahul populations that diverge from the rest of Asia (O'Connell et al., 2018). Within the descendant populations there are several further divergences. It is likely that these patterns reflect original dispersals of early modern humans, and subsequent dispersals and range shifts across the Upper Pleistocene and throughout the Holocene (Pugach et al., 2013; Reyes-Centeno et al., 2015). However, this 'dispersal and divergence model' is a major oversimplification, as each of these is overlain by repeated contact, gene flow and admixture, both between populations of modern humans, and with archaic species (Reich, 2018). Figure 7.5 shows the pattern of human geographical diversity based on major

sources of ancestry, thus reflecting the dispersal and divergence model without taking into account the overlay of gene flow.

The timing of these divergences is still lacking fine resolution. The early African divergences probably date between 100 and 200 Ka; the primary Africa-Eurasia split is in the region of 70 – 50 Ka; the divergence of the Sunda-Sahul populations is around 45 Ka, while the later main divergences all occur after about 30 Ka. It should be emphasized that there are broad errors on these estimates, but the issue here is the branching sequence rather than hypothesized chronology.

We can match, to some extent, the Major Human Subdivisions and Continental Groups on to the genomic results. Figure 7.5 shows a phylogenetic tree of human populations based on ancient and contemporary genomics, using dominant ancestry to construct the tree – in other words, the tree reflects the primary ancestral contribution to the descendant populations, and does not take into account high levels of admixture and gene flow which would greatly reduce the resolution of the tree.

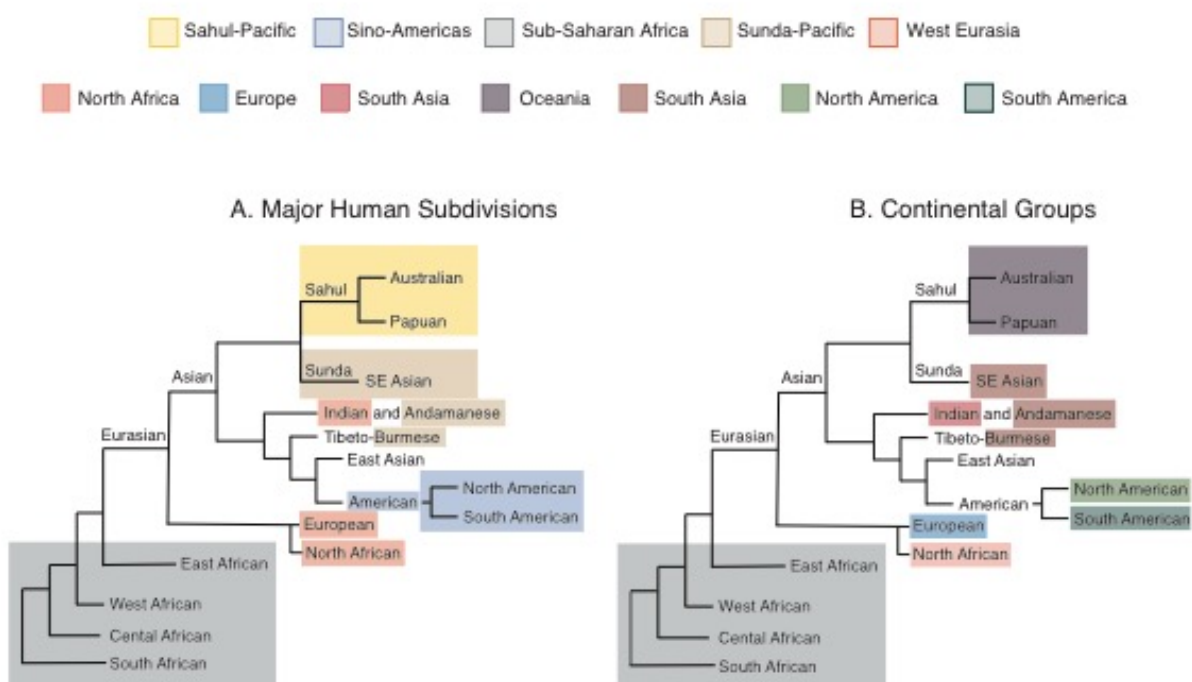


Figure 7.5: Phylogenetic tree of human populations based on ancient and contemporary genomics after Cavalli-Sforza (1994). Overlaid colours represent (A) Geographical Level 1: Major Human Subdivisions and (B) Geographical Level 2: Continental Groups. Tree is only used for visualisation of groups and is not calculated from actual phylogenetic distances.

The groups identified in the Major Human Sub-division analyses here do reflect the tree to a large extent (Figure 7.5A), in that the results show that the groupings that arise out of the analysis are ones that coincide with the dominant ancestry tree. The exception is our West-Eurasian category, which combines South Asian and European populations, which is inconsistent with the genomics. However, Indian ancestry is highly variable, with strong genetic and linguistic links between some Indo-European and Afro-Asiatic populations. Similar groupings are reflected in tooth crown phenotypes, and have been attributed to a relatively recent immigration of Europeans into the Indian-Subcontinent that comprise the majority of North Indian populations (Wells et al., 2001; Cordaux et al., 2004; Scott and Hemphill, 2012).

In terms of comparison of phenetic similarity shown in the results here, and phylogenetic affinity represented genomically, one would expect there to be some patterning that reflects the broad 'out of Africa model'. The MHS plots (Figure 7.2) show that Sub-Saharan Africa and Sino-American populations are most distant from one another, and this may reflect the more ancestral and derived condition of each respectively. The Sino-American group, which is primarily comprised of North-American populations, is likely to have been most influenced by distance from Africa and isolation. The two most linked groups (Sunda and Sahul) are the most similar, as one would expect.

When we look at the continental subdivisions (Figure 7.4) the resulting groupings are also generally consistent with genomic reconstructions. Again, Sub-Saharan African and Sino-American populations are distinct from all other groups. Ancient populations expanded rapidly across the Americas around 14,000 years ago, and are a genetically and culturally distinctive group (Moreno-Mayar et al., 2018; Posth et al., 2018). South American groups have been difficult to classify using tooth crowns. This is because previous studies of South American tooth crowns were sampled from Peru, Chile, and the Caribbean, and these groups might reflect introgression from African or European populations, or be obscured by crown wear (see Burnett et al., 2013 for an in depth discussion of these studies). However, FDA was able to use tooth roots to classify North and South American groups with 96% accuracy (Table 6.7). Though the sample includes specimens from Peru, Chile, and the Caribbean populations, they groups are known to have strong Native American ancestry (Wang et al., 2008; Homburger et al., 2015). Increased genomic and phenotypic resolution will help resolve these groupings.

Human occupation of South East Asia (Sunda) and Sahul (New Guinea and Australia) encompasses the first out-of-Africa expansion of *H. sapiens* during the Upper Pleistocene. With the exception of Australia and some Melanesian Islands, subsequent dispersals of especially Austronesian speakers added to the populational diversity and extended the range of human occupation to the Pacific Islands (Polynesia). Australia and Melanesia, therefore, link ancestrally to the early South East Asia populations, while the parts of Melanesia and all of Polynesia link to the Taiwanese (i.e., East Asian) source populations. In the results presented here for the Major Human Subdivisions (Figure 7.2) support this pattern, showing firstly that there is a strong overlap between the Sahul-Pacific and Sunda-Pacific populations in Canonical Variables 1 and 2, and the Canonical Variable 3 brings them together with Sub-Saharan Africa, as would be expected if they were part of an earlier southern dispersal (Lahr and Foley, 2005). The same pattern can be observed in the Geographical Level 2 (Continental Groups), where Australia & Melanesia (Sahul) are very similar to South East Asia, and Africa is similar when Canonical Variable 3 is included (Figure 7.4). Together these are perhaps strong support for a southern dispersal, as is indicated by some genetic evidence (Malaspinas et al., 2016).

### 7.5.3 The problem of scale and classificatory criteria in human populations

One of the problems in any sort of analysis of human biological and evolutionary diversity is to select the appropriate geographical scale. In principle one can operate at any scale from, perhaps, Africa versus non-Africa, down to individual linguistic or cultural groups. In these analyses we have selected only two scales, the Major Human Subdivisions and the Continental Groups: two levels which represent a pragmatic mix of geographical location, historically recognized phenotypic groups, and linguistic affiliation (Cavalli-Sforza, 1994; Scott et al., 2018). As discussed in the previous section, selecting populations on the basis of dominant ancestry would be an alternative, and it is likely that the growing consensus on the details of long-term patterns of dispersal and admixture will provide the best basis for groupings. However, what should be emphasized is that the appropriate scale and criteria should be question-dependent. If, for example, we are interested in small scale, recent patterns, then using linguistic and cultural affiliation are likely to be the best ones. If, on the other hand it is deeper time depths that are of interest, then it is unlikely that

linguistic affiliation is appropriate as most language families are likely to only have a time depth of less than ten thousand years. Equally, if we are interested in the role of selection on the distribution of phenotypes economic or habitat categories might provide a better framework. Further research is required to explore analytically the underlying structure of global diversity in root phenotypes, at different population levels.

#### 7.5.4 Archaic and older AMH admixture

In discussing these geographical patterns, the emphasis has been placed on dominant ancestry, but it is worth stressing two further elements that might compound these effects. The first is that the genetic evidence, certainly in terms of chronology, is not always consistent with the archaeological and fossil evidence. Two examples can be given. The first is Sahul-Pacific. The genomic evidence (Malaspinas et al., 2016) would suggest an age of colonization of Australia and New Guinea around 48 Ka (i.e. the split date for Sahul populations from Sunda ones). However, there is strong evidence for colonization as early as 65 Ka (Clarkson et al., 2017). The second is East Asia. The divergence of East and West Eurasians is thought to be around 42 Ka (Yang et al., 2017; Matsumura et al., 2019). This would fit a large amount of evidence for the spread of Upper Palaeolithic populations, but there is also evidence for substantially older populations in East Asia at 80 Ka (Liu et al., 2015).

In addition to the evidence for earlier modern human presence in parts of Eurasia, there is also extensive evidence for admixture (Figure 7.6). Much stress has been placed on the evidence for admixture between modern humans and archaic populations (Kelso and Prüfer, 2014; Vattathil and Akey, 2015; Nielsen et al., 2017), but there is also extensive admixture between different early (i.e. Upper Pleistocene) modern humans in Eurasia (Prüfer et al., 2014; Fu et al., 2016; Meyer et al., 2016; Rogers et al., 2020). The significance of these two observations is that the expectation that root phenotypic patterns will necessarily reflect dominant ancestry patterns is an oversimplification, and we should expect further work to focus in more detail on the complex relationships of genotype-phenotype relationships.

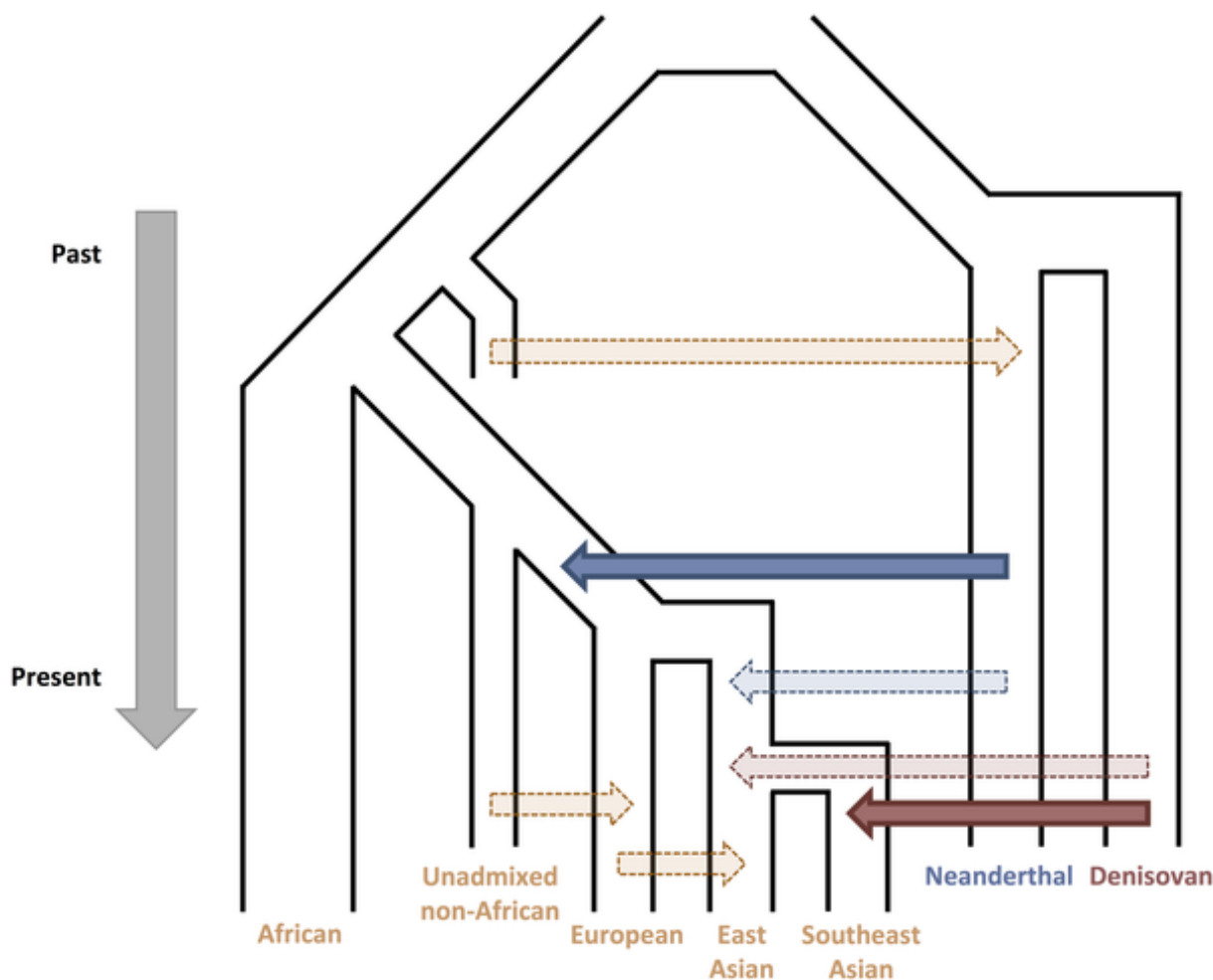


Figure 7.6: Characterization of archaic gene flow into early modern humans. Figure from Wolf and Akey, 2018.

In terms of tooth roots, this may be particularly pertinent when considering rare phenotypes, or ones that have been found in archaic hominins. Several dental traits identified in Late Pleistocene *H. sapiens* from China have been attributed to archaic hominins (Shang et al., 2007; Liao et al., 2019). A three-rooted 2nd mandibular molar belonging to the Denisovan hemimandible from Xiahe, China has also been attributed to introgression (Bailey et al., 2019; Chen et al., 2019). This interpretation has proven controversial, as while the trait does appear in modern humans, it is usually found in the 1st molar (Scott et al., 2018), and with key differences in its morphological expression (Scott et al., 2020).

### 7.5.5 The potential of AI and Machine learning approaches

While machine learning falls under the umbrella of Artificial Intelligence (AI) it is only making its decisions according to what it has learned from the data. In this study we were able to supply the classifier with a robust data set of known samples. 'Known' is the key word here, as the machine learning methods employed in this paper are a type of 'supervised' pattern recognition (supervised because the data has been labelled and processed by humans). This is the reason we have introduced an exclusion criterion. The classifier cannot be trained to classify phenotypes or groups that appear once as it has no labelled data for training. For example, the Central American individual was removed during analysis of G2, as without other Central Americans to train itself on FDA was unable to generate a classification.

One of the strengths of machine learning techniques is that they allow the use of advanced algorithms to parse data, learn from it, and discover meaningful patterns that a human user may fail to recognize due to the size or complexity of the data set. Another is that machine learning models are adaptive, in that they can learn through new sample data. A step up from supervised machine learning is the application of neural networks. A neural network, once trained, is not limited to labelled data. Instead, it will process unlabelled data in multiple layers, with each layer classifying characteristics and information from the previous one and make decisions based on the patterns it pulls from the data. For our analyses this would mean the recovery of all individuals and phenotypes removed by our exclusion criteria, which would enable accurate classification at more refined levels of geographical subdivisions such as the continental, country or state, or even tribal or local levels. We have shown in this study that mixed metric and non-parametric data can be utilized for these types of studies, and with great effect.

## 7.6 Conclusions

This paper presents a novel method for using tooth root phenotypes to classify population structure from a global sample of modern humans. This was accomplished by training a non-parametric machine learning classifier with tooth root phenotypic data: root and canal number, morphology and canal orientation, coded into a novel phenotyping system, and continental and sub-continental geographic data. Results show that tooth roots

capture population and sub-population heterogeneity in a way that provides accurate (88-100%) classification of groups. These results are comparable with those of genomic studies, in that group structures reflect the primary ancestral contribution to the descendant populations. While results show that geographically-based human groups can be identified and separated with a high level of statistical probability, we propose that future studies will benefit from the inclusion of a neural network in order to reconcile rare (n=1) phenotypes and outliers, and to assist in classification in smaller populations subdivisions.

## Chapter 8: Conclusions

Discussions of the major results of the research presented here have been provided in each of the chapters. This chapter summarizes these results and discusses some of the broader issues tying them together. Directions for future research are also discussed.

### 8.1 Summary of conclusions

Chapter 4 presents a novel study of the relationship between canal and root number. We show that for all teeth, canal number is equal to, or exceeds, root number; that these canal to root relationships are significantly different between tooth types (i.e., molars and premolars), within and between the maxilla and mandible. These results suggest that canals lead the way developmentally, and that root count as a phenotypic trait is influenced by canal count. Results also show that the relationship between canal and root number differ between global populations, with a reduction of root number and canal number in non-African populations.

Having established the connection between root and canal number, Chapter 5 presents a novel study on the relationship between canal number, morphology, and orientation to external root morphology. Results indicate that canal number, and certain canal morphologies and orientations are strongly associated with, and predictive of certain external root morphologies. Results also include a description and discussion of the MFP of individual roots and root complexes of teeth within the maxilla, mandible, and combined jaws. Certain roots of the teeth and jaws appear to be more variable than others. Why this should be is unclear. Future studies will most likely require an interdisciplinary approach combining developmental biology and the effects of masticatory loadings and directions on root form and function.

In Chapter 6, a novel system for defining and analysing the phenotypic set of the human tooth root complex was developed and tested on the maxillary and mandibular teeth of a modern human sample. This system focuses on five elements (E): root presence/absence (E1), canal root presence/absence (E2), canal location (E3), external root morphology (E4), and canal morphology and configuration (E5). These elements can be applied individually and/or in combination to investigations of phenotypic diversity,

population affinity and history, and biomechanical and spatial hypotheses of growth and development. The phenotyping system is also shown to be applicable to non-human primates and fossil hominins.

The results of this system demonstrate its utility and effectiveness in delineating distributions of phenotypes in populations of modern humans; and that these groups occupy overlapping, but ultimately different positions in tooth root morphospace. The phenotypic set of our sample is comprised of 841 phenotypes, a number which seems quite large, especially as it approaches the number of individuals used for this study ( $n = 945$ ). However, the large numbers of phenotypes can be explained as variations on a theme, by which the change of one element in the root complex can result in multiple, nearly identical tooth roots being described with different phenotypes. This variation increases rapidly when multi-rooted teeth are included.

Chapter 7 applies machine learning techniques to the tooth root phenotypic set. Traditionally, studies of population affinities and histories rely on biological distance statistics. The aim of these approaches is to understand movements and mixtures of human populations across time, and how geographically distant groups are related. This analysis takes things one step further, asking if tooth roots can accurately classify populations. This novel application of machine learning methods reveals that tooth root phenotypes can classify populations with a high degree of accuracy at the global and continental population levels. Further, populations at both levels are classified in a way that may reflect ancestral and derived conditions, with Sub-Saharan African and Sino-American populations being the most distinct and distant from one another based on their cumulative variance.

## 8.2 Tooth roots as a model phenotype

This dissertation consists of an in-depth examination of a relatively understudied dental morphological complex that has the potential to be highly informative for anthropology and human evolutionary studies. Teeth, including roots, are well represented in the fossil record, and so can play an important role in the reconstruction of evolutionary and biogeographical history. The results in the individual chapters of this dissertation have attempted to demonstrate this. However, it is also important to consider that they are just one of a vast array of potential phenotypes useful for studying humans, non-human

primates, and fossil hominins. In this context they can be viewed as a model system, and that the methods developed here – building up the assessment of the diversity of forms from elements that can be combined – can be applied to other systems. A recent study has made a similar approach in testing the for the most efficient combination of dental traits of the ASUDAS by first defining all possible combinations, and then assessing which combinations are most effective for detecting variation (Rathmann and Reyes-Centeno, 2020).

The value of tooth roots as a model system can also be considered in terms of the fact that they are clearly integrated with other elements of morphology. The most obvious of these are tooth crowns, but equally important are the bony matrix of the mandible and maxilla. Developing similar approaches to other parts of the masticatory system will contribute to the important issues of surrounding the phenotypic integration, modularity and evolvability of biological structures. A classic example of this in hominin evolution is the reduction of facial prognathism and encephalization of the cranium. These changes are the results of selection and adaptive strategies at different points in hominin evolutionary history. At some point the integration of cranio-dental features is reduced, leading to potential increased variability of some elements via selection, while other elements remain fixed, or phenotypically constrained (Gómez-Robles and Polly, 2012).

While tooth roots are in one sense just one of many of these possible phenotypic models, they also have unique elements which set them apart. The stems from their composition of epithelial tissues - dentine and cementum. These, in some ways drastically different tissues, and their resultant phenotypes, stem from their reciprocal and sequential developmental trajectories. It is these unique properties that make roots such an excellent morphological complex for testing ideas about phenotypic integration, modularity and evolvability. As shown in this dissertation, each one of the 5 elements is dependent on one or more of the other elements. Results indicate that the 'root' phenotype from which variation is derived is element 2 - canal number.

## 8.3 Evolutionary and methodological issues

### 8.3.1 The use of key teeth vs. the total phenotypic set

As discussed in Section 3.5 the use of ‘key teeth’ has long history in dental anthropological studies. From a statistical analysis standpoint this is to avoid issues with how linearly correlated and/or non-independent variables violate statistical assumptions of independence. In modern humans, this approach is problematic as (a) it leaves out a wide range of tooth root and canal morphologies that are either not found in ‘key teeth’ (e.g., M<sub>2</sub>s with C-shaped roots and canals), or have a higher degree of expression than the most mesial member of a morphogenetic field (e.g., fused roots; see Table 3.9); and (b) many of these traits, such as C-shaped molars, Tomes’ roots, and three rooted M<sub>1</sub>s have an ethnic component, with high frequencies in Asian, European, and Sino-American populations respectively (Tomes, 1889; Wang et al., 2012; Ballullaya et al., 2013; Fernandes et al., 2014). These traits are of great importance for population studies based on tooth root phenotypes, and it may be that the inclusion of all teeth rather than just ‘key teeth’ are necessary for generating higher resolution classification analyses such as the one carried out in Chapter 7.

From an adaptive framework, ‘key teeth’ are also problematic as they potentially biased towards adaptive traits at the expense of ‘populations specific’ traits. In humans, M<sup>1</sup>s/M<sub>1</sub>s, the ‘key teeth’ in molar morphogenetic fields, have the highest bite-force magnitudes of all teeth (Ledogar et al., 2016). Chapter 6 shows that M<sup>1</sup>s/M<sub>1</sub>s have the most phenotypic permutations (Table 6.9). However, it is unclear if this is due to adaptive pressures of dietary differences within and between geographic groups, some other selective pressure. Further work on tooth root trait expression and frequency, and how these correlate with masticatory behaviours will need to be carried out in order to determine how and what traits are adaptive versus which ones are population specific.

### 8.3.2 Tooth root morphospace

One of the great questions in evolutionary biology regards the evolution of organismal shape, and in particular, why certain forms are repetitive, others rare, and others not at all. Central to this dissertation is finding a rigorous and comprehensive way of defining tooth root diversity. To accomplish this, we find the concept and application of the morphospace, the space which describes and relates phenotypes, to be critical. The concept

of the morphospace underlies the statistical description of biological shape and form in studies of morphometrics (Bennett, 1983; Mitteroecker and Huttegger, 2009). However, it is also fundamental to the conception of theoretical considerations of adaptive landscapes, and distance or direction between actual and theoretical phenotypes in topological spaces.

Numerically, a single root can have only one of 8 external morphologies. If this single root contains a single canal, then the internal morphologies are limited to 2. A single root with two canals is limited to 9 internal morphological configurations. In aggregate, the number of traits observable in a single root are 20. Compared to the 27 traits of the ASUDAS (Turner II et al., 1991; Scott et al., 2018), of which root count is one, tooth root morphology appears to be more constrained, but more diverse than previously accounted for. However, the majority of teeth are not single-rooted, and the number of phenotypes for a single root becomes additive as root number increases. The description of the tooth root morphospace from this sample reaches 841 phenotypes, many of these based on multi-rooted forms. While this number may seem high, and with little utility for analyses, the 27 traits of the ASUDAS, of which multiple combinations are found in each tooth crown, produce >134 million combinations (Rathmann and Reyes-Centeno, 2020).

The definition of tooth root morphospace, and the distribution of phenotypes within such a space allows for inferences and hypotheses about phenotypic relationships, which may not be evident from pair-wise phenotype comparisons or singular descriptions. In this dissertation, these comparisons are limited to elements only found within the tooth root complex. Thus, not only is the diversity of tooth root morphospace defined and explored, but through its very definition, new questions and testable hypotheses are generated. This dissertation addresses only some of them.

### 8.3.3 The phenotypic set

The concept of a morphospace effectively defines the totality of forms that are theoretically possible – in other words, all the combinations. This very large number is, however, the number of possible phenotypes. The number of actual phenotypes is likely to be much smaller. Physical incompatibilities make this inevitable as there exists an upwards boundary or biological constraint on phenotypes. For example, while it is theoretically possible to have 10 roots in a single tooth, the biological reality of this is effectively nil due

to spatial restrictions alone. Conversely, hominins can theoretically have more or less teeth in each quadrant of the dental arcade than the usual 8 (2:1:2:3). The spatial constraints for this are quite low, and the ancestral Eutherian mammalian pattern possesses 3 incisors and four premolars (Jheon et al., 2013). Thus, additional (or reduced) numbers of teeth exist in mammalian dental phenotypic set, yet the realized phenotypic set of hominin dental phenotypes does not match this variation.

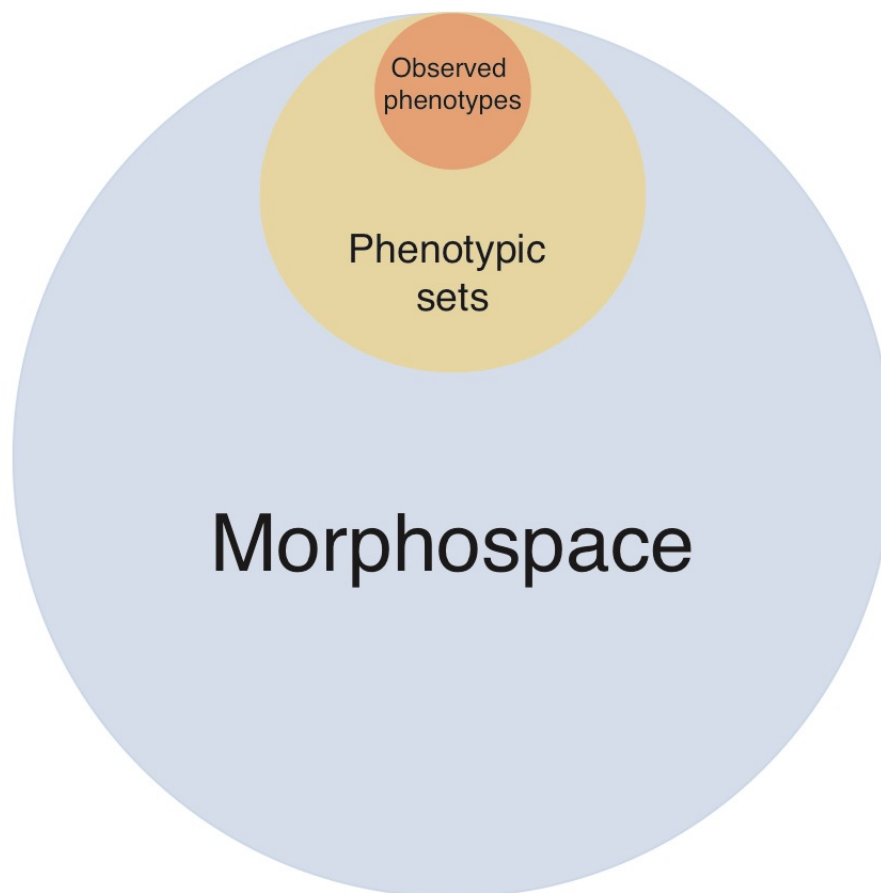


Figure 8.1: Morphospace, phenotypic sets and observed phenotypes. The morphospace is the totality of possible combinations. However, many of these are not possible (what are classically considered to be physical constraints), so that much of morphospace (brown) is 'impossible'. What remains is the phenotypic set (orange), the possible forms. Not all of these in turn may actually occur, or occur in a particular sample, or may have once occurred but are now extinct (pale green). These are the observed phenotypes. The value of these concepts is to understand what factors and conditions, physical, biological or historical, determine these three interlocking concepts.

Furthermore, not all possible phenotypes actually occur. Some may never have occurred, in that while they may be possible, they are seldom beneficial. Others may have occurred in ancestral species that have now become extinct, such as the ancestral hominin

3-rooted maxillary premolars (Abbot, 1984; Emonet et al., 2012), or the Eutherian tooth pattern discussed above. These too constitute the phenotypic set. Although this concept was developed by Maynard Smith (1976) for modelling behaviour, it has broader value, as it defines the phenotypes that are at play in the functional and selective arena, and therefore the group that must be considered in any assessment of patterns of diversity in space or change over time (Figure 8.1).

In creating the tooth root phenotyping system, an attempt has been made to develop a methodology that allows a definition of the total morphospace – the full range of possible combination of all five elements and their states. In the analyses we have explored the broad principles underlying the relationships and combinations of elements, and so defined what might be considered the phenotypic set; and then, for the sample available, we have determined the number of observed phenotypes.

This may appear a cumbersome system, but it has the advantage of not being limited to particular samples, or in the case of dental anthropology, individual teeth. Instead, it allows comparisons to be made with all possible phenotypes, and hence expand the range of evolutionary and functional comparisons and hypotheses. The method can be simplified – using fewer of the elements or reducing the number of states that each element can have or be appended to account for newly identified phenotypes. But these are easily available analytical options, rather than conceptual ones.

## 8.4 Evolutionary implications and applications

Mentioned throughout this dissertation is the poor understanding of tooth root phenotypic diversity. This extends to, and stems from, the developmental processes underlying tooth root number, morphology, and patterning (Li et al., 2017). For evolutionary studies, the clarification of these developmental pathways here, in modern humans, may offer novel insights on hominin evolution. While core processes are generally conserved in biological systems, their number and stability give rise to phenotypic diversity (Kirschner and Gerhart, 1998), are heritable, and under selective pressure (Earl and Deem, 2004; Bloom et al., 2006). It is highly probable that the developmental processes underlying tooth root diversity in humans are identical in fossil hominins. It is only their phenotypic expression that is different. Compared to humans, canal number, and root number and

orientation of certain teeth do exhibit greater variability between and within great apes and Plio-Pleistocene hominins (Wood et al., 1988; Moore et al., 2013, 2015, 2016; Kupczik et al., 2018). The link between canal number and orientation to root number and morphology may help explain why this variation in hominins exists from a developmental context.

The application of the phenotype system to fossil hominins also allows for the definition of a genus' or species' unique tooth root morphospace; adding new morphological data that can be utilized for a number of research tracts. From a comparative standpoint, the identification and classification of unreported external and internal non-metric morphologies will prove beneficial in cladistic and phylogenetic analyses. This may be especially useful for clarifying questions of robust australopith mono- and polyphyly (Wood and Constantino, 2007).

Recent research in dental morphology (Hanihara, 2008), and population and quantitative genetics (Ramachandran et al., 2005) have shown that genotypic and phenotypic variation decreases with increased geographical distance from Africa; and that neutral genetic variation and tooth crown morphological variation are significantly correlated (Hubbard et al., 2015; Rathmann et al., 2017). This dissertation has shown that like tooth crowns, tooth root variation decreases with distance from Africa; and that this variation can be used to compare and accurately classify groups at multiple levels that match, to some extent, genomic results.

In terms of future research, it will be necessary to apply the method to the increasing number of CT and micro-CT scans of extinct hominins that are available. This is likely to expand the observed number of phenotypes and allow different taxa to be placed into the sort of analyses presented in Chapter 6. It has already been discussed with the previous chapters that fossil hominins can differ in root morphology, but there has not been a systematic comparison in the way that has been appearing for studies of the enamel-dentine junction (Davies et al., 2019a, 2019b). Although not attempted here, due to the question of how applicable they are to within species variation, phylogenetic approaches can be applied to root variation among hominins and hominids.

## 8.5 Machine learning methods in human evolutionary studies

The application of supervised machine learning to large data sets is becoming the norm in biology (Shalev-Shwartz and Ben-David, 2013). This is especially true of genomics and medical studies (Brown et al., 2000; Wang et al., 2005; Vervier et al., 2018). As we have already shown, tooth root morphospace is large, and the potential combinations of dental traits, and thus tooth crown morphospace is larger (Rathmann and Reyes-Centeno, 2020). The data set used in this dissertation is also vast (75,637 data points). One of the inspirations behind this work was to develop approaches and methodologies suitable for the field of palaeoanthropology, and to raise the resolution of morphological data to that of genomics. Incorporating these data into these analyses presents a major computational challenge, and timewise the ability to analyse data increases significantly as the size and availability of data increases. Machine learning methods work best on large data sets as the abundance of data can be leveraged for training (Hastie et al., 1994). In fact, without an abundance of high-quality data, machine learning algorithms are rendered useless.

In Chapter 6, 20% of the data set (189 individuals, 15,127 data points) are used to train the FDA machine classifier. The results speak for themselves. The majority of populations are classified with 100% accuracy. Only in one case does classification accuracy fall below 90%. While these approaches do not directly provide explanations for the observed patterns (a limitation of machine learning), by discriminating groups so powerfully they offer the opportunity to test evolutionary hypotheses (and more broadly, adaptive, geographical and functional ones) in a more comprehensive way, and, perhaps, integrate them analytically with genomic results.

This dissertation shows that theoretical and realized phenotype morphospaces benefit from the application of machine learning methods. This is only a first attempt. The next step is the application of a neural network as they are designed to recognize patterns in raw input (unlabelled data). Like machine learning techniques they require training. However, once trained neural networks can be applied to classify unlabelled and unknown data. For palaeoanthropology, these approaches are promising for delineating species and/or genus boundaries (*Australopithecus* or *Paranthropus*? *Homo heidelbergensis* or *Homo neanderthalensis*?) and providing comparative insights about similarities and differences in fossil morphologies. Importantly, future works will need to consider if and/or

how different phenotypes influence classification. As discussed above, the defining of a phenotype's morphospace for use with machine learning techniques will contribute greatly to this.

## 8.6 Strengths, limitations, and future directions

The greatest strengths of this dissertation are four-fold: 1) The investigation, defining, and codifying of tooth root internal and external morphologies. Until now, a systematic investigation and description of these morphologies constituted a large gap in the literature. Whereas before, tooth roots were an afterthought to dental crown morphology, they can now be utilized more fully for anthropological studies. 2) The development of a simple, robust, and flexible system for classifying and describing tooth root phenotypes. Like the ASUDAS, this system was developed to enable the user to systematically classify not only the phenotypes discussed here, but to be appended for additional and/or new phenotypes. 3) The links between internal and external morphologies. Working from the simple assumption that a single root must include at least a single canal (Huang and Chai, 2013; Miller, 2013; Martins and Versiani, 2019), chapter 3 has shown that not only is this assumption correct, but that there exists a strong linear relationship between canal and root number. For the first time, the relationship between canal number and orientation and external root morphology are also explored, showing that the former is strong predictor of the latter. 4) The use of tooth root phenotypes as a genomic proxy for investigating human biogeography. As teeth, roots included, are often the best-preserved fossil remains of individuals and populations past, whatever information can be gleaned from them is crucial to investigations of population identity, affinity, and movement. As shown here, tooth roots can provide a wealth of information, especially in the absence of genomic material.

This study is limited in that it does not include all features of tooth root morphology. For example, metric traits (e.g., root length and width) other than root and canal number have been omitted. The reasons for this are because the genes and environmental factors controlling root size are poorly investigated and understood (Huang and Chai, 2013; Wang et al., 2013; Jing et al., 2019). While the same can be said of the morphologies used in this dissertation, the morphologies discussed here are better understood in terms of their

development (ibid.) and have been shown through this dissertation to be developmentally 'linked' (Chapters 3 & 4). An analysis of tooth root surface area and volume, which have been particularly important in hominoid and dietary and biomechanical studies (Plavcan and Daegling, 2006; Le Cabec et al., 2012, 2013; Kirilova et al., 2014; Kupczik et al., 2018; Xing et al., 2018), has also been excluded. This is because root surface is less a morphology than a function of shape and size. Finally, the populations used, while diverse, are not truly global. Notably absent from the Sino-American samples are individuals from China and Russia. Populations sizes are also uneven. While they are large enough for comparative purposes, it is likely that the morphological and phenotypic diversity of all populations are not fully represented.

Future studies will benefit from the use of  $\mu$ CT rather than CT scans. While the resolution of CT scans is sufficient for this study as designed, they are insufficient for surface and volumetric studies, as well as the segmentation of internal structures such as canals and accessory canals, or dentine from cementum and enamel. There is also the unaddressed issue of genetically uninformative traits. Chapter 2 presents descriptive statistics on internal and external counts, morphologies and orientations, while chapters 4 and 6 discuss the most frequent morphologies and phenotypes respectively. However, while it is clear which morphologies and/or phenotypes are the most frequent in populations, it is not always clear which phenotypes are the most informative. While it is true that infrequent or rare phenotypes such as C-shaped molars, Tomes' roots, three rooted  $M_1$ s have high frequencies in several out-of-Africa populations (Tomes, 1889; Wang et al., 2012; Ballullaya et al., 2013; Fernandes et al., 2014), it is unclear if other infrequent or rare phenotype permutations generated in this study are of utility for populations studies; or if they are indeed rare and infrequent at all, and instead are underrepresented in this sample. Future studies of how adjacent and opposing teeth affect one another will also help clarify questions of environmental, biomechanical, and hereditary factors on tooth root phenotypes.

## Chapter 9: Appendices

### 9.1 Glossary

#### 9.1.1 Tooth and Mandibular Anatomy

**Alveoli:** Tooth sockets.

**Alveolar process/bone** (maxillary and mandibular): Thick ridge of bone containing the tooth sockets.

**Apex:** The tip of a tooth cusp.

**Apical foramen:** opening at tip of the tooth root (apex) through which nerves pass from the alveolar bone to the pulp cavity.

**Bell stage:** Developmental stage in which the cells of the enamel organ differentiate into the separate tissues of the root.

**Bifurcated root:** Roots with bifurcated apices less than 33% of the total root length are bifurcated.

**Bud stage:** Developmental stage characterized by the appearance of a tooth bud with no clear arrangement of cells.

**C-shaped:** C-shape molars are primarily found in the second molars of the mandible, though they rarely appear in the first and third mandibular molars as well. There is a substantial clinical literature covering their distinct morphology and prevalence. Unlike Tomes' roots they do not appear to be splitting into two roots. Rather, they are a single, continuous root structure. Like kidney shaped roots they have opposite convex and concave sides. However, their curvature is more pronounced, in nearly a 180o arc with ends that are parallel to one another.

**Cementum:** a bone-like tissue, which covers the external surface of tooth roots.

**Cervix** (or **neck**): the constricted part of the tooth where the crown meets the root.

**Cementoenamel junction (CEJ):** a line, encircling crown at the cervix. The CEJ marks the border of the root and crown. Synonymous with cervix and cervical line.

**Cingulum:** ridge of enamel either partially or fully encircling the crown. More prominent in incisors and canines than molars (see tuberculum).

**Coronal pulp:** Pulp that resides in the crown of the tooth.

**Crown:** The part of the tooth that extends above the gum line and is covered with enamel (also: anatomical crown).

**Cusp:** Bony eminence on the occlusal surface of the tooth crown. Canines possess a single cusp, while premolars have two, and are referred to as “bicuspid”. Molars normally possess four or five cusps.

**Dentin (or dentine):** a tissue, which forms the core of the tooth. While it has no vascular supply, it is supported by the tooth pulp’s vascular system. It is lined with odontoblasts.

**Dentoenamel junction (DEJ):** marks the boundary between the enamel cap and the underlying dentin.

**Diverticle:** conical hollow beneath a tooth cusp.

**Elliptical:** While size, and distance of the edges from the centre vary, elliptical shaped roots are distinct from others in that they look like a squashed circle. Sometimes these forms are perfectly symmetrical and other times they resemble an egg. However, a consistent feature are there continuously smooth edges which are concentric to the canals.

**Enamel:** A hard tissue that covers the crown. It is 97% mineralized.

**Entomolaris:** Accessory root arising from the lingual surface of the distal root.

**Furcation root:** accessory projecting from the point of bifurcation between roots.

**Gingiva:** Soft tissue lining the palate and mandible. The gums.

**Globular:** Round or circular in shape. While this form varies greatly in size, it is relatively invariant in shape in that all edges are relatively equidistant from the centre.

**Hertwig’s epithelial root sheath (HERS):** A proliferation of epithelial cells extending from the cervical loop of the enamel organ in a developing tooth.

**Hourglass:** Hourglass shaped roots have often been confused with plate-shaped roots, or occasionally, elliptical roots. However, this form is distinct and easily identified by its bulbous ends and constricted centre. This constriction can be so pronounced that the root appears almost as a lemniscate in cross-section.

**Hydroxyapatite:** Hydroxyl end member of a naturally occurring mineral form of calcium apatite.

**Interradicular process (IRP):**

**Isthmus:** Complete or incomplete connections between two canals.

**Kidney:** Kidney shaped roots are defined by their opposite convex and concave sides. Sometimes these curvatures are pronounced, and other times they are more subtle. However, these two features are always apparent, and distinct from other forms.

**Mandible:** Lowest bone of the jaws.

**Maxilla:** Upper bones (two fused maxillary bones) of the jaws.

**Paramolaris:** accessory root arising from buccal side of the distal root.

**Pegged:** Pegged third molar roots are associated with a reduced crown and root size and are globular shaped in cross section.

**Plate:** Plate shape roots are similar to hourglass and elliptical roots in their dimensions but are easily distinguished by their flat edges. In some variants the corners are rounded, while in others they are square.

**Pulp:** Soft tissue containing nerves, connective fibres and blood vessels

**Pulp chamber:** Contains the pulp of the tooth.

**Radical:** unseparated, root-like division of the root.

**Radicular pulp:** pulp found in the root canal.

**Root:** The part of the tooth that extends below the gum line and into the alveolus of the jaws. Different teeth have different numbers of roots. Incisors, canines, and premolars normally have single roots, while mandibular molars have two roots, and maxillary molars have three.

**Taurodont:** A condition in which the root trunk and internal pulp cavity are enlarged, and the roots are short. This form was first classified by Keith (1913) in *Homo neanderthalensis*.

**Tomes' Root:** A distinctive root form variant seen in pre-molars in which the mesiolingual groove deepens into a C-shaped cleft or divides the apical portion of the root into a distinct mesiobuccal rootlet. First described by Sir Charles Tomes (Tomes, 1889).

**Tooth germ:** Embryonic cell that is a precursor to a tooth.

**Tuberculum:** a bulge on the lingual surface of incisors and canines. Derives from the cingulum.

**Wedge:** Wedge shaped roots are easily distinguished by their 'tapered' appearance. Sometimes these forms take the shape of a triangle with three edges and corners, while other times they appear more tear drop shaped with a slight constriction in the middle. However, they are easily distinguished as one end is always noticeably wider than the other.

### 9.1.2 Directional Terms

**Mesial:** The portion of the tooth closest to where the central incisors contact one another.

**Distal:** The distal portion of the tooth is farthest from the point where the central incisors contact one another.

**Lingual:** The surface of the tooth crown that faces the tongue.

**Labial:** The surface of the tooth crown that touches the lips. This term is reserved for the incisors and canines.

**Buccal:** The surface of the tooth crown that touches the cheeks. This term is reserved for the premolars and molars.

**Occlusal:** The chewing/biting surfaces of tooth crowns.

**Interproximal:** where tooth surfaces contact one another between adjacent teeth.

### 9.1.3 Tooth identity

**Categorical:** Indicates whether a tooth is an incisor (**I**), canine (**C**), premolar (**P**), or molar (**M**).

**Position:** Each tooth is represented by a supra- or subscript number, which corresponds to that tooth's category and position in the tooth row. In modern humans, incisors are numbered either **1** or **2**, canines are marked **1**, premolars are marked **3** or **4**, and molars are marked **1**, **2**, or **3**. This system can be represented as a dental formula

$$\frac{2: 1: 2: 3}{2: 1: 2: 3}$$

**Dental arcade (or arch):** Indicates if the tooth originates in the maxilla or mandible. A shorthand notation for indicating the arch consists of the use of a superscript for maxillary teeth and a subscript for mandibular teeth. Thus,  $M^1$  would indicate the maxillary first molar while  $M_1$  would indicate the mandibular first molar.

**Side:** Indicate which side of the dental arcade the tooth originates from – right (**R**) or left (**L**).

## 9.2 List of individuals used in this dissertation

Table 9.1: Collection information for individuals used in this dissertation

ID	Collection	Sex	Years BP*	G1 <sup>†</sup>	G2	G3	G4	G5
99_1_102	AMNH	F	~1600	Sino-Americas	North America	American Arctic	Alaska	Ipiutak
99_1_103	AMNH	M	~1600	Sino-Americas	North America	American Arctic	Alaska	Ipiutak
99_1_105	AMNH	M	~1600	Sino-Americas	North America	American Arctic	Alaska	Ipiutak
99_1_161	AMNH	F	~1600	Sino-Americas	North America	American Arctic	Alaska	Ipiutak
99_1_163	AMNH	F	~1600	Sino-Americas	North America	American Arctic	Alaska	Ipiutak
99_1_165	AMNH	M	~1600	Sino-Americas	North America	American Arctic	Alaska	Ipiutak
99_1_166	AMNH	M	~1600	Sino-Americas	North America	American Arctic	Alaska	Ipiutak
99_1_168	AMNH	F	~1600	Sino-Americas	North America	American Arctic	Alaska	Ipiutak
99_1_181	AMNH	M	~1600	Sino-Americas	North America	American Arctic	Alaska	Ipiutak
99_1_192	AMNH	M	~1600	Sino-Americas	North America	American Arctic	Alaska	Ipiutak
99_1_194	AMNH	M	~1600	Sino-Americas	North America	American Arctic	Alaska	Ipiutak
99_1_196	AMNH	M	~1600	Sino-Americas	North America	American Arctic	Alaska	Ipiutak
99_1_197	AMNH	F	~1600	Sino-Americas	North America	American Arctic	Alaska	Ipiutak
99_1_198	AMNH	NA	~1600	Sino-Americas	North America	American Arctic	Alaska	Ipiutak
99_1_201	AMNH	F	~1600	Sino-Americas	North America	American Arctic	Alaska	Ipiutak
99_1_252	AMNH	M	~1600	Sino-Americas	North America	American Arctic	Alaska	Ipiutak
99_1_684	AMNH	F	~1600	Sino-Americas	North America	American Arctic	Alaska	Ipiutak
99_1_72	AMNH	M	~1600	Sino-Americas	North America	American Arctic	Alaska	Ipiutak
99_1_80	AMNH	M	~1600	Sino-Americas	North America	American Arctic	Alaska	Ipiutak
99_1_90	AMNH	F	~1600	Sino-Americas	North America	American Arctic	Alaska	Ipiutak
99_1_92	AMNH	M	~1600	Sino-Americas	North America	American Arctic	Alaska	Ipiutak
99_1_93	AMNH	M	~1600	Sino-Americas	North America	American Arctic	Alaska	Ipiutak
99_1_94	AMNH	M	~1600	Sino-Americas	North America	American Arctic	Alaska	Ipiutak
99_1_95	AMNH	NA	~1600	Sino-Americas	North America	American Arctic	Alaska	Ipiutak
99_1_256	AMNH	M	Unkw	Sino-Americas	North America	American Arctic	Alaska	NA
99_1_569	AMNH	F	Unkw	Sino-Americas	North America	American Arctic	Alaska	NA
99_1_575	AMNH	F	Unkw	Sino-Americas	North America	American Arctic	Alaska	NA
99_1_586	AMNH	F	Unkw	Sino-Americas	North America	American Arctic	Alaska	NA
99_1_592	AMNH	F	Unkw	Sino-Americas	North America	American Arctic	Alaska	NA
99_1_606	AMNH	F	Unkw	Sino-Americas	North America	American Arctic	Alaska	NA
99_1_607	AMNH	M	Unkw	Sino-Americas	North America	American Arctic	Alaska	NA
99_1_608	AMNH	F	Unkw	Sino-Americas	North America	American Arctic	Alaska	NA
99_1_61	AMNH	M	Unkw	Sino-Americas	North America	American Arctic	Alaska	NA
99_1_619	AMNH	M	Unkw	Sino-Americas	North America	American Arctic	Alaska	NA







99_1_542	AMNH	M	~800	Sino-Americas	North America	American Arctic	Alaska	Tigara
99_1_543	AMNH	F	~800	Sino-Americas	North America	American Arctic	Alaska	Tigara
99_1_544	AMNH	F	~800	Sino-Americas	North America	American Arctic	Alaska	Tigara
99_1_546	AMNH	F	~800	Sino-Americas	North America	American Arctic	Alaska	Tigara
99_1_549	AMNH	M	~800	Sino-Americas	North America	American Arctic	Alaska	Tigara
99_1_551	AMNH	F	~800	Sino-Americas	North America	American Arctic	Alaska	Tigara
99_1_552	AMNH	M	~800	Sino-Americas	North America	American Arctic	Alaska	Tigara
99_1_643	AMNH	F	~800	Sino-Americas	North America	American Arctic	Alaska	Tigara
99_1_644	AMNH	M	~800	Sino-Americas	North America	American Arctic	Alaska	Tigara
99_1_666	AMNH	F	~800	Sino-Americas	North America	American Arctic	Alaska	Tigara
99_1_667	AMNH	F	~800	Sino-Americas	North America	American Arctic	Alaska	Tigara
99_1_675	AMNH	F	~800	Sino-Americas	North America	American Arctic	Alaska	Tigara
99_1_69	AMNH	M	~800	Sino-Americas	North America	American Arctic	Alaska	Tigara
226086	NMNH	F	Unkw	Sahul-Pacific	Oceania	Australia	Victoria	Hexham
226087	NMNH	F	Unkw	Sahul-Pacific	Oceania	Australia	Victoria	Hexham
226089	NMNH	M	Unkw	Sahul-Pacific	Oceania	Australia	Australia South	Murray River
226090	NMNH	F	Unkw	Sahul-Pacific	Oceania	Australia	Australia South	Murray River
329778	NMNH	F	Unkw	Sahul-Pacific	Oceania	Australia	Australia South	Cape Spencer Aborigine
329779	NMNH	M	Unkw	Sahul-Pacific	Oceania	Australia	Australia South	Murray River
330604	NMNH	M	Unkw	Sahul-Pacific	Oceania	Australia	Australia Western	Derby Coast Aborigine
331242	NMNH	M	Unkw	Sahul-Pacific	Oceania	Australia	Australia Central	Aborigine
331243	NMNH	M	Unkw	Sahul-Pacific	Oceania	Australia	Australia South	Plympton Aborigine
331247	NMNH	F	Unkw	Sahul-Pacific	Oceania	Australia	Australia South	Swanport Aborigine
344711	NMNH	M	Unkw	Sahul-Pacific	Oceania	Australia	Victoria	Loddon River Aborigine
344712	NMNH	F	Unkw	Sahul-Pacific	Oceania	Australia	Victoria	Mortlake Aborigine
344713	NMNH	F	Unkw	Sahul-Pacific	Oceania	Australia	Victoria	Murray River Aborigine
344714	NMNH	F	Unkw	Sahul-Pacific	Oceania	Australia	Victoria	Murray River Aborigine
344715	NMNH	F	Unkw	Sahul-Pacific	Oceania	Australia	Victoria	Murray River Aborigine
350096	NMNH	M	Unkw	Sahul-Pacific	Oceania	Australia	Australia South	Aborigine
242687	NMNH	M	Unkw	Sino-Americas	North America	American Arctic	Greenland	Inuit
242690	NMNH	F	Unkw	Sino-Americas	North America	American Arctic	Greenland	Inuit
242693	NMNH	F	Unkw	Sino-Americas	North America	American Arctic	Greenland	Inuit
242694	NMNH	F	Unkw	Sino-Americas	North America	American Arctic	Greenland	Inuit
242695	NMNH	M	Unkw	Sino-Americas	North America	American Arctic	Greenland	Inuit
242697	NMNH	M	Unkw	Sino-Americas	North America	American Arctic	Greenland	Inuit
242698	NMNH	M	Unkw	Sino-Americas	North America	American Arctic	Greenland	Inuit
242699	NMNH	F	Unkw	Sino-Americas	North America	American Arctic	Greenland	Inuit
242702	NMNH	F	Unkw	Sino-Americas	North America	American Arctic	Greenland	Inuit
242704	NMNH	F	Unkw	Sino-Americas	North America	American Arctic	Greenland	Inuit



242761	NMNH	M	Unkw	Sino-Americas	North America	American Arctic	Greenland	Inuit
242831	NMNH	M	Unkw	Sino-Americas	North America	American Arctic	Greenland	Inuit
242832	NMNH	M	Unkw	Sino-Americas	North America	American Arctic	Greenland	Inuit
242835	NMNH	F	Unkw	Sino-Americas	North America	American Arctic	Greenland	Inuit
225044	NMNH	M	Unkw	Sunda-Pacific	South East Asia	Malay Archipelago	Indonesia	Java
225046	NMNH	M	Unkw	Sunda-Pacific	South East Asia	Malay Archipelago	Indonesia	Java
225047	NMNH	M	Unkw	Sunda-Pacific	South East Asia	Malay Archipelago	Indonesia	Java
225053	NMNH	F	Unkw	Sunda-Pacific	South East Asia	Malay Archipelago	Indonesia	Java
225054	NMNH	M	Unkw	Sunda-Pacific	South East Asia	Malay Archipelago	Indonesia	Java
225055	NMNH	F	Unkw	Sunda-Pacific	South East Asia	Malay Archipelago	Indonesia	Java
225399	NMNH	M	Unkw	Sunda-Pacific	South East Asia	Malay Archipelago	Indonesia	Java
225120	NMNH	NA	Unkw	Sunda-Pacific	South East Asia	Malay Archipelago	Indonesia	Java
225007	NMNH	NA	Unkw	Sahul-Pacific	Oceania	Melanesia	Papua New Guinea	New Britain
226096	NMNH	M	Unkw	Sahul-Pacific	Oceania	Melanesia	Papua New Guinea	New Britain
226099	NMNH	F	Unkw	Sahul-Pacific	Oceania	Melanesia	Papua New Guinea	New Britain
226101	NMNH	F	Unkw	Sahul-Pacific	Oceania	Melanesia	Papua New Guinea	New Britain
226102	NMNH	F	Unkw	Sahul-Pacific	Oceania	Melanesia	Papua New Guinea	New Britain
226103	NMNH	M	Unkw	Sahul-Pacific	Oceania	Melanesia	Papua New Guinea	New Britain
226105	NMNH	F	Unkw	Sahul-Pacific	Oceania	Melanesia	Papua New Guinea	New Britain
226107	NMNH	M	Unkw	Sahul-Pacific	Oceania	Melanesia	Papua New Guinea	New Britain
226108	NMNH	M	Unkw	Sahul-Pacific	Oceania	Melanesia	Papua New Guinea	New Britain
226109	NMNH	F	Unkw	Sahul-Pacific	Oceania	Melanesia	Papua New Guinea	New Britain
226110	NMNH	F	Unkw	Sahul-Pacific	Oceania	Melanesia	Papua New Guinea	New Britain
226111	NMNH	M	Unkw	Sahul-Pacific	Oceania	Melanesia	Papua New Guinea	New Britain
226112	NMNH	F	Unkw	Sahul-Pacific	Oceania	Melanesia	Papua New Guinea	New Britain
226113	NMNH	M	Unkw	Sahul-Pacific	Oceania	Melanesia	Papua New Guinea	New Britain
226114	NMNH	M	Unkw	Sahul-Pacific	Oceania	Melanesia	Papua New Guinea	New Britain
226115	NMNH	M	Unkw	Sahul-Pacific	Oceania	Melanesia	Papua New Guinea	New Britain
226116	NMNH	F	Unkw	Sahul-Pacific	Oceania	Melanesia	Papua New Guinea	New Britain
226117	NMNH	F	Unkw	Sahul-Pacific	Oceania	Melanesia	Papua New Guinea	New Britain
226118	NMNH	M	Unkw	Sahul-Pacific	Oceania	Melanesia	Papua New Guinea	New Britain
227464	NMNH	F	Unkw	Sahul-Pacific	Oceania	Melanesia	Papua New Guinea	New Britain
381080	NMNH	F	Unkw	Sahul-Pacific	Oceania	Melanesia	Papua New Guinea	New Britain
381082	NMNH	F	Unkw	Sahul-Pacific	Oceania	Melanesia	Papua New Guinea	New Britain
381083	NMNH	M	Unkw	Sahul-Pacific	Oceania	Melanesia	Papua New Guinea	New Britain
205333	NMNH	M	Unkw	Sahul-Pacific	Oceania	Polynesia	New Zealand	NA
225113	NMNH	F	Unkw	Sahul-Pacific	Oceania	Polynesia	New Zealand	NA
225114	NMNH	M	Unkw	Sahul-Pacific	Oceania	Polynesia	New Zealand	NA
225115	NMNH	M	Unkw	Sahul-Pacific	Oceania	Polynesia	New Zealand	NA
226140	NMNH	F	Unkw	Sahul-Pacific	Oceania	Polynesia	New Zealand	NA
226142	NMNH	M	Unkw	Sahul-Pacific	Oceania	Polynesia	New Zealand	NA

226145	NMNH	M	Unkw	Sahul-Pacific	Oceania	Polynesia	New Zealand	NA
226147	NMNH	F	Unkw	Sahul-Pacific	Oceania	Polynesia	New Zealand	NA
226150	NMNH	M	Unkw	Sahul-Pacific	Oceania	Polynesia	New Zealand	NA
226151	NMNH	F	Unkw	Sahul-Pacific	Oceania	Polynesia	New Zealand	NA
226152	NMNH	F	Unkw	Sahul-Pacific	Oceania	Polynesia	New Zealand	NA
226153	NMNH	F	Unkw	Sahul-Pacific	Oceania	Polynesia	New Zealand	NA
226154	NMNH	F	Unkw	Sahul-Pacific	Oceania	Polynesia	New Zealand	NA
226159	NMNH	F	Unkw	Sahul-Pacific	Oceania	Polynesia	New Zealand	NA
381086	NMNH	F	Unkw	Sahul-Pacific	Oceania	Polynesia	New Zealand	NA
381087	NMNH	F	Unkw	Sahul-Pacific	Oceania	Polynesia	New Zealand	NA
221998	NMNH	F	Unkw	Sunda-Pacific	South East Asia	Malay Archipelago	Indonesia	Pagi Island
221999	NMNH	F	Unkw	Sunda-Pacific	South East Asia	Malay Archipelago	Indonesia	Pagi Island
222000	NMNH	F	Unkw	Sunda-Pacific	South East Asia	Malay Archipelago	Indonesia	Pagi Island
222002	NMNH	F	Unkw	Sunda-Pacific	South East Asia	Malay Archipelago	Indonesia	Pagi Island
222003	NMNH	M	Unkw	Sunda-Pacific	South East Asia	Malay Archipelago	Indonesia	Pagi Island
276076	NMNH	F	Unkw	Sahul-Pacific	Oceania	Melanesia	Papua New Guinea	NA
276077	NMNH	M	Unkw	Sahul-Pacific	Oceania	Melanesia	Papua New Guinea	NA
276078	NMNH	F	Unkw	Sahul-Pacific	Oceania	Melanesia	Papua New Guinea	NA
276079	NMNH	M	Unkw	Sahul-Pacific	Oceania	Melanesia	Papua New Guinea	NA
276080	NMNH	F	Unkw	Sahul-Pacific	Oceania	Melanesia	Papua New Guinea	NA
225129	NMNH	M	Unkw	Sunda-Pacific	South East Asia	Malay Archipelago	Philippines	NA
259353	NMNH	F	Unkw	Sunda-Pacific	South East Asia	Malay Archipelago	Philippines	NA
227456	NMNH	M	Unkw	Sahul-Pacific	Oceania	Melanesia	Solomon Islands	NA
227457	NMNH	F	Unkw	Sahul-Pacific	Oceania	Melanesia	Solomon Islands	NA
227458	NMNH	M	Unkw	Sahul-Pacific	Oceania	Melanesia	Solomon Islands	NA
ANI_23	DW	F	<200	Sunda-Pacific	South East Asia	Andaman Archipelago	Andaman Island	NA
ANI_16	DW	F	<200	Sunda-Pacific	South East Asia	Andaman Archipelago	Andaman Island	NA
ANI_35	DW	F	<200	Sunda-Pacific	South East Asia	Andaman Archipelago	Andaman Island	NA
ANI_37	DW	M	<200	Sunda-Pacific	South East Asia	Andaman Archipelago	Andaman Island	NA
ANI_39_40	DW	F	<200	Sunda-Pacific	South East Asia	Andaman Archipelago	Andaman Island	NA
ANI_32	DW	F	<200	Sunda-Pacific	South East Asia	Andaman Archipelago	Andaman Island	NA
ANI_27	DW	F	<200	Sunda-Pacific	South East Asia	Andaman Archipelago	Andaman Island	NA
ANI_36	DW	M	<200	Sunda-Pacific	South East Asia	Andaman Archipelago	Andaman Island	NA
ANI_29	DW	F	<200	Sunda-Pacific	South East Asia	Andaman Archipelago	Andaman Island	NA
ANI_31	DW	M	<200	Sunda-Pacific	South East Asia	Andaman Archipelago	Andaman Island	NA
ANI_33	DW	M	<200	Sunda-Pacific	South East Asia	Andaman Archipelago	Andaman Island	NA
ANI_26	DW	F	<200	Sunda-Pacific	South East Asia	Andaman Archipelago	Andaman Island	NA
ANI_28	DW	M	<200	Sunda-Pacific	South East Asia	Andaman Archipelago	Andaman Island	NA
ANI_30	DW	F	<200	Sunda-Pacific	South East Asia	Andaman Archipelago	Andaman Island	NA
ANI_17	DW	F	<200	Sunda-Pacific	South East Asia	Andaman Archipelago	Andaman Island	NA
ANI_07	DW	F	<200	Sunda-Pacific	South East Asia	Andaman Archipelago	Andaman Island	NA
ANI_11	DW	M	<200	Sunda-Pacific	South East Asia	Andaman Archipelago	Andaman Island	NA
ANI_18	DW	F	<200	Sunda-Pacific	South East Asia	Andaman Archipelago	Andaman Island	NA

ANI_15	DW	F	<200	Sunda-Pacific	South East Asia	Andaman Archipelago	Andaman Island	NA
ANI_10	DW	F	<200	Sunda-Pacific	South East Asia	Andaman Archipelago	Andaman Island	NA
ANI_12	DW	F	<200	Sunda-Pacific	South East Asia	Andaman Archipelago	Andaman Island	NA
ANI_13	DW	M	<200	Sunda-Pacific	South East Asia	Andaman Archipelago	Andaman Island	NA
ANI_19	DW	M	<200	Sunda-Pacific	South East Asia	Andaman Archipelago	Andaman Island	NA
ANI_38	DW	M	<200	Sunda-Pacific	South East Asia	Andaman Archipelago	Andaman Island	NA
ANI_34	DW	F	<200	Sunda-Pacific	South East Asia	Andaman Archipelago	Andaman Island	NA
ANI_43	DW	M	<200	Sunda-Pacific	South East Asia	Andaman Archipelago	Nicobar Island	NA
ANI_42	DW	M	<200	Sunda-Pacific	South East Asia	Andaman Archipelago	Nicobar Island	NA
ANI_54	DW	M	<200	Sunda-Pacific	South East Asia	Andaman Archipelago	Nicobar Island	NA
ANI_41	DW	M	<200	Sunda-Pacific	South East Asia	Andaman Archipelago	Nicobar Island	NA
ANI_44	DW	F	<200	Sunda-Pacific	South East Asia	Andaman Archipelago	Nicobar Island	NA
ANI_59	DW	M	<200	Sunda-Pacific	South East Asia	Andaman Archipelago	Nicobar Island	NA
ANI_56	DW	M	<200	Sunda-Pacific	South East Asia	Andaman Archipelago	Nicobar Island	NA
ANI_50	DW	M	<200	Sunda-Pacific	South East Asia	Andaman Archipelago	Nicobar Island	NA
ANI_55	DW	M	<200	Sunda-Pacific	South East Asia	Andaman Archipelago	Nicobar Island	NA
ANI_61	DW	M	<200	Sunda-Pacific	South East Asia	Andaman Archipelago	Nicobar Island	NA
ANI_57	DW	M	<200	Sunda-Pacific	South East Asia	Andaman Archipelago	Nicobar Island	NA
ANI_58	DW	M	<200	Sunda-Pacific	South East Asia	Andaman Archipelago	Nicobar Island	NA
ANI_47	DW	M	<200	Sunda-Pacific	South East Asia	Andaman Archipelago	Nicobar Island	NA
ANI_49	DW	M	<200	Sunda-Pacific	South East Asia	Andaman Archipelago	Nicobar Island	NA
ANI_51	DW	M	<200	Sunda-Pacific	South East Asia	Andaman Archipelago	Nicobar Island	NA
ANI_48	DW	M	<200	Sunda-Pacific	South East Asia	Andaman Archipelago	Nicobar Island	NA
BU_28	DW	F	<200	Sunda-Pacific	South East Asia	Indochinese Peninsula	Myanmar	NA
BU_29	DW	M	<200	Sunda-Pacific	South East Asia	Indochinese Peninsula	Myanmar	NA
BU_21	DW	M	<200	Sunda-Pacific	South East Asia	Indochinese Peninsula	Myanmar	NA
BU_19	DW	M	<200	Sunda-Pacific	South East Asia	Indochinese Peninsula	Myanmar	NA
BU_04	DW	M	<200	Sunda-Pacific	South East Asia	Indochinese Peninsula	Myanmar	NA
BU_32	DW	M	<200	Sunda-Pacific	South East Asia	Indochinese Peninsula	Myanmar	NA
BU_14	DW	M	<200	Sunda-Pacific	South East Asia	Indochinese Peninsula	Myanmar	NA
BU_01	DW	F	<200	Sunda-Pacific	South East Asia	Indochinese Peninsula	Myanmar	NA
BU_31	DW	M	<200	Sunda-Pacific	South East Asia	Indochinese Peninsula	Myanmar	NA
BU_16	DW	M	<200	Sunda-Pacific	South East Asia	Indochinese Peninsula	Myanmar	NA
BU_10	DW	M	<200	Sunda-Pacific	South East Asia	Indochinese Peninsula	Myanmar	NA
MEL_120	DW	M	<200	Sahul-Pacific	Oceania	Melanesia	Papua New Guinea	Oriomo River Daudai
MEL_219	DW	F	<200	Sahul-Pacific	Oceania	Melanesia	Papua New Guinea	Murua Island Muyuw
MEL_264	DW	M	<200	Sahul-Pacific	Oceania	Melanesia	Papua New Guinea	NA
MEL_104	DW	F	<200	Sahul-Pacific	Oceania	Melanesia	Papua New Guinea	Kwaiawata Island Muyuw

MEL_197	DW	M	<200	Sahul-Pacific	Oceania	Melanesia	Papua New Guinea	Murua Island Muyuw
MEL_258	DW	M	<200	Sahul-Pacific	Oceania	Melanesia	Papua New Guinea	Kwaiawata Island Muyuw
MEL_259	DW	M	<200	Sahul-Pacific	Oceania	Melanesia	Papua New Guinea	Kwaiawata Island Muyuw
MEL_272	DW	M	<200	Sahul-Pacific	Oceania	Melanesia	Papua New Guinea	Kwaiawata Island Muyuw
MEL_273	DW	M	<200	Sahul-Pacific	Oceania	Melanesia	Papua New Guinea	Kwaiawata Island Muyuw
MEL_189	DW	M	<200	Sahul-Pacific	Oceania	Melanesia	Papua New Guinea	Murua Island Muyuw
SAS_13	DW	F	<200	West Eurasia	South Asia	Indian Sub-Continent	North India	Punjab
SAS_19	DW	M	<200	West Eurasia	South Asia	Indian Sub-Continent	Pakistan	NA
SAS_16	DW	M	<200	West Eurasia	South Asia	Indian Sub-Continent	Pakistan	Pathan
SAS_44	DW	F	<200	West Eurasia	South Asia	Indian Sub-Continent	South India	Deccan Berars
SAS_45	DW	M	<200	West Eurasia	South Asia	Indian Sub-Continent	East India	Patna
SAS_08	DW	F	<200	West Eurasia	South Asia	Indian Sub-Continent	North India	Naharhmpikya Sinhalese
SAS_29	DW	M	<200	West Eurasia	South Asia	Indian Sub-Continent	North India	Punjab
SAS_23	DW	F	<200	West Eurasia	South Asia	Indian Sub-Continent	North India	Punjab
SAS_07	DW	M	<200	West Eurasia	South Asia	Indian Sub-Continent	North India	NA
SAS_04	DW	F	<200	West Eurasia	South Asia	Indian Sub-Continent	North India	Veddah
SAS_31	DW	F	<200	West Eurasia	South Asia	Indian Sub-Continent	North India	Punjab
SAS_81	DW	F	<200	West Eurasia	South Asia	Indian Sub-Continent	India	NA
SAS_57	DW	F	<200	West Eurasia	South Asia	Indian Sub-Continent	East India	Hindustan Bihar
SAS_10	DW	M	<200	West Eurasia	South Asia	Indian Sub-Continent	Sri Lanka	Colombo
SAS_17	DW	F	<200	West Eurasia	South Asia	Indian Sub-Continent	Pakistan	Pathan
SAS_15	DW	M	<200	West Eurasia	South Asia	Indian Sub-Continent	Pakistan	Pathan
SAS_27	DW	F	<200	West Eurasia	South Asia	Indian Sub-Continent	North India	Punjab
SAS_20	DW	F	<200	West Eurasia	South Asia	Indian Sub-Continent	North India	Punjab
SAS_03	DW	F	<200	West Eurasia	South Asia	Indian Sub-Continent	North India	Veddah
SAS_60	DW	M	<200	West Eurasia	South Asia	Indian Sub-Continent	North India	NA
SAS_54	DW	M	<200	West Eurasia	South Asia	Indian Sub-Continent	North India	Hindustan
SAS_71	DW	F	<200	West Eurasia	South Asia	Indian Sub-Continent	Bangladesh	Bengal
SAS_46	DW	M	<200	West Eurasia	South Asia	Indian Sub-Continent	East India	Bihari
SAS_61	DW	M	<200	West Eurasia	South Asia	Indian Sub-Continent	North India	Pakistan
SAS_39	DW	F	<200	West Eurasia	South Asia	Indian Sub-Continent	East India	Bengal
SAS_35	DW	M	<200	West Eurasia	South Asia	Indian Sub-Continent	East India	Bengal
SAS_47	DW	F	<200	West Eurasia	South Asia	Indian Sub-Continent	East India	Bihari
SAS_02	DW	M	<200	West Eurasia	South Asia	Indian Sub-Continent	North India	Veddah
SAS_51	DW	M	<200	West Eurasia	South Asia	Indian Sub-Continent	South India	Coorg
SAS_40	DW	M	<200	West Eurasia	South Asia	Indian Sub-Continent	East India	Bengal
SAS_84	DW	F	<200	West Eurasia	South Asia	Indian Sub-Continent	India	NA
SAS_34	DW	F	<200	West Eurasia	South Asia	Indian Sub-Continent	East India	Bengal

SAS_01	DW	F	<200	West Eurasia	South Asia	Indian Sub-Continent	North India	Veddah
SAS_09	DW	M	<200	West Eurasia	South Asia	Indian Sub-Continent	Sri Lanka	Colombo
SAS_69	DW	M	<200	West Eurasia	South Asia	Indian Sub-Continent	Bangladesh	Bengal
SAS_83	DW	M	<200	West Eurasia	South Asia	Indian Sub-Continent	India	Hindu
SAS_77	DW	M	<200	West Eurasia	South Asia	Indian Sub-Continent	South India	Dravidian
SAS_56	DW	F	<200	West Eurasia	South Asia	Indian Sub-Continent	West India	Mumbai Parsi
SAS_38	DW	M	<200	West Eurasia	South Asia	Indian Sub-Continent	East India	Bengal
SAS_53	DW	F	<200	West Eurasia	South Asia	Indian Sub-Continent	Sri Lanka	Ballam Coffa
SAS_78	DW	M	<200	West Eurasia	South Asia	Indian Sub-Continent	South India	NA
SAS_36	DW	M	<200	West Eurasia	South Asia	Indian Sub-Continent	East India	Bengal
SAS_42	DW	M	<200	West Eurasia	South Asia	Indian Sub-Continent	India Unkw	Ballam Coffa
SAS_11	DW	M	<200	West Eurasia	South Asia	Indian Sub-Continent	North India	NA
SAS_55	DW	M	<200	West Eurasia	South Asia	Indian Sub-Continent	Sri Lanka	Eingenadu
SAS_67	DW	F	<200	West Eurasia	South Asia	Indian Sub-Continent	India Unkw	NA
SAS_70	DW	F	<200	West Eurasia	South Asia	Indian Sub-Continent	Bangladesh	Bengal
SAS_75	DW	F	<200	West Eurasia	South Asia	Indian Sub-Continent	India Unkw	NA
SAS_79	DW	F	<200	West Eurasia	South Asia	Indian Sub-Continent	India	Hindu
SAS_37	DW	F	<200	West Eurasia	South Asia	Indian Sub-Continent	East India	Bengal Bangladesh
SAS_28	DW	F	<200	West Eurasia	South Asia	Indian Sub-Continent	North India	Punjab
SAS_26	DW	M	<200	West Eurasia	South Asia	Indian Sub-Continent	North India	Punjab
SAS_30	DW	M	<200	West Eurasia	South Asia	Indian Sub-Continent	North India	Punjab
SAS_52	DW	M	<200	West Eurasia	South Asia	Indian Sub-Continent	South India	Paliyan Tribe
SAS_25	DW	M	<200	West Eurasia	South Asia	Indian Sub-Continent	North India	Punjab
SAS_24	DW	M	<200	West Eurasia	South Asia	Indian Sub-Continent	North India	Punjab
SAS_21	DW	F	<200	West Eurasia	South Asia	Indian Sub-Continent	North India	Punjab
SAS_33	DW	M	<200	West Eurasia	South Asia	Indian Sub-Continent	East India	Bengal
SAS_05	DW	M	<200	West Eurasia	South Asia	Indian Sub-Continent	North India	Veddah
SAS_62	DW	M	<200	West Eurasia	South Asia	Indian Sub-Continent	East India	NA
SAS_48	DW	M	<200	West Eurasia	South Asia	Indian Sub-Continent	East India	Hindustan Bihar
SAS_68	DW	F	<200	West Eurasia	South Asia	Indian Sub-Continent	East India	Bengal Bangladesh
5423	DW	F	<200	Sub-Saharan Africa	Sub-Saharan Africa	Western Africa	Nigeria	Kagoro
6087	DW	F	<200	Sub-Saharan Africa	Sub-Saharan Africa	Western Africa	Nigeria	Kaduna
1734	DW	M	<200	Sub-Saharan Africa	Sub-Saharan Africa	Southern Africa	South Africa	Basuto
1743	DW	F	<200	Sub-Saharan Africa	Sub-Saharan Africa	Southern Africa	South Africa	Port Elizabeth
5340	DW	F	<200	Sub-Saharan Africa	Sub-Saharan Africa	Eastern Africa	Kenya	Akamba
AF1082	DW	F	<200	Sub-Saharan Africa	Sub-Saharan Africa	Eastern Africa	Kenya	NA
1755	DW	F	<200	Sub-Saharan Africa	Sub-Saharan Africa	Southern Africa	South Africa	Wynberg San
3731	DW	F	<200	Sub-Saharan Africa	Sub-Saharan Africa	Southern Africa	South Africa	Knysna Cave

1728	DW	M	<200	Sub-Saharan Africa	Sub-Saharan Africa	Western Africa	Guinea	NA
5585	DW	F	<200	Sub-Saharan Africa	Sub-Saharan Africa	Southern Africa	Namibia	Walvis Bay
5651	DW	M	<200	Sub-Saharan Africa	Sub-Saharan Africa	Western Africa	Nigeria	Muri Province
1735	DW	M	<200	Sub-Saharan Africa	Sub-Saharan Africa	Southern Africa	South Africa	Manatee Cradock
5425	DW	M	<200	Sub-Saharan Africa	Sub-Saharan Africa	Western Africa	Nigeria	Gannawarri
1747	DW	M	<200	Sub-Saharan Africa	Sub-Saharan Africa	Southern Africa	South Africa	Korana
5060	DW	M	<200	Sub-Saharan Africa	Sub-Saharan Africa	Central Africa	Congo	Brazaville
4_93	DW	M	<200	Sub-Saharan Africa	Sub-Saharan Africa	Western Africa	Nigeria	NA
1733	DW	M	<200	Sub-Saharan Africa	Sub-Saharan Africa	Southern Africa	South Africa	Amaponda
6097	DW	F	<200	Sub-Saharan Africa	Sub-Saharan Africa	Western Africa	Nigeria	Yola
AF_35_0_1	DW	M	<200	Sub-Saharan Africa	Sub-Saharan Africa	Southern Africa	South Africa	NA
1731	DW	M	<200	Sub-Saharan Africa	Sub-Saharan Africa	Southern Africa	Angola	Luanda
4697	DW	F	<200	Sub-Saharan Africa	Sub-Saharan Africa	Western Africa	Nigeria	NA
6110	DW	F	<200	Sub-Saharan Africa	Sub-Saharan Africa	Southern Africa	South Africa	Bechuanaland
1732	DW	M	<200	Sub-Saharan Africa	Sub-Saharan Africa	Southern Africa	SSA Unkw	NA
6109	DW	F	<200	Sub-Saharan Africa	Sub-Saharan Africa	Southern Africa	South Africa	Bechuanaland
5424	DW	M	<200	Sub-Saharan Africa	Sub-Saharan Africa	Western Africa	Nigeria	Kagoro
6093	DW	M	<200	Sub-Saharan Africa	Sub-Saharan Africa	Eastern Africa	Uganda	Teso
4197	DW	M	<200	Sub-Saharan Africa	Sub-Saharan Africa	Southern Africa	South Africa	NA
6089	DW	F	<200	Sub-Saharan Africa	Sub-Saharan Africa	Eastern Africa	Nigeria	Kaduna
AF_0_1	DW	F	<200	Sub-Saharan Africa	Sub-Saharan Africa	Eastern Africa	Mozambique	Makua
1721	DW	M	<1000	West Eurasia	North Africa	Northern Africa	Canary Islands	Guanche
1769	DW	M	<200	West Eurasia	North Africa	Northern Africa	Egypt	NA
1777	DW	F	<200	Sub-Saharan Africa	Sub-Saharan Africa	Central Africa	Congo	Upper Congo River
1751	DW	M	<200	Sub-Saharan Africa	Sub-Saharan Africa	Southern Africa	South Africa	Kalahari
5058	DW	M	<200	Sub-Saharan Africa	Sub-Saharan Africa	Central Africa	Congo	Bambuti Pygmy
5643	DW	M	<200	Sub-Saharan Africa	Sub-Saharan Africa	Western Africa	Ghana	Ashanti
1749	DW	F	<200	Sub-Saharan Africa	Sub-Saharan Africa	Southern Africa	South Africa	NA
1729	DW	F	<200	Sub-Saharan Africa	Sub-Saharan Africa	Central Africa	Congo	NA
1709	DW	M	<1000	West Eurasia	North Africa	Northern Africa	Canary Islands	Guanche
1722	DW	F	<1000	West Eurasia	North Africa	Northern Africa	Canary Islands	Guanche
6094	DW	M	<200	Sub-Saharan Africa	Sub-Saharan Africa	Eastern Africa	Uganda	Teso
1711	DW	M	<1000	West Eurasia	North Africa	Northern Africa	Canary Islands	Guanche
3732	DW	F	<200	Sub-Saharan Africa	Sub-Saharan Africa	Southern Africa	South Africa	Knysna Cave
6092	DW	M	<200	Sub-Saharan Africa	Sub-Saharan Africa	Eastern Africa	Uganda	NA
1737	DW	M	<200	Sub-Saharan Africa	Sub-Saharan Africa	Southern Africa	South Africa	Amakhosa Great Winterberg
1727	DW	F	<200	Sub-Saharan Africa	Sub-Saharan Africa	Eastern Africa	Tanzania	Makua

1774	DW	M	<200	Sub-Saharan Africa	Sub-Saharan Africa	Eastern Africa	Tanzania	NA
4696	DW	M	<200	Sub-Saharan Africa	Sub-Saharan Africa	Western Africa	Nigeria	NA
Af_31_0_1	DW	M	<200	Sub-Saharan Africa	Sub-Saharan Africa	Eastern Africa	Zimbabwe	NA
1730	DW	M	<200	Sub-Saharan Africa	Sub-Saharan Africa	Western Africa	Guinea	NA
1739	DW	M	<200	Sub-Saharan Africa	Sub-Saharan Africa	Southern Africa	South Africa	Khoikhoi
6096	DW	M	<200	Sub-Saharan Africa	Sub-Saharan Africa	Western Africa	Nigeria	Yola
1744	DW	M	<200	Sub-Saharan Africa	Sub-Saharan Africa	Southern Africa	South Africa	Knysna Cave
149	DW	M	<200	Sub-Saharan Africa	Sub-Saharan Africa	Southern Africa	South Africa	NA
Af_44_0_2	DW	M	<200	Sub-Saharan Africa	Sub-Saharan Africa	Western Africa	Nigeria	Yoruba Ilorin
1738	DW	F	<200	Sub-Saharan Africa	Sub-Saharan Africa	Southern Africa	South Africa	NA
Af_20_0_1	DW	M	<200	Sub-Saharan Africa	Sub-Saharan Africa	SSA Unkw	SSA Unkw	Bantu Kaoisoudo
6085	DW	M	<200	Sub-Saharan Africa	Sub-Saharan Africa	Eastern Africa	Kenya	NA
1778	DW	F	<200	Sub-Saharan Africa	Sub-Saharan Africa	Central Africa	Congo	NA
AF_30_0_1	DW	M	<200	Sub-Saharan Africa	Sub-Saharan Africa	Southern Africa	South Africa	NA
5418	DW	F	<200	Sub-Saharan Africa	Sub-Saharan Africa	Eastern Africa	Kenya	Kikuyu
AF_44_0_4	DW	F	<200	Sub-Saharan Africa	Sub-Saharan Africa	Western Africa	Nigeria	Yoruba Ilorin
1725	DW	M	200	Sub-Saharan Africa	Sub-Saharan Africa	Western Africa	Ghana	Fanti
5428	DW	F	<200	Sub-Saharan Africa	Sub-Saharan Africa	Western Africa	Nigeria	Kagoro
5701	DW	M	<200	Sub-Saharan Africa	Sub-Saharan Africa	Western Africa	Nigeria	Muri Province
AF_15_0_6	DW	F	<200	Sub-Saharan Africa	Sub-Saharan Africa	Eastern Africa	Somalia	Jilibi
AF_15_0_27	DW	M	<200	Sub-Saharan Africa	Sub-Saharan Africa	Eastern Africa	Somalia	Darood
AF_15_0_30	DW	F	<200	Sub-Saharan Africa	Sub-Saharan Africa	Eastern Africa	Somalia	NA
AF_15_0_22	DW	M	<200	Sub-Saharan Africa	Sub-Saharan Africa	Eastern Africa	Somalia	Darood
AF_15_0_34	DW	M	<200	Sub-Saharan Africa	Sub-Saharan Africa	Eastern Africa	Somalia	Darood Hawiya
AF_15_0_17	DW	M	<200	Sub-Saharan Africa	Sub-Saharan Africa	Eastern Africa	Somalia	Darood
AF_15_0_50	DW	M	<200	Sub-Saharan Africa	Sub-Saharan Africa	Eastern Africa	Somalia	Darood Hawiya
AF_15_0_48	DW	M	<200	Sub-Saharan Africa	Sub-Saharan Africa	Eastern Africa	Somalia	Darood Hawiya
AF_15_0_19	DW	M	<200	Sub-Saharan Africa	Sub-Saharan Africa	Eastern Africa	Somalia	Darood
AF_15_0_11	DW	M	<200	Sub-Saharan Africa	Sub-Saharan Africa	Eastern Africa	Somalia	Tegera Well
AF_15_0_23	DW	M	<200	Sub-Saharan Africa	Sub-Saharan Africa	Eastern Africa	Somalia	Darood
AF_15_0_70	DW	M	<200	Sub-Saharan Africa	Sub-Saharan Africa	Eastern Africa	Somalia	Darood Hawiya
AF_15_0_62	DW	M	<200	Sub-Saharan Africa	Sub-Saharan Africa	Eastern Africa	Somalia	NA
AF_15_0_5	DW	M	<200	Sub-Saharan Africa	Sub-Saharan Africa	Eastern Africa	Somalia	Didali
AF_15_0_55	DW	M	<200	Sub-Saharan Africa	Sub-Saharan Africa	Eastern Africa	Somalia	Darood Hawiya
AF_15_0_53	DW	M	<200	Sub-Saharan Africa	Sub-Saharan Africa	Eastern Africa	Somalia	Darood Hawiya
AF_15_0_12	DW	M	<200	Sub-Saharan Africa	Sub-Saharan Africa	Eastern Africa	Somalia	Ainaho, Hahr Jalo or Daldshantu tribe
AF_15_0_18	DW	M	<200	Sub-Saharan Africa	Sub-Saharan Africa	Eastern Africa	Somalia	Darood

AF_15_0_69	DW	M	<200	Sub-Saharan Africa	Sub-Saharan Africa	Eastern Africa	Somalia	Darood Hawiya
AF_15_0_1	DW	M	<200	Sub-Saharan Africa	Sub-Saharan Africa	Eastern Africa	Somalia	Ali Kush
AF_15_0_41	DW	M	<200	Sub-Saharan Africa	Sub-Saharan Africa	Eastern Africa	Somalia	Darood Hawiya
AF_15_0_64	DW	M	<200	Sub-Saharan Africa	Sub-Saharan Africa	Eastern Africa	Somalia	Darood Hawiya
AF_15_0_32	DW	M	<200	Sub-Saharan Africa	Sub-Saharan Africa	Eastern Africa	Somalia	Darood Hawiya
AF_15_0_42	DW	M	<200	Sub-Saharan Africa	Sub-Saharan Africa	Eastern Africa	Somalia	Darood Hawiya
AF_15_0_65	DW	M	<200	Sub-Saharan Africa	Sub-Saharan Africa	Eastern Africa	Somalia	Darood Hawiya
AF_15_0_02	DW	M	<200	Sub-Saharan Africa	Sub-Saharan Africa	Eastern Africa	Somalia	Hariya
AF_15_0_31	DW	M	<200	Sub-Saharan Africa	Sub-Saharan Africa	Eastern Africa	Somalia	NA
AF_15_0_25	DW	M	<200	Sub-Saharan Africa	Sub-Saharan Africa	Eastern Africa	Somalia	Darood
AF_15_0_16	DW	M	<200	Sub-Saharan Africa	Sub-Saharan Africa	Eastern Africa	Somalia	Ainaho, Burao
AF_15_0_13	DW	F	<200	Sub-Saharan Africa	Sub-Saharan Africa	Eastern Africa	Somalia	Ainaho, Burao
AF_15_0_03	DW	M	<200	Sub-Saharan Africa	Sub-Saharan Africa	Eastern Africa	Somalia	Hadad
AF_15_0_47	DW	M	<200	Sub-Saharan Africa	Sub-Saharan Africa	Eastern Africa	Somalia	Darood Hawiya
AF_15_0_67	DW	M	<200	Sub-Saharan Africa	Sub-Saharan Africa	Eastern Africa	Somalia	Darood Hawiya
AF_15_0_33	DW	M	<200	Sub-Saharan Africa	Sub-Saharan Africa	Eastern Africa	Somalia	Darood Hawiya
AF_23_0_22	DW	M	<200	Sub-Saharan Africa	Sub-Saharan Africa	Eastern Africa	Tanzania	Haya
AF_23_0_30	DW	F	<200	Sub-Saharan Africa	Sub-Saharan Africa	Eastern Africa	Tanzania	Haya
AF_23_0_19	DW	M	<200	Sub-Saharan Africa	Sub-Saharan Africa	Eastern Africa	Tanzania	Haya
AF_23_0_23	DW	M	<200	Sub-Saharan Africa	Sub-Saharan Africa	Eastern Africa	Tanzania	Haya
AF_23_0_32	DW	M	<200	Sub-Saharan Africa	Sub-Saharan Africa	Eastern Africa	Tanzania	Haya
AF_23_0_112	DW	F	<200	Sub-Saharan Africa	Sub-Saharan Africa	Eastern Africa	Tanzania	Haya
AF_23_0_113	DW	M	<200	Sub-Saharan Africa	Sub-Saharan Africa	Eastern Africa	Tanzania	Haya
AF_23_0_17	DW	M	<200	Sub-Saharan Africa	Sub-Saharan Africa	Eastern Africa	Tanzania	Haya
AF_23_0_31	DW	M	<200	Sub-Saharan Africa	Sub-Saharan Africa	Eastern Africa	Tanzania	Haya
AF_23_0_109	DW	M	<200	Sub-Saharan Africa	Sub-Saharan Africa	Eastern Africa	Tanzania	Haya
AF_23_0_04	DW	M	<200	Sub-Saharan Africa	Sub-Saharan Africa	Eastern Africa	Tanzania	Haya
AF_23_0_20	DW	F	<200	Sub-Saharan Africa	Sub-Saharan Africa	Eastern Africa	Tanzania	Haya
AF_23_0_219	DW	F	<200	Sub-Saharan Africa	Sub-Saharan Africa	Eastern Africa	Tanzania	Haya
AF_23_0_223	DW	M	<200	Sub-Saharan Africa	Sub-Saharan Africa	Eastern Africa	Tanzania	Haya
AF_23_0_228	DW	F	<200	Sub-Saharan Africa	Sub-Saharan Africa	Eastern Africa	Tanzania	Haya
AF_23_0_224	DW	F	<200	Sub-Saharan Africa	Sub-Saharan Africa	Eastern Africa	Tanzania	Haya
AF_23_0_39	DW	M	<200	Sub-Saharan Africa	Sub-Saharan Africa	Eastern Africa	Tanzania	Haya
AF_23_0_27	DW	F	<200	Sub-Saharan Africa	Sub-Saharan Africa	Eastern Africa	Tanzania	Haya
AF_23_0_37	DW	M	<200	Sub-Saharan Africa	Sub-Saharan Africa	Eastern Africa	Tanzania	Haya
AF_23_0_111	DW	M	<200	Sub-Saharan Africa	Sub-Saharan Africa	Eastern Africa	Tanzania	Haya
AF_23_0_21_	DW	F	<200	Sub-Saharan Africa	Sub-Saharan Africa	Eastern Africa	Tanzania	Haya
AF_23_0_209	DW	F	<200	Sub-Saharan Africa	Sub-Saharan Africa	Eastern Africa	Tanzania	Haya

AF_23_0_35	DW	M	<200	Sub-Saharan Africa	Sub-Saharan Africa	Eastern Africa	Tanzania	Haya
AF_23_0_118	DW	M	<200	Sub-Saharan Africa	Sub-Saharan Africa	Eastern Africa	Tanzania	Haya
AF_23_0_115	DW	M	<200	Sub-Saharan Africa	Sub-Saharan Africa	Eastern Africa	Tanzania	Haya
AF_23_0_225	DW	F	<200	Sub-Saharan Africa	Sub-Saharan Africa	Eastern Africa	Tanzania	Haya
AF_23_0_119	DW	M	<200	Sub-Saharan Africa	Sub-Saharan Africa	Eastern Africa	Tanzania	Haya
AF_23_0_110	DW	M	<200	Sub-Saharan Africa	Sub-Saharan Africa	Eastern Africa	Tanzania	Haya
AF_23_0_44	DW	F	<200	Sub-Saharan Africa	Sub-Saharan Africa	Eastern Africa	Tanzania	Haya
AF_23_0_38	DW	M	<200	Sub-Saharan Africa	Sub-Saharan Africa	Eastern Africa	Tanzania	Haya
AF_23_0_213	DW	M	<200	Sub-Saharan Africa	Sub-Saharan Africa	Eastern Africa	Tanzania	Haya
AF_23_0_36	DW	M	<200	Sub-Saharan Africa	Sub-Saharan Africa	Eastern Africa	Tanzania	Haya
AF_23_0_218	DW	M	<200	Sub-Saharan Africa	Sub-Saharan Africa	Eastern Africa	Tanzania	Haya
AF_23_0_25	DW	F	<200	Sub-Saharan Africa	Sub-Saharan Africa	Eastern Africa	Tanzania	Haya
AF_23_0_42	DW	F	<200	Sub-Saharan Africa	Sub-Saharan Africa	Eastern Africa	Tanzania	Haya
AF_23_0_114	DW	M	<200	Sub-Saharan Africa	Sub-Saharan Africa	Eastern Africa	Tanzania	Haya
AF_23_0_200	DW	M	<200	Sub-Saharan Africa	Sub-Saharan Africa	Eastern Africa	Tanzania	Haya
AF_23_0_18	DW	M	<200	Sub-Saharan Africa	Sub-Saharan Africa	Eastern Africa	Tanzania	Haya
AF_23_0_202	DW	M	<200	Sub-Saharan Africa	Sub-Saharan Africa	Eastern Africa	Tanzania	Haya
AF_23_0_116	DW	M	<200	Sub-Saharan Africa	Sub-Saharan Africa	Eastern Africa	Tanzania	Haya
AF_23_0_227	DW	F	<200	Sub-Saharan Africa	Sub-Saharan Africa	Eastern Africa	Tanzania	Haya
AF_23_0_226	DW	M	<200	Sub-Saharan Africa	Sub-Saharan Africa	Eastern Africa	Tanzania	Haya
AF_23_0_34	DW	F	<200	Sub-Saharan Africa	Sub-Saharan Africa	Eastern Africa	Tanzania	Haya
AF_23_0_8	DW	F	<200	Sub-Saharan Africa	Sub-Saharan Africa	Eastern Africa	Tanzania	Haya
AF_23_0_16	DW	M	<200	Sub-Saharan Africa	Sub-Saharan Africa	Eastern Africa	Tanzania	Haya
AF_23_0_2	DW	M	<200	Sub-Saharan Africa	Sub-Saharan Africa	Eastern Africa	Tanzania	Haya
1067	DW	M	<200	West Eurasia	Europe	Western Europe	France	NA
1065	DW	M	<200	West Eurasia	Europe	Central Europe	Switzerland	St Bernard
Eu_25_00_2	DW	F	<200	West Eurasia	Europe	Central Europe	Switzerland	Graubunden Saint Moritz
Eu_25_00_1	DW	M	<200	West Eurasia	Europe	Central Europe	Switzerland	Graubunden Saint Moritz
1036	DW	M	<200	West Eurasia	Europe	Western Europe	France	NA
1181	DW	M	<200	West Eurasia	Europe	Central Europe	Austrian	NA
1178	DW	M	<200	West Eurasia	Europe	Northern Europe	Sweden	NA
2235	DW	M	<200	West Eurasia	Europe	Western Europe	France	Paris
3000	DW	M	<200	West Eurasia	Europe	Central Europe	Hungary	NA
1143	DW	M	<200	West Eurasia	Europe	Central Europe	Austrian	Vienna
Eu_26_00_2	DW	M	<200	West Eurasia	Europe	Central Europe	Germany	Halle
1150	DW	F	<200	West Eurasia	Europe	Central Europe	Austrian	NA
Eu_31_0_1	DW	M	<200	West Eurasia	Europe	Eastern Europe	Ukraine	Crime Sebastopol
1051	DW	M	<200	West Eurasia	Europe	Western Europe	France	Brittany

1042	DW	M	<200	West Eurasia	Europe	Western Europe	France	NA
Eu_26_00_1	DW	M	<200	West Eurasia	Europe	Central Europe	Germany	Halle
Eu_31_00_1	DW	M	<200	West Eurasia	Europe	Eastern Europe	Russia	Khanty Kondinski
1155	DW	M	<200	West Eurasia	Europe	Central Europe	Czechoslovakia	NA
Eu_31_00_2	DW	F	<200	West Eurasia	Europe	Eastern Europe	Russia	Salekhard
1173	DW	F	<200	West Eurasia	Europe	Northern Europe	Finland	Lapland
Eu_42_00_1	DW	F	<200	West Eurasia	Europe	Southern Europe	Italy	NA
Eu_34_4_1	DW	F	<200	West Eurasia	Europe	Central Europe	Hungary	Toszeg
Eu_24_00_2	DW	F	<200	West Eurasia	Europe	Western Europe	France	NA
Eu_45_4_1	DW	M	<200	West Eurasia	Europe	Southern Europe	Spain	Minorca
Eu_44_0_3	DW	M	<200	West Eurasia	Europe	Southern Europe	Italy	Sardinia
1114	DW	M	<200	West Eurasia	Europe	Southern Europe	Italy	Paestum
Eu_42_00_5	DW	F	<200	West Eurasia	Europe	Southern Europe	Italy	Lazio
Eu_44_00_1	DW	F	<200	West Eurasia	Europe	Southern Europe	Italy	Sardinia
Eu_24_00_1	DW	M	<200	West Eurasia	Europe	Western Europe	France	NA
Eu_1_5_67	DW	M	<200	West Eurasia	Europe	Western Europe	England	NA
1121	DW	M	<200	West Eurasia	Europe	Southern Europe	Italy	Rome
Eu_43_00_4	DW	F	<200	West Eurasia	Europe	Southern Europe	Malta	Bingemma
Eu_1_5_82	DW	M	<200	West Eurasia	Europe	Western Europe	England	South Wilshire
Eu_45_4_2	DW	F	<200	West Eurasia	Europe	Southern Europe	Spain	Minorca
Eu_45_4_3	DW	F	<200	West Eurasia	Europe	Southern Europe	Spain	Minorca
1118	DW	F	<200	West Eurasia	Europe	Southern Europe	Italy	Sardinia
Eu_42_00_2	DW	F	<200	West Eurasia	Europe	Southern Europe	Italy	NA
Eu_43_00_3	DW	M	<200	West Eurasia	Europe	Southern Europe	Malta	Tal Horr
5903	DW	M	<200	West Eurasia	Europe	Southern Europe	Greece	Thessaly
1120	DW	M	<200	West Eurasia	Europe	Southern Europe	Italy	Rome
6044	DW	M	<200	West Eurasia	Europe	Southern Europe	Italy	Sicily
1898	DW	M	<200	Sino-Americas	South America	Andean	Argentina	Rio Gallegos
CA019	DW	F	<200	Sino-Americas	North America	Carribbean	Jamaica	NA
CA004	DW	F	<200	Sino-Americas	Central America	Central America	Guatemala	Gondaiaio
CA025	DW	M	<200	Sino-Americas	North America	Carribbean	Jamaica	NA
CA017	DW	M	<200	Sino-Americas	North America	Carribbean	Jamaica	NA
NA023	DW	F	<200	Sino-Americas	North America	Northeast Woodlands	United States	Iroquois
SA032	DW	M	<200	Sino-Americas	South America	Andean	Peru	NA
SA010	DW	F	<200	Sino-Americas	South America	Andean	Chile	Valparaiso
SA008	DW	M	<200	Sino-Americas	South America	Andean	Chile	NA
SA021	DW	M	<200	Sino-Americas	South America	Andean	Peru	NA
SA038	DW	M	<200	Sino-Americas	South America	Andean	Peru	Pasamayo
SA001	DW	F	<200	Sino-Americas	South America	SA Unkw	SA Unkw	NA
CA001	DW	M	<200	Sino-Americas	South America	Carribbean	Barbados	Arawak
NA065	DW	F	<200	Sino-Americas	North America	NA Unkw	NA Unkw	NA
NA024	DW	F	<700	Sino-Americas	North America	NA South West	United States	Ketchipawan
CA014	DW	M	<200	Sino-Americas	North America	Carribbean	Jamaica	NA
NA015	DW	F	<700	Sino-Americas	North America	NA South West	United States	Ketchipawan

NA011	DW	F	<700	Sino-Americas	North America	NA South West	United States	Ketchipawan
SA045	DW	F	<200	Sino-Americas	South America	Andean	Peru	NA
SA019	DW	M	<200	Sino-Americas	South America	Andean	Peru	NA
NA52	DW	M	<700	Sino-Americas	North America	NA South West	United States	Ketchipawan
SA26	DW	F	<200	Sino-Americas	South America	Andean	Peru	NA
NA72	DW	M	<200	Sino-Americas	North America	NA Plains	United States	Sioux
SA23	DW	F	<200	Sino-Americas	South America	Andean	Peru	NA
NA001	DW	F	<700	Sino-Americas	North America	NA South West	United States	Ketchipawan
NA46	DW	F	<700	Sino-Americas	North America	NA South West	United States	Ketchipawan
SA39	DW	M	<200	Sino-Americas	South America	Andean	Peru	NA
SA37	DW	M	<200	Sino-Americas	South America	Andean	Peru	NA
SA44	DW	F	<200	Sino-Americas	South America	Andean	Peru	NA
SA17	DW	M	<200	Sino-Americas	South America	Andean	Peru	NA
SA007	DW	M	<200	Sino-Americas	South America	Andean	Chile	NA
SA020	DW	F	<200	Sino-Americas	South America	Andean	Peru	NA
NA002	DW	F	<700	Sino-Americas	North America	NA South West	United States	Ketchipawan
NA071	DW	M	<200	Sino-Americas	North America	NA South West	United States	Apache
NA034	DW	F	<700	Sino-Americas	North America	NA South West	United States	Ketchipawan
SA18	DW	F	<200	Sino-Americas	South America	Andean	Peru	NA
CA10	DW	F	<200	Sino-Americas	North America	Caribbean	Jamaica	NA
SA15	DW	F	<200	Sino-Americas	South America	Andean	Peru	NA
SA006	DW	M	<200	Sino-Americas	South America	Andean	Chile	NA
NA_12	DW	F	<700	Sino-Americas	North America	NA South West	United States	Ketchipawan
CA95	DW	F	<200	Sino-Americas	North America	Caribbean	Jamaica	NA
CA26	DW	M	<200	Sino-Americas	North America	Caribbean	Jamaica	NA
NA45	DW	F	<700	Sino-Americas	North America	NA South West	United States	Ketchipawan
SA16	DW	M	<200	Sino-Americas	South America	Andean	Peru	NA
SA25	DW	M	<200	Sino-Americas	South America	Andean	Peru	NA
NA68	DW	F	<200	Sino-Americas	North America	NA Plains	United States	NA
SA_58	DW	F	<200	Sino-Americas	South America	Andean	Peru	NA
POL_41	DW	F	<200	Sahul-Pacific	Oceania	Polynesia	New Zealand	Maori
POL_43	DW	F	<200	Sahul-Pacific	Oceania	Polynesia	New Zealand	Maori
POL_002	DW	M	<200	Sahul-Pacific	Oceania	Polynesia	New Zealand	Maori
POL_11	DW	F	<200	Sahul-Pacific	Oceania	Polynesia	New Zealand	Maori
POL_19	DW	M	<200	Sahul-Pacific	Oceania	Polynesia	New Zealand	Maori
POL_05	DW	F	<200	Sahul-Pacific	Oceania	Polynesia	New Zealand	Maori
POL_24	DW	M	<200	Sahul-Pacific	Oceania	Polynesia	New Zealand	Maori
POL_22	DW	M	<200	Sahul-Pacific	Oceania	Polynesia	New Zealand	Maori
POL_09	DW	M	<200	Sahul-Pacific	Oceania	Polynesia	New Zealand	Maori
POL_40	DW	F	<200	Sahul-Pacific	Oceania	Polynesia	New Zealand	Maori
NA_138	DW	M	<200	Sino-Americas	North America	American Arctic	American Arctic Unkw	Inuit
POL_15	DW	M	<200	Sahul-Pacific	Oceania	Polynesia	New Zealand	Maori
POL_23	DW	F	<200	Sahul-Pacific	Oceania	Polynesia	New Zealand	Maori
NA_139	DW	F	<200	Sino-Americas	North America	American Arctic	American Arctic Unkw	Inuit
POL_12	DW	M	<200	Sahul-Pacific	Oceania	Polynesia	New Zealand	Maori
NA_163	DW	F	<200	Sino-Americas	North America	American Arctic	American Arctic Unkw	Inuit
NA_147	DW	M	<200	Sino-Americas	North America	American Arctic	American Arctic Unkw	Inuit
POL_17	DW	M	<200	Sahul-Pacific	Oceania	Polynesia	New Zealand	Maori
NA_173	DW	F	<200	Sino-Americas	North America	NA Unkw	NA Unkw	NA
NA_110	DW	NA	<200	Sino-Americas	North America	Northwest Coast	Canada	Vancouver Island
NA_154	DW	F	<200	Sino-Americas	North America	American Arctic	American Arctic Unkw	Inuit
POL_45	DW	M	<200	Sahul-Pacific	Oceania	Polynesia	New Zealand	Maori
NA_149	DW	M	<200	Sino-Americas	North America	American Arctic	American Arctic Unkw	Inuit
NA_87	DW	M	<200	Sino-Americas	North America	NA Northwest Coast	Canada	New Westminster
POL_06	DW	M	<200	Sahul-Pacific	Oceania	Polynesia	New Zealand	Maori
POL_18	DW	M	<200	Sahul-Pacific	Oceania	Polynesia	New Zealand	Maori

NA_137	DW	F	<200	Sino-Americas	North America	American Arctic	American Arctic Unkw	Inuit
POL_13	DW	M	<200	Sahul-Pacific	Oceania	Polynesia	New Zealand	Maori
NA_145	DW	F	<200	Sino-Americas	North America	American Arctic	American Arctic Unkw	Inuit
NA_67	DW	F	<200	Sino-Americas	North America	Northwest Coast	United States	NA
NA_133	DW	F	<200	Sino-Americas	North America	American Arctic	American Arctic Unkw	Inuit
NA_151	DW	F	<200	Sino-Americas	North America	American Arctic	American Arctic Unkw	Inuit
NA_123	DW	M	<200	Sino-Americas	North America	American Arctic	American Arctic Unkw	Inuit
NA_124	DW	F	<200	Sino-Americas	North America	American Arctic	Greenland	Inuit
NA_136	DW	M	<200	Sino-Americas	North America	American Arctic	American Arctic Unkw	Inuit
NA_140	DW	M	<200	Sino-Americas	North America	American Arctic	American Arctic Unkw	Inuit
NA_105	DW	F	<200	Sino-Americas	North America	Northwest Coast	Canada	Vancouver Island
NA_62	DW	M	<200	Sino-Americas	North America	NA South West	United States	Zuni
NA_135	DW	M	<200	Sino-Americas	North America	American Arctic	American Arctic Unkw	Inuit
NA_68	DW	F	<200	Sino-Americas	North America	NA Plains	United States	NA
NA_111	DW	F	<200	Sino-Americas	North America	Northwest Coast	United States	Makah
NA_150	DW	F	<200	Sino-Americas	North America	American Arctic	American Arctic Unkw	Inuit
NA_144	DW	F	<200	Sino-Americas	North America	American Arctic	American Arctic Unkw	Inuit
NA_121	DW	F	<200	Sino-Americas	North America	American Arctic	Greenland	Inuit Eleanor Bay
NA_182	DW	M	<200	Sino-Americas	North America	NA Unkw	NA Unkw	Native American
NA_82	DW	M	<200	Sino-Americas	North America	NA	Canada	Huron
POL_44	DW	M	<200	Sahul-Pacific	Oceania	Northeast Woodlands	New Zealand	Maori
NA_95	DW	M	<200	Sino-Americas	North America	Polynesia	Canada	Vancouver Island
NA_72	DW	M	<200	Sino-Americas	North America	Northwest Coast	United States	Sioux
NA_89	DW	M	<200	Sino-Americas	North America	NA Plains	United States	NA
NA_132	DW	F	<200	Sino-Americas	North America	Northwest Coast	Canada	New Westminister
NA_75	DW	F	<200	Sino-Americas	North America	American Arctic	American Arctic Unkw	Inuit
NA_71	DW	M	<200	Sino-Americas	North America	American Arctic	United States	Iroquois
NA_84	DW	F	<200	Sino-Americas	North America	NA South West	United States	Apache
NA_153	DW	M	<200	Sino-Americas	North America	NA	Canada	Manitoba
NA_98	DW	F	<200	Sino-Americas	North America	Subarctic	American Arctic Unkw	Inuit
NA_164	DW	F	<200	Sino-Americas	North America	American Arctic	Canada	Vancouver Island
NA_102	DW	M	<200	Sino-Americas	North America	NA	American Arctic Unkw	Inuit
NA_97	DW	F	<200	Sino-Americas	North America	Northwest Coast	Canada	Vancouver Island
NA_183	DW	M	<200	Sino-Americas	North America	Northwest Coast	Canada	Vancouver Island
NA_61	DW	F	<200	Sino-Americas	North America	NA Unkw	NA Unkw	Native American
						NA South West	United States	Zuni

NA_83	DW	M	<200	Sino-Americas	North America	NA Northeast Woodlands	Canada	Huron
NA_104	DW	M	<200	Sino-Americas	North America	NA Northwest Coast	Canada	Vancouver Island
NA_76	DW	M	<200	Sino-Americas	North America	NA Northeast Woodlands	United States	Iroquois
NA_101	DW	F	<200	Sino-Americas	North America	NA Northwest Coast	Canada	Vancouver Island
NA_92	DW	M	<200	Sino-Americas	North America	NA Northwest Coast	Canada	Vancouver Island
NA_81	DW	M	<200	Sino-Americas	North America	NA Northeast Woodlands	Canada	Huron
NA_74	DW	M	<200	Sino-Americas	North America	NA Northeast Woodlands	Canada	Huron
NA_134	DW	F	<200	Sino-Americas	North America	American Arctic	American Arctic Unkw	Inuit
NU_761	DW	M	<200	Sub-Saharan Africa	Sub-Saharan Africa	SSA Unkw	SSA Unkw	NA
AUS_001	DW	M	<200	Sahul-Pacific	Oceania	Australia	Australia Unkw	NA
AUS_016	DW	M	<200	Sahul-Pacific	Oceania	Australia	Australia Unkw	Aborigine
AUS_017	DW	F	<200	Sahul-Pacific	Oceania	Australia	Australia Unkw	NA
AUS_020	DW	M	<200	Sahul-Pacific	Oceania	Australia	Australia Unkw	NA
AUS_022	DW	F	<200	Sahul-Pacific	Oceania	Australia	Australia Unkw	NA
AUS_023	DW	M	<200	Sahul-Pacific	Oceania	Australia	Australia Unkw	NA
AUS_024	DW	M	<200	Sahul-Pacific	Oceania	Australia	Australia Unkw	Aborigine
AUS_025	DW	M	<200	Sahul-Pacific	Oceania	Australia	Australia Unkw	Aborigine
AUS_027	DW	F	<200	Sahul-Pacific	Oceania	Australia	Australia Unkw	NA
AUS_028	DW	F	<200	Sahul-Pacific	Oceania	Australia	Australia Unkw	NA
AUS_029	DW	M	<200	Sahul-Pacific	Oceania	Australia	Australia Unkw	NA
AUS_030	DW	M	<200	Sahul-Pacific	Oceania	Australia	Australia Unkw	Aborigine
AUS_032	DW	M	<200	Sahul-Pacific	Oceania	Australia	Australia Unkw	NA
AUS_037	DW	M	<200	Sahul-Pacific	Oceania	Australia	Victoria	NA
AUS_046	DW	F	<200	Sahul-Pacific	Oceania	Australia	Australia Unkw	Aborigine
AUS_047	DW	F	<200	Sahul-Pacific	Oceania	Australia	Australia Unkw	NA
AUS_048	DW	F	<200	Sahul-Pacific	Oceania	Australia	Australia Unkw	NA
AUS_049	DW	F	<200	Sahul-Pacific	Oceania	Australia	Australia Unkw	NA
AUS_050	DW	F	<200	Sahul-Pacific	Oceania	Australia	Australia Unkw	NA
AUS_051	DW	M	<200	Sahul-Pacific	Oceania	Australia	Australia Unkw	Aborigine
AUS_053	DW	M	<200	Sahul-Pacific	Oceania	Australia	Australia Unkw	Aborigine
AUS_054	DW	F	<200	Sahul-Pacific	Oceania	Australia	Australia Unkw	NA
AUS_055	DW	M	<200	Sahul-Pacific	Oceania	Australia	Australia Unkw	NA
AUS_056	DW	F	<200	Sahul-Pacific	Oceania	Australia	Australia Unkw	NA
AUS_058	DW	M	<200	Sahul-Pacific	Oceania	Australia	Australia Unkw	NA
AUS_059	DW	F	<200	Sahul-Pacific	Oceania	Australia	Western Australia	Baiono
AUS_062	DW	M	<200	Sahul-Pacific	Oceania	Australia	Western Australia	Perth
AUS_077	DW	M	<200	Sahul-Pacific	Oceania	Australia	Australia Unkw	Aborigine
AUS_078	DW	M	<200	Sahul-Pacific	Oceania	Australia	Australia Unkw	NA
AUS_079	DW	F	<200	Sahul-Pacific	Oceania	Australia	South Australia	NA
AUS_080	DW	M	<200	Sahul-Pacific	Oceania	Australia	South Australia	NA
AUS_081	DW	M	<200	Sahul-Pacific	Oceania	Australia	South Australia	NA
AUS_082	DW	M	<200	Sahul-Pacific	Oceania	Australia	South Australia	NA
AUS_083	DW	F	<200	Sahul-Pacific	Oceania	Australia	Australia Unkw	NA
AUS_093	DW	F	<200	Sahul-Pacific	Oceania	Australia	South Australia	NA
AUS_094	DW	F	<200	Sahul-Pacific	Oceania	Australia	South East Australia	NA
AUS_095	DW	F	<200	Sahul-Pacific	Oceania	Australia	South East Australia	NA
AUS_096	DW	F	<200	Sahul-Pacific	Oceania	Australia	Victoria	NA
AUS_102	DW	M	<200	Sahul-Pacific	Oceania	Australia	New South Wales	Aborigine
AUS_104	DW	M	<200	Sahul-Pacific	Oceania	Australia	South East Australia	NA

AUS_105	DW	M	<200	Sahul-Pacific	Oceania	Australia	New South Wales	Aborigine
AUS_106	DW	M	<200	Sahul-Pacific	Oceania	Australia	Australia Unkw	NA
AUS_107	DW	F	<200	Sahul-Pacific	Oceania	Australia	New South Wales	Mem Mem
AUS_108	DW	M	<200	Sahul-Pacific	Oceania	Australia	New South Wales	Berida
AUS_109	DW	M	<200	Sahul-Pacific	Oceania	Australia	New South Wales	Wollongong
AUS_110	DW	F	<200	Sahul-Pacific	Oceania	Australia	New South Wales	Newcastle
AUS_113	DW	M	<200	Sahul-Pacific	Oceania	Australia	New South Wales	Murray River
AUS_114_1	DW	M	<200	Sahul-Pacific	Oceania	Australia	New South Wales	Murray River
AUS_116	DW	F	<200	Sahul-Pacific	Oceania	Australia	New South Wales	Murray River
AUS_119	DW	F	<200	Sahul-Pacific	Oceania	Australia	New South Wales	Murray River
AUS_120	DW	M	<200	Sahul-Pacific	Oceania	Australia	New South Wales	Murray River
AUS_121	DW	F	<200	Sahul-Pacific	Oceania	Australia	New South Wales	Murray River
AUS_122	DW	M	<200	Sahul-Pacific	Oceania	Australia	Queensland	NA
AUS_123	DW	F	<200	Sahul-Pacific	Oceania	Australia	Queensland	Mackay Aborigine
AUS_124	DW	M	<200	Sahul-Pacific	Oceania	Australia	Queensland	Aborigine
AUS_125	DW	F	<200	Sahul-Pacific	Oceania	Australia	Queensland	Croydon
AUS_126	DW	M	<200	Sahul-Pacific	Oceania	Australia	Queensland	Queensland Croydon
AUS_127	DW	M	<200	Sahul-Pacific	Oceania	Australia	Queensland	Queensland North
AUS_128	DW	M	<200	Sahul-Pacific	Oceania	Australia	Queensland	Queensland North
AUS_129	DW	M	<200	Sahul-Pacific	Oceania	Australia	Queensland	Queensland North
AUS_130	DW	F	<200	Sahul-Pacific	Oceania	Australia	Queensland	Queensland North
AUS_131	DW	F	<200	Sahul-Pacific	Oceania	Australia	Queensland	Queensland North
AF_11_5_28	DW	F	6400-6000	West Eurasia	North Africa	North East Africa	Egypt	Badari
AF_11_5_21	DW	F	6400-6000	West Eurasia	North Africa	North East Africa	Egypt	Badari
AF_11_5_42	DW	M	6400-6000	West Eurasia	North Africa	North East Africa	Egypt	Badari
AF_11_5_04	DW	F	6400-6000	West Eurasia	North Africa	North East Africa	Egypt	Badari
AF_11_5_17	DW	F	6400-6000	West Eurasia	North Africa	North East Africa	Egypt	Badari
AF_11_5_10	DW	M	6400-6000	West Eurasia	North Africa	North East Africa	Egypt	Badari
AF_11_5_40	DW	M	6400-6000	West Eurasia	North Africa	North East Africa	Egypt	Badari
AF_12_4_25	DW	M	2100-1400	West Eurasia	North Africa	North East Africa	Sudan	Jebel Moya
AF_11_5_22	DW	F	6400-6000	West Eurasia	North Africa	North East Africa	Egypt	Badari
AF_11_5_25	DW	F	6400-6000	West Eurasia	North Africa	North East Africa	Egypt	Badari
AF_12_4_28	DW	M	2100-1400	West Eurasia	North Africa	North East Africa	Sudan	Jebel Moya
AF_12_4_18	DW	M	2100-1400	West Eurasia	North Africa	North East Africa	Sudan	Jebel Moya
AF_12_4_08	DW	M	2100-1400	West Eurasia	North Africa	North East Africa	Sudan	Jebel Moya
AF_11_5_27	DW	F	6000-5200	West Eurasia	North Africa	North East Africa	Egypt	Nagada
AF_11_5_59	DW	M	6000-5200	West Eurasia	North Africa	North East Africa	Egypt	Nagada
AF_11_5_55	DW	M	6000-5200	West Eurasia	North Africa	North East Africa	Egypt	Nagada
AF_11_5_34	DW	M	6000-5200	West Eurasia	North Africa	North East Africa	Egypt	Nagada

AF_11_5_53	DW	M	6000-5200	West Eurasia	North Africa	North East Africa	Egypt	Nagada
AF_11_5_02	DW	F	6000-5200	West Eurasia	North Africa	North East Africa	Egypt	Nagada
AF_12_4_07	DW	M	6000-5200	West Eurasia	North Africa	North East Africa	Egypt	Nagada
AF_11_5_12	DW	F	6000-5200	West Eurasia	North Africa	North East Africa	Egypt	Nagada
AF_12_4_15	DW	M	2100-1400	West Eurasia	North Africa	North East Africa	Sudan	Jebel Moya
AF_12_4_103	DW	M	2100-1400	West Eurasia	North Africa	North East Africa	Sudan	Jebel Moya
AF_11_5_07	DW	F	6000-5200	West Eurasia	North Africa	North East Africa	Egypt	Nagada
AF_11_5_44	DW	M	6000-5200	West Eurasia	North Africa	North East Africa	Egypt	Nagada
AF_11_5_54	DW	F	6000-5200	West Eurasia	North Africa	North East Africa	Egypt	Nagada
AF_11_5_24	DW	F	6000-5200	West Eurasia	North Africa	North East Africa	Egypt	Nagada
AF_11_5_32	DW	M	6000-5200	West Eurasia	North Africa	North East Africa	Egypt	Nagada
AF_11_5_43	DW	M	6000-5200	West Eurasia	North Africa	North East Africa	Egypt	Nagada
AF_11_5_16	DW	M	6000-5200	West Eurasia	North Africa	North East Africa	Egypt	Nagada
AF_12_4_91	DW	M	2100-1400	West Eurasia	North Africa	North East Africa	Sudan	Jebel Moya
AF_11_5_18	DW	M	6000-5200	West Eurasia	North Africa	North East Africa	Egypt	Nagada
AF_12_4_21	DW	F	2100-1400	West Eurasia	North Africa	North East Africa	Sudan	Jebel Moya
AF_11_5_41	DW	F	6000-5200	West Eurasia	North Africa	North East Africa	Egypt	Nagada
AF_11_5_52	DW	F	6000-5200	West Eurasia	North Africa	North East Africa	Egypt	Nagada
AF_12_4_17	DW	NA	2100-1400	West Eurasia	North Africa	North East Africa	Sudan	Jebel Moya
AF_12_4_19	DW	M	2100-1400	West Eurasia	North Africa	North East Africa	Sudan	Jebel Moya
AF_11_5_58	DW	F	6000-5200	West Eurasia	North Africa	North East Africa	Egypt	Nagada
AF_12_4_10	DW	M	2100-1400	West Eurasia	North Africa	North East Africa	Sudan	Jebel Moya
AF_11_5_39	DW	M	6000-5200	West Eurasia	North Africa	North East Africa	Egypt	Nagada
AF_11_5_46	DW	F	6000-5200	West Eurasia	North Africa	North East Africa	Egypt	Nagada
AF_11_5_33	DW	F	6000-5200	West Eurasia	North Africa	North East Africa	Egypt	Nagada
AF_11_5_47	DW	F	6000-5200	West Eurasia	North Africa	North East Africa	Egypt	Nagada
AF_11_5_35	DW	F	6000-5200	West Eurasia	North Africa	North East Africa	Egypt	Nagada
AF_11_5_37	DW	M	6000-5200	West Eurasia	North Africa	North East Africa	Egypt	Nagada
AF_11_536	DW	M	6000-5200	West Eurasia	North Africa	North East Africa	Egypt	Nagada
AF_11_5_57	DW	M	6000-5200	West Eurasia	North Africa	North East Africa	Egypt	Nagada
AF_12_4_22	DW	F	2100-1400	West Eurasia	North Africa	North East Africa	Sudan	Jebel Moya
AF_11_5_26	DW	F	6000-5200	West Eurasia	North Africa	North East Africa	Egypt	Nagada
AF_11_5_29	DW	F	6000-5200	West Eurasia	North Africa	North East Africa	Egypt	Nagada
AF_12_4_26	DW	M	2100-1400	West Eurasia	North Africa	North East Africa	Sudan	Jebel Moya
AF_12_4_108	DW	M	2100-1400	West Eurasia	North Africa	North East Africa	Sudan	Jebel Moya
AF_11_5_31	DW	F	6000-5200	West Eurasia	North Africa	North East Africa	Egypt	Nagada
AF_11_5_56	DW	F	6000-5200	West Eurasia	North Africa	North East Africa	Egypt	Nagada
AF_11_5_38	DW	F	6000-5200	West Eurasia	North Africa	North East Africa	Egypt	Nagada

SUD_11	DW	M	3750-3500	West Eurasia	North Africa	North East Africa	Sudan	Kerma
SUD_05	DW	M	3750-3500	West Eurasia	North Africa	North East Africa	Sudan	Kerma
SUD_13	DW	M	3750-3500	West Eurasia	North Africa	North East Africa	Sudan	NA
SUD_5343	DW	M	3750-3500	West Eurasia	North Africa	North East Africa	Sudan	NA
SUD_08	DW	M	3750-3500	West Eurasia	North Africa	North East Africa	Sudan	Kerma
SUD_14	DW	M	3750-3500	West Eurasia	North Africa	North East Africa	Sudan	Kerma
SUD_04	DW	M	3750-3500	West Eurasia	North Africa	North East Africa	Sudan	Kerma
SUD_20	DW	M	3750-3500	West Eurasia	North Africa	North East Africa	Sudan	Kerma
SUD_10	DW	M	3750-3500	West Eurasia	North Africa	North East Africa	Sudan	Kerma
SUD_01	DW	M	3750-3500	West Eurasia	North Africa	North East Africa	Sudan	Kerma
SUD_26	DW	M	3750-3500	West Eurasia	North Africa	North East Africa	Sudan	Kerma
SUD_38	DW	M	3750-3500	West Eurasia	North Africa	North East Africa	Sudan	Kerma
SUD_16	DW	M	3750-3500	West Eurasia	North Africa	North East Africa	Sudan	Kerma
SUD_27	DW	M	3750-3500	West Eurasia	North Africa	North East Africa	Sudan	Kerma
SUD_15	DW	M	3750-3500	West Eurasia	North Africa	North East Africa	Sudan	Kerma
SUD_02	DW	M	3750-3500	West Eurasia	North Africa	North East Africa	Sudan	Kerma
SUD_5053	DW	F	<200	West Eurasia	North Africa	North East Africa	Sudan	NA
SUD_4438	DW	M	<200	West Eurasia	North Africa	North East Africa	Sudan	NA
MEL_255	DW	F	<200	Sahul-Pacific	Oceania	Melanesia	Papua New Guinea	Muyuw Kwaiawata Island
AF_11_5_48	DW	NA	<200	West Eurasia	North Africa	North East Africa	Egypt	NA
4434	DW	M	200	Sub-Saharan Africa	Sub-Saharan Africa	Western Africa	Ghana	Ashanti
5419	DW	F	<200	Sub-Saharan Africa	Sub-Saharan Africa	Western Africa	Nigeria	Kagoro
AF_21_0_14	DW	M	<200	Sub-Saharan Africa	Sub-Saharan Africa	Eastern Africa	Kenya	Teita
AF_21_0_62	DW	F	<200	Sub-Saharan Africa	Sub-Saharan Africa	Eastern Africa	Kenya	Teita
AF_21_0_102	DW	F	<200	Sub-Saharan Africa	Sub-Saharan Africa	Eastern Africa	Kenya	Teita
AF_21_0_100	DW	F	<200	Sub-Saharan Africa	Sub-Saharan Africa	Eastern Africa	Kenya	Teita
AF_21_0_48	DW	M	<200	Sub-Saharan Africa	Sub-Saharan Africa	Eastern Africa	Kenya	Teita
AF_21_0_108	DW	F	<200	Sub-Saharan Africa	Sub-Saharan Africa	Eastern Africa	Kenya	Teita
AF_21_0_107	DW	F	<200	Sub-Saharan Africa	Sub-Saharan Africa	Eastern Africa	Kenya	Teita
AF_21_0_93	DW	F	<200	Sub-Saharan Africa	Sub-Saharan Africa	Eastern Africa	Kenya	Teita
AF_21_0_95	DW	F	<200	Sub-Saharan Africa	Sub-Saharan Africa	Eastern Africa	Kenya	Teita
AF_21_0_50	DW	M	<200	Sub-Saharan Africa	Sub-Saharan Africa	Eastern Africa	Kenya	Teita
AF_21_0_45	DW	M	<200	Sub-Saharan Africa	Sub-Saharan Africa	Eastern Africa	Kenya	Teita
AF_21_0_68	DW	M	<200	Sub-Saharan Africa	Sub-Saharan Africa	Eastern Africa	Kenya	Teita
AF_21_0_71	DW	F	<200	Sub-Saharan Africa	Sub-Saharan Africa	Eastern Africa	Kenya	Teita
AF_21_0_41	DW	M	<200	Sub-Saharan Africa	Sub-Saharan Africa	Eastern Africa	Kenya	Teita
AF_21_0_82	DW	F	<200	Sub-Saharan Africa	Sub-Saharan Africa	Eastern Africa	Kenya	Teita

AF_21_0_94	DW	F	<200	Sub-Saharan Africa	Sub-Saharan Africa	Eastern Africa	Kenya	Teita
AF_21_0_67	DW	F	<200	Sub-Saharan Africa	Sub-Saharan Africa	Eastern Africa	Kenya	Teita
AF_21_0_70	DW	F	<200	Sub-Saharan Africa	Sub-Saharan Africa	Eastern Africa	Kenya	Teita
AF_21_0_60	DW	M	<200	Sub-Saharan Africa	Sub-Saharan Africa	Eastern Africa	Kenya	Teita
AF_21_0_34	DW	M	<200	Sub-Saharan Africa	Sub-Saharan Africa	Eastern Africa	Kenya	Teita
AF_21_0_24	DW	M	<200	Sub-Saharan Africa	Sub-Saharan Africa	Eastern Africa	Kenya	Teita
AF_21_0_9	DW	M	<200	Sub-Saharan Africa	Sub-Saharan Africa	Eastern Africa	Kenya	Teita
AF_21_0_20	DW	M	<200	Sub-Saharan Africa	Sub-Saharan Africa	Eastern Africa	Kenya	Teita
AF_21_0_18	DW	M	<200	Sub-Saharan Africa	Sub-Saharan Africa	Eastern Africa	Kenya	Teita
AF_21_0_43	DW	M	<200	Sub-Saharan Africa	Sub-Saharan Africa	Eastern Africa	Kenya	Teita
AF_21_0_16	DW	M	<200	Sub-Saharan Africa	Sub-Saharan Africa	Eastern Africa	Kenya	Teita
AF_21_0_13	DW	M	<200	Sub-Saharan Africa	Sub-Saharan Africa	Eastern Africa	Kenya	Teita
AF_21_0_40	DW	M	<200	Sub-Saharan Africa	Sub-Saharan Africa	Eastern Africa	Kenya	Teita
AF_21_0_25	DW	M	<200	Sub-Saharan Africa	Sub-Saharan Africa	Eastern Africa	Kenya	Teita
AF_21_0_12	DW	M	<200	Sub-Saharan Africa	Sub-Saharan Africa	Eastern Africa	Kenya	Teita
AF_21_0_29	DW	M	<200	Sub-Saharan Africa	Sub-Saharan Africa	Eastern Africa	Kenya	Teita
AF_21_0_118	DW	F	<200	Sub-Saharan Africa	Sub-Saharan Africa	Eastern Africa	Kenya	Teita
AF_21_0_121	DW	F	<200	Sub-Saharan Africa	Sub-Saharan Africa	Eastern Africa	Kenya	Teita
AF_21_0_133	DW	F	<200	Sub-Saharan Africa	Sub-Saharan Africa	Eastern Africa	Kenya	Teita
AF_21_0_129	DW	F	<200	Sub-Saharan Africa	Sub-Saharan Africa	Eastern Africa	Kenya	Teita
AF_21_0_123	DW	F	<200	Sub-Saharan Africa	Sub-Saharan Africa	Eastern Africa	Kenya	Teita
AF_21_0_126	DW	F	<200	Sub-Saharan Africa	Sub-Saharan Africa	Eastern Africa	Kenya	Teita
AF_21_0_113	DW	M	<200	Sub-Saharan Africa	Sub-Saharan Africa	Eastern Africa	Kenya	Teita
1742	DW	F	<200	Sub-Saharan Africa	Sub-Saharan Africa	Southern Africa	South Africa	NA
AF_23_0_28	DW	F	<200	Sub-Saharan Africa	Sub-Saharan Africa	Eastern Africa	Tanzania	Bukoba
AF_15_0_2	DW	M	<200	Sub-Saharan Africa	Sub-Saharan Africa	Eastern Africa	Somalia	Hariya
AF112	DW	F	<200	Sub-Saharan Africa	Sub-Saharan Africa	Southern Africa	South Africa	NA
SAS_14	DW	M	<200	West Eurasia	South Asia	Indian Sub-Continent	Pakistan	NA
209305	NMNH	M	<200	Sunda-Pacific	South East Asia	Malay Archipelago	Philippines	Tagalog Island
209307	NMNH	F	<200	Sunda-Pacific	South East Asia	Malay Archipelago	Philippines	Tagalog Island
209310	NMNH	F	<200	Sunda-Pacific	South East Asia	Malay Archipelago	Philippines	Tagalog Island
226155	NMNH	F	<200	Sahul-Pacific	Oceania	Polynesia	New Zealand	NA
226156	NMNH	F	<200	Sahul-Pacific	Oceania	Polynesia	New Zealand	NA
226158	NMNH	M	<200	Sahul-Pacific	Oceania	Polynesia	New Zealand	NA
222001	NMNH	M	<200	Sunda-Pacific	South East Asia	Malay Archipelago	Indonesia	Pagi Island
381079	NMNH	F	<200	Sahul-Pacific	Oceania	Melanesia	Papua New Guinea	New Britain
99_1_109	NMNH	M	~1600	Sino-Americas	North America	American Arctic	Alaska	Ipiutak
99_1_199	NMNH	F	~1600	Sino-Americas	North America	American Arctic	Alaska	Ipiutak
99_1_209	NMNH	M	~1600	Sino-Americas	North America	American Arctic	Alaska	Ipiutak

99_1_211	NMNH	F	~1600	Sino-Americas	North America	American Arctic	Alaska	Ipiutak
99_1_174	NMNH	F	~1600	Sino-Americas	North America	American Arctic	Alaska	NA
99_1_568	NMNH	M	~1600	Sino-Americas	North America	American Arctic	Alaska	NA
99_1_594	NMNH	M	~1600	Sino-Americas	North America	American Arctic	Alaska	NA
99_1_593	NMNH	F	~1600	Sino-Americas	North America	American Arctic	Alaska	NA
99_1_64	NMNH	F	~800	Sino-Americas	North America	American Arctic	Alaska	Tigara
99_1_642	NMNH	M	~800	Sino-Americas	North America	American Arctic	Alaska	Tigara
99_1_649	NMNH	M	~800	Sino-Americas	North America	American Arctic	Alaska	Tigara
99_1_222	NMNH	F	~800	Sino-Americas	North America	American Arctic	Alaska	Tigara
99_1_231	NMNH	M	~800	Sino-Americas	North America	American Arctic	Alaska	Tigara
99_1_231A	NMNH	F	~800	Sino-Americas	North America	American Arctic	Alaska	Tigara
99_1_232	NMNH	F	~800	Sino-Americas	North America	American Arctic	Alaska	Tigara
99_1_260	NMNH	F	~800	Sino-Americas	North America	American Arctic	Alaska	Tigara
99_1_262	NMNH	F	~800	Sino-Americas	North America	American Arctic	Alaska	Tigara
99_1_402	NMNH	M	~800	Sino-Americas	North America	American Arctic	Alaska	Tigara
99_1_403	NMNH	M	~800	Sino-Americas	North America	American Arctic	Alaska	Tigara
99_1_404	NMNH	M	~800	Sino-Americas	North America	American Arctic	Alaska	Tigara
99_1_415	NMNH	F	~800	Sino-Americas	North America	American Arctic	Alaska	Tigara
99_1_420	NMNH	F	~800	Sino-Americas	North America	American Arctic	Alaska	Tigara
99_1_435	NMNH	M	~800	Sino-Americas	North America	American Arctic	Alaska	Tigara
99_1_462	NMNH	M	~800	Sino-Americas	North America	American Arctic	Alaska	Tigara
99_1_503	NMNH	F	~800	Sino-Americas	North America	American Arctic	Alaska	Tigara
226098	NMNH	NA	<200	Sahul-Pacific	Oceania	Melanesia	Papua New Guinea	New Britain
227454	NMNH	NA	<200	Sahul-Pacific	Oceania	Melanesia	Papua New Guinea	New Britain
227459	NMNH	NA	<200	Sahul-Pacific	Oceania	Melanesia	Papua New Guinea	New Britain
227465	NMNH	NA	<200	Sahul-Pacific	Oceania	Melanesia	Papua New Guinea	New Britain
242755	NMNH	NA	<200	Sino-Americas	North America	American Arctic	Canada	Baffin Island
242834	NMNH	NA	<200	Sino-Americas	North America	American Arctic	Canada	Baffin Island
259354	NMNH	NA	<200	Sunda-Pacific	South East Asia	Malay Archipelago	Philippines	NA
342024	NMNH	NA	Unkw	Sino-Americas	North America	American Arctic	Greenland	Inuit
379058	NMNH	NA	<200	Sunda-Pacific	South East Asia	Malay Archipelago	Philippines	NA
380430	NMNH	F	<200	Sunda-Pacific	South East Asia	Malay Archipelago	NA	Malaysian
380447	NMNH	M	<200	Sunda-Pacific	South East Asia	Malay Archipelago	NA	NA
380448	NMNH	M	<200	Sunda-Pacific	South East Asia	Malay Archipelago	NA	Malaysian
380450	NMNH	M	Unkw	Sahul-Pacific	Oceania	Australia	Northern Territory	Crocodile Island

**ID** = collection identification number, **M** = Male, **F** = female, **\*BP** = before present, **DW** = Duckworth, **AMNH** = American Museum of Natural History, **NMNH** = Smithsonian National Museum of Natural History, **†G1** = Major Human Subdivisions, **G2** = Continental Group, **G3** = Continental Region, **G4** = Country/State, **G5** = Locality/Tribe, **Unkw** = unknown.

## 9.3 Chapter 4 supplementary statistics

### 9.3.1 Tukey Pair-wise comparisons by tooth

Table 9.2: Tukey Pair-wise comparisons of from GLM model of canal to root number by tooth

Contrast	Estimate	Odds Ratio	Std. Error	z-value	P-value
P <sup>3</sup> - P <sup>4</sup>	0.0911	1.0953	0.0123	7.4180	<.00001
P <sup>3</sup> - M <sup>1</sup>	-0.6923	0.5004	0.0165	-41.9106	<.00001
P <sup>3</sup> - M <sup>2</sup>	-0.6476	0.5233	0.0165	-39.2830	<.00001
P <sup>3</sup> - M <sup>3</sup>	-0.6500	0.5221	0.0164	-39.6955	<.00001
P <sup>3</sup> - P <sub>3</sub>	0.1272	1.1356	0.0129	9.8777	<.00001
P <sup>3</sup> - P <sub>4</sub>	0.1197	1.1272	0.0128	9.3303	<.00001
P <sup>3</sup> - M <sub>1</sub>	-0.2871	0.7504	0.0186	-15.4013	<.00001
P <sup>3</sup> - M <sub>2</sub>	-0.3234	0.7237	0.0145	-22.2508	<.00001
P <sup>3</sup> - M <sub>3</sub>	-0.3557	0.7006	0.0141	-25.1822	<.00001
P <sup>4</sup> - M <sup>1</sup>	-0.7834	0.4569	0.0183	-42.9011	<.00001
P <sup>4</sup> - M <sup>2</sup>	-0.7386	0.4778	0.0183	-40.3220	<.00001
P <sup>4</sup> - M <sup>3</sup>	-0.7410	0.4766	0.0179	-41.3743	<.00001
P <sup>4</sup> - P <sub>3</sub>	0.0361	1.0368	0.0073	4.9477	<.00001
P <sup>4</sup> - P <sub>4</sub>	0.0286	1.0290	0.0071	4.0477	<.00001
P <sup>4</sup> - M <sub>1</sub>	-0.3782	0.6851	0.0208	-18.1390	<.00001
P <sup>4</sup> - M <sub>2</sub>	-0.4145	0.6607	0.0158	-26.2447	<.00001
P <sup>4</sup> - M <sub>3</sub>	-0.4468	0.6397	0.0152	-29.4156	<.00001
M <sup>1</sup> - M <sup>2</sup>	0.0448	1.0458	0.0061	7.2915	<.00001
M <sup>1</sup> - M <sup>3</sup>	0.0423	1.0433	0.0072	5.8984	<b>0.0001</b>
M <sup>1</sup> - P <sub>3</sub>	0.8195	2.2694	0.0174	47.1051	<.00001
M <sup>1</sup> - P <sub>4</sub>	0.8120	2.2525	0.0178	45.6536	<.00001
M <sup>1</sup> - M <sub>1</sub>	0.4052	1.4997	0.0055	73.7824	<.00001
M <sup>1</sup> - M <sub>2</sub>	0.3689	1.4461	0.0053	69.3361	<.00001
M <sup>1</sup> - M <sub>3</sub>	0.3366	1.4002	0.0055	61.0848	<.00001
M <sup>2</sup> - M <sup>3</sup>	-0.0024	0.9976	0.0078	-0.3101	0.0222
M <sup>2</sup> - P <sub>3</sub>	0.7748	2.1701	0.0177	43.6840	<.00001
M <sup>2</sup> - P <sub>4</sub>	0.7673	2.1539	0.0181	42.3303	<.00001
M <sup>2</sup> - M <sub>1</sub>	0.3605	1.4340	0.0085	42.4873	<.00001
M <sup>2</sup> - M <sub>2</sub>	0.3241	1.3828	0.0071	45.3929	<.00001
M <sup>2</sup> - M <sub>3</sub>	0.2918	1.3389	0.0074	39.2476	<.00001
M <sup>3</sup> - P <sub>3</sub>	0.7772	2.1753	0.0174	44.7211	<.00001
M <sup>3</sup> - P <sub>4</sub>	0.7697	2.1591	0.0177	43.4366	<.00001
M <sup>3</sup> - M <sub>1</sub>	0.3629	1.4375	0.0094	38.4709	<.00001
M <sup>3</sup> - M <sub>2</sub>	0.3265	1.3862	0.0078	41.6325	<.00001
M <sup>3</sup> - M <sub>3</sub>	0.2942	1.3421	0.0080	36.9683	<.00001 <sup>#</sup>
P <sub>3</sub> - P <sub>4</sub>	-0.0075	0.9925	0.0019	-3.8619	<.00001
P <sub>3</sub> - M <sub>1</sub>	-0.4143	0.6608	0.0200	-20.6987	<.00001
P <sub>3</sub> - M <sub>2</sub>	-0.4506	0.6372	0.0147	-30.7287	<.00001
P <sub>3</sub> - M <sub>3</sub>	-0.4829	0.6170	0.0141	-34.2334	<.00001
P <sub>4</sub> - M <sub>1</sub>	-0.4068	0.6658	0.0204	-19.9481	<.00001
P <sub>4</sub> - M <sub>2</sub>	-0.4431	0.6420	0.0151	-29.3666	<.00001
P <sub>4</sub> - M <sub>3</sub>	-0.4754	0.6216	0.0145	-32.8780	<.00001
M <sub>1</sub> - M <sub>2</sub>	-0.0364	0.9643	0.0078	-4.6724	<.00001
M <sub>1</sub> - M <sub>3</sub>	-0.0687	0.9336	0.0079	-8.7160	<.00001
M <sub>2</sub> - M <sub>3</sub>	-0.0323	0.9682	0.0050	-6.4832	<.00001

<sup>#</sup> Does not meet Bonferroni correction of  $0.05/45 \approx 0.001$ , where 45 is the number of pair-wise tests.

\* Significant values in bold after Bonferroni correction. Model fitted without intercept. Results are given on the log (not the response) scale.

### 9.3.2 Tukey pair-wise comparisons by geographical region

Table 9.3: Tukey pair-wise comparisons of canal to root number by geographical region

Contrast	Estimate	Odds Ratio	Std. Error	z-ratio	P-value*
Sahul-Pacific - Sino-Americas	-0.022	0.978	0.007	-3.165	0.014
Sahul-Pacific - Sub-Saharan Africa	-0.047	0.955	0.007	-6.191	<b>&lt;.0001</b>
Sahul-Pacific - Sunda-Pacific	-0.008	0.993	0.011	-0.688	0.9591
Sahul-Pacific - West Eurasia	0.019	1.019	0.008	2.539	0.082
Sino-Americas - Sub-Saharan Africa	-0.024	0.976	0.007	-3.457	<b>0.005</b>
Sino-Americas - Sunda-Pacific	-0.015	1.015	0.011	1.402	0.626
Sino-Americas - West Eurasia	-0.003	0.997	0.007	-0.438	0.992
Sub-Saharan Africa - Sunda-Pacific	0.039	1.040	0.011	3.584	0.003
Sub-Saharan Africa - West Eurasia	-0.027	0.973	0.008	-3.622	0.003
Sunda-Pacific - West Eurasia	0.012	1.012	0.008	1.066	0.824

Model fitted without intercept. Results are averaged over tooth. \* significant values in bold

## 9.4 Chapter 6: Most prevalent phenotypes by geographical grouping

Table 9.4: A-E provide the most prevalent phenotype codes for each geographical group

<b>9.4 A - Sahul Pacific</b>				
Tooth	Phenotype Code*	n	Frequency	
<b>Maxilla</b>				
I <sup>1</sup> , n= 34	R1-C1-A-G-R	14	41.18	
I <sup>2</sup> , n= 58	R1-C1-A-P-O	21	36.21	
C <sup>1</sup> , n=74	R1-C1-A-P-O/	25/	44.31/	
	R1-C1-A-W-O	25	44.31	
P <sup>3</sup> , n=86	R2-C2-B1L1-BGLG-BRLR	37	43.02	
P <sup>4</sup> , n=85	R1-C1-A-P-O	26	30.59	
M <sup>1</sup> , n=124	R3-C4-M2D1L1-MWDPLP-MR2DRLO	6	4.84	
M <sup>2</sup> , n=112	R2-C3-M1D1L1-MDFLG-MRDRLR	5	4.46	
M <sup>3</sup> , n=75	R3-C3-M1D1L1-MWDGLG-MRDRLR/	5/	6.67/	
	R1-C3-M1D1L1-MLFDLF-MRDRLR	5	6.67	
M <sup>4</sup> = 0	-	-	-	
<b>Mandible</b>				
I <sub>1</sub> , n=35	R1-C1-A-P-O	29	82.86	
I <sub>2</sub> , n=36	R1-C1-A-P-O	24	66.67	
C <sub>1</sub> , n=43	R1-C1-A-W-O	17	39.53	
P <sub>3</sub> , n=55	R1-C1-A-P-O	17	30.91	
P <sub>4</sub> , n=47	R1-C1-A-P-O	19	40.43	
M <sub>1</sub> , n=66	R2-C3-M2D1-MHDP-MR2DO	5	7.46	
M <sub>2</sub> , n=67	R2-C3-M2D1-MKDK-MR2DO	6	8.96	
M <sub>3</sub> , n=63	R2-C3-M2D1-MKDK-MR4DO	6	9.52	
M <sub>4</sub> = 0	-	-	-	

\*In some cases, two phenotypes appear in equal frequency. These are separate by a "/"

<b>9.4 B - Sino-Americas</b>				
Tooth	Phenotype Code	n	Frequency	
<b>Maxilla</b>				
I <sup>1</sup> , n= 104	R1-C1-A-G-R	77	74.04	
I <sup>2</sup> , n=103	R1-C1-A-E-R	63	61.17	
C <sup>1</sup> , n=163	R1-C1-A-E-R	60	36.81	

P <sup>3</sup> , n= 175	R1-C1-A-P-O	46	26.3
P <sup>4</sup> , n= 156	R1-C1-A-P-O	96	61.54
M <sup>1</sup> , n= 248	R3-C3-M1D1L1-MWDELG-MODRLR	9	3.6
M <sup>2</sup> , n= 204	R2-C3-M1D1L1-MLFDE-MRDRLR/ R3-C3-M1D1L1-MPDELG-MODRLR	10/ 10	4.90/ 4.90
M <sup>3</sup> , n=129	R1-C1-A-P-O	13	10.08
M <sup>4</sup> = 0	-	-	-
<b>Mandible</b>			
I <sub>1</sub> , n=100	R1-C1-A-P-O	42	42.0
I <sub>2</sub> , n=127	R1-C1-A-P-O	69	54.3
C <sub>1</sub> , n=153	R1-C1-A-P-O	54	35.3
P <sub>3</sub> , n=158	R1-C1-A-P-O	60	37.97
P <sub>4</sub> , n=155	R1-C1-A-P-O	53	34.19
M <sub>1</sub> , n= 172	R2-C2-M1D1-MPDP-MODO	18	10.47
M <sub>2</sub> , n= 151	R2-C2-M1D1-MPDP-MODO	16	10.60
M <sub>3</sub> , n=104	R2-C2-M1D1-MPDG-MODR	10	9.62
M <sub>4</sub> = 0	-	-	-

#### 9.4 C - Sub-Saharan Africa

Tooth	Phenotype Code	n	Frequency
<b>Maxilla</b>			
I <sub>1</sub> , n=19	R1-C1-A-E-R	13	68.4
I <sub>2</sub> , n=32	R1-C1-A-E-R	11	34.4
C <sub>1</sub> , n=77	R1-C1-A-E-R	31	40.3
P <sub>3</sub> , n= 121	R2-C2-B1L1-BGLG-BRLR	62	51.24
P <sub>4</sub> , n= 107	R2-C2-B1L1-BGLG-BRLR	23	21.5
M <sub>1</sub> , n=144	R3-C3-M1D1L1-MWDPLP-MRDRLR	6	4.2
M <sub>2</sub> , n= 132	R3-C3-M1D1L1-MPDGLG-MRDRLR	7	5.3
M <sub>3</sub> , n= 105	R3-C3-M1D1L1-MWDGLG-MRDRLR	11	10.48
M <sub>4</sub> n= 1	R1-C1-A-P-R	1	100.0
<b>Mandible</b>			
I <sub>1</sub> , n=24	R1-C1-A-P-R	10	41.67
I <sub>2</sub> , n=27	R1-C1-A-P-O	15	55.56
C <sub>1</sub> , n=34	R1-C1-A-P-O	21	61.8
P <sub>3</sub> , n=52	R1-C2-B1L1-T-i5	19	36.54
P <sub>4</sub> , n= 39	R1-C1-A-P-O	15	38.5
M <sub>1</sub> , n= 70	R2-C3-M2D1-MHDP-MR2DO	13	18.57
M <sub>2</sub> , n=67	R2-C3-M2D1-MHDK-MR4DO/ R2-C3-M2D1-MHDP-MR4DO	6/ 6	8.96/ 8.96
M <sub>3</sub> , n=58	R2-C2-M1D1-MKDK-MRDR	3	5.17
M <sub>4</sub> = 0	-	-	-

#### 9.4 D - Sunda-Pacific

Tooth	Phenotype Code	n	Frequency
<b>Maxilla</b>			
I <sup>1</sup> , n=1	R1-C1-A-E-O	1	100.0
I <sup>2</sup> , n=4	R1-C1-A-E-O	2	50.00
C <sup>1</sup> , n= 10	R1-C1-A-E-O/ R1-C1-A-W-O	3/ 3	33.30/ 33.30
P <sup>3</sup> , n= 19	R2-C2-B1L1-BGLG-BRLR	6	31.57
P <sup>4</sup> , n= 19	R1-C1-A-P-O	6	31.58
M <sup>1</sup> , n=45	R3-C4-M2D1L1-MWDELG-MR4DRLR	3	6.67
M <sup>2</sup> , n= 35	R3-C3-M1D1L1-MWDGLG-MRDRLR	4	11.43
M <sup>3</sup> , n= 17	R4-C4-M1B1D1L1-MWBEDELG-MRBRDRLR	2	11.76
M <sup>4</sup> = 0	-	-	-
<b>Mandible</b>			

I <sub>1</sub> , n=5	R1-C1-A-P-O/ R1-C2-B1L1-P-R2	2/ 2	40.0/ 40.0
I <sub>2</sub> , n=8	R1-C1-A-P-O	3	37.50
C <sub>1</sub> , n= 5	R1-C1-A-W-O	4	80.0
P <sub>3</sub> , n= 15	R1-C2-B1L1-T-i5	6	40.00
P <sub>4</sub> , n= 11	R1-C1-A-E-O	5	45.45
M <sub>1</sub> , n= 25	R2-C3-M2D1-MHDK-MR2DO	3	12.00
M <sub>2</sub> , n= 20	R2-C3-M2D1-MHDK-MR2DO/ R2-C3-M2D1-MPDK-MR4DO/ R2-C4-M2D2-MPDP-MR2DR4	2/ 2/ 2	10.0/ 10.0/ 10.0
M <sub>3</sub> , n= 16	R2-C3-M2D1-MPDK-MR4DO	3	18.75
M <sub>4</sub> = 0	-	-	-

#### 9.4 E - West Eurasia

Tooth	Phenotype Code	n	Frequency
<b>Maxilla</b>			
I <sup>1</sup> , n= 46	R1-C1-A-G-R	18	39.1
I <sup>2</sup> , n=52	R1-C1-A-P-R	23	44.2
C <sup>1</sup> , n= 81	R1-C1-A-P-O	20	24.7
P <sup>3</sup> , n= 116	R2-C2-B1L1-BGLG-BRLR	61	52.59
P <sup>4</sup> , n= 101	R1-C1-A-P-O	22	21.78
M <sup>1</sup> , n= 136	R3-C4-M2D1L1-MWDELE-MR4DRLR	10	7.35
M <sup>2</sup> , n= 114	R3-C3-M1D1L1-MWDGLG-MRDRLR	7	6.14
M <sup>3</sup> , n= 66	R3-C3-M1D1L1-MWDGLG-MRDRLR	13	19.70
M <sup>4</sup> = 0	-	-	-
<b>Mandible</b>			
I <sub>1</sub> , n=40	R1-C1-A-P-O	17	42.5
I <sub>2</sub> , n= 50	R1-C1-A-P-O	18	36.0
C <sub>1</sub> , n=60	R1-C1-A-P-O	22	36.7
P <sub>3</sub> , n= 63	R1-C1-A-P-O	22	34.92
P <sub>4</sub> , n= 61	R1-C1-A-P-O	29	47.54
M <sub>1</sub> , n= 77	R2-C3-M2D1-MHDP-MR4DO	7	9.10
M <sub>2</sub> , n= 80	R2-C3-M2D1-MHDK-MR4DO	8	10.0
M <sub>3</sub> , n= 62	R2-C3-M2D1-MKDK-MR4DO/ R2-C3-M2D1- MKDK-MR4DO	4/ 4	6.45/ 6.45
M <sub>4</sub> = 0	-	-	-

## 9.5 Chapter 7: Canonical variables with outliers

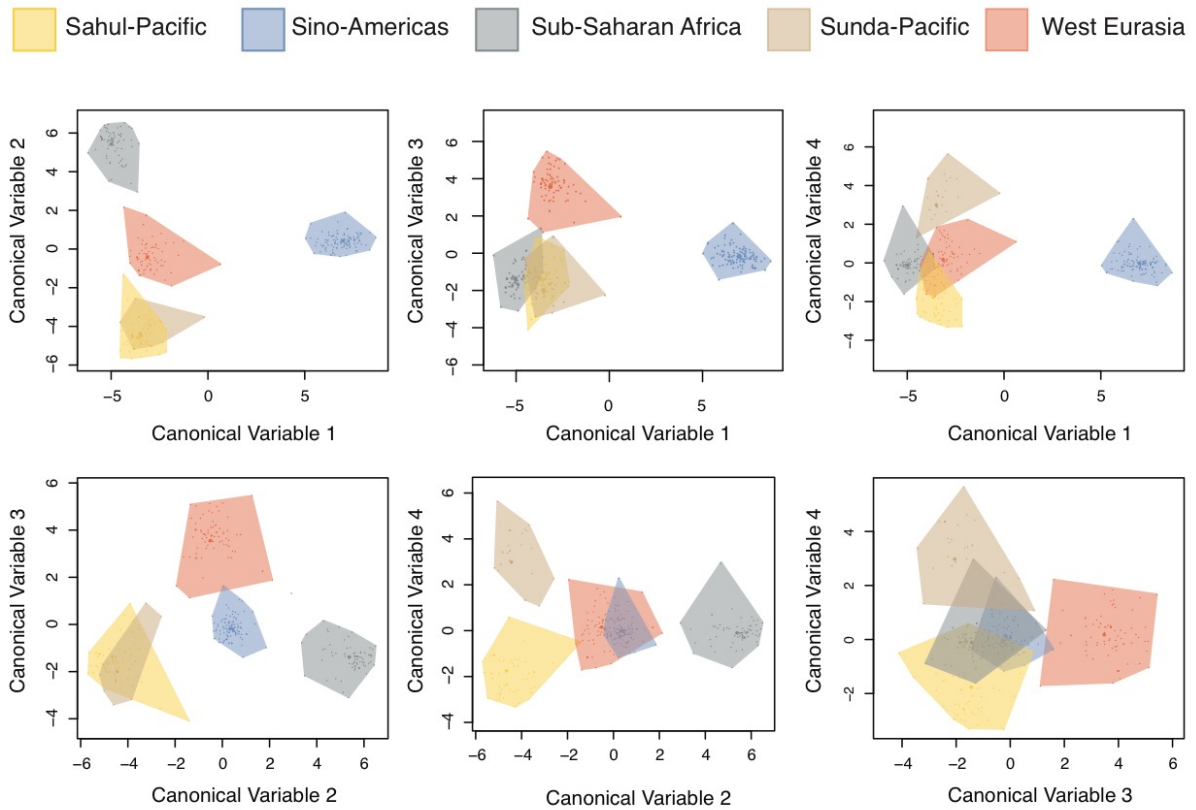


Figure 9.1: Canonical variables 1-4 for G1: Major Human Subdivisions. No outliers removed.

## Chapter 10: References

- Abbott, S.A., 1984. A comparative study of tooth root morphology in the great apes, modern man and early hominids [unpublished Ph.D Dissertation]. University of London.
- Abrahams, L.C., 1947. The masticatory apparatus of the people of Calvinia and Namaqualand in the North Western Cape of the Union of South Africa. *Journal of the Dental Association of South Africa*. 1, 5–51.
- Ackerman, J.L., Ackerman, A.L., Ackerman, A.B., 1973. Taurodont, pyramidal and fused molar roots associated with other anomalies in a kindred. *American Journal of Physical Anthropology*. 38, 681–694.
- Agresti, A., 2002. *Categorical Data Analysis*. Somerset: John Wiley & Sons, Incorporated, Somerset.
- Ahmed, H.M.A., Hashem, A.A., 2016. Accessory roots and root canals in human anterior teeth: a review and clinical considerations. *International Endodontic Journal*.
- Ahmed, H.M.A., Versiani, M.A., De-Deus, G., Dummer, P.M.H.H., 2017. A new system for classifying root and root canal morphology. *International Endodontic Journal*. 50, 761–770.
- Akoglu, H., 2018. User's guide to correlation coefficients. *Turkish Journal of Emergency Medicine*. 18, 91–93.
- Anton, S.C., 2003. Natural history of *Homo erectus*. *American Journal of Physical Anthropology*. 122, 126–170.
- Arthur, W., 2004. The effect of development on the direction of evolution: toward a twenty-first century consensus. *Evolution and Development*. 6, 282–288.
- Ash, N., 2013. Summary for Policymakers. In: Intergovernmental Panel on Climate Change (Ed.), *Climate Change 2013 - The Physical Science Basis*. Cambridge University Press, Cambridge, pp. 1–30.
- Bailey, S.E., Hublin, J.-J., Antón, S.C., 2019. Rare dental trait provides morphological evidence of archaic introgression in Asian fossil record. *Proceedings of the National Academy of Sciences*. 116, 14806–14807.
- Ballullaya, S., Vemuri, S., Kumar, P., 2013. Variable permanent mandibular first molar: Review of literature. *Journal of Conservative Dentistry*. 16, 99.
- Baragar, F.A., Osborn, J.W., 1987. Efficiency as a predictor of human jaw design in the sagittal plane. *Journal of Biomechanics*. 20, 447–457.
- Barker, B.C.W., Parsons, K.C., Mills, P.R., Williams, G.L., 1974. Anatomy of root canals. III. permanent mandibular molars. *Australian Dental Journal*. 19, 408–413.
- Barnes, D.S., 1969. Tooth morphology and other aspects of the Teso dentition. *American Journal of Physical Anthropology*. 30, 183–193.
- Bastir, M., Rosas, A., 2005. Hierarchical nature of morphological integration and modularity in the human posterior face. *American Journal of Physical Anthropology*. 128, 26–34.
- Bei, M., 2009. Molecular genetics of tooth development. *Current Opinion in Genetics & Development*. 19, 504–510.
- Benazzi, S., Nguyen, H.N., Kullmer, O., Hublin, J.J., 2015. Exploring the biomechanics of taurodontism. *Journal of Anatomy*. 226, 180–188.
- Benazzi, S., Viola, B., Kullmer, O., Fiorenza, L., Harvati, K., Paul, T., Gruppioni, G., Weber, G.W., Mallegni, F., 2011. A reassessment of the Neanderthal teeth from Taddeo cave (Southern Italy). *Journal of Human Evolution*. 61, 377–387.
- Bennett, P., 1983. Evolution and the theory of games. *European Journal of Operational*

- Research. 13, 409–410.
- Berg, G.E., Ta'ala, S.C., 2014. Biological Affinity in Forensic Identification of Human Skeletal Remains, *Biological Affinity in Forensic Identification of Human Skeletal Remains: Beyond Black and White*. CRC Press.
- Betti, L., Balloux, F., Amos, W., Hanihara, T., Manica, A., 2009. Distance from Africa, not climate, explains within-population phenotypic diversity in humans. *Proceedings of the Royal Society B: Biological Sciences*. 276, 809–814.
- Black, G.V., 1902. *Descriptive anatomy of the human teeth*. S.S. White Dental Manufacturing Company, Philadelphia.
- Blattner, T.C., George, N., Lee, C.C., Kumar, V., Yelton, C.D.J., 2010. Efficacy of Cone-Beam Computed Tomography as a Modality to Accurately Identify the Presence of Second Mesiobuccal Canals in Maxillary First and Second Molars: A Pilot Study. *Journal of Endodontics*. 36, 867–870.
- Bloom, J.D., Labthavikul, S.T., Otey, C.R., Arnold, F.H., 2006. Protein stability promotes evolvability. *Proceedings of the National Academy of Sciences of the United States of America*. 103, 5869–5874.
- Bouvier, M., 1986. Biomechanical scaling of mandibular dimensions in New World Monkeys. *International Journal of Primatology*. 7, 551–567.
- Brabant, H.E., 1964. Observations sur revolution de la denture permanente humaine en Europe Occidentale. *Bulletin du Groupement International pour la Recherche Scientifique en Stomatologie et Odontologie*. 7, 11–84.
- Brewer-Carias, C.A., le Blanc, S., Neel, J. V., 1976. Genetic structure of a tribal population, the Yanomama Indians. XIII. Dental microdifferentiation. *American Journal of Physical Anthropology*. 44, 5–14.
- Brook, A.H., 2009. Multilevel complex interactions between genetic, epigenetic and environmental factors in the aetiology of anomalies of dental development. *Archives of Oral Biology*. 54, S3–S17.
- Brook, A.H., Jernvall, J., Smith, R.N., Hughes, T.E., Townsend, G.C., 2014. The dentition: The outcomes of morphogenesis leading to variations of tooth number, size and shape. *Australian Dental Journal*. 59, 131–142.
- Brothwell, D.R., 1963. *Dental Anthropology*. Symposium Publications Division, Pergamon Press.
- Brown, M.P.S., Grundy, W.N., Lin, D., Cristianini, N., Sugnet, C.W., Furey, T.S., Ares, M., Haussler, D., 2000. Knowledge-based analysis of microarray gene expression data by using support vector machines. *Proceedings of the National Academy of Sciences of the United States of America*. 97, 262–267.
- Buck, T., Viðarsdóttir, U.S., 2012. Craniofacial evolution in polynesia: A geometric morphometric study of population diversity. *American Journal of Human Biology*. 24, 776–785.
- Burnett, S.E., Irish, J.D., Fong, M.R., 2013. Wear's the problem? Examining the effect of dental wear on studies of crown morphology. In: Scott, G.R., Irish, J.D. (Eds.), *Anthropological Perspectives on Tooth Morphology*. Cambridge University Press, Cambridge, pp. 535–554.
- Busse, W.D., Carpenter, F.H., 1976. Synthesis and properties of carbonylbis(methionyl)insulin, a proinsulin analog which is convertible to insulin by cyanogen bromide cleavage. *Biochemistry*. 15, 1649–1657.
- Butler, P.M., 1937. *Studies of the Mammalian Dentition*.–I. The Teeth of *Centetes ecaudatus*

- and its Allies. Proceedings of the Zoological Society of London. B107, 103–132.
- Butler, P.M., 1939. Studies of the Mammalian Dentition.—Differentiation of the Post-canine Dentition. Proceedings of the Zoological Society of London. B109, 1–36.
- Butler, P.M., 1956. THE ONTOGENY OF MOLAR PATTERN. Biological Reviews. 31, 30–69.
- Butler, P.M., 1963. Tooth morphology and primate evolution. In: Brothwell, D.R. (Ed.), Dental Anthropology. Pergamon Press, New York, pp. 1–13.
- Calberson, F.L., De Moor, R.J., Deroose, C.A., 2007. The Radix Entomolaris and Paramolaris: Clinical Approach in Endodontics. Journal of Endodontics. 33, 58–63.
- Calışkan, M.K., Pehlivan, Y., Sepetçioğlu, F., Türkün, M., Tuncer, S.S., 1995. Root canal morphology of human permanent teeth in a Turkish population. Journal of endodontics. 21, 200–4.
- Campbell, M.C., Tishkoff, S.A., 2010. The Evolution of Human Genetic and Phenotypic Variation in Africa. Current Biology. 20, R166–R173.
- Campbell, T.D., 1925. Dentition and palate of the Australian Aboriginal, University of Adelaide Publications under the Keith Sheridan Foundation. Hassell Press, Adelaide.
- Carlsen, O., Alexandersen, V., 1990. Radix entomolaris: identification and morphology. Scandinavian Journal of Dental Research. 98, 363–73.
- Carlsen, O., Alexandersen, V., 1991. Radix paramolaris in permanent mandibular molars: identification and morphology. European Journal of Oral Sciences. 99, 189–195.
- Carns, E.J., Skidmore, A.E., 1973. Configurations and deviations of root canals of maxillary first premolars. Oral Surgery, Oral Medicine, Oral Pathology. 36, 880–886.
- Carstairs-McCarthy, A., Ruhlen, M., 1997. The Origin of Language: Tracing the Evolution of the Mother Tongue. Language. 73, 611.
- Cavalli-Sforza, L.L., 1994. The History and Geography of Human Genes. Princeton : Princeton University Press, 1994., Princeton.
- Cavalli-Sforza, L.L., Menozzi, P., Piazza, A., 2018. The History and Geography of Human Genes, The History and Geography of Human Genes. Princeton University Press.
- Chen, F., Welker, F., Shen, C.-C., Bailey, S.E., Bergmann, I., Davis, S., Xia, H., Wang, H., Fischer, R., Freidline, S.E., Yu, T.-L., Skinner, M.M., Stelzer, S., Dong, Guangrong, Fu, Q., Dong, Guanghui, Wang, J., Zhang, D., Hublin, J.-J., 2019. A late Middle Pleistocene Denisovan mandible from the Tibetan Plateau. Nature. 569, 409–412.
- Chen, J., Sokal, R.R., Ruhlen, M., 2012. Worldwide analysis of genetic and linguistic relationships of human populations. Human Biology. 84, 553–570.
- Christie, W.H., Peikoff, M.D., Fogel, H.M., 1991. Maxillary molars with two palatal roots: A retrospective clinical study. Journal of Endodontics. 17, 80–84.
- Clarkson, C., Jacobs, Z., Marwick, B., Fullagar, R., Wallis, L., Smith, M., Roberts, R.G., Hayes, E., Lowe, K., Carah, X., Florin, S.A., McNeil, J., Cox, D., Arnold, L.J., Hua, Q., Huntley, J., Brand, H.E.A., Manne, T., Fairbairn, A., Shulmeister, J., Lyle, L., Salinas, M., Page, M., Connell, K., Park, G., Norman, K., Murphy, T., Pardoe, C., 2017. Human occupation of northern Australia by 65,000 years ago. Nature. 547, 306–310.
- Cleghorn, B.M., Christie, W.H., Dong, C.C.S., 2006. Root and Root Canal Morphology of the Human Permanent Maxillary First Molar: A Literature Review. Journal of Endodontics. 32, 813–821.
- Copes, L.E., 2012. Comparative and Experimental Investigations of Cranial Robusticity in Mid-Pleistocene Hominins [unpublished Ph.D Dissertation]. Arizona State University.
- Cordaux, R., Auger, R., Bentley, G., Nasidze, I., Sirajuddin, S.M., Stoneking, M., 2004. Independent Origins of Indian Caste and Tribal Paternal Lineages. Current Biology. 14,

231–235.

- Corruccini, R.S., 1976. The interaction between nonmetric and metric cranial variation. *American Journal of Physical Anthropology*. 44, 285–293.
- Corruccini, R.S., McHenry, H.M., 1980. Cladometric analysis of Pliocene hominids. *Journal of Human Evolution*. 9, 209–221.
- Corruccini, R.S., Sharma, K., Potter, R.H.Y., 1986. Comparative genetic variance and heritability of dental occlusal variables in U.S. and Northwest Indian twins. *American Journal of Physical Anthropology*. 70, 293–299.
- Daegling, D.J., Grine, F.E., 1991. Compact bone distribution and biomechanics of early hominid mandibles. *American journal of physical anthropology*. 86, 321–39.
- Dahlberg, A.A., 1945. The paramolar tubercle. *American Journal of Physical Anthropology*. 3, 97–103.
- Dahlberg, A.A., 1945. The Changing Dentition of Man. *The Journal of the American Dental Association*. 32, 676–690.
- Dahlberg, A.A., 1950. The evolutionary significance of the protostylid. *American Journal of Physical Anthropology*. 8, 15–26.
- Daito, M., Tanaka, T., Hieda, T., 1992. Clinical observations on the development of third molars. *Journal of Osaka Dental University*. 26, 91–104.
- Davies, T.W., Delezene, L.K., Gunz, P., Hublin, J.-J., Skinner, M.M., 2019a. Endostructural morphology in hominoid mandibular third premolars: Geometric morphometric analysis of dentine crown shape. *Journal of Human Evolution*. 133, 198–213.
- Davies, T.W., Delezene, L.K., Gunz, P., Hublin, J.-J., Skinner, M.M., 2019b. Endostructural morphology in hominoid mandibular third premolars: Discrete traits at the enamel-dentine junction. *Journal of Human Evolution*. 136, 102670.
- De Pablo, Ó.V., Estevez, R., Péix Sánchez, M., Heilborn, C., Cohenca, N., 2010. Root anatomy and canal configuration of the permanent mandibular first molar: A systematic review. *Journal of Endodontics*.
- Demes, B., Creel, N., 1988. Bite force, diet, and cranial morphology of fossil hominids. *Journal of Human Evolution*. 17, 657–670.
- Dempsey, P.J., Townsend, G.C., 2001. Genetic and environmental contributions to variation in human tooth size. *Heredity*. 86, 685–693.
- Dempster, W.T., Adams, W.J., Duddles, R.A., 1963. Arrangement in the Jaws of the Roots of the Teeth. *The Journal of the American Dental Association*. 67, 779–797.
- Diggle, P., Heagerty, P., Liang, K.-Y., Zeger, S., 2002. *Analysis of Longitudinal Data*. Oxford: Oxford University Press, Incorporated, Oxford.
- Domark, J.D., Hatton, J.F., Benison, R.P., Hildebolt, C.F., 2013. An ex vivo comparison of digital radiography and cone-beam and micro computed tomography in the detection of the number of canals in the mesiobuccal roots of maxillary molars. *Journal of Endodontics*. 39, 901–905.
- Drennan, M.R., 1929. The dentition of a Bushman tribe. *Annals of the South African Museum*. 61–88.
- Du Brul, E.L., 1977. Early hominid feeding mechanisms. *American Journal of Physical Anthropology*. 47, 305–320.
- Earl, D.J., Deem, M.W., 2004. Evolvability is a selectable trait. *Proceedings of the National Academy of Sciences of the United States of America*. 101, 11531–11536.
- Emonet, E.-G., Kullmer, O., 2014. Variability in Premolar and Molar Root Number in a Modern Population of P an troglodytes versus. *The Anatomical Record*. 297, 1927–1934.

- Emonet, E.-G., Tafforeau, P., Chaimanee, Y., Guy, F., de Bonis, L., Koufos, G., Jaeger, J.-J., 2012. Three-dimensional analysis of mandibular dental root morphology in hominoids. *Journal of Human Evolution*. 62, 146–154.
- Evans, A.R., Daly, E.S., Catlett, K.K., Paul, K.S., King, S.J., Skinner, M.M., Nesse, H.P., Hublin, J.-J., Townsend, G.C., Schwartz, G.T., Jernvall, J., 2016. A simple rule governs the evolution and development of hominin tooth size. *Nature*. 530, 477–80.
- Fahid, A., Taintor, J.F., 1988. Maxillary second molar with three buccal roots. *Journal of Endodontics*. 14, 181–183.
- Fan, B., Cheung, G.S.P., Fan, M., Gutmann, J.L., Bian, Z., 2004a. C-shaped canal system in mandibular second molars: Part I - Anatomical features. *Journal of Endodontics*. 30, 899–903.
- Fan, B., Cheung, G.S.P., Fan, M., Gutmann, J.L., Fan, W., 2004b. C-shaped canal system in mandibular second molars: Part II - Radiographic features. *Journal of Endodontics*. 30, 904–908.
- Fathi, Z., Rahimi, S., Tavakoli, R., Amini, M., 2014. A Three-rooted Mandibular Second Premolar: A Case Report. *Journal of Dental Research, Dental Clinics, Dental Prospects*. 8, 184–186.
- Fernandes, M., de Ataide, I., Wagle, R., 2014. C-shaped root canal configuration: A review of literature. *Journal of Conservative Dentistry*. 17, 312.
- Fischischweiger, W., Clausnitzer, E., 1988. Root formation in molar teeth of the CD-1 mouse. *Journal of Endodontics*. 14, 163–168.
- FitzGerald, C.M., 1998. Do enamel microstructures have regular time dependency? Conclusions from the literature and a large-scale study. *Journal of Human Evolution*. 35, 371–386.
- Fleagle, J., 2013. *Primate Adaptation and Evolution*, 3rd ed. Academic Press, Cambridge.
- Forster, P., Matsumura, S., 2005. Did Early Humans Go North or South? *Science*. 308, 965–966.
- Fu, Q., Posth, C., Hajdinjak, M., Petr, M., Mallick, S., Fernandes, D., Furtwängler, A., Haak, W., Meyer, M., Mittnik, A., Nickel, B., Peltzer, A., Rohland, N., Slon, V., Talamo, S., Lazaridis, I., Lipson, M., Mathieson, I., Schiffels, S., Skoglund, P., Derevianko, A.P., Drozdov, N., Slavinsky, V., Tsybankov, A., Cremonesi, R.G., Mallegni, F., Gély, B., Vacca, E., Morales, M.R.G., Straus, L.G., Neugebauer-Maresch, C., Teschler-Nicola, M., Constantin, S., Moldovan, O.T., Benazzi, S., Peresani, M., Coppola, D., Lari, M., Ricci, S., Ronchitelli, A., Valentin, F., Thevenet, C., Wehrberger, K., Grigorescu, D., Rougier, H., Crevecoeur, I., Flas, D., Semal, P., Mannino, M.A., Cupillard, C., Bocherens, H., Conard, N.J., Harvati, K., Moiseyev, V., Drucker, D.G., Svoboda, J., Richards, M.P., Caramelli, D., Pinhasi, R., Kelso, J., Patterson, N., Krause, J., Pääbo, S., Reich, D., 2016. The genetic history of Ice Age Europe. *Nature*. 534, 200–205.
- Garn, S.M., 1971. *Human Races*, 3rd ed. Charles C. Thomas, Springfield.
- Garn, S.M., Lewis, A.B., Kerewsky, R.S., 1963. Third Molar Agenesis and Size Reduction of the Remaining Teeth. *Nature*. 200, 488–489.
- Garn, S.M., Lewis, A.B., Kerewsky, R.S., 1965. Size Interrelationships of the Mesial and Distal Teeth. *Journal of Dental Research*. 44, 350–354.
- Garn, S.M., Lewis, A.B., Kerewsky, R.S., 1968. Relationship Between Buccolingual and Mesiodistal Tooth Diameters. *Journal of Dental Research*. 47, 495–495.
- Garson, G.D., 2015. *Missing values analysis and data imputation*. Statistical Associates Publishers, Raleigh, North Carolina.

- Gehring, W.J., 1993. Exploring the homeobox. *Gene*. 135, 215–221.
- Giambersio, E., Barile, V., Giambersio, A.M., 2019. Klinefelter's syndrome and taurodontism. *Archivio Italiano di Urologia e Andrologia*. 91, 130–132.
- Gómez-Robles, A., Martínón-Torres, M., Bermúdez de Castro, J.M., Margvelashvili, A., Bastir, M., Arsuaga, J.L., Pérez-Pérez, A., Estebaranz, F., Martínez, L.M., 2007. A geometric morphometric analysis of hominin upper first molar shape. *Journal of Human Evolution*. 53, 272–285.
- Gómez-Robles, A., Polly, P.D., 2012. MORPHOLOGICAL INTEGRATION IN THE HOMININ DENTITION: EVOLUTIONARY, DEVELOPMENTAL, AND FUNCTIONAL FACTORS. *Evolution*. 66, 1024–1043.
- Gordon, K.R., 1984. Microfracture patterns of abrasive wear striations on teeth indicate directionality. *American Journal of Physical Anthropology*. 63, 315–322.
- Gregory, W.K., 1921. The Origin and Evolution of the Human Dentition. *Journal of Dental Research*. 3, 87–228.
- Gu, Y., Tang, Y., Zhu, Q., Feng, X., 2016. Measurement of root surface area of permanent teeth with root variations in a Chinese population—A micro-CT analysis. *Archives of Oral Biology*. 63, 75–81.
- Halekoh, U., Højsgaard, S., Yan, J., 2006. The R Package geepack for Generalized Estimating Equations. *Journal of Statistical Software*. 15, 1–11.
- Hamon, N., Emonet, E.-G., Chaimanee, Y., Guy, F., Tafforeau, P., Jaeger, J.-J., 2012. Analysis of Dental Root Apical Morphology: A New Method for Dietary Reconstructions in Primates. *The Anatomical Record: Advances in Integrative Anatomy and Evolutionary Biology*. 295, 1017–1026.
- Handley, L.J.L., Manica, A., Goudet, J., Balloux, F., 2007. Going the distance: human population genetics in a clinal world. *Trends in Genetics*. 23, 432–439.
- Hanihara, T., 2008. Morphological variation of major human populations based on nonmetric dental traits. *American Journal of Physical Anthropology*. 136, 169–182.
- Hanihara, T., 2009. Metric and nonmetric dental variation and the population structure of the Ainu. *American Journal of Human Biology*. 22, 163–71.
- Hanihara, T., 2013. Geographic structure of dental variation in the major human populations of the world. In: Scott, G.R., Irish, J.D. (Eds.), *Anthropological Perspectives on Tooth Morphology*. Cambridge University Press, Cambridge, pp. 479–509.
- Hanihara, T., Ishida, H., 2005. Metric dental variation of major human populations. *American Journal of Physical Anthropology*. 128, 287–298.
- Hanihara, T., Ishida, H., 2009. Regional differences in craniofacial diversity and the population history of Jomon Japan. *American Journal of Physical Anthropology*. 139, 311–322.
- Haque, S., Alam, M.K., 2015. Common dental anomalies in cleft lip and palate patients. *Malaysian Journal of Medical Sciences*. 22, 55–60.
- Harris, E.F., Lease, L.R., 2005. Mesiodistal tooth crown dimensions of the primary dentition: A worldwide survey. *American Journal of Physical Anthropology*. 128, 593–607.
- Hastie, T., Tibshirani, R., Buja, A., 1994. Flexible discriminant analysis by optimal scoring. *Journal of the American Statistical Association*. 89, 1255–1270.
- Hemphill, B.E., 2002. The Anthropology of Modern Human Teeth: Dental Morphology and Its Variation in Recent Human Populations. G. Richard Scott, Christy G. Turner II. *Journal of Anthropological Research*. 58, 412–414.
- Henn, B.M., Cavalli-Sforza, L.L., Feldman, M.W., 2012. The great human expansion.

- Proceedings of the National Academy of Sciences. 109, 17758–17764.
- Henn, B.M., Gignoux, C.R., Jobin, M., Granka, J.M., Macpherson, J.M., Kidd, J.M., Rodriguez-Botigue, L., Ramachandran, S., Hon, L., Brisbin, A., Lin, A.A., Underhill, P.A., Comas, D., Kidd, K.K., Norman, P.J., Parham, P., Bustamante, C.D., Mountain, J.L., Feldman, M.W., 2011. Hunter-gatherer genomic diversity suggests a southern African origin for modern humans. *Proceedings of the National Academy of Sciences*. 108, 5154–5162.
- Hershkovitz, I., Weber, G.W., Quam, R., Duval, M., Grün, R., Kinsley, L., Ayalon, A., Bar-Matthews, M., Valladas, H., Mercier, N., Arsuaga, J.L., Martín-Torres, M., De Castro, J.M.B., Fornai, C., Martín-Francés, L., Sarig, R., May, H., Krenn, V.A., Slon, V., Rodríguez, L., García, R., Lorenzo, C., Carretero, J.M., Frumkin, A., Shahack-Gross, R., Mayer, D.E.B.Y., Cui, Y., Wu, X., Peled, N., Groman-Yaroslavski, I., Weissbrod, L., Yeshurun, R., Tsatskin, A., Zaidner, Y., Weinstein-Evron, M., 2018. The earliest modern humans outside Africa. *Science*. 359, 456–459.
- Hillson, S., 1996. *Dental Anthropology*. Cambridge University Press, Cambridge.
- Hjellman, G., 1929. Morphologische Beobachtungen an den Zähnen der Finnen. *Acta Societas Medicorum Fennicae "Duodecim."* 1–132.
- Hlusko, L.J., Schmitt, C.A., Monson, T.A., Brasil, M.F., Mahaney, M.C., 2016. The integration of quantitative genetics, paleontology, and neontology reveals genetic underpinnings of primate dental evolution. *Proceedings of the National Academy of Sciences of the United States of America*. 113, 9262–9267.
- Hoffmann, J.P., 2004. *Generalized linear models: an applied approach*, Generalized linear models : an applied approach. Pearson Allyn and Bacon, Boston.
- Holly Smith, B., 1986. Development and evolution of the helicoidal plane of dental occlusion. *American Journal of Physical Anthropology*. 69, 21–35.
- Homburger, J.R., Moreno-Estrada, A., Gignoux, C.R., Nelson, D., Sanchez, E., Ortiz-Tello, P., Pons-Estel, B.A., Acevedo-Vasquez, E., Miranda, P., Langefeld, C.D., Gravel, S., Alarcón-Riquelme, M.E., Bustamante, C.D., 2015. Genomic Insights into the Ancestry and Demographic History of South America. *PLOS Genetics*. 11, e1005602.
- Hrdlička, A., 1920. Shovel-shaped teeth. *American Journal of Physical Anthropology*. 3, 429–465.
- Hsu, Y.Y., Kim, S., 1997. The resected root surface. The issue of canal isthmuses. *Dental clinics of North America*. 41, 529–540.
- <https://www.horosproject.org>, 2016. Horos Dicom Viewer.
- <https://www.R-project.org>, 2017. R: A Language and Environment for Statistical Computing.
- Huang, X.F., Chai, Y., 2013. Molecular regulatory mechanism of tooth root development. *International Journal of Oral Science*.
- Hubbard, A.R., Guatelli-Steinberg, D., Irish, J.D., 2015. Do nuclear DNA and dental nonmetric data produce similar reconstructions of regional population history? An example from modern coastal Kenya. *American Journal of Physical Anthropology*. 157, 295–304.
- Hylander, W.L., 1975. Incisor Size and Diet in Anthropoids with Special Reference to Cercopithecidae. *Science*. 189, 1095–1098.
- Irish, D.J.D., 2005. Population continuity vs. discontinuity revisited: Dental affinities among late Paleolithic through Christian-era Nubians. *American Journal of Physical Anthropology*. 128, 520–535.
- Irish, J.D., 1998. Ancestral dental traits in recent Sub-Saharan Africans and the origins of modern humans. *Journal of Human Evolution*. 34, 81–98.
- Irish, J.D., Bailey, S.E., Guatelli-Steinberg, D., Deleuzene, L.K., Berger, L.R., 2018. Ancient

- teeth, phenetic affinities, and African hominins: Another look at where *Homo naledi* fits in. *Journal of Human Evolution*. 122, 108–123.
- Irish, J.D., Guatelli-Steinberg, D., 2003. Ancient teeth and modern human origins: An expanded comparison of African Plio-Pleistocene and recent world dental samples. *Journal of Human Evolution*. 45, 113–144.
- Irish, J.D., Guatelli-Steinberg, D., Legge, S.S., de Ruiter, D.J., Berger, L.R., 2013. Dental Morphology and the Phylogenetic “Place” of *Australopithecus sediba*. *Science*. 340, 1233062.
- Irish, J.D., Konigsberg, L., 2007. The ancient inhabitants of Jebel Moya Redux: Measures of Population Affinity based on dental morphology. *International Journal of Osteoarchaeology*. 17, 138–156.
- Jernvall, J., Thesleff, I., 2000. Reiterative signaling and patterning during mammalian tooth morphogenesis. *Mechanisms of Development*. 92, 19–29.
- Jheon, A.H., Seidel, K., Biehs, B., Klein, O.D., 2013. From molecules to mastication: the development and evolution of teeth. *Wiley Interdisciplinary Reviews: Developmental Biology*. 2, 165–182.
- Jing, J., Feng, J., Li, J., Han, X., He, J., Ho, T.-V., Du, J., Zhou, X., Urata, M., Chai, Y., 2019. Antagonistic interaction between *Ezh2* and *Arid1a* coordinates root patterning and development via *Cdkn2a* in mouse molars. *eLife*. 8.
- Josse, J., Husson, F., 2016. missMDA: A package for handling missing values in multivariate data analysis. *Journal of Statistical Software*. 70.
- Kakkar, P., Singh, A., 2012. Mandibular first premolar with three roots: a case report. *Iranian Endodontic Journal*. 7, 207–10.
- Kavanagh, K.D., Evans, A.R., Jernvall, J., 2007. Predicting evolutionary patterns of mammalian teeth from development. *Nature*. 449, 427–432.
- Kay, R.F., 1975. The functional adaptations of primate molar teeth. *American Journal of Physical Anthropology*. 43, 195–215.
- Kayser, M., 2010. The Human Genetic History of Oceania: Near and Remote Views of Dispersal. *Current Biology*. 20, R194–R201.
- Keith, A., 1913. Problems Relating to the Teeth of the Earlier Forms of Prehistoric Man. *Proceedings of the Royal Society of Medicine*. 6, 103–124.
- Kelso, J., Prüfer, K., 2014. Ancient humans and the origin of modern humans. *Current Opinion in Genetics & Development*. 29, 133–138.
- Kirilova, J., Topalova-Pirinska, S., Kirov, D., 2014. VARIATION OF MAXILLARY FIRST PREMOLAR WITH THREE ROOT CANALS. *Journal of IMAB - Annual Proceeding (Scientific Papers)*. 20, 584–588.
- Kirkham, J., Kaur, R., Stillman, E.C., Blackwell, P.G., Elcock, C., Brook, A.H., 2005. The patterning of hypodontia in a group of young adults in Sheffield, UK. *Archives of Oral Biology*. 50, 287–291.
- Kirschner, M., Gerhart, J., 1998. Evolvability. *Proceedings of the National Academy of Sciences*. 95, 8420–8427.
- Kovacs, I., 1971. A systematic description of dental roots. In: Dahlberg, A.A. (Ed.), *Dental Morphology and Evolution*. The University of Chicago Press, Chicago, pp. 211–256.
- Kullmer, O., Sandrock, O., Kupczik, K., Frost, S.R., Volpato, V., Bromage, T.G., Schrenk, F., 2011. New primate remains from Mwenirondo, Chiwondo Beds in northern Malawi. *Journal of Human Evolution*. 61, 617–623.
- Kupczik, K., Dean, M.C., 2008. Comparative observations on the tooth root morphology of

- Gigantopithecus blacki. *Journal of Human Evolution*. 54, 196–204.
- Kupczik, K., Delezene, L.K., Skinner, M.M., 2019. Mandibular molar root and pulp cavity morphology in *Homo naledi* and other Plio-Pleistocene hominins. *Journal of Human Evolution*. 130, 83–95.
- Kupczik, K., Hublin, J.-J., 2010. Mandibular molar root morphology in Neanderthals and Late Pleistocene and recent *Homo sapiens*. *Journal of Human Evolution*. 59, 525–541.
- Kupczik, K., Olejniczak, A.J., Skinner, M.M., Hublin, J.-J., 2009. Molar Crown and Root Size Relationship in Anthropoid Primates. In: *Comparative Dental Morphology*. KARGER, Basel, pp. 16–22.
- Kupczik, K., Spoor, F., Pommert, A., Dean, M., 2005. Premolar root number variation in hominoids: genetic polymorphism vs. functional significance. In: *Current Trends in Dental Morphology Research*. pp. 257–268.
- Kupczik, K., Toro-Ibacache, V., Macho, G.A., 2018. On the relationship between maxillary molar root shape and jaw kinematics in *Australopithecus africanus* and *Paranthropus robustus*. *Royal Society Open Science*. 5, 180825.
- Lahr, M.M., Foley, R., 2005. Multiple dispersals and modern human origins. *Evolutionary Anthropology: Issues, News, and Reviews*. 3, 48–60.
- Larsen, H.E., Rainey, F.G., 1948. Ipiutak and the Arctic whale hunting culture. *Anthropological papers of the AMNH* ; v. 42.
- Le Cabec, A., Gunz, P., Kupczik, K., Braga, J., Hublin, J.-J., 2013. Anterior tooth root morphology and size in Neanderthals: Taxonomic and functional implications. *Journal of Human Evolution*. 64, 169–193.
- Le Cabec, A., Kupczik, K., Gunz, P., Braga, J., Hublin, J.-J., 2012. Long anterior mandibular tooth roots in Neanderthals are not the result of their large jaws. *Journal of Human Evolution*. 63, 667–681.
- Ledogar, J.A., Dechow, P.C., Wang, Q., Gharpure, P.H., Gordon, A.D., Baab, K.L., Smith, A.L., Weber, G.W., Grosse, I.R., Ross, C.F., Richmond, B.G., Wright, B.W., Byron, C., Wroe, S., Strait, D.S., 2016. Human feeding biomechanics: performance, variation, and functional constraints. *PeerJ*. 4, e2242.
- Li, H., Durbin, R., 2011. Inference of human population history from individual whole-genome sequences. *Nature*. 475, 493–496.
- Li, J., Parada, C., Chai, Y., 2017. Cellular and molecular mechanisms of tooth root development. *Development*. 144, 374–384.
- Li, J.Z., Absher, D.M., Tang, H., Southwick, A.M., Casto, A.M., Ramachandran, S., Cann, H.M., Barsh, G.S., Feldman, M., Cavalli-Sforza, L.L., Myers, R.M., 2008. Worldwide Human Relationships Inferred from Genome-Wide Patterns of Variation. *Science*. 319, 1100–1104.
- Liao, W., Xing, S., Li, D., Martínón-Torres, M., Wu, X., Soligo, C., Bermúdez de Castro, J.M., Wang, W., Liu, W., 2019. Mosaic dental morphology in a terminal Pleistocene hominin from Dushan Cave in southern China. *Scientific Reports*. 9, 2347.
- Lieberman, P., 2006. *Toward an evolutionary biology of language*. Belknap Press of Harvard University Press.
- Lipson, M., Ribot, I., Mallick, S., Rohland, N., Olalde, I., Adamski, N., Broomandkhoshbacht, N., Lawson, A.M., López, S., Oppenheimer, J., Stewardson, K., Asombang, R.N., Bocherens, H., Bradman, N., Culleton, B.J., Cornelissen, E., Crevecoeur, I., de Maret, P., Fomine, F.L.M., Lavachery, P., Mindzie, C.M., Orban, R., Sawchuk, E., Semal, P., Thomas, M.G., Van Neer, W., Veeramah, K.R., Kennett, D.J., Patterson, N., Hellenthal,

- G., Lalueza-Fox, C., MacEachern, S., Prendergast, M.E., Reich, D., 2020. Ancient West African foragers in the context of African population history. *Nature*. 577, 665–670.
- Liu, H., Prugnolle, F., Manica, A., Balloux, F., 2006. A Geographically Explicit Genetic Model of Worldwide Human-Settlement History. *American Journal of Human Genetics*. 79, 230–237.
- Liu, W., Martínón-Torres, M., Cai, Y.J., Xing, S., Tong, H.W., Pei, S.W., Sier, M.J., Wu, X.H., Edwards, R.L., Cheng, H., Li, Y.Y., Yang, X.X., De Castro, J.M.B., Wu, X.J., 2015. The earliest unequivocally modern humans in southern China. *Nature*. 526, 696–699.
- Luca, F., Perry, G.H., Di Rienzo, A., 2010. Evolutionary adaptations to dietary changes. *Annual Review of Nutrition*.
- Luder, H.U., 2015. Malformations of the tooth root in humans. *Frontiers in Physiology*. 6, 307.
- Luo, Z.-X., Wible, J.R., 2005. A Late Jurassic Digging Mammal and Early Mammalian Diversification. *Science*. 308, 103–107.
- Luo, Z.X., Meng, Q.J., Ji, Q., Liu, D., Zhang, Y.G., Neander, A.I., 2015. Evolutionary development in basal mammaliaforms as revealed by a docodontan. *Science*. 347, 760–764.
- Macho, G.A., 2015. *Trends in Biological Anthropology*, 1st ed. Oxbow, Oxford.
- Macho, G.A., Spears, I.R., 1999. Effects of loading on the biochemical behavior of molars of Homo, Pan, and Pongo. *American Journal of Physical Anthropology*. 109, 211–227.
- Malaspina, A.-S., Westaway, M.C., Muller, C., Sousa, V.C., Lao, O., Alves, I., Bergström, A., Athanasiadis, G., Cheng, J.Y., Crawford, J.E., Heupink, T.H., Macholdt, E., Peischl, S., Rasmussen, S., Schiffels, S., Subramanian, S., Wright, J.L., Albrechtsen, A., Barbieri, C., Dupanloup, I., Eriksson, A., Margaryan, A., Moltke, I., Pugach, I., Korneliusson, T.S., Levkivskiy, I.P., Moreno-Mayar, J.V., Ni, S., Racimo, F., Sikora, M., Xue, Y., Aghakhanian, F.A., Brucato, N., Brunak, S., Campos, P.F., Clark, W., Ellingvåg, S., Fourmile, G., Gerbault, P., Injie, D., Koki, G., Leavesley, M., Logan, B., Lynch, A., Matisoo-Smith, E.A., McAllister, P.J., Mentzer, A.J., Metspalu, M., Migliano, A.B., Murgha, L., Phipps, M.E., Pomat, W., Reynolds, D., Ricaut, F.-X., Siba, P., Thomas, M.G., Wales, T., Wall, C.M., Oppenheimer, S.J., Tyler-Smith, C., Durbin, R., Dortch, J., Manica, A., Schierup, M.H., Foley, R.A., Lahr, M.M., Bown, C., Wall, J.D., Mailund, T., Stoneking, M., Nielsen, R., Sandhu, M.S., Excoffier, L., Lambert, D.M., Willerslev, E., 2016. A genomic history of Aboriginal Australia. *Nature*. 538, 207–214.
- Mallineni, S.K., 2014. Supernumerary Teeth: Review of the Literature with Recent Updates. *Conference Papers in Science*. 2014, 1–6.
- Manica, A., Amos, W., Balloux, F., Hanihara, T., 2007. The effect of ancient population bottlenecks on human phenotypic variation. *Nature*. 448, 346–348.
- Manning, S.A., 1990. Root canal anatomy of mandibular second molars. *International Endodontic Journal*. 23, 40–45.
- Marean, C.W., 2015. An Evolutionary Anthropological Perspective on Modern Human Origins. *Annual Review of Anthropology*. 44, 533–556.
- Maret, D., Peters, O.A., Galibourg, A., Dumoncel, J., Esclassan, R., Kahn, J.L., Sixou, M., Telmon, N., 2014. Comparison of the accuracy of 3-dimensional cone-beam computed tomography and micro-computed tomography reconstructions by using different voxel sizes. *Journal of endodontics*. 40, 1321–1326.
- Markowski, J., 1995. Non-metric traits: remarks on sex dependence, age dependence, and on intercorrelations among characters. *Acta Theriologica*. 40, 65–74.

- Martin, G., 2014. Fisher's geometrical model emerges as a property of complex integrated phenotypic networks. *Genetics*. 197, 237–255.
- Martinón-Torres, M., Bermúdez De Castro, J.M., Gómez-Robles, A., Arsuaga, J.L., Carbonell, E., Lordkipanidze, D., Manzi, G., Margvelashvili, A., 2007. Dental evidence on the hominin dispersals during the Pleistocene. *Proceedings of the National Academy of Sciences of the United States of America*. 104, 13279–13282.
- Martinón-Torres, M., Bermúdez de Castro, J.M., Gómez-Robles, A., Margvelashvili, A., Prado, L., Lordkipanidze, D., Vekua, A., 2008. Dental remains from Dmanisi (Republic of Georgia): Morphological analysis and comparative study. *Journal of Human Evolution*. 55, 249–273.
- Martins, J.N.R., Versiani, M.A., 2019. CBCT and Micro-CT on the Study of Root Canal Anatomy. In: *The Root Canal Anatomy in Permanent Dentition*. Springer International Publishing, Cham, pp. 89–180.
- Matsumura, H., Hung, H., Higham, C., Zhang, C., Yamagata, M., Nguyen, L.C., Li, Z., Fan, X., Simanjuntak, T., Oktaviana, A.A., He, J., Chen, C., Pan, C., He, G., Sun, G., Huang, W., Li, X., Wei, X., Domett, K., Halcrow, S., Nguyen, K.D., Trinh, H.H., Bui, C.H., Nguyen, K.T.K., Reinecke, A., 2019. Craniometrics Reveal “Two Layers” of Prehistoric Human Dispersal in Eastern Eurasia. *Scientific Reports*. 9, 1451.
- McCollum, M., Sharpe, P.T., 2001. Evolution and development of teeth. *Journal of Anatomy*. 199, 153–159.
- McGhee, G.R., 2015. Limits in the evolution of biological form: a theoretical morphologic perspective. *Interface Focus*. 5, 20150034.
- McKeown, H.F., 2002. Tooth dimensions in hypodontia patients, their unaffected relatives and a control group measured by a new image analysis system. *The European Journal of Orthodontics*. 24, 131–141.
- Meyer, M., Arsuaga, J.-L., de Filippo, C., Nagel, S., Aximu-Petri, A., Nickel, B., Martínez, I., Gracia, A., de Castro, J.M.B., Carbonell, E., Viola, B., Kelso, J., Prüfer, K., Pääbo, S., 2016. Nuclear DNA sequences from the Middle Pleistocene Sima de los Huesos hominins. *Nature*. 531, 504–507.
- Meyer, M., Kircher, M., Gansauge, M.T., Li, H., Racimo, F., Mallick, S., Schraiber, J.G., Jay, F., Prüfer, K., De Filippo, C., Sudmant, P.H., Alkan, C., Fu, Q., Do, R., Rohland, N., Tandon, A., Siebauer, M., Green, R.E., Bryc, K., Briggs, A.W., Stenzel, U., Dabney, J., Shendure, J., Kitzman, J., Hammer, M.F., Shunkov, M. V., Derevianko, A.P., Patterson, N., Andrés, A.M., Eichler, E.E., Slatkin, M., Reich, D., Kelso, J., Pääbo, S., 2012. A high-coverage genome sequence from an archaic Denisovan individual. *Science*. 338, 222–226.
- Michetti, J., Maret, D., Mallet, J.P., Diemer, F., 2010. Validation of cone beam computed tomography as a tool to explore root canal anatomy. *Journal of Endodontics*. 36, 1187–1190.
- Miller, N., 2013. *Ten Cate's Oral Histology*, 8th ed. Mosby, St. Louis, Mo.
- Mirazón-Lahr, M., 2011. A Brief History of the Duckworth Collections [WWW Document]. URL <https://www.human-evol.cam.ac.uk/history.html> (accessed 12.20.21).
- Mitsiadis, T.A., Smith, M.M., 2006. How do genes make teeth to order through development? *Journal of Experimental Zoology Part B: Molecular and Developmental Evolution*. 306B, 177–182.
- Mitteroecker, P., Huttegger, S.M., 2009. The Concept of Morphospaces in Evolutionary and Developmental Biology: Mathematics and Metaphors. *Biological Theory*. 4, 54–67.
- Miyabara, T., 1994. An anthropological study of the masticatory system in the Japanese the

- teeth. *Dental Cosmos*. 58, 739–749.
- Moggi-Cecchi, J., Boccone, S., 2007. Maxillary molars cusp morphology of South African australopithecines. In: *Vertebrate Paleobiology and Paleoanthropology*. Springer Netherlands, pp. 53–64.
- Moore, N.C., Hublin, J.-J., Skinner, M.M., 2015. Premolar root and canal variation in extant non-human hominoids. *American Journal of Physical Anthropology*. 158, 209–226.
- Moore, N.C., Skinner, M.M., Hublin, J.-J., 2013. Premolar root morphology and metric variation in *Pan troglodytes* versus. *American Journal of Physical Anthropology*. 150, 632–646.
- Moore, N.C., Thackeray, J.F., Hublin, J.-J., Skinner, M.M., 2016. Premolar root and canal variation in South African Plio-Pleistocene specimens attributed to *Australopithecus africanus* and *Paranthropus robustus*. *Journal of Human Evolution*. 93, 46–62.
- Moorrees, C.F.A., 1957. *The Aleut dentition*. Harvard University Press, Cambridge.
- Moreno-Mayar, J.V., Vinner, L., de Barros Damgaard, P., de la Fuente, C., Chan, J., Spence, J.P., Allentoft, M.E., Vimala, T., Racimo, F., Pinotti, T., Rasmussen, S., Margaryan, A., Iraeta Orbegozo, M., Mylopotamitaki, D., Wooller, M., Bataille, C., Becerra-Valdivia, L., Chivall, D., Comeskey, D., Deviese, T., Grayson, D.K., George, L., Harry, H., Alexandersen, V., Primeau, C., Erlandson, J., Rodrigues-Carvalho, C., Reis, S., Bastos, M.Q.R., Cybulski, J., Vullo, C., Morello, F., Vilar, M., Wells, S., Gregersen, K., Hansen, K.L., Lynnerup, N., Mirazón Lahr, M., Kjær, K., Strauss, A., Alfonso-Durruty, M., Salas, A., Schroeder, H., Higham, T., Malhi, R.S., Rasic, J.T., Souza, L., Santos, F.R., Malaspinas, A.-S., Sikora, M., Nielsen, R., Song, Y.S., Meltzer, D.J., Willerslev, E., 2018. Early human dispersals within the Americas. *Science*. 362.
- Moss, M.L., Chase, P.S., Howes, R.I., 1967. Comparative odontometry of the permanent post-canine dentition of American Whites and Negroes. *American Journal of Physical Anthropology*. 27, 125–142.
- Müller, M.M., Kals, E., Pansa, R., 2009. Adolescents' emotional affinity toward nature: A cross-societal study. *The Journal of Developmental Processes*. 4, 59–69.
- Muoka, A.K., Mwambi, H., Agogo, G.O., Ngesa, O., 2021. Dealing with covariate measurement error in a clustered cross-sectional survey. *RMS: Research in Mathematics & Statistics*. 8.
- Næs, T., Mevik, B.H., 2001. Understanding the collinearity problem in regression and discriminant analysis. *Journal of Chemometrics*. 15, 413–426.
- Nelson, C.T., 1938. The teeth of the Indians of Pecos Pueblo. *American Journal of Physical Anthropology*. 23, 261–293.
- Nelson, S.J., Ash, M.M., 2010. *Wheeler's dental anatomy, physiology, and occlusion*, 9th ed. Saunders/Elsevier, St. Louis, Mo.
- Nichol, C.R., Turner, C.G., Dahlberg, A.A., 1984. Variation in the convexity of the human maxillary incisor labial surface. *American Journal of Physical Anthropology*. 63, 361–370.
- Nicholls, W., 2016. Dental anomalies in children with cleft lip and palate in Western Australia. *European Journal of Dentistry*. 10, 254–258.
- Nielsen, R., Akey, J.M., Jakobsson, M., Pritchard, J.K., Tishkoff, S., Willerslev, E., 2017. Tracing the peopling of the world through genomics. *Nature*. 541, 302–310.
- Nieminen, P., 2009. Genetic basis of tooth agenesis. *Journal of Experimental Zoology Part B: Molecular and Developmental Evolution*. 312B, 320–342.
- Novacek, M.J., 1986. The primitive eutherian dental formula. *Journal of Vertebrate*

- Paleontology. 6, 191–196.
- O’Connell, J.F., Allen, J., Williams, M.A.J., Williams, A.N., Turney, C.S.M., Spooner, N.A., Kamminga, J., Brown, G., Cooper, A., 2018. When did homo sapiens first reach Southeast Asia and Sahul? *Proceedings of the National Academy of Sciences of the United States of America*. 115, 8482–8490.
- Orban, B.J., Bhaskar, S.N., 1980. *Orban’s Oral histology and embryology*, 9th ed. ed. Mosby, St. Louis.
- Orhan, A., Sari, S., 2006. Double-rooted primary canines: A report of three cases. *Journal of Indian Society of Pedodontics and Preventive Dentistry*. 24, 204.
- Osborn, J.W., 1978. Morphogenetic gradients: Fields versus clones. In: Butler, P.M., Joysey, K. (Eds.), *Development, Function and Evolution of Teeth*. Academic Press, New York, pp. 171–201.
- Pagani, L., Schiffels, S., Gurdasani, D., Danecek, P., Scally, A., Chen, Y., Xue, Y., Haber, M., Ekong, R., Oljira, T., Mekonnen, E., Luiselli, D., Bradman, N., Bekele, E., Zalloua, P., Durbin, R., Kivisild, T., Tyler-Smith, C., 2015. Tracing the Route of Modern Humans out of Africa by Using 225 Human Genome Sequences from Ethiopians and Egyptians. *American Journal of Human Genetics*. 96, 986–991.
- Pallmann, P., Schaarschmidt, F., Hothorn, L.A., Fischer, C., Nacke, H., Priesnitz, K.U., Schork, N.J., 2012. Assessing group differences in biodiversity by simultaneously testing a user-defined selection of diversity indices. *Molecular Ecology Resources*. 12, 1068–1078.
- Pécora, J.D., Estrela, C., Bueno, M.R., Porto, O.C., Alencar, A.H.G., Sousa-Neto, M.D., de Araújo, C.R.E., 2013. Detection of root canal isthmuses in molars by map-reading dynamic using CBCT images. *Brazilian Dental Journal*. 24, 569–574.
- Pedersen, P.O., 1949. The East Greenland Eskimo dentition, numerical variations and anatomy : a contribution to comparative ethnic odontography. *Meddelelser om Grønland*. 142, 1–244.
- Peiris, R., Malwatte, U., Abayakoon, J., Wettasinghe, A., 2015. Variations in the Root Form and Root Canal Morphology of Permanent Mandibular First Molars in a Sri Lankan Population. *Anatomy Research International*. 2015, 1–7.
- Pickrell, J.K., Reich, D., 2014. Toward a new history and geography of human genes informed by ancient DNA. *Trends in Genetics*. 30, 377–389.
- Plavcan, J.M., Daegling, D.J., 2006. Interspecific and intraspecific relationships between tooth size and jaw size in primates. *Journal of Human Evolution*. 51, 171–184.
- Posth, C., Nakatsuka, N., Lazaridis, I., Skoglund, P., Mallick, S., Lamnidis, T.C., Rohland, N., Nägele, K., Adamski, N., Bertolini, E., Broomandkshobacht, N., Cooper, A., Culleton, B.J., Ferraz, T., Ferry, M., Furtwängler, A., Haak, W., Harkins, K., Harper, T.K., Hünemeier, T., Lawson, A.M., Llamas, B., Michel, M., Nelson, E., Oppenheimer, J., Patterson, N., Schiffels, S., Sedig, J., Stewardson, K., Talamo, S., Wang, C.-C., Hublin, J.-J., Hubbe, M., Harvati, K., Nuevo Delaunay, A., Beier, J., Francken, M., Kaulicke, P., Reyes-Centeno, H., Rademaker, K., Trask, W.R., Robinson, M., Gutierrez, S.M., Prufer, K.M., Salazar-García, D.C., Chim, E.N., Müller Plumm Gomes, L., Alves, M.L., Liryo, A., Inglez, M., Oliveira, R.E., Bernardo, D. V., Barioni, A., Wesolowski, V., Scheifler, N.A., Rivera, M.A., Plens, C.R., Messineo, P.G., Figuti, L., Corach, D., Scabuzzo, C., Eggers, S., DeBlasis, P., Reindel, M., Méndez, C., Politis, G., Tomasto-Cagigao, E., Kennett, D.J., Strauss, A., Fehren-Schmitz, L., Krause, J., Reich, D., 2018. Reconstructing the Deep Population History of Central and South America. *Cell*. 175, 1185-1197.e22.
- PRADO-SIMÓN, L., MARTINÓN-TORRES, M., BACA, P., GÓMEZ-ROBLES, A., LAPRESA, M.,

- CARBONELL, E., BERMÚDEZ DE CASTRO, J.M., 2012. A morphological study of the tooth roots of the Sima del Elefante mandible (Atapuerca, Spain): a new classification of the teeth—biological and methodological considerations. *Anthropological Science*. 120, 61–72.
- Prado-Simón, L., Martínón-Torres, M., Baca, P., Olejniczak, A.J., Gómez-Robles, A., Lapresa, M., Luis Arsuaga, J., María Bermúdez de Castro, J., 2012. Three-dimensional evaluation of root canal morphology in lower second premolars of early and middle pleistocene human populations from atapuerca (Burgos, Spain). *American Journal of Physical Anthropology*. 147, 452–461.
- Prüfer, K., Racimo, F., Patterson, N., Jay, F., Sankararaman, S., Sawyer, S., Heinze, A., Renaud, G., Sudmant, P.H., de Filippo, C., Li, H., Mallick, S., Dannemann, M., Fu, Q., Kircher, M., Kuhlwilm, M., Lachmann, M., Meyer, M., Ongyerth, M., Siebauer, M., Theunert, C., Tandon, A., Moorjani, P., Pickrell, J., Mullikin, J.C., Vohr, S.H., Green, R.E., Hellmann, I., Johnson, P.L.F., Blanche, H., Cann, H., Kitzman, J.O., Shendure, J., Eichler, E.E., Lein, E.S., Bakken, T.E., Golovanova, L. V., Doronichev, V.B., Shunkov, M. V., Derevianko, A.P., Viola, B., Slatkin, M., Reich, D., Kelso, J., Pääbo, S., 2014. The complete genome sequence of a Neanderthal from the Altai Mountains. *Nature*. 505, 43–49.
- Prugnolle, F., Manica, A., Balloux, F., 2005. Geography predicts neutral genetic diversity of human populations. *Current Biology*. 15, R159–R160.
- Pugach, I., Delfin, F., Gunnarsdóttir, E., Kayser, M., Stoneking, M., 2013. Genome-wide data substantiate Holocene gene flow from India to Australia. *Proceedings of the National Academy of Sciences of the United States of America*. 110, 1803–1808.
- Quam, R., Bailey, S., Wood, B.A., 2009. Evolution of M1 crown size and cusp proportions in the genus *Homo*. *Journal of Anatomy*. 214, 655–670.
- Ragsdale, C.S., Edgar, H.J.H., 2015. Cultural interaction and biological distance in postclassic period Mexico. *American Journal of Physical Anthropology*. 157, 121–133.
- Rahim, N.G., Harismendy, O., Topol, E.J., Frazer, K.A., 2008. Genetic determinants of phenotypic diversity in humans. *Genome Biology*. 9, 215.
- Rainey, F., 1941. The Ipiutak Culture at Point Hope, Alaska. *American Anthropologist*. 43, 364–375.
- Rainey, F.G., 1947. The whale hunters of Tigara. *Anthropological papers of the AMNH ; v. 41, pt. 2*.
- Rainey, F.G., 1971. *The Ipiutak Culture: Excavations at Point Hope, Alaska*. Addison-Wesley Publishing.
- Rakhshan, V., 2015. Congenitally missing teeth (hypodontia): A review of the literature concerning the etiology, prevalence, risk factors, patterns and treatment. *Dental Research Journal*. 12, 1.
- Ralph, P., Coop, G., 2013. The Geography of Recent Genetic Ancestry across Europe. *PLoS Biology*. 11, e1001555.
- Ramachandran, S., Deshpande, O., Roseman, C.C., Rosenberg, N.A., Feldman, M.W., Cavalli-Sforza, L.L., 2005. Support from the relationship of genetic and geographic in human populations for a serial founder effect originating in Africa. *Proceedings of the National Academy of Sciences of the United States of America*. 102, 15942–15947.
- Rathmann, H., Reyes-Centeno, H., 2020. Testing the utility of dental morphological trait combinations for inferring human neutral genetic variation. *Proceedings of the National Academy of Sciences*. 117, 10769–10777.

- Rathmann, H., Reyes-Centeno, H., Ghirotto, S., Creanza, N., Hanihara, T., Harvati, K., 2017. Reconstructing human population history from dental phenotypes. *Scientific Reports*. 7, 12495.
- Reed, K.E., 1997. Early hominid evolution and ecological change through the African Plio-Pleistocene. *Journal of Human Evolution*. 32, 289–322.
- Reich, D., 2018. *Who we are and how we got here : ancient DNA and the new science of the human past*. Oxford University Press: Oxford.
- Reid, D.J., Schwartz, G.T., Dean, C., Chandrasekera, M.S., 1998. A histological reconstruction of dental development in the common chimpanzee, *Pan troglodytes*. *Journal of Human Evolution*. 35, 427–448.
- Reyes-Centeno, H., Ghirotto, S., Détoit, F., Grimaud-Hervé, D., Barbujani, G., Harvati, K., 2014. Genomic and cranial phenotype data support multiple modern human dispersals from Africa and a southern route into Asia. *Proceedings of the National Academy of Sciences of the United States of America*. 111, 7248–7253.
- Reyes-Centeno, H., Hubbe, M., Hanihara, T., Stringer, C., Harvati, K., 2015. Testing modern human out-of-Africa dispersal models and implications for modern human origins. *Journal of Human Evolution*. 87, 95–106.
- Reyes-Centeno, H., Rathmann, H., Hanihara, T., Harvati, K., 2017. Testing modern human out-of-Africa dispersal models using dental nonmetric data. *Current Anthropology*. 58, S406–S417.
- Rivera, F., Mirazón Lahr, M., 2017. New evidence suggesting a dissociated etiology for cribra orbitalia and porotic hyperostosis. *American Journal of Physical Anthropology*. 164, 76–96.
- Roberts, D.F., Molnar, S., 1975. *Races, Types and Ethnic Groups: The Problem of Human Variation*. *Man*. 10, 628.
- Robinson, J.T., 1954. Prehominid dentition and dental evolution. *Evolution*. 8, 324–334.
- Robinson, J.T., 1956. The dentition of the Australopithecinae: Australopithecines and hominid phylogenesis. *Transvaal Museum Memoirs*. 9, 158–175.
- Rogers, A.R., Harris, N.S., Achenbach, A.A., 2020. Neanderthal-Denisovan ancestors interbred with a distantly related hominin. *Science Advances*. 6, eaay5483.
- Roy, A., 2013. Mandibular Second Molar with a Single Root and a Single Canal: Case Series. *Journal of Clinical and Diagnostic Research*. 7, 2637–2638.
- Sankararaman, S., Mallick, S., Patterson, N., Reich, D., 2016. The Combined Landscape of Denisovan and Neanderthal Ancestry in Present-Day Humans. *Current Biology*. 26, 1241–1247.
- Savell, K.R.R., Auerbach, B.M., Roseman, C.C., 2016. Constraint, natural selection, and the evolution of human body form. *Proceedings of the National Academy of Sciences of the United States of America*. 113, 9492–9497.
- Schiffels, S., Durbin, R., 2014. Inferring human population size and separation history from multiple genome sequences. *Nature Genetics*. 46, 919–925.
- Scott, G.R., 1977. Interaction Between Shoveling of the Maxillary and Mandibular Incisors. *Journal of Dental Research*. 56, 1423.
- Scott, G.R., 1988. Dental Anthropology. *Annual Review of Anthropology*. 17, 99–126.
- Scott, G.R., Hemphill, B.E., 2012. *Officers of the Dental Anthropology Association*. 25.
- Scott, G.R., Irish, J.D., 2017. *Human Tooth Crown and Root Morphology, Human Tooth Crown and Root Morphology*. Cambridge University Press.
- Scott, G.R., Irish, J.D., Martínón-Torres, M., 2020. A more comprehensive view of the

- Denisovan 3-rooted lower second molar from Xiahe. *Proceedings of the National Academy of Sciences*. 117, 37–38.
- Scott, G.R., Turner, C.G., 1988. Dental Anthropology. *Annual Review of Anthropology*. 17, 99–126.
- Scott, G.R., Turner, C.G., 1997. *The Anthropology of Modern Human Teeth*, The Anthropology of Modern Human Teeth. Cambridge University Press.
- Scott, G.R., Turner II, C.G., Townsend, G.C., Martínón-Torres, M., 2018. *The Anthropology of Modern Human Teeth*, The Anthropology of Modern Human Teeth: Dental Morphology and its Variation in Recent and Fossil Homo Sapien. Cambridge University Press.
- Scott, J.E., Lockwood, C.A., 2004. Patterns of tooth crown size and shape variation in great apes and humans and species recognition in the hominid fossil record. *American Journal of Physical Anthropology*. 125, 303–319.
- Selmer-Olsen, R., 1949. *An odontometric study of the Norwegian Lapps*. Det Norske Videnskaps Akademi, Oslo.
- Shalev-Shwartz, S., Ben-David, S., 2013. Understanding machine learning: From theory to algorithms, *Understanding Machine Learning: From Theory to Algorithms*. Cambridge University Press, Cambridge.
- Shang, H., Tong, H., Zhang, S., Chen, F., Trinkaus, E., 2007. An early modern human from Tianyuan Cave, Zhoukoudian, China. *Proceedings of the National Academy of Sciences*. 104, 6573–6578.
- Shaw, J., 1931. *The teeth, the bony palate and the mandible in Bantu races of South Africa*. John Bale Sons & Danielsson, London.
- Shields, E.D., 2005. Mandibular premolar and second molar root morphological variation in modern humans: What root number can tell us about tooth morphogenesis. *American Journal of Physical Anthropology*. 128, 299–311.
- Skoglund, P., Posth, C., Sirak, K., Spriggs, M., Valentin, F., Bedford, S., Clark, G.R., Reepmeyer, C., Petchey, F., Fernandes, D., Fu, Q., Harney, E., Lipson, M., Mallick, S., Novak, M., Rohland, N., Stewardson, K., Abdullah, S., Cox, M.P., Friedlaender, F.R., Friedlaender, J.S., Kivisild, T., Koki, G., Kusuma, P., Merriwether, D.A., Ricaut, F.X., Wee, J.T.S., Patterson, N., Krause, J., Pinhasi, R., Reich, D., 2016. Genomic insights into the peopling of the Southwest Pacific. *Nature*. 538, 510–513.
- Smith, B.H., 1991. Dental development and the evolution of life history in Hominidae. *American Journal of Physical Anthropology*. 86, 157–174.
- Smith, J.M., Burian, R., Kauffman, S., Alberch, P., Campbell, J., Goodwin, B., Lande, R., Raup, D., Wolpert, L., 1985. Developmental Constraints and Evolution: A Perspective from the Mountain Lake Conference on Development and Evolution. *The Quarterly Review of Biology*. 60, 265–287.
- Sofaer, J.A., Niswander, J.D., MacLean, C.J., Workman, P.L., 1972. Population studies on Southwestern Indian tribes V. Tooth morphology as an indicator of biological distance. *American Journal of Physical Anthropology*. 37, 357–366.
- Spears, I.R., Macho, G.A., 1998. Biomechanical behaviour of modern human molars: Implications for interpreting the fossil record. *American Journal of Physical Anthropology*. 106, 467–482.
- Spencer, M.A., 2003. Tooth-root form and function in platyrrhine seed-eaters. *American Journal of Physical Anthropology*. 122, 325–335.
- Sperber, G.H., 1973. *Morphology of the Cheek Teeth of Early South African Hominids*. Witwatersrand University: Johannesburg.

- Sterne, J.A.C., White, I.R., Carlin, J.B., Spratt, M., Royston, P., Kenward, M.G., Wood, A.M., Carpenter, J.R., 2009. Multiple imputation for missing data in epidemiological and clinical research: potential and pitfalls. *BMJ*. 338, b2393–b2393.
- Stinchcombe, J.R., Hoekstra, H.E., 2008. Combining population genomics and quantitative genetics: finding the genes underlying ecologically important traits. *Heredity*. 100, 158–170.
- Stojanowski, C.M., Paul, K.S., Seidel, A.C., Duncan, W.N., Guatelli-Steinberg, D., 2018. Heritability and genetic integration of anterior tooth crown variants in the South Carolina Gullah. *American Journal of Physical Anthropology*. 167, 124–143.
- Stojanowski, C.M., Paul, K.S., Seidel, A.C., Duncan, W.N., Guatelli-Steinberg, D., 2019. Quantitative genetic analyses of postcanine morphological crown variation. *American Journal of Physical Anthropology*. 168, 606–631.
- Stringer, C.B., Humphrey, L.T., Compton, T., 1997. Cladistic analysis of dental traits in recent humans using a fossil outgroup. *Journal of Human Evolution*. 32, 389–402.
- Taylor, A.B., 2006. Feeding behavior, diet, and the functional consequences of jaw form in orangutans, with implications for the evolution of Pongo. *Journal of Human Evolution*. 50, 377–393.
- Taylor, A.E., 1899. Variations in the Human Tooth-form as met with in Isolated Teeth. *Journal of Anatomy and Physiology*. 33, 268–72.
- Tomes, C.S., 1889. *A Manual of Dental Anatomy: Human and Comparative*. J. & A. Churchill, London.
- Townsend, G., Hughes, T., Luciano, M., Bockmann, M., Brook, A., 2009. Genetic and environmental influences on human dental variation: A critical evaluation of studies involving twins. *Archives of Oral Biology*. 54, S45–S51.
- Tratman, E.K., 1938. Three-rooted lower molars in man and their racial distribution. *British Dental Journal*. 264–274.
- Turner, C.G., 1971. Three-rooted mandibular first permanent molars and the question of American Indian Origins. *American Journal of Physical Anthropology*. 34, 229–241.
- Turner, C.G., 1981. Root number determination in maxillary first premolars for modern human populations. *American Journal of Physical Anthropology*. 54, 59–62.
- Turner, C.G., 1987. Late Pleistocene and Holocene population history of east Asia based on dental variation. *American Journal of Physical Anthropology*. 73, 305–321.
- Turner II, C.G., 1989. Teeth and Prehistory in Asia. *Scientific American*. 260, 88–96.
- Turner II, C.G., Nichol, C.R., Scott, G.R., 1991. Scoring procedures for key morphological traits of the permanent dentition : the Arizona State University dental anthropology system. In: Kelley, M.A., Larson, C.S. (Eds.), *Advances in Dental Anthropology*. Wiley-Liss Inc., New York, pp. 13–31.
- van Eijden, T.M.G.J., 1991. Three-dimensional analyses of human bite-force magnitude and moment. *Archives of Oral Biology*. 36, 535–539.
- Vattathil, S., Akey, J.M., 2015. Small Amounts of Archaic Admixture Provide Big Insights into Human History. *Cell*. 163, 281–284.
- Versiani, M.A., Basrani, B., Sousa-Neto, M.D., 2019. *The Root Canal Anatomy in Permanent Dentition*. Springer International Publishing, Cham.
- Vertucci, F., Seelig, A., Gillis, R., 1974. Root canal morphology of the human maxillary second premolar. *Oral Surgery, Oral Medicine, Oral Pathology*. 38, 456–464.
- Vertucci, F.J., 2005. Root canal morphology and its relationship to endodontic procedures.

- Endodontic Topics. 10, 3–29.
- Vertucci, F.J., Gegauff, A., 1979. Root canal morphology of the maxillary first premolar. *The Journal of the American Dental Association*. 99, 194–198.
- Vervier, K., Mahé, P., Vert, J.-P., 2018. MetaVW: Large-Scale Machine Learning for Metagenomics Sequence Classification. In: *Methods in Molecular Biology*. Humana Press Inc., pp. 9–20.
- von Cramon-Taubadel, N., Lycett, S.J., 2008. Brief Communication: Human cranial variation fits iterative founder effect model with African origin. *American Journal of Physical Anthropology*. 136, 108–113.
- Walker, A., 1981. Diet and teeth: Dietary hypotheses and human evolution. *Philosophical Transactions of the Royal Society of London. B, Biological Sciences*. 292, 57–64.
- Wang, K. e., Yang, Y., Shen, F., Tao, J., Xu, H., Portnof, J.E., Wang, G., Salyer, K.E., 2009. Utilization of three-dimensional computed tomography for craniofacial phenotypic analysis in children with velocardiofacial syndrome. *Journal of Craniofacial Surgery*. 20, 2013–2019.
- Wang, S., Ray, N., Rojas, W., Parra, M. V., Bedoya, G., Gallo, C., Poletti, G., Mazzotti, G., Hill, K., Hurtado, A.M., Camrena, B., Nicolini, H., Klitz, W., Barrantes, R., Molina, J.A., Freimer, N.B., Bortolini, M.C., Salzano, F.M., Petzl-Erler, M.L., Tsuneto, L.T., Dipierri, J.E., Alfaro, E.L., Bailliet, G., Bianchi, N.O., Llop, E., Rothhammer, F., Excoffier, L., Ruiz-Linares, A., 2008. Geographic Patterns of Genome Admixture in Latin American Mestizos. *PLoS Genetics*. 4, e1000037.
- Wang, Y., Cox, M.K., Coricor, G., MacDougall, M., Serra, R., 2013. Inactivation of *Tgfb2* in Osterix-Cre expressing dental mesenchyme disrupts molar root formation. *Developmental Biology*. 382, 27–37.
- Wang, Y., Guo, J., Yang, H.-B., Han, X., Yu, Y., 2012. Incidence of C-shaped root canal systems in mandibular second molars in the native Chinese population by analysis of clinical methods. *International Journal of Oral Science*. 4, 161–165.
- Wang, Y., Tetko, I. V., Hall, M.A., Frank, E., Facius, A., Mayer, K.F.X., Mewes, H.W., 2005. Gene selection from microarray data for cancer classification—a machine learning approach. *Computational Biology and Chemistry*. 29, 37–46.
- Ward, S.C., Johanson, D.C., Coppens, Y., 1982. Subocclusal morphology and alveolar process relationships of hominid gnathic elements from the Hadar formation: 1974-1977 collections. *American Journal of Physical Anthropology*. 57, 605–630.
- Ward, S.C., Molnar, S., 1980. Experimental stress analysis of topographic diversity in early hominid gnathic morphology. *American Journal of Physical Anthropology*. 53, 383–395.
- Weine, F.S., 1984. The enigma of the lateral canal. *Dental Clinics of North America*. 28, 833–852.
- Wells, R.S., Yuldasheva, N., Ruzibakiev, R., Underhill, P.A., Evseeva, I., Blue-Smith, J., Jin, L., Su, B., Pitchappan, R., Shanmugalakshmi, S., Balakrishnan, K., Read, M., Pearson, N.M., Zerjal, T., Webster, M.T., Zholoshvili, I., Jamarjashvili, E., Gambarov, S., Nikbin, B., Dostiev, A., Aknazarov, O., Zalloua, P., Tsoy, I., Kitaev, M., Mirrakhimov, M., Chariev, A., Bodmer, W.F., 2001. The Eurasian heartland: A continental perspective on Y-chromosome diversity. *Proceedings of the National Academy of Sciences of the United States of America*. 98, 10244–10249.
- White, T.D., Black, M.T., Folkens, P.A., White, T.D., Black, M.T., Folkens, P.A., 2012. Teeth. In: *Human Osteology*. Academic Press, pp. 101–128.
- Wilkins, A.S., 2007. Between “design” and “bricolage”: Genetic networks, levels of selection,

- and adaptive evolution. *Proceedings of the National Academy of Sciences of the United States of America*. 104, 8590–8596.
- Wilsey, B.J., Chalcraft, D.R., Bowles, C.M., Willig, M.R., 2005. RELATIONSHIPS AMONG INDICES SUGGEST THAT RICHNESS IS AN INCOMPLETE SURROGATE FOR GRASSLAND BIODIVERSITY. *Ecology*. 86, 1178–1184.
- Winder, I.C., Devès, M.H., King, G.C.P., Bailey, G.N., Inglis, R.H., Meredith-Williams, M., 2015. Evolution and dispersal of the genus *Homo* : A landscape approach. *Journal of Human Evolution*. 87, 48–65.
- Wolf, A.B., Akey, J.M., 2018. Outstanding questions in the study of archaic hominin admixture. *PLOS Genetics*. 14, e1007349.
- Wood, B., Collard, M., 1999. The changing face of genus *Homo*. *Evolutionary Anthropology: Issues, News, and Reviews*. 8, 195–207.
- Wood, B.A., Abbott, S.A., 1983. Analysis of the dental morphology of Plio-pleistocene hominids. I. Mandibular molars: crown area measurements and morphological traits. *Journal of Anatomy*. 136, 197–219.
- Wood, B.A., Abbott, S.A., Uytterschaut, H., 1988. Analysis of the dental morphology of Plio-Pleistocene hominids. IV. Mandibular postcanine root morphology. *Journal of Anatomy*. 156, 107–39.
- Wood, B.A., Constantino, P., 2007. *Paranthropus boisei*: Fifty years of evidence and analysis. *American Journal of Physical Anthropology*. 134, 106–132.
- Wood, B.A., Engleman, C.A., 1988. Analysis of the dental morphology of Plio-Pleistocene hominids V. Maxillary postcanine tooth morphology. *Journal of Anatomy*. 161, 1–35.
- Wood, B.A., Uytterschaut, H., 1987. Analysis of the dental morphology of Plio-Pleistocene hominids. III. Mandibular premolar crowns. *Journal of anatomy*. 154, 121–56.
- Wright, T., 2007. The Molecular Control of and Clinical Variations in Root Formation. *Cells Tissues Organs*. 186, 86–93.
- Xing, S., Martínón-Torres, M., Bermúdez de Castro, J.M., 2018. The fossil teeth of the Peking Man. *Scientific Reports*. 8, 2066.
- Yang, M.A., Gao, X., Theunert, C., Tong, H., Aximu-Petri, A., Nickel, B., Slatkin, M., Meyer, M., Pääbo, S., Kelso, J., Fu, Q., 2017. 40,000-Year-Old Individual from Asia Provides Insight into Early Population Structure in Eurasia. *Current Biology*. 27, 3202–3208.e9.
- Zanoli, C., Mazurier, A., 2013. Endostructural characterization of the *H. heidelbergensis* dental remains from the early Middle Pleistocene site of Tighenif, Algeria. *Comptes Rendus Palevol*. 12, 293–304.
- Zeger, S.L., Liang, K.-Y., 1986. Longitudinal Data Analysis for Discrete and Continuous Outcomes. *Biometrics*. 42, 121.
- Zeileis, A., Kleiber, C., Jackman, S., 2008. Regression Models for Count Data in R. *Journal of Statistical Software*. 27, 1–25.
- Zhang, Yuqing, Alyass, A., Vanniyasingam, T., Sadeghirad, B., Flórez, I.D., Pichika, S.C., Kennedy, S.A., Abdulkarimova, U., Zhang, Yuan, Iljon, T., Morgano, G.P., Colunga Lozano, L.E., Aloweni, F.A.B., Lopes, L.C., Yepes-Nuñez, J.J., Fei, Y., Wang, L., Kahale, L.A., Meyre, D., Akl, E.A., Thabane, L., Guyatt, G.H., 2017. A systematic survey of the methods literature on the reporting quality and optimal methods of handling participants with missing outcome data for continuous outcomes in randomized controlled trials. *Journal of Clinical Epidemiology*. 88, 67–80.
- Zheng, Q., Zhang, L., Zhou, X., Wang, Q., Wang, Y., Tang, L., Song, F., Huang, D., 2011. C-shaped root canal system in mandibular second molars in a Chinese population

- evaluated by cone-beam computed tomography. *International Endodontic Journal*. 44, 857–862.
- Zichello, J.M., Baab, K.L., McNulty, K.P., Raxworthy, C.J., Steiper, M.E., 2018. Hominoid intraspecific cranial variation mirrors neutral genetic diversity. *Proceedings of the National Academy of Sciences of the United States of America*. 115, 11501–11506.
- Zorba, E., Vanna, V., Moraitis, K., 2014. Sexual dimorphism of root length on a Greek population sample. *HOMO*. 65, 143–154.
- Zuur, A.F., Ieno, E.N., Walker, N., Saveliev, A.A., Smith, G.M., 2009. *Mixed effects models and extensions in ecology with R, Statistics for Biology and Health*. Springer New York, New York, NY.
- Zwemer, T., 1985. Bioengineering analysis of orthodontic mechanics. *American Journal of Orthodontics*. 88, 446–447.